

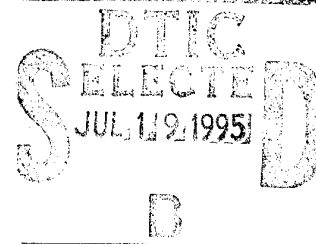
# AGARD

ADVISORY GROUP FOR AEROSPACE RESEARCH & DEVELOPMENT

7 RUE ANCELLE, 92200 NEUILLY-SUR-SEINE, FRANCE

DISTRIBUTION STATEMENT A

Approved for public release  
Distribution Unlimited



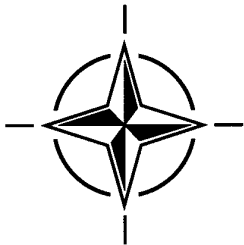
AGARD CONFERENCE PROCEEDINGS NO 556

## Dual Usage in Military and Commercial Technology in Guidance and Control

(Technologies duales militaires et civiles  
de guidage/pilotage)

*Papers presented at the Guidance and Control Panel 59th Symposium held in  
Pratica di Mare (Rome) from 20th October to 21st October 1994.*

19950718 006



NORTH ATLANTIC TREATY ORGANIZATION

# AGARD

ADVISORY GROUP FOR AEROSPACE RESEARCH & DEVELOPMENT

7 RUE ANCELLE, 92200 NEUILLY-SUR-SEINE, FRANCE

---

**AGARD CONFERENCE PROCEEDINGS NO 556**

## **Dual Usage in Military and Commercial Technology in Guidance and Control**

(Technologies duales militaires et civiles  
de guidage/pilotage)

Papers presented at the Guidance and Control Panel 59th Symposium held in  
Pratica di Mare (Rome) from 20th October to 21st October 1994.



North Atlantic Treaty Organization  
*Organisation du Traité de l'Atlantique Nord*

---

# The Mission of AGARD

According to its Charter, the mission of AGARD is to bring together the leading personalities of the NATO nations in the fields of science and technology relating to aerospace for the following purposes:

- Recommending effective ways for the member nations to use their research and development capabilities for the common benefit of the NATO community;
- Providing scientific and technical advice and assistance to the Military Committee in the field of aerospace research and development (with particular regard to its military application);
- Continuously stimulating advances in the aerospace sciences relevant to strengthening the common defence posture;
- Improving the co-operation among member nations in aerospace research and development;
- Exchange of scientific and technical information;
- Providing assistance to member nations for the purpose of increasing their scientific and technical potential;
- Rendering scientific and technical assistance, as requested, to other NATO bodies and to member nations in connection with research and development problems in the aerospace field.

The highest authority within AGARD is the National Delegates Board consisting of officially appointed senior representatives from each member nation. The mission of AGARD is carried out through the Panels which are composed of experts appointed by the National Delegates, the Consultant and Exchange Programme and the Aerospace Applications Studies Programme. The results of AGARD work are reported to the member nations and the NATO Authorities through the AGARD series of publications of which this is one.

Participation in AGARD activities is by invitation only and is normally limited to citizens of the NATO nations.

The content of this publication has been reproduced directly from material supplied by AGARD or the authors.

Accession For	
NTIS GRA&I	<input checked="checked" type="checkbox"/>
DTIC TAB	<input type="checkbox"/>
Unannounced	<input type="checkbox"/>
Justification	
By	
Distribution/	
Availability Codes	
Dist	Avail and/or Special
A-1	

Published March 1995

Copyright © AGARD 1995  
All Rights Reserved

ISBN 92-836-1016-4



Printed by Canada Communication Group  
45 Sacré-Cœur Blvd., Hull (Québec), Canada K1A 0S7

## Theme

In the past decade, the development of components, techniques, and tools in the commercial world has had a significant impact upon the aerospace community. Such things as the personal computer, highly sophisticated operating environments, commercial computer chip developments, optical disks and fiber optics are examples. Alternatively, in cases where developmental costs are high for a limited production base, or in which commercial spin-offs are not immediately evident, the military has developed technologies which have had, or will have, a significant impact on the commercial sector. Examples are GPS, Fly-by-wire flight control systems, integrated avionics, and automatic landing systems.

Major reductions in military procurements within NATO countries has led to concern over the long-term viability of the military industrial base. Dual-use technologies provide new markets for the military industrial base. Future military options are retained by the commercial market development of products which address important military needs. Commercial volumes are often higher for these products resulting in enhanced affordability for the military.

Guidance and control is a natural dual-use technology because of the rich applications to commercial as well as military aircraft in areas such as navigation, control systems, flight management, automated vehicle operations and space G, N, and C.

This Symposium will focus on commercial and military system producers throughout NATO countries who can create cooperative international products and markets. In a new spirit of international cooperation, technologists from former Warsaw Pact countries have been invited to participate.

They will cover:

- Dual-use Opportunities and Missions
- Navigation Sensors for Dual-use Applications
- Multi-sensor Navigation Applied to Dual-uses
- Dual-use Technology for Air-Ground Operations
- Dual-use Applications of G&C Technology

## Thème

Au cours de la dernière décennie, le développement de composantes, de techniques et d'outils par l'industrie civile a eu un impact sensible sur la communauté aérospatiale. Des éléments tels que l'ordinateur individuel, les systèmes d'exploitation hautement sophistiqués, le développement commercial des circuits intégrés, les disques optiques et les fibres optiques en sont des exemples.

Inversement, dans les cas où les coûts de développement étaient trop élevés par rapport à une production limitée, ou lorsque les débouchés civils ne semblaient pas d'emblée évidents, les militaires ont développé des technologies qui ont eu, ou qui auront, un impact considérable sur le secteur civil. Exemples de ces technologies: le GPS, les commandes de vol électriques, l'avionique intégrée et les systèmes d'atterrissage automatique.

Les réductions importantes qui ont été opérées dans les programmes militaires au sein des pays membres de l'OTAN, ont soulevé des inquiétudes concernant la viabilité à long terme de l'assise industrielle militaire. Les technologies duales ouvrent de nouvelles perspectives de marché pour l'industrie militaire. Les options militaires futures sont tributaires du développement commercial de produits qui répondent aux besoins militaires. Les volumes de production de ces produits sont souvent plus importants, ce qui les rend plus accessibles financièrement pour les autorités militaires.

Le «guidage et pilotage» est une discipline bien adaptée aux technologies duales en raison de la multiplicité d'applications civiles et militaires qui existent dans des domaines tels que la navigation, les systèmes de commande, la gestion des vols, la conduite automatisée des véhicules et le guidage, la navigation et le pilotage de véhicules spatiaux.

Ce symposium portera principalement sur les fournisseurs de systèmes civils et militaires des pays de l'OTAN, susceptibles de créer des produits pour les marchés de la coopération internationale. Dans un nouvel esprit de coopération internationale, des technologues de différents pays de l'ancien Pacte de Varsovie ont été invités à participer à la conférence. Les sujets suivants seront examinés:

- les possibilités et les missions duales
- les senseurs de navigation pour les applications duales
- les applications duales de la navigation multi-senseur
- les technologies duales dans les opérations air-sol
- les applications duales des technologies de guidage et de pilotage



# Guidance and Control Panel

**Acting Chairman:** Mr. J.K. Ramage  
Chief, Flight Control  
Flight Dynamics Directorate  
WL/FIGS, Bldg 146  
2210 Eighth St, Ste 11  
WRIGHT-PATTERSON AFB,  
OH 45433-7521, USA

## TECHNICAL PROGRAMME COMMITTEE

<b>Co-Chairmen:</b>	Dr. T. Cunningham	US
	Dr. E. Zimet	US
<b>Members:</b>	Mr. J. Cymbalista	FR
	Prof. Dr. H. Sorg	GE
	Mr. K. Helps	UK
	Dr. J. Niemela	US

## PANEL EXECUTIVE

### From Europe:

AGARD-OTAN  
Lieutenant-Colonel P. FORTABAT, FAF  
MSP Executive  
7 rue Ancelle  
F-92200 NEUILLY-SUR-SEINE,  
FRANCE

### From the USA or Canada:

AGARD-NATO  
Attention: MSP Executive  
PSC 116  
APO AE 09777

Telephone 33-1-4738 5780/82 — Telex: 610 176 — Telefax: 33-1-4738 6720/5799

## HOST NATION LOCAL COORDINATOR

Colonel F. CELEGATO  
Aeronautica Militare  
Ufficio D N AGARD  
Aeroporto Pratica di Mare  
00040 POMEZIA (Roma)  
Tel: (39) 6 910 926 83  
FAX: (39) 6 910 5887

## ACKNOWLEDGEMENTS/REMERCIEMENTS

The Panel wishes to express its thanks to the Italian National Delegates to AGARD for the invitation to hold this Symposium in Pratica di Mare and for the facilities and personnel which made the Symposium possible.

Le Panel tient à remercier les délégués nationaux d'Italie auprès de l'AGARD de leur invitation à tenir ce symposium à Pratica di Mare et de la mise à disposition de personnel et des installations nécessaires.

# Contents

	Page
Theme/Thème	iii
Panel Officer and Programme Committee	iv
	Reference
Technical Evaluation Report by S. Leek	TER
 <b>SESSION I — DUAL USE OPPORTUNITIES AND MISSIONS</b> Chairman: Dr. E. Zimet (US)	
Dual Use: Opportunities, Payoffs and Challenges by T.B. Cunningham	1
The Concept of the Space System Based on the "ROCKOT" Launch Vehicle of Light-Weight Class for Direct Sounding of Large-Scale Natural Hazards by V.I. Loukiachtchenko, G.A. Tsyboulskii, A.K. Nedaivoda, V.K. Karrask, A.A. Medvedev, N.A. Meliankow, S.N. Philosophov, V.P. Karmasin	2
 <b>SESSION II — NAVIGATION SENSORS FOR DUAL-USE APPLICATIONS</b> Chairman: Dr. H. Sorg (GE)	
Commercial Usage of Navy Components Developed and Manufactured by CRI "DELFIN" by A.V. Novgorodsky, M.V. Chichinadze	3
Some Results of International Cooperation in Military to Commercial Conversation of Laser Gyro Technology by Y.V. Filatov, D.P. Loukianov, A.V. Mochalov, R. Probst, R. Rodloff, B. Stieler	4
Navigational Technology of Dual Usage by V.G. Peshekhonov, I.M. Okon, L.P. Nesenyuk, Y.B. Belous	5
Dual Use Micromechanical Inertial Sensors by J.M. Elwell Jr.	6
Laser Gyroscopy Tendencies and their Analysis of Development in the Ukraine by A. Dovbeshko	7
 <b>SESSION III — MULTI-SENSOR NAVIGATION APPLIED TO DUAL-USES</b> Chairman: Dr. J. Niemela (US)	
Effects of the Specific Military Aspects of Satellite Navigation on the Civil Use of GPS/GLONASS by D. Kayser, G. Schanzer	8
The DLR Research Programme on an Integrated Multi-Sensor System for Surface Movement Guidance and Control by K. Klein	9

<b>Low-Level Data Fusion: Applications for Landing Runways Detection</b> by L. Sliwa, X. Briottet	<b>10</b>
<b>Paper 11 withdrawn</b>	
<b>SESSION IV — DUAL-USE TECHNOLOGY FOR AIR/GROUND OPERATIONS</b> <b>Chairman: Dr. T. Cunningham</b>	
<b>HeliRadar — Rotating Antenna Synthetic Aperture Radar for Helicopter Allweather Operations</b> by W. Kreitmair-Steck, A.P. Wolframm	<b>12</b>
<b>Identification of Terrain Imagery with Unstable Reflectivity</b> by Y.A. Kozko, V.V. Saveliev	<b>13</b>
<b>Integrated Navigation and Landing System/A System for Autoland of Military and Civil Aircraft</b> by T. Jacob, U. Wacker, H. Schmidt	<b>14*</b>
<b>Development and Application of the Methods for Pilot-Aircraft System Research to the Manual Control Tasks of Modern Vehicles</b> by A.V. Efremov, A.V. Oglobin	<b>15</b>
<b>Successful Flight Testing of an Automatic Low Altitude Avoidance and Navigation System — LATAN</b> by H.-D. Lerche	<b>16*</b>
<b>Paper 17 withdrawn</b>	
<b>Application of Advanced Safety Technique to Ring Laser Gyro Inertial Navigation System Integration</b> by J. Blaylock, D. Swihart, C. Stribula	<b>18</b>
<b>SESSION V — DUAL-USE APPLICATIONS OF G &amp; C TECHNOLOGY</b> <b>Chairman: Mr. K. Helps (UK)</b>	
<b>Paper 19 withdrawn</b>	
<b>Sea Wave Parameters, Small Altitudes and Distances Measurers Design for Movement Control Systems of Ships, Wing-in-Surface Effect Crafts and Seaplanes</b> by A.V. Nebylov, A.P. Vanayev, V.V. Chernyavets	<b>20</b>
<b>The Application of ADA and Formal Methods to a Safety Critical Engine Control System</b> by W.C. Dolman, A.M. Ashdown, K.J. McCallion	<b>21</b>
<b>Solid-State Data Recorder, Next Development and Use</b> by J. Vidiečan, J. Kozák, K. Horák, J. Svoboda	<b>22†</b>
<b>GPS-Based Navigation For Space Applications</b> by C. Champetier, T. Duhamel, M. Frezet	<b>23</b>
<b>Integrated Special Mission Flight Management for a Flight Inspection Aircraft</b> by A. Redeker, M. Haverland	<b>24</b>

\* Not available at time of printing.

† Paper prepared for the meeting, but not presented.

## TECHNICAL EVALUATION REPORT

Stanley Leek  
8 Sunnyfield  
Hatfield  
Hertfordshire AL9 5DX  
United Kingdom

### INTRODUCTION

The 59th - and last - symposium of the Guidance and Control Panel, was held in the Pratica di Mare Air Force Base, near Rome, Italy, on the 20th and 21st of October, 1994.\*

The subject of this symposium - dual usage in military and commercial technology - was very timely in view of the major reductions taking place in military procurement and consequent concern over the long-term viability of its supporting industrial base. In addressing these concerns there is some hope that future military options may be supported by the commercial market development of products which fulfill important military needs. Equally important, higher commercial production volumes for these products could enhance the affordability of military systems. Guidance and control is a natural field for dual-use of technology because of its rich applications, in commercial as well as military aircraft, to such areas as navigation, control systems, flight management, automated vehicle operations and space vehicles.

In the past decade, the development of components, techniques and tools in the commercial world has already had a significant impact upon the aerospace community. Good examples are: the personal computer, highly sophisticated operating environments, commercial computer chip developments, optical disks and fibre optics. Alternatively, in cases where development costs are high for a limited production base, or in which commercial spin-offs are not immediately evident, the military has developed technologies which have had, or will have, a significant impact on the commercial sector. Examples addressed in the symposium were GPS, inertial sensors, automatic landing systems, and integrated guidance, control and navigation systems.

The symposium was noteworthy in including a large proportion of papers from Russia and Ukraine, as Cooperation Partners under the terms of AGARD's Technical Cooperation programme. The subject of dual civil/military use was considered highly appropriate to the spirit of international cooperation that informs that initiative.

### PARTNERSHIP FOR PEACE

As an introduction to the symposium, Col. Ir Willem Kauw, Royal Netherlands Air Force, presented an overview of

AGARD's Technical Cooperation Programme.

The programme had its origins in the Declaration at the London Summit Meeting of 1990, of steps to adapt NATO's policies and objectives in the light of the changes that had taken place in Europe. In 1991, the Alliance furthered this process with its historic Declaration on Peace and Cooperation and the publication of a new Strategic Concept to bring NATO's overall strategy in line with future needs. The North Atlantic Cooperation Council was subsequently created, with membership from countries of NATO and the former Warsaw Pact, and a Military Cooperation Work Plan agreed.

The 1994 "Partnership for Peace Invitation," by the North Atlantic Council, went a stage further in expressing the desire for consultation and evolutionary eastward extension of membership to the whole of Europe. The PFP aims to achieve its objectives through bilateral agreements in areas of common interest, expressed through Partnership Work Programmes. AGARD's Technical Cooperation Programme aims to provide a catalyst for cooperative activities in the field of Aerospace.

AGARD's cooperation initiatives include co-sponsoring symposia with Cooperation Partners (for example, the Flight Safety Symposium at TsAGI in Zhukovsky, near Moscow in 1993), lecture series by Cooperation Partners for Western audiences, technical consultations, and invitations to participate in AGARD-sponsored activities, such as the present symposium. These activities are aimed at encouraging links with technologists and making knowledge of their skills and resources more widely available.

The present symposium provided an excellent example of participation by Cooperation Partners in an activity which represents one of AGARD's greatest strengths - the opportunities it offers for international communication at a working level.

### KEYNOTE ADDRESS

The keynote address, "Dual-Usage in Military and Commercial Technology" was given by Dr D A Rossi, Director of the US Navy Industrial Program in the Office of Naval Research, Harlington, Virginia. In his address he gave an overview of the Dual-Usage aims of the US Department of Defence and US Navy initiatives to meet them.

Dr Rossi first dealt with the separate, but related, issue of defence conversion. As he explained, the DoD perceives potential benefits from defence conversion by mitigating "defense drawdown impacts" through conversion of military production facilities and the creation of new jobs. At the same time, an initiative to develop an integrated commercial/

---

\* The Guidance and Control Panel was one of four AGARD specialist panels that have recently been replaced by three new panels. One of these new panels, the Mission Systems Panel (which embraces many of the interests of the former Avionics Panel and Guidance & Control Panel), held a symposium during the following week.

defence technology base will provide opportunities for Industry to augment already planned investment, funnel resources to specific geographical areas that need it, and focus additional R&D resources.

In meeting the DoD's aims however, the Navy faces the dilemma of satisfying the differently orientated goals of its main mission (to provide an adequate maritime defence) and the new mission of creating commercial jobs by a Defense Conversion programme. The Navy's solution is to adopt a bi-directional R&D paradigm, in which defence industry R&D spin-offs to commercial industry are matched by "spin-on" in the reverse direction, with additional collaboration in areas of mutually beneficial technology - in effect a dual-use approach.

Dr Rossi, outlining specific military/commercial steps being taken in pursuit of Defense Conversion, referred to the DoD Acquisition Reform process, recently initiated by the US Secretary of State for Defense, which supports the achievement of the twin goals of defence conversion/dual-use through its aims of removing MILSPEC barriers to the military utilisation of commercial equipment, and accepting commercial technical and accounting standards. Turning to the specific issue of dual-use, which Dr Rossi defined from a US perspective as

"the process by which DoD leverages the US industrial base towards affordable defense procurement by partnering with industry,"

he mentioned the cultural changes needed at the science and technology level to achieve leverage of S&T funds through economic development of emerging dual-use technologies, their relevance to Navy needs, commercial marketability, and the technical partnerships required between industry, academia and Navy laboratories. Military benefits were expected to follow from the development of new technologies, from assured access to existing commercial technologies in times of political stress (and in a form usable by the DoD), from increased DoD awareness of commercial opportunities and influence over commercial strategies to make DoD a smart buyer, and from preservation of DoD-critical industries by fostering new sustaining markets.

In pursuit of the US Navy's Industrial Program Mission, Dr Rossi described a number of initiatives whose combined effect is intended to enhance the Navy's warfighting capabilities. They include the Navy Dual-Use Technology Program, the Technology Reinvestment Program, Small Business Innovation Research, Domestic Technology Transfer, and Manufacturing Science and Technology (MAN-TECH) aims.

The remainder of Dr Rossi's address concentrated on the Technology Reinvestment Project (TRP) whose aim is to "stimulate the transition to a growing, integrated, national industrial capability which provides the most advanced, affordable, military systems and the most competitive commercial products". Its three elements of technology development, technology deployment, and manufacturing education and training, are being implemented through a phased programme of part-funded activities conducted jointly by six Federal agencies. The Department of Defense (ARPA) provide the lead, with involvement by the Departments of

Commerce (NIST), Energy, and Transportation, plus the National Aeronautics and Space Administration (NASA) and the National Science Foundation (NSF). All activities of the TRP must meet statutory requirements for competitive award, specific participation (with the emphasis on partnerships) cost sharing of at least fifty percent, and an emphasis on applicability to defence.

Dr Rossi completed his address with a review of the TRP activities to date. In 1993, 280 awards were made, selected from 2,800 applications (of which 5 were foreign) to a total value of \$465 million. It was interesting that approximately 50% of awards were to small businesses, and universities were also significant participants. The 1994 TRP competition, with a smaller budget, was more focused - mainly on IT/software plus specific areas of military interest such as uncooled infrared detectors.

In answer to a question, Dr Rossi confirmed interest in open system architectures for their potential to allow diverse systems to operate together - though security of modems remained a problem.

The Keynote Address was particularly interesting for its focus on specific Government programmes and their practical implementation. Dr Rossi also included the important and related US Defense Conversion plans. Though not originally highlighted as a principal theme for the Symposium (as reflected in the Introduction to this Technical Evaluation), his comments on the US Navy Defense Conversion programmes were particularly interesting in relation to the later Russian papers which showed somewhat different economic concerns.

## SESSION I - DUAL USE OPPORTUNITIES AND MISSIONS

The first paper, "Dual Use: Opportunities, Pay-Offs and Challenges," was delivered by one of the co-Chairmen of the Symposium, Dr Thomas B Cunningham of the Honeywell Technology Center, Minneapolis, MN, US. In addition to describing examples of the opportunities available, he emphasised the relevance of guidance, navigation and control technologists to non-military problems, the pay-offs from common military/civil solutions in terms of affordable military systems, and exploitation of commercial aviation technologies in particular for reducing military system development cost and timescales.

The civil spin-offs described were remarkable for their variety, ranging from drill bit navigation for off-shore oil facilities to automatic guidance of automobiles to ease highway congestion. Spin-on opportunities for the military were exemplified by the ring laser gyro which, through large scale use in civil aviation, had fallen in price by a factor of five or more in the last decade. Similar spin-on in electronics (though potentially a "gold mine") is however inhibited by differences in military and commercial environments, standards and specifications. The need for changes in military specifications and procurement practices was one of his key conclusions.

The other paper in Session I, "the Concept of the Space System Based on the SS-19 Missile for Direct Sounding of Large-Scale Natural Hazards" by V I Loukiatchenko et al of the Central Research Institute of Machine-Building

(TSNIMash), Kaliningrad (Moscow), RU, was at the opposite end of the spectrum of technology spin-off from the applications in Dr Cunningham's paper. He described a programme for utilising the "Rockot" SS-19 ICBM derivative for meteorological measurements with parachute-retarded weather radio-probes deployed from ballistic re-entry capsules. Two applications were described: the first having up to 50 probes for monitoring pressure, relative humidity, temperature, and wind velocity components in tropical typhoons; the second application, for monitoring ozone-depleted regions has up to 25 probes and provides additional ozone concentration measurements. The paper, in its direct approach to defence conversion through utilisation of military systems, raises major questions regarding the redeployment and funding of personnel, facilities and systems for productive civil use.

## SESSION II - NAVIGATION SENSORS FOR DUAL-USE APPLICATIONS

The first paper of the session, "Commercial usage of Navy Components Developed by CRI DELPHIN", was given by Prof A V Novgorodsky of the Delphin Institute, Moscow, RU. The motivation for dual-use of equipments was, like the previous paper, driven largely by the desire to retain skilled and valuable personnel in a climate of military procurement cut-backs. This has led the Institute to diversify into the development and production of equipment and instruments for oil and gas prospecting, extraction and transportation.

Prof Novgorodsky described examples of the precision equipment developed by the Institute, including a high performance dynamically tuned gyro, a miniature accelerometer and a torquer, together with a miniature gyrocompass, a compact heading and attitude reference system (which includes a GPS input mode), a non-gyro ship's roll, rate and acceleration measurement system, and a gyro inclinometer for oil well bore hole use. He also described the recent development of a gas-propelled projectile with strapdown INS position measuring system, for checking trunk gas pipes. In answer to questions on foreign sales, Mr Novgorodski cited interest from Western countries, particularly in the bore hole sensor system and in the gyro compass.

Next in this session was a joint effort by authors from the St Petersburg State Electromechanical University, RU, the Physikalisch Technische Bundesanstalt, Braunschweig and the Institut für Flugführung, DLR, Braunschweig, GE. The paper, "Some Results of International Cooperation in Military to Commercial Conversion of Laser Gyro Technology," and delivered by D P Loukianov, highlighted the fruitful cooperation in recent years between the three institutes, based on earlier separate pre-"perestroika" work in Russia and Germany in the field of high precision goniometry with laser gyro technology. The applications described included railway track surveying, measurement of deformation of long objects (ships, very large aircraft, etc.) and rapid, high precision, angular measurements of drift in inertial navigation systems. Work on the railway track surveying system is in partnership with the Deutsche Bahn AG.

The paper "Navigational Technology of Dual Usage" was delivered by Prof V G Peshekhonov of the Central R&D Institute "Elektropribor", St Petersburg, RU, a centre for R&D, Prototyping and Production of precision G&C equip-

ment. Like the previous speaker, he also stressed the economic importance to his Institute of finding civil applications for technology originally developed for military use. As an indication of the magnitude of change, military orders have reduced from a figure of more than 90% of its total production in 1961 to less than 50% in 1993.

Elektropribor's diversification of interests was indicated by the present breakdown of R&D as: IN systems 26%, marine navigation and control 30%, gravimetric systems 17%, wind power and electro-mechanisms 17%, and medical equipment 10% (in answer to a question, he said that 30-40% of funding was from Government). He described the "Marshrut" application of a marine INS to railway track monitoring and the parallel investigation of its application to inertial geodesy. He also described the "Chekan" universal gyro-stabilised gravimeter for ship-and-air-borne geological survey/prospecting (with measurement accuracies of 1 mGal or less in airborne applications, utilising GPS and/or GLONASS inputs) and the ECDIS electronic chart display information system.

The next paper, "Dual-Use Micromechanical Inertial Sensors," by John M Elwell Jr of the Charles Stark Draper Laboratory Inc, Cambridge, MA, US, followed a significantly different line from that of the three previous papers; the development of completely new technology aimed simultaneously at civil and military applications. He described the Draper Labs' work on micromechanical inertial sensors fabricated directly on silicon chips. The aim is to reduce the cost of inertial sensors and systems to a level that will facilitate their use in a wide range of commercial products, for example automobiles, cameras, toys, medical implants and so on.

The Draper Lab is essentially an R&D organisation and is teamed with the Rockwell Corporation for commercial exploitation of their work in this field. His projection of the relationship between price and market potential (as indicated by performance) suggested an order of magnitude reduction in the cost of rate sensors for each order of magnitude relaxation in accuracy - assuming equivalent production volumes: concluding that rate sensors produced in large volumes for the automotive market could be manufactured for less than 1\$ per axis.

The final paper in Session II, "Laser Gyroscopy Tendencies and their Analysis - Development in the Ukraine", was by Aleksander A Dovbeshko of the Research Institute of Mechanics Problems (RITM), Kiev, UKRAINE. Mr Dovbeshko's paper was mainly concerned with mathematical analysis, in which the Eastern European nations have traditionally been extremely strong. Unfortunately, assimilation of his presentation was severely hindered by lack of readable overhead projection vugraphs, reflecting the current - and one hopes, temporary - difficulties encountered by some authors from Eastern European countries in adapting to unfamiliar Western presentation methods and equipment. In the absence of a readable projection of his equations during his presentation or of a printed copy of his paper, it is not possible to make any useful comment on the authors' methodology, although the performance figures quoted for laser gyroscopic devices developed by the Institute were impressive.

### SESSION III - MULTI-SENSOR NAVIGATION APPLIED TO DUAL-USE

The first paper in Session III, "Low-Level Data Fusion for Landing Runways Detection," was by Laure Sliwa and Xavier Briottet of the Centre d'Etudes et de Recherches de Toulouse, ONERA, Toulouse, FR. Miss Sliwa, presenting the paper, explained the relevance of their work to both civil and military operations. Their low-level fusion uses electro-optical images essentially as measured, with no more than calibration pre-processing. She reviewed the theoretical background and analytical methods for correlation of data from different spectral bands (visible and infrared) at the pixel level, and showed results using different optimisation methods. With some a priori knowledge of surface materials, successful results have been obtained, demonstrating the advantages of pixel fusion in terms of real-time processing and detection of runways at long range with a wide field of view. In answer to a question, Miss Sliwa said that, despite the availability of GPS for accurately locating runways, multi-spectral electro-optical devices were of value in detecting runway obstructions.

The second paper, "The DLR Research Programme on an Integrated Multisensor System for Surface Movement Guidance and Control" by Dipl Ing Kurt Klein of the German Aerospace Research Establishment, was also concerned with both civil and military airfield operations. Although primarily a civil aviation issue, military aspects had to be included because of the interactions between civil and military air traffic. The work also makes use of techniques and system concepts originally developed for military use. The SMGCS research includes a variety of candidate sensors, including differential GPS and SSMR (Secondary Surveillance Mode Radar) Mode S, and data fusion techniques. The research activities are centred on an installation at Braunschweig Airport with a master station and peripheral measurement stations connected by a high speed fibre-optic data network. The derived situation information can then be downloaded to planning tools and to the DLR's control tower simulator. Integration into Air Traffic Management will follow as standards and architectures are developed.

The final paper in Session III, "Effects of the Specific Military Aspects of Satellite Navigation on the Civil Use of GPS/GLONASS," was delivered by Dipl-Ing Detlef Kayser of the Institut für Flugführung and written in conjunction with Prof Dr-Ing Gunther Schänzer of the Technische Universität, Braunschweig, GE. As Mr Kayser pointed out, satellite navigation is one of today's most promising infrastructure technologies, and offers improvements over terrestrial navigation in accuracy, coverage, availability, and system capacity. Nevertheless, despite their rapidly growing civil utilisation, complete acceptance of GPS and GLONASS for civil aviation and maritime use is hindered, in part by unsolved technical problems such as integrity, but also by limitations deriving from their military origins. After describing the history and background to satellite navigation he dealt at length with the military aspects - particularly the strong feelings aroused by the Selective Availability (SA) policy of downgrading the Standard Positioning Service (SPS) of the GPS system for users without access to specially authorised Precision Position Service (PPS) equipment.

The present limitations on civil utilisation can be overcome

by, for example, combined GPS/GLONASS receivers and differential GPS, but a strong commercial case can be made for a new system: from the multitudinous civil applications he cited the Hamburg container terminal which, in only one year, has recouped the cost of a carrier location system to keep track of containers. During the following discussion, he elaborated on the civil GNSS I/GNSS II programme which has gained European Union/ESA/Eurocontrol support with proposed funding under ESA's ARTES Element 9 for the first phase of up to 100 million Ecus. He also expressed the hope that domestic pressure might encourage the US Authorities to abandon SA coding.

### SESSION IV - DUAL-USE TECHNOLOGY FOR AIR/ GROUND OPERATIONS

The first paper in Session IV, "Heliradar, a Rotating Antenna Synthetic Aperture Radar for Helicopter Allweather Operations," was presented by W Kreitmair-Steck of Eurocopter Deutschland GmbH and written in cooperation with A P Wolfram of Deutsche Aerospace AG, Munich, GE. The technology of ROSAR (Synthetic Aperture Radar based on Rotating Antennas) is aimed at overcoming the limitations of conventional radar and electro-optical sensors for poor weather helicopter operations - particularly civil operations.

By mounting the antenna on the rotor blade, ROSAR achieves forward-looking high resolution SAR operation by sweeping the antenna field of view in an arc across the flight path at the rotor frequency. Mr Kreitmair-Steck reviewed the requirements for flight guidance by synthetic vision together with the basic principles of ROSAR, and concluded by describing the technical details of Heliradar and its proposed civil and military applications. In discussion, he quoted the effect on performance of antenna installation as the equivalent of 10-15km/hr reduction in maximum speed, though he expected this to be improved in further development.

The second paper, by Prof Y A Kozko and Dr V V Saveliev of the Institute for Precision Instrumentation, Moscow, RU, "Identification of Terrain Imagery with Unstable Reflectivity," was delivered by Prof Kozko. It dealt with the problem of statistical object identification from terrestrial images, obtained from airborne or spaceborne remote sensing in various spectral ranges, using comparison with idealised reference images. He reviewed several forms of recognition procedures or "classifiers" and outlined the difficulties encountered when the observed image deviated from the reference image due to differences in reflectivity arising from seasonal, weather, or illumination fluctuations, and, in the case of SAR imagery, random noise. He presented an analysis of a digital image model and recognition algorithms, from which an adaptive zonal SAR image model had been developed that has been confirmed experimentally.

The third paper, by Dr-Ing Thomas Jacob et al of Deutsche Aerospace AG, Ulm, GE, described an "Integrated Navigation and Landing System - a System for Autoland of Military and Civil Aircraft". The system combines GPS (using the civil C/A code) with an inertial measurement unit (IMU). A ground installation provides a reference for differential GPS operation, transmitted to the aircraft via a VHF/VOR data link, enabling the in-flight calibration of the

IMU by Kalman filter. This robust combination ensures integrity during GPS satellite masking and high accuracy - with measurement errors less than 1m. Flight tests have demonstrated the systems' ability to meet the requirements for autoland with or without a ground installation at the airfield itself. It copes with straight or curved approach paths and is suitable for any airfield, including unprepared military airstrips. When asked, Dr Jacob agreed that the system could function without the IMU but it is important for the integrity of civil operations.

The fourth paper, "Development and Application of the Methods for Pilot-Aircraft System Research to the Manual Control Tasks of Modern Vehicles," by A V Efremov and A V Ogloblin of the Moscow Aviation Institute, Moscow, RU, addressed the problem of the pilot-machine interface for highly-augmented aircraft, whether military or civil. Mr Efremov outlined the problems posed by the "superaugmented" aircraft that have appeared since the early 1980's and presented the results of studies of pilot control and physiological response characteristics, mentioning the development of a non-linear prefilter for the Buran aerospace vehicle and experimental determination of permissible pilot limits for maximum acceleration as a function of frequency. He then presented an analysis of flight control system (FCS) design and flying qualities, covering development of new dynamics/configuration standards and criteria and their use in vehicle design; particularly in overcoming FCS time delay effects on handling qualities, pilot psycho-physiological limitations, pilot induced oscillation (PIO) limits, and undesirable non-linear effects.

The fifth paper, "Successful Flight Testing of an Automatic Low Altitude Terrain and Navigation System - LATAN," by Horst-Dieter Lerche of Deutsche Aerospace AG, Bremen, GE, was a straightforward description of a system designed primarily for military low-altitude operations. The author reviewed the system design and architecture, which combines terrain referenced navigation and passive terrain following. The system, which utilises existing sensors and displays, (INS, radio altimeter, terrain following radar and display, navigation display, and HUD) has been proven in a Tornado demonstrator programme, including extreme manoeuvre conditions and clearance of discrete obstacles such as power lines and tv towers. In addition to the system's application to low altitude penetration of GA aircraft, it has potential in civil applications for obstacle avoidance and for controlled flight into terrain (CFIT), a situation that accounts for a large proportion of deaths in civil aviation. In the subsequent discussion the author cited NATO's Digital Mapping Agency as a principal source of terrain data and stated that the terrain following radar had been used during Tornado flight tests for integrity monitoring only.

The final paper of Session IV, "Application of Advanced Safety Technique to Ring Laser Gyro Inertial Navigation System Integration," was presented by James Blaylock of Lockheed Corporation, Fort Worth, TE and Donald Swihart, Wright Laboratory, Wright Patterson AFB, OH, US. Captain Chuck Stribula, Aeronautical Systems Center, Wright Patterson AFB, was co-author. Like the previous paper, it was concerned with a terrain following (TF) system - in this case for the F-16. The main thrust of the present paper however was the application of System Wide Integrity Management (SWIM), particularly in connection with the integration of

ring laser gyro INS units with the TF system. The SWIM technique, which originated in the AFTI F-16 AMAS programme and fully implemented in the F-16 TF programme, is based on the concept of functional self-test, embracing the total system, as distinct from the traditional self-test of individual subsystems (in answer to a question, it was stated that the system nevertheless identified failure at the LRU level). Major improvements in cost-effectiveness were claimed and the technique is expected to find applications in military and civil systems which demand high integrity - for example, ILS, ATC and autopilot control.

## SESSION V - DUAL-USE APPLICATIONS OF G&C TECHNOLOGY

The first paper in Session V, by W C Dolman and A M Ashdown of Lucas Aerospace, Birmingham, UK, with K J McCallion, Ministry of Defence, London, described "The Application of Ada and Formal Methods to a Safety Critical Engine Control System." The background to the work described by Mr Dolman was the UK MoD's identification of Ada as the single preferred high level language for real time operational systems from 1987: the HOLD (high order language demonstrator) programme was undertaken to demonstrate its practical application to a FADEC (full authority digital engine control).

The programme included in its aims the formal specification and verification of some components of the system in line with Interim Defence Standard 00-55 for safety-critical software. As Mr Dolman explained, there are difficulties in combining formal methods with high level languages which required a special approach. He described the software tools and development techniques, and concluded with the observations: a safe subset of Ada such as SPARK is essential, allowance has to be made in the system for the Ada overhead, and verification is limited to Ada source code level which puts a great emphasis on validating compilers, procedures and tools. During discussion, he agreed there was a problem with the accessibility of formal languages and a need for alternatives such as structured everyday language.

The second paper, by A V Nebylov, A P Vanayev and V V Chernyavets of the State Academy of Aerospace Applications," was concerned with sea wave parameter measurement at small altitudes/clearances and the control of ships, wing-in-ground-effect (WIG) craft and seaplanes. Mr Nebylov described applications to the "Ekranoplane" class of over-water WIG vehicles, which "fly" clear of the surface, utilizing wings of moderate aspect ratio operating in the aerodynamic ground effect regime to minimise lift-induced drag. Projects include the "Orlyonok" 140 tonne vehicle capable of 450km/hr, and an assault amphibian development. Second generation projects are expected to be economically competitive with conventional seaplanes.

The work on sea wave measurement and control has also been applied to hydrofoil craft such as the Taifun. He described in detail a controller based on a three-dimensional seaway model derived from two-dimensional wave components measured by phase radioaltimeters. He expressed the hope that the work, aimed at practical seaway operation of displacement and non-displacement craft, could be a proving ground for international cooperation based on Russian non-commercial applications, supported by a strong theoretical base, and Western commercial product strengths.



In answer to a question regarding the extent of GEV/WIG vehicle development in Russia, Mr Nebylov, replied that there were some thousands of such craft, as shown in Janes'.

The third paper of the session, "GPS-Based Navigation for Space Applications," by C Champetier, T Duhamel and M Frezet of Matra Marconi Space, Toulouse, FR, was interesting as the only paper that dealt with satellite-based navigation applied to space vehicles, rather than terrestrial vehicles. Mr Duhamel, after surveying various approaches, presented an analysis of four different applications: autonomous navigation for geostationary spacecraft; relative navigation for rendez-vous; differential navigation for landing vehicles; and absolute navigation for launchers and re-entry vehicles.

The authors' examples demonstrated some unusual techniques: in the case of absolute navigation, use is made of single sequential measurements in a hybridised orbital model while, in the case of relative navigation, measurements transmitted from one vehicle to another are processed in a model of their relative dynamics. The geostationary spacecraft application, exhibiting totally different orientations from terrestrial applications, involves special consideration of earth ionospheric effects. In conclusion, the authors claim to have demonstrated the usefulness of GPS navigation for many space missions and the improvements in performance, autonomy and costs relative to other forms of navigation. They anticipate that experiments and commercial utilisations in the pipeline could result in it becoming the future preferred system for space navigation. The ensuing questions and clarifications were indicative of the unfamiliarity with the special requirements of space applications by many of the delegates.

The final paper, "Integrated Special Mission Flight Management for a Flight Inspection Aircraft," by A Redeker and M Haverland of Aerodata GmbH, Braunschweig, GE, was concerned with flight inspection operations for ATC using specially instrumented aircraft. Mr Redeker, showed illustrations of FIS (flight inspection system) installations in HS748 and King Air aircraft, mentioning the utilisation of existing aircraft equipment together with the additional FIS elements, and on-line presentation of results. He pointed out that the move towards privatisation of ATC was likely to lead to a greater drive towards improved air inspection efficiency. In this context, size reduction as well as improved system effectiveness is important: the aim for the future is to replace four existing HS748 aircraft with two, much smaller, King Air 350s. International cooperation is also an important issue in terms of regulations and increasingly involves Eastern European countries. The effects are being seen in increasing international sales prospects for the system, leaving aside the USA and Russia, which both have flight inspection fleets.

#### ROUND TABLE DISCUSSION

The discussion opened with some observations on the absence of contributions from the military side - apart from the Keynote Speaker - in comparison to the many papers on dual-use from research institutes and commercial companies. Although the Technology Reinvestment Programme involves significant expenditure by the US, the Symposium had revealed very few examples. Nevertheless, as Dr Rossi pointed out, the effects of US defence downsizing (30-50%),

first on personnel and then on infrastructure, is encouraging a focus on readiness and supporting technology investment and, although being scaled down somewhat, the TRP will be producing results in about two years time.

The human aspects of downsizing were raised by Prof Novgorodsky: academics, scientists and technicians, previously employed on military-aligned activities, must now find alternatives. The negative effect on student intake was also a serious problem - student exchange with the West was potentially valuable in this context. It was generally agreed that, although in the past the extent of military-orientated post-graduate studies had been limited in Western countries, it could be advantageous to encourage such a trend.

A question was raised regarding the influence of standardisation on dual-use, particularly the growing relative importance of commercial, as distinct from military, specifications and standards. For example, the ARINC 650 standard for modular avionics was already being applied while equivalent MILSPEC development was moving slowly. This might lead to a situation where the military would be forced to follow the ARINC standard. International standardisation was an important area where there had been much success in the commercial world. In comparison, it was stated that some 80% of NATO STANAGS had never been applied. It was expected that Industry will set de facto standards, driven by cost considerations in the commercial, industrial, domestic, and games markets, which the military would then adopt - as for example with the VME bus and backplane architectures. In this connection there were some reservations expressed regarding the danger of single-supplier dependency which demanded greater emphasis on open standards.

The need for coordinated international activity was particularly apparent in pervasive developments such as GPS/GLONASS, though the difficult question of international control arises. It was suggested that satellite navigation systems and standards might eventually be determined by the market, as had happened with mobile telephone networks. Lower cost solutions than the military systems, such as Motorola's proposal for a very low orbit system, could facilitate this process. History suggested that it was only a matter of time before civil use developed independently of the military, as with earlier "advanced" technologies such as radio. While a potential danger was recognised from terrorist/criminal use of widely available low-cost precision navigation, it was conceded that this would not be avoided merely by delaying commercial development.

The round table discussion concluded with further examples of dual-use and its implications, concentrating on the civil use of military technology. They ranged from instrumented prosthetic devices, electronic "guide dogs" (it was stated that Germany for example had some 60,000 blind persons but only 2000 guide dogs) to railway train management systems. In considering the practical limits to this process, it was claimed there were few areas of military technology that do not have potential for civil use: examples were cited of the US manufacturer of warhead fuzes now involved in automobile safety air-bag development and manufacture, and military engine health monitoring systems applied to civil buildings. The general feeling in regard to civil conversion was positive and it was pointed out that, not only products, but also skills and resources have the potential to be

re-directed. In addition it is becoming clear that the proportion of governments' funding on civil R&D is rising, relative to military R&D.

### CONCLUDING REMARKS

It is necessary first to recognise the valuable contribution made to this symposium by authors from the Cooperation Partner countries. The subject and theme were highly appropriate to East-West cooperation and revealed deep common concerns at the effects on people and facilities of military downsizing, plus the potential rewards from technology spin-off. Two Russian papers, dealing directly with the civil application of systems developed for military purposes, also touched on the maintenance of technological expertise: their subjects were; the conversion of the SS-19 ICBM for weather monitoring, and G&C aspects of the unique Russian Ekranoplane wing-in-ground-effect vehicles.

The other major concern of the symposium, the maintenance of a military technological capability, was highlighted by the Keynote Speaker, Dr Rossi, in his review of the US Navy's programmes for Defense Conversion and Technology Reinvestment. It is too early to assess the practical benefits of such planned joint Government/Industry investments, but in the meantime the unplanned commercial exploitation of "military" technology is already making a major impact on manufacturing costs with potential benefits for military procurement. Order of magnitude reductions in the cost of ring laser gyros achieved over the last decade through widespread civil aircraft use, and the potential for extremely low cost commercial micromechanical inertial sensors, are two striking examples quoted. Utilising commercial products for military systems poses some difficulties however; the main one being the differences between military and civil standards and specifications. Some of these differences are admittedly a consequence of dissimilar operating environments but there is still plenty of room for applying MILSPECs with more flexibility as proposed in the recent initiative of the US Secretary of State for Defense.

A quite different problem was raised in regard to the civil applications of satellite navigation. The civil use of GPS is expanding extremely rapidly, as evidenced by the examples in the paper by Kayser and Schanzer on the "effects of specific military aspects ----", and the paper by Champetier, Duhamel and Frezet on space applications. However, the deliberate degradation of accuracy imposed on civil users by the GPS SA coding is a deterrent to wider use, despite the ingenuity displayed in circumventing the problem by differential GPS navigation and the potential of dual GPS/GLONASS receivers which make use of the different coverage and orbital characteristics of the US and Russian systems. There is a clear need for international coordination of satellite navigation as for example in the collaborative European studies, though there was some interesting speculation on the possibilities of commercial systems.

Although not directly relevant to dual-use, the symposium also provided opportunities to compare the different approaches of Eastern and Western nations in guidance and

control. For example, significant differences of detail surfaced in areas of INS technology, a subject that featured largely in the symposium: this was especially true of ring laser gyro design issues such as the use of Faraday or Zeeman biasing rather than mechanical dither, and RF excitation instead of high-voltage DC discharge. There also appeared to be a difference in emphasis in the greater number of theoretical papers from the Eastern Cooperation Partner countries. This may have been due to a proportionally greater representation by academic institutions but in any case is indicative of a strength in applied mathematics.

The dual-use significance of guidance and control was well demonstrated by the symposium, including the important subject area of civil and military air traffic operations, management and control, which reflects a long-standing interest by the GCP. Papers were presented on runway detection, landing aids, terrain navigation, and ATM/ATC inspection systems. In other fields, examples of dual-use opportunities ranged widely from the use of existing G&C equipment in oil drilling and gas pipeline applications to new techniques such as the Heliradar forward-looking synthetic aperture radar for poor weather navigation of helicopters. In the field of multi sensor data processing and software applications generally, papers revealed common military/civil interests in high integrity systems. Software integrity was a problem addressed directly in a paper on a research/demonstrator programme for a full-authority engine control system which gave an outline of the problems of combining a high level language (ADA) with formal methods for software generation and verification, together with an approach to resolving them. This is an important subject which demands greater attention, as does modular avionics architectures, in which the civil aviation ARINC standards appear to be leading the way.

Several important general needs emerged from the symposium. They are:

Effective international collaboration to achieve a universally acceptable high-integrity satellite navigation system. In the meantime there are strong commercial pressures to "switch off" the SA coding of GPS.

Improved awareness - particularly in Western nations - of the wealth of expertise available in the Cooperation Partner nations. Student exchanges could assist this process.

Increased compatibility of civil and military aviation/electronics standards and specifications, including relaxations in applying MILSPECs and the adoption of civil standards where appropriate.

In conclusion, the symposium was very successful in achieving both its aims: it provided a comprehensive forum for dual-use technology in guidance and control, and it was a valuable example of East-West cooperation, pointing the way for similar initiatives by AGARD in the future.

# Dual Use: Opportunities, Payoffs and Challenges

Thomas Cunningham  
Honeywell Technology Center  
3660 Technology Drive  
Minneapolis, Minnesota 55418  
USA

## 1. Summary

Significant payoffs can be achieved by increasing the interaction between military and commercial business and technology communities.

This paper describes a few of the opportunities available to practitioners of guidance, navigation and control technologies to work in this dual use world. Examined from the point of view of an engineer who has been solving primarily military problems, it is hoped that the NATO AGARD reader as well as our new friends from the Cooperating Countries will benefit.

The paper emphasizes three major themes:

1. Guidance, Navigation, and Control (G, N, and C) technologies and engineers are highly qualified to solve important non-military problems.
2. The use of common solutions to commercial and military problems, from components to systems, has significant cost payoffs to future affordable military systems.
3. Commercial systems, particularly aviation, offer technology advantages which should be exploited for affordable non-recurring developments and reduced cycle times in future military systems.

- Experiences over decades with custom parts and rigid specifications result in systems that are expensive to repair and maintain.

With these issues in mind this paper describes opportunities for G, N, and C companies to find profitable ways to use their core competencies, and better prepare for scaled back, much more affordability-driven military markets.

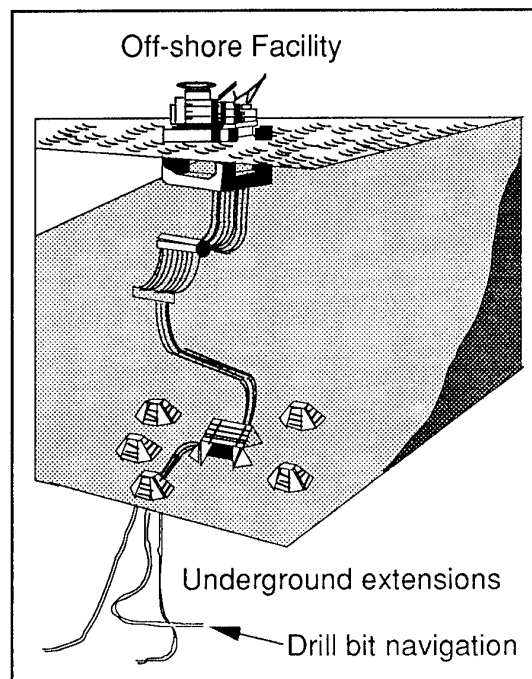


Figure 1. Oil Drilling Navigator

## 2. Background

Payoffs for developing and exploiting dual usage have always existed, however recent events mark a significant rise in these benefits:

- The dominant users of new technology have shifted from the military to the commercial sectors.
- The reduced tension of major military powers resulting in scaling back of arms places much more emphasis on affordability in weapon systems.

## 3. Spin Off Opportunities in Guidance, Navigation, and Control

With the shift away from military emphasis, the need to shift to commercial payoffs for technology developments is key to the economic success of NATO countries. The G, N and C community has impressive skills to offer the commercial sector. Navigation, in particular, offers good potential for spin-offs.

Automotive applications of GPS coupled with digital map displays are being developed to

provide low-cost personal navigation. Use of inertial information overcomes multipath problems of GPS in cities.

Another application of inertial navigation is in oil well drilling, shown in Figure 1. Business issues and financial payoffs drive high accuracy requirements. The drilling temperature and vibration environment could provide engineers with a far greater technical challenge than aerospace applications.

Machine tool alignment is another application. Working in vibration over long periods of time, machine tools, such as milling machine heads, could benefit from automatic realignment based upon inertial sensing.

Exciting opportunities exist for guidance and control technology applied to automatic cars and

automated highways. Displayed in Figure 2., a concept for an automated highway system poses clear challenges and very difficult technical problems.

A major benefit to the public will be closer spacing of traffic which increases the capacity of roadway systems without adding more concrete highways. Because of safety implications from such close spacing, vehicles using automatic driving systems will deal with some familiar problems:

- Hands and feet-off driving. Faults must be contained and vehicles continue to operate:
  - within narrow highway widths
  - in high traffic volume conditions
  - at high speeds
  - in very close proximity to other vehicles and barriers

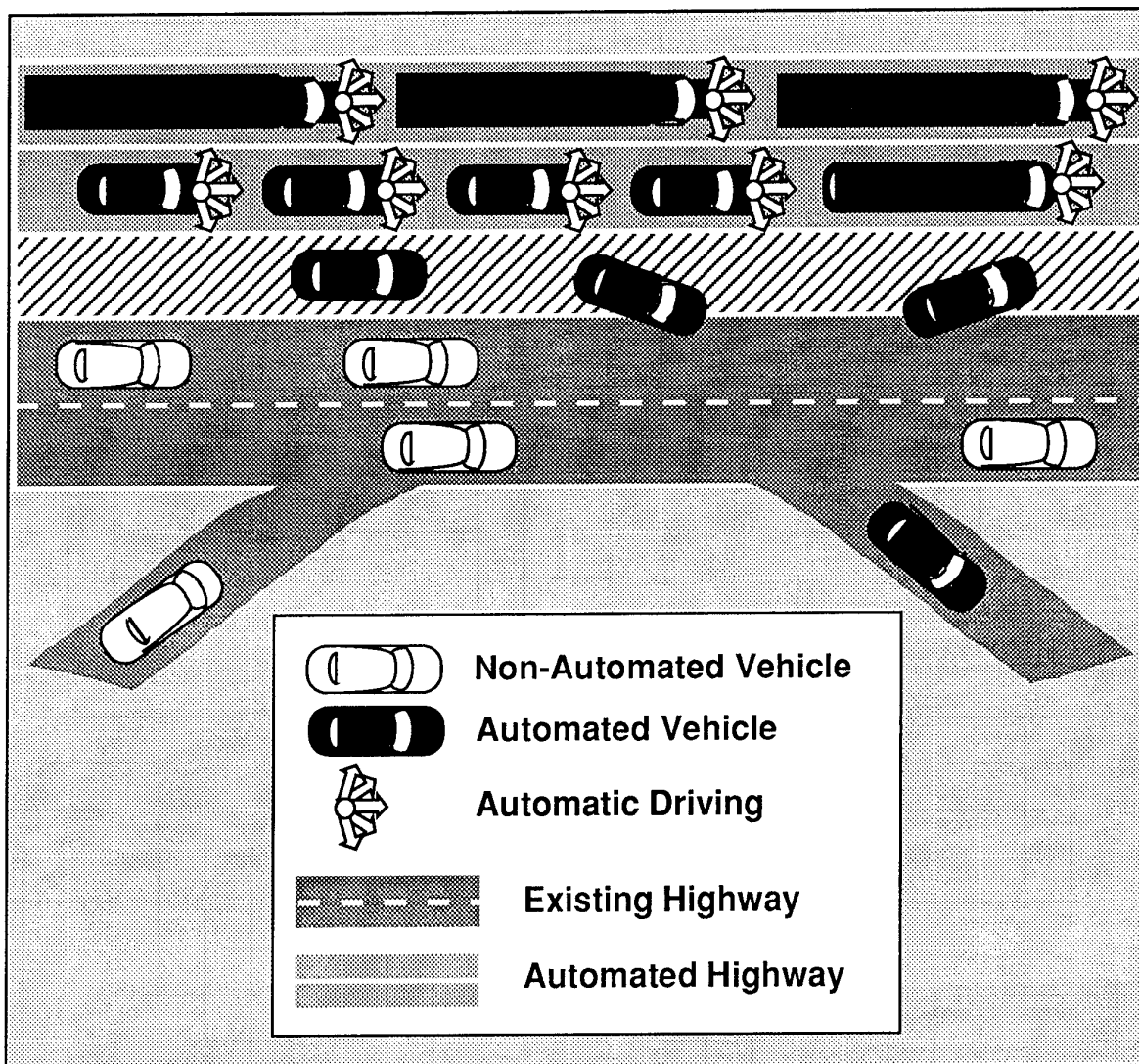


Figure 2. Automated Highway System

- Driver fault recovery limits
  - Human response time limitations
  - Limited or non-existent situation awareness
- Fault tolerant sensors, actuators, computers, communications components, and software.
- A thorough system checkout (BIT) phase prior to entry onto the automated highway and an operator effectiveness assessment prior to exit.
- A complete failure tolerant highway traffic control system which is robust to a complex set of accident, weather, and aging situations.

An ongoing study currently projects an on-vehicle redundant positioning control system must have a probability of accident of  $1 \times 10^{-6}$  per hour of driving. Engineers who design aerospace controls systems are very familiar with these types of fault tolerant requirements.

Besides automated highways, there are other opportunities for fault tolerant concepts to be applied. Within the aerospace community, application of military technology to commercial aerospace has produced significant results in the past ten years:

- Commercial transport fly-by-wire controls have been using military technology in the A-320 and Boeing 777 aircraft designs.

- The Boeing 777 integrated avionics concept, Aircraft Information Management System (AIMS), has used basic fault tolerant and automated maintenance concepts from military aircraft R&D<sup>1,2</sup> developments.

Other application opportunities include:

- Feedback controls in automobiles to provide stability augmentation for less stable modes of driving, e.g., torque steering skid control.
- Automated buses could be the ground transportation equivalent of a fly-by-wire aircraft providing additional cost savings in fuel and increased passenger capacity.
- Extensive application of current G, N, and C technology to civil helicopters will enable wider use in urban transportation with fault tolerant assurances for safe controlled flight into terrain.

#### 4. Spin On Opportunities

Because of technology issues of affordability and availability in the future, military systems must make maximum use of commercially available technology and production commonality.

The Ring Laser Gyro (RLG), A Common Product - One historical case demonstrates the payoffs that can be achieved through effective use of common technology and production. The RLG development and its application to a number of commercial and military systems has

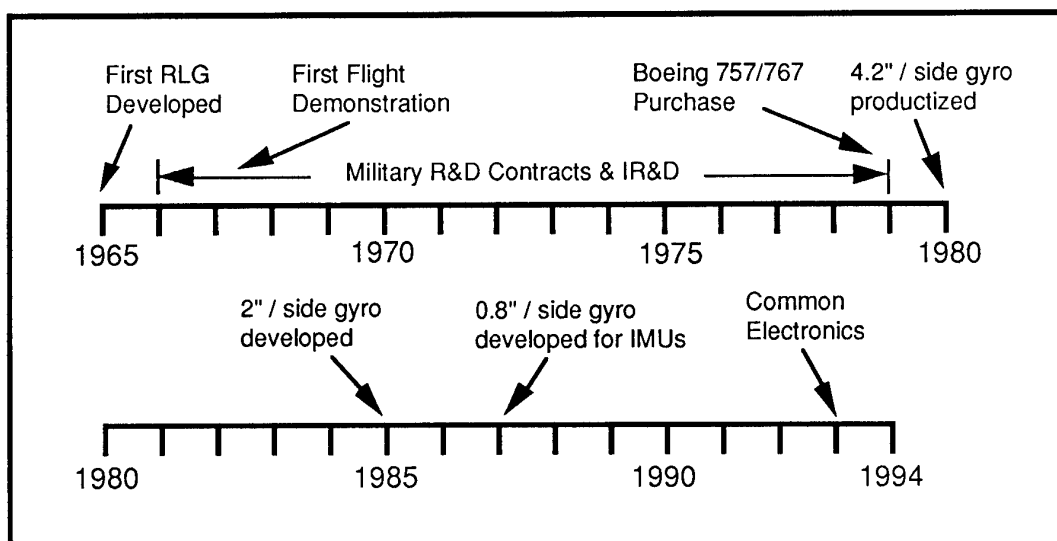


Figure 3. Honeywell RLG Technology Development History

provided impressive cost savings to both communities.

Looking at the history of the RLG technology development at Honeywell, Figure 3., shows the lengthy development period and improvements of the RLG. The emphasis, indeed, the vast majority of the funding and technology pull, came from military funded programs and government recovered internal research and development (IR&D). Most of the payoff applications in the 80's came in the commercial

most important opportunity for dual use spin-on.

Electronics. The Dual Use Gold Mine - The largest area of untapped cost savings is creation and application of common commercial and military electronic parts and systems. The savings in recurring costs should be similar to the cost savings associated with the RLG. The challenge is to overcome decades of methods and experiences the military had with specifications, industry practices and certain technologies.

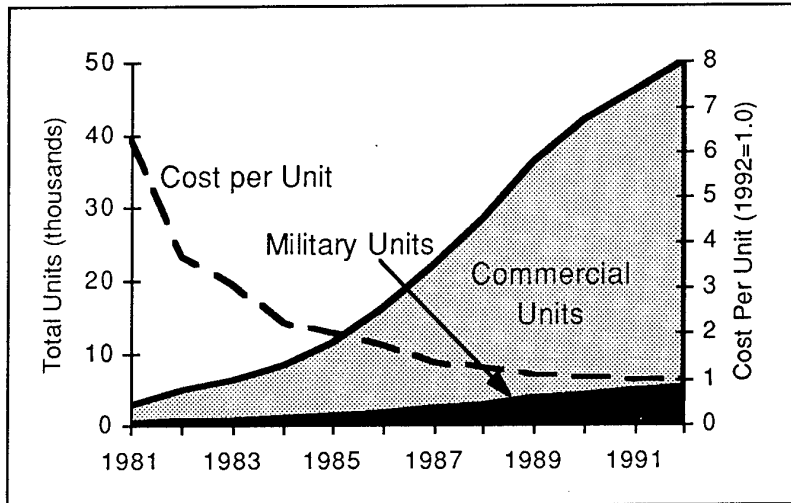


**Figure 4. RLG Production History and Cost Trend**

transport business.

The payoffs to the military is the cost leverage shown in Figure 4.

Although the ratio of commercial to military production volumes are roughly 9 to 1, all customers benefit from the recurring cost savings of common production. This case demonstrates nothing more than simple cost/volume learning curve concepts.

Benefits demonstrated by the common RLG production were achieved for the basic sensor block. The RLG control electronics costs have been borne by individual customers based upon distinct requirements for commercial versus military use. The impressive cost savings demonstrated by the sensor block assembly, therefore, have not been achieved in the electronics portion of the RLG or inertial systems in general. This is the

To illustrate the differences in practices and technologies, Figure 5. shows the reliability of electronics developed by military versus commercial requirements. The case described contains a number of development distinctions:

- The hermetic curve illustrates military practices and specifications
  - Rigid Mil Spec inspection of all parts
  - Designed for high reliability
  - Expensive manufacturing
  - High cost per part due to low volumes
  - Few suppliers
- The non-hermetic curve refers to plastic parts using commercial practices and procedures.
  - Commercial statistical process control
  - Designed for high reliability
  - Low cost manufacturing
  - Low cost per part due to high volumes

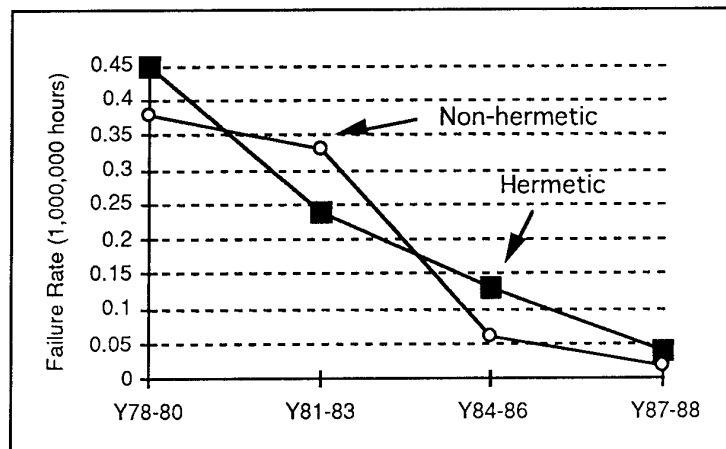


**Figure 5. Military versus Commercial Parts**

- Many suppliers to guarantee availability

Remarkably, over time, the commercial products have proven to be as reliable as the military products.

In recognition of this kind of performance, the U.S. Secretary of Defense, William Perry, recently announced a bold new initiative concerning the use of commercial parts and practices. The following statement is part of this initiative:

***Military specs and standards: Performance specs shall be used when purchasing new systems, major modifications, upgrades to current systems, and non-developmental and commercial items for programs in any acquisition category,...the use of mil-specs and standards is authorized as a last resort with an appropriate waiver.***

In anticipation of these changes, a recent development in RLG's at Honeywell added a self

**Fault Tolerant Architectures - Dual use returns to the military** - Some technologies have crossed the military to commercial boundary and have been further developed. The results of commercial investments should be examined for a form of "Spin back" to the military. In the aerospace G, N, and C community a list of technologies would include:

- Flight management
- On board maintenance
- Flight controls and displays
- Fault tolerant navigation
- Fault tolerant architectures

Although, all of these topics are worthy of discussion, focus on architectures will yield significant savings in recurring and non-recurring costs to the military.

Two examples of integrated modular avionics have been developed recently, the F-22 fighter avionics and the Boeing 777 Aircraft Information Management System (AIMS). The F-22 is characterized by the following features:

- Functions
  - Electronic Warfare
  - Radar
  - Controls & Displays
  - Com/Nav/Ident
  - Inertial Reference
  - Stores Management
- Cabinet Architecture
  - Backplane Bus - Pi Bus
- Common Modules with functional separations
- Multiple 1553 Busses
- Vehicle Management System (VMS) separated for fault tolerance

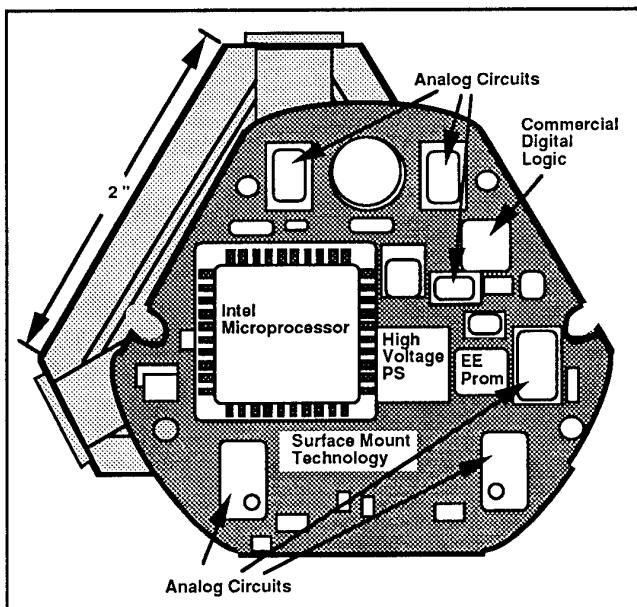


**Figure 6. Digital RLG Electronics**

contained sensor electronic package collocated with the sensor block. This design uses commercial practices and parts to the maximum extent allowable. This concept, illustrated in Figure 6., creates a self contained digital gyro (Dig-Gyro™ RLG) applied to the common commercial and military customer base.

The AIMS architecture followed the F-22. Pave Pillar concepts were also followed for the basic design philosophy of common modules. The AIMS design is distinct from the F-22 as follows:

- Functions
  - Displays (including graphics generation)
  - Flight Management (incl. Auto throttle)
  - Central Maintenance
  - Communication Management
  - Airplane Condition Monitoring

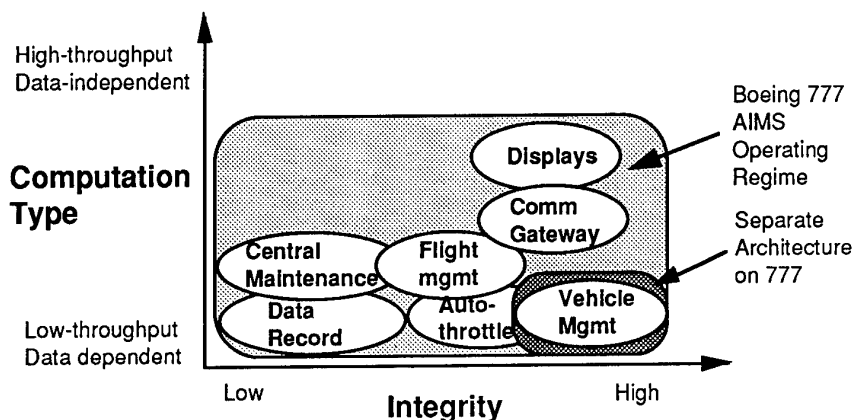


**Figure 7. Boeing 777 Integrated Avionics**

- Flight Data Recorder Interface
- Data Conversion Gateway
- Quick Access Recorder Interface
- Cabinet Architecture
  - Backplane Bus - SAFEbus™
- Common Modules with multiple criticality levels
- Fault-Tolerant ARINC 659 Bus
- Vehicle Management System separate

AIMS architecture incorporates extensive fault tolerance in the basic design. Developed under Air Force R&D funding<sup>1</sup>, a key element of the AIMS fault tolerance is the backplane Bus - SAFEbus™.

Another way to describe the AIMS function is shown in Figure 7. Although the architecture did not include the VMS, the integrity requirements of the communications gateway and display functions require high integrity ( $1 \times 10^{-8}$  failure probability per flight hour).

Neither architectural concepts include the high integrity functions of the Vehicle Management System, which typically contains flight control and navigation. The F-22 integrated avionics concept was not designed with sufficient fault tolerance to include the flight-critical VMS. Unlike the F-22, however, the Boeing 777

The application of new fault tolerance experiences on the Boeing 777 design should be exploited in the next generation military design for the VMS. This would bring the Pave Pillar/Pave Pace payoffs to the VMS with the associated cost savings. The functions that could be addressed by an AIMS like concept are shown

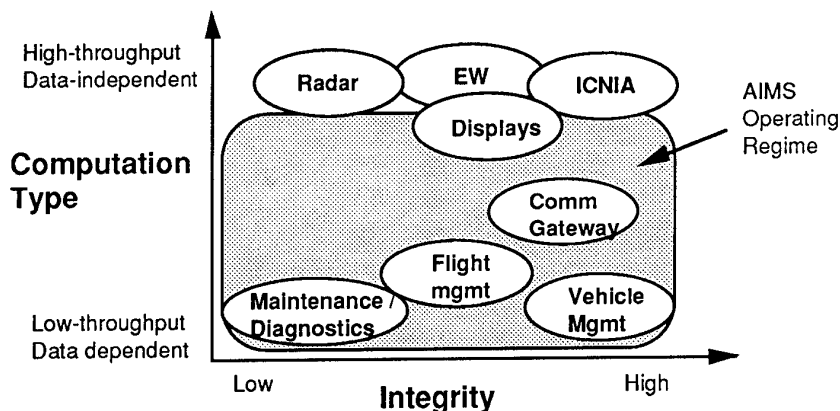


**Figure 8. Next Generation Military Fault Tolerant Integrated Avionics**



in Figure 8.

## 5. Conclusions

This paper dealt with a number of opportunities and challenges for the guidance, navigation and control community for dual use in commercial and military applications.

The military G, N, & C engineer can make enormous contributions to the commercial world. Examples cited relate to the ability of such engineers to solve very difficult problems dealing with harsh environments and high integrity designs. The G, N, and C designer is uniquely qualified to attack these problems and the military companies employing their skills can create profitable businesses in these areas.

Future military systems will require fundamental changes in design, manufacturing and product specification in order to be affordable to procure and maintain over the life cycle. Use of commercial technology has been shown to significantly reduce non-recurring development costs and schedule. Common use of parts and practices from the commercial world has a huge impact on recurring costs.

NATO countries must make fundamental changes in specifications and procurement practices to achieve these savings.

## References

- <sup>1</sup> K. Driscoll, G. Papadopoulos, S. Nelson, G. Hartmann, G. Ramohalli, Multi-microprocessor Flight Control System, AFWAL-TR-84-3076, September 1984.
- <sup>2</sup> P. Bursch, J. Meisner, M. Jeppson, Flight Control Maintenance Diagnostic System, Wright Laboratory TR-93-3022, March 1993.
- <sup>3</sup> *Military & Aerospace Electronics*, Vol. 5, No. 9, August 1994.

# THE CONCEPT OF THE SPACE SYSTEM BASED OF THE "ROCKOT" LAUNCH VEHICLE OF LIGHT-WEIGHT CLASS FOR DIRECT SOUNDING OF LARGE-SCALE NATURAL HAZARDS

V.I. Loukiachtchenko

G.A. Tsybouskii

Central Research Institute of Machine Building,

Kaliningrad, Moscow region, RU

A.K. Nedaivoda, V.K. Karrask, A.A. Medvedev

N.A. Meliankov, S.N. Philosophov

Design Bureau "Salyut" of Khrunichev SRPSC, Moscow, RU

V.P. Karmasin

NPO "Typhoon" Obninsk, RU

## Summary

The report contains the description of proposal on development and using of space system intended for direct (contact) exploration of such natural hazards as, for example, tropical cyclones or ozone hole which are heavy influencing on humanity life activity.

This system would be developed on base of Russian (former Soviet) SS-19 ICBM, which should be removed from battle duty according to the START Treaty. Recently developed on base of that ICBM Russian "Rockot" launch vehicle can deliver with high accuracy to hazard region up to 50 reentry probes which should transmit the information through space, airborne or sea retransmitters. That efficient collection of information on atmosphere conditions in altitude range of 40...0 kilometers should be the effective tool for investigation of large-scale natural phenomena which are very dangerous for people and economics of Earth.

## 1. Introduction

Tropical cyclones (or typhoons, hurricanes) are one of most destructive natural phenomena. Annual loss caused by them to economics of tropical zone countries is 6-8 billions USD on the average.

The main destructive factors when the tropical cyclone (TC) reaches the land are a heavy precipitation (up to 500 mm/day) and entailed it floods; a strong wind (up to 80 m/sec); a storm rising tide onto sea-coast and a destruction of coast buildings by waves.

A reduction of damage caused by typhoons is possible at first of all owing to a rise of accuracy of typhoon shift and intensity forecast.

The accurate forecast for time and location of typhoon reaching the land made two days before will let to take necessary preventing measures exactly at that (sea-coast zone with width of 250-300 km) where the maximum destructions are possible.

At present the accuracy of that forecast for the TC's center made one day before is 400 km, made three days before is about 700 km.

It is necessary to note that this error has not been reduced during two recent decades in spite of all achievements in a creation of more and more complex numerical models for the TC and

it's displacement, a development of satellite meteorology and a using of technological innovations.

The main reason of that statement is an absence of clear understanding for physical processes and mechanisms which are determining both TC itself evolution and it's interaction with surrounding atmosphere and laid under it surface.

In it's turn, an absence of clear understanding for the physical nature of TC is connected first of all with a shortage of experimental data on the parameters of atmosphere in TC and around it with the dispersion of 20-30 km by horizontal line and 300 m by vertical line.

The modern methods and means for a receiving of experimental data on tropical cyclones (the measurements by special aircrafts-laboratories; the aerological measurements from island and coastal stations and also from ships (episodically); the satellite measurements, mainly from geostationary satellites) are not able to provide a receiving of such information.

An appearance of the "ozone holes" in the higher layer of atmosphere is the natural phenomena which is not more less dangerous by it's consequences.

The atmospherical ozone is a natural protection for all animate nature of the Earth against the influence of hard ultra-violet Sun radiation. Even small decrease of ozone content in atmosphere leads to a unhealthy influence for people.

The discovery of "ozone hole" above Antarctic Continent in 1985 was a stimulating incitement for international investigations of that phenomena. Today the investigation of Antarctic "ozone hole" and determination of it's appearance initial reason are the central link of ozone investigations of whole world's commonwealth.

At present there is no a monosemantic understanding for this phenomena till now, first of all because of an absence of sufficient experimental data, a receiving of which in the Antarctic Continent environment (especially in polar night) is connected with great complications because of difficulty of access into the region of investigations and it's severe natural environment.

In accordance with the theory accepted at present time, the main reason of ozone anomaly appearance is a throwing out of chlorine-fluorine-carbons into the atmosphere.

The total volume of world's output for chlorine - fluorine - carbons (trade names - freons, arctons, eskimons, khladons) is reaching of 1 million tons per year.

The practical measures, which are consequences of the hypothesis about destructive influence of chlorine - fluorine - carbons to ozone layer, require a sharp shortening of chlorine - fluorine - carbons production and using, that is connected with very high financial expenses.

It is necessary to take into account that the Antarctic ozone anomaly is formed in polar night when the modern means and methods for a measurement of ozone concentration would not be used.

The common feature for an investigation of such large - scale nature phenomena as tropical cyclones and ozone holes is a necessity in receiving of the detail information on atmosphere parameters (the temperature, humidity, pressure, wind velocity, ozone concentration) along whole large - scale volume of investigated phenomena (for a typhoon: the altitude - from 0 up to 25 km, the diameter - up to 500 km; for the Antarctic ozone anomaly: the altitude - from 5 up to 40 km, the diameter - up to 5000 km) practically simultaneously (during the time about 1 hour) at all points of measurement while the structure of typhoon or "ozone hole" can be assumed as stationary one.

The proposed by "Salyut" DB of Khrunichev State Research and Productional Space Center (SRPSC) and Central Research Institute of Machine Building (TsNIIMASH) experimental space - rocket complex for investigation of tropical cyclones and ozone anomalies lets to make up the existing deficiency in system of collection of experimental data on parameters of atmosphere inside TCs and the ozone layer.

The received by it's using experimental data will let to take the unique science - capacious information which in connection with the data received by other means of measurement will make deeper the understanding of physical nature of processes, which are occurring in tropical cyclones and ozone layer and will raise an effectiveness of methods for a counteraction against these dangerous nature phenomena.

The studies carried out in the "Salyut" DB of Khrunichev SRPSC have confirmed the technical passibility for creation of space - rocket complex intended for contact sounding of tropical cyclones and ozone layer. This complex should be developed on base of the "Rockot" launch vehicle and will use the equipment of "Scut" or "Orbita" telemetry systems for a collection of information from meteorological probes and the GLONASS satellite navigation system for a determination of probes coordinates.

The "Salyut" DB of Khrunichev SRPSC together with "Typhoon" Research and Production Corporation (NPO) has the experience of development and operation of the key elements for space - rocket complex (launch vehicles, spacecrafts, reentry capsules and means for their pulling apart, means for collection and processing of information) and also the means and methods for a measurement of parameters of tropical cyclones and ozone concentration in

the atmosphere (the sensor equipment, ejected and aerostatic meteorological probes).

## 2. The review of modern means and methods for tropical cyclones investigation

At present time, in spite of enormous volume of accomplished theoretical and experimental investigations, there is still no an understanding of physical processes and mechanisms inside TC, which is necessary both for exact forecast of it's movement and intensity and for development of conteption for it's artificial relaxation.

The main sources of experimental data on TC and surrounding it atmosphere are at present the followings:

2.1. The measurements by special aircrafts - meteorological laboratories, including the measurements at the centre of TC. The turboprop aircrafts (P-3 Orion, C-130 Hercules, Il-18, An-12) having a cruise speed about 400 km/h are used for this mission.

The information is collected by contact sensors, on-board meteorological radars and other equipment, including ejected airborne probes. A duration of research flight is in average 3-4 hours, a maximum altitude is no more than 6 km. The measurements are performed mainly at the TC's central zone having a radius of 150-180 km. During TC's approach to the land 1-2 flights per day are performed.

The aviation investigations of TC's are most informative ones, however they have two significant limitations. First of them is connected with the maximum altitude of flight - only one third of total TC's height is investigated, although this height is investigated in details. The second limitation is connected with the fact that it is wrong, in general, to assume that the TC's characteristics and structure would be stationary ones during 3-4 hours because of their natural changeableness and fluctuations.

2.2. The aerological measurements at islands and coastal stations and also, episodically, from ships.

The measurements are performed usually once-twice a day, the altitude of measurement is of 20-30 km. The temperature, humidity, horizontal wind velocity and pressure are measured. The shortcomings of this method are: too much distance between stations (some hundreds kilometers) and the fact that measurements are performed only at TC's periphery because the radio-probe launch is possible at wind velocity which is no more than 20 m/s.

2.3. The satellite measurements. The measurements from geostationary meteorological satellites can be performed in half an hour or more frequently, from polar - orbital satellites once or twice a day with duration of about 5 minutes. The measurements are performed in visual, IR and SHF ranges. However only limited number of parameters are measured because of the features of radiation spreading in cloudy atmosphere and the spatial discrepancy by vertical is poor.

2.4. When the TC approaches to the land, it's observations would be performed by meteorological radars including Doppler's radars. The sufficiently dense network of such radars having reciprocally overlapped fields of vision is

at the Atlantic Coast of USA, at coast of India, China, Japan and Korea. The range of meteorological radars is of up to 400 km, however the spatial discrepancy, which is sufficient for an investigation of one cloud, is possible at distance which is no more than 100 km only.

2.5. Weather science - research ships provide a receiving of the large volume of information on the nearest TC's periphery.

However these measurements have given no any significant contribution to the TC study. The main limitation for ships using for TC study is that than the ships can be only at the rear part of TC and at significant (200 km and more) distance from it's centre by safety reasons.

2.6. There are two main approaches to the analysis of experimental data which are received by using of one or technical means. The first approach includes the analysis and study of separate event, for example, the data of research flight together with the satellite data. Such approach can sufficiently illuminate in details any event or process in the TC, however in this case there is no certainty that this event is the typical one because the measurements have been restricted both in space and in time. The second approach is based on the supposition that it is possible to try to reconstruct some typical averaged structure of TC or the mechanism of it's interaction with surrounding atmosphere. Such reconstruction should be performed with using of the composition (putting together) of separate measurements which have been performed in different times in different TCs. It is clear that with this average many important features of TC's structure, which are necessary for the understanding of it's physical nature, will be lost.

### 3. The review of modern means and methods for the "ozone hole" investigation

Today there are three types of technical means for receiving of experimental data on the Antarctic "ozone hole":

- satellite systems of remote monitoring;
- aircraft laboratories;
- on-ground measuring stations.

3.1. The satellite systems of remote monitoring are performing a cartography of general ozone content only during day-light hours (because the equipment used on them is based on the analysis of spectrum and intensity of solar radiation dispersed by ozone layer). That does not give a possibility to know the initial history of "ozone hole" formation during a winter ("dark") period. Besides that, in the first turn it is necessary to know the ozone distribution along altitudes, not only it's general content. The satellite systems of remote monitoring don't provide such information.

The restriction of principle even for prospective satellite monitoring of ozone layer is an impossibility of measurements for ozone concentrations in the atmosphere layers which are situated under the layer of ozone concentration maximum, and also the circumstance that during the measurement of ozone content it is necessary to take the information on the atmosphere composition and on the parameters of atmospheric processes (the

temperature, humidity, pressure, wind velocity) in the environment of points of ozone concentration measurement.

3.2. The aircraft laboratories are used periodically because of a remoteness of measurement performing region from airfields and maintenance bases and in connection with that they give a possibility only for investigation of "ozone hole" local regions and don't provide a receiving of information on a change of ozone concentration along an altitude.

3.3. The ground measuring stations are carrying out the measurements by radio-probes launched by balloons. At present they are a sole source of information on the vertical distribution of ozone and atmosphere parameters.

However, the existing at the Antarctic Continent ground measuring stations are situated at the coast, are small in number and don't provide a scope of significant area of "ozone hole" by measurements.

The technology of preparation for a using of balloons equipped with radio-probes (some days) is hampering their group (mass) launch simultaneously from all ground polar stations of the world's commonwealth. That sharply decreases a value of received information for a clearing up the mechanism of "ozone hole" formation.

Thus, in spite of the task importance and significant means allotted for the investigation of Antarctic ozone anomaly, the technical means which are used at present for that don't provide in principle a simultaneous receiving of information on the ozone content distribution and on the atmosphere parameters in altitudes range of 0-35 km, at large area (5000 \* 5000 km) not only in conditions of polar night but even in condition of polar day.

### 4. The possible consumers of information on experimental contact investigation of tropical cyclones and "ozone hole"

On the base of above mentioned it is possible to make the following conclusions. Used at present technical means for receiving of experimental data on TCs and "ozone hole" both separately and in total don't allow to receive the detailed three-dimensional picture which should characterize the atmosphere parameters along whole volume of the TC or "ozone hole" space with the acceptable discrepancy by horizontal line (20-50 km) and by vertical line (hundreds meters) during a time about 1 hour.

The instrumental measurements in the central part of TC (with radius of 150 - 180 km) at altitudes of above 5-8 km are practically absent.

The analogous situation has a place regarding experimental investigations of the leading stream in radius of up to 100 km from the TC's centre.

The instrumental investigations of Antarctic zone anomaly is carried out only in separate points with great discreteness by the time and by the space.

The experimental information on TC's central part has the main value first of all for the development of fundamental science investigations of TCs and, in more less degree, for the efficient forecast of TC's trajectory and intensity. Their consumers in world's commonwealth would be only some countries having the science potential which can process

this information: USA, Japan, Russia, China and Australia.

This information would be transferred to consumers in some weeks or months after the experiment.

The information on leading stream has a pronounced significance for the efficient forecast of TC direction and speed of movement, while the data bank for the leading stream has a great value for development of new effective schemes of forecasting.

On purposes to efficient forecasting the information should be transferred to consumers (in form of variables approved in meteorology) as soon as possible, however it should be transferred not later than 1 hour after the ending of measurements. The consumers for this information, in spite of abovementioned already countries, would be also the hydro-meteorological services of Philippines, South Korea, Taiwan, Viet-Nam, Hong Kong, India, Mexico, and island countries of Caribbean basin.

### 5. The main tasks which would be realized with using of space-rocket technology for experimental contact investigation of tropical cyclones and "ozone hole"

At present on purpose to solve effectively the problems of typhoons and ozone anomalies it is necessary to solve the following tasks:

5.1. Massed measurements of the atmosphere parameters (wind, temperature, humidity, pressure) in the individual TCs at different stages of their development, which are necessary for more complete understanding of physical defining the structure and power potential during transfer from one stage to other.

The characteristic distance between soundered vertical sections of atmosphere should be of 20-30 km near the centre of TC's circulation and would be twice as much at distance of 150-200 km from the centre.

The range of measurement rate for meteorological probes should be from 20-18 km (for 25% of probes total number a decrease of this altitude is possible of up to 16-15 km) up to the Earth surface.

A vertical displacement velocity for meteorological probes should be not more than 10 m/s. A number of soundered vertical sections should be of up to 40.

It is possible if the probe will hit in a circle of 5 km radius having a centre in the calculated point.

It is most important that the absolute coordinates of probe should be known at the moments of measurements during whole time of sounding from maximum altitude up to minimum altitude with accuracy not less than 0.5 km. It is desirable to launch the meteorological probes during 5-7 days with the rate of 1-2 launches per day. The decision on first launch of some launches serial in the individual TC would be taken approximately a day before the launch.

5.2. The measurements of parameters of atmosphere, surrounding TC, in the first turn, the leading stream, on purpose to efficient forecast for TC's movement. It is desirable that these measurements would be carried out surround of the TC in a ring having the radius of

from 500 to 1000 km with the spacial discrepancy of about 200 km.

According the current conceptions these measurements will let more precisely forecast the probability of TC's trajectory turn and calculate the time and coordinates of turn point.

The characteristic distance between the probes in that case is about 200 km. The total number of probes is up to 40. The possible tolerance of probe from calculated point in the moment of it's work beginning is up to 20 km. The coordinates of probe in measurements process should be known with error no more than 1 km. The range of sounding altitudes is from 20-18 km up to the Earth surface. The vertical displacement velocity of meteorological probe should be not more than 10 m/s. The measurements should be performed during some days with rate of 2-4 measurements per day with the synchronization of measurements by the time with the existing search network operation (the ground, satellite and aviation measurements). The decision on first measurement would be taken a day before the experiment.

5.3 The soundered area of "ozone hole" would have a shape of stripe with the length of 5000 km and width about 500 km with the uniform-regular structure of ozone-aerological probes disposition.

The range of altitudes for measurements carrying out should be from 35-40 km to 0-5 km.

The possible vertical velocity of ozone probe displacement should be about 10 m/s. The discreteness of measurements for parameters by altitude is up to 1 km. The accuracy of measurement altitude determination - up to 200 m, the accuracy of measurement horizontal situation determination - up to 300 km.

The main registred parameters are: the ozone concentration, pressure, wind velocity and direction.

The periodicity of information receiving is once a week (10-15 measurements during 3 months) at the period of evident "ozone hole" appearance and once a month at the rest time of year.

The duration of period of receiving of experimental information on "ozone hole" phenomena study should be 6-10 years.

The total number of simultaneously operated probes should be up to 50.

The using of space-rocket technology for simultaneous delivery of significant number of measuring probes directly into the TC or "ozone hole" atmosphere is presented as very prospective affair.

By the space-rocket technology the measuring probes would be distributed by the upper boundary of investigated area of atmosphere on purpose to carry out the measurements with required discrepancy during their descent simultaneously for some tens of vertical profiles of such atmosphere parameters as wind velocity, temperature, humidity, pressure, ozone concentration.

The performed by "Salyut" DB of Khrunichev SRPSC together with "Typhoon" NPO preliminary estimations (on base of analysis of the sensor equipment for meteorological and ozone probes and also the features of experiments on contact sounding of large scale atmospheric phenomenas) showed that the

required experimental information on parameters of atmosphere in the zone of TC and "ozone holes" would be received by space-rocket complex (SRC) for contact sounding which can deliver some tens of small (with mass of 10-12 kg) automatic radio-probes to the required region and distribute them by required area practically simultaneously by the "Rockot" launch vehicle of light-weight class developed by the "Salyut" DB on base of removed ICBM equipped with the "Breaz" upper stage.

#### 6. The scheme of space-rocket complex functioning during contact investigation of tropical cyclones and ozone layer

The functioning of space purpose missile (SPM) is performed by the strict program. In the process of that the preparation of SPM for the launch and the trajectory part on injection into the circular orbit including the functioning of spacecraft with the "Breaz" upper stage are performed in accordance with the established cyclogram of "Rockot" LV operation. After the injection part ending the flight is performed along the circular orbit with required inclination and height of 250-400 km (see the Fig. 1).

When the spacecraft (SC) approaches to the calculated point the orientation of SC into position for a separation of reentry capsules with radio-probes is performed.

The engine units of radio-probes reentry capsules distribution are started with the calculated time delay after the separation from SC (the pyro-delay). In the result of engine units running the reentry capsules (RCs) gain the radial speed which is necessary for their distribution along required area.

After the entry into dense layers of atmosphere the RCs are aerodynamically stabilized and braked with using of the braking system and parachute.

When the altitude of sounding is achieved, an ejection of thermal-protection envelopes is performed. The following descent and functioning of radio-probes are provided by the parachute.

In the version of TC sounding the probe-retransmitter is used for a providing of the aerological-meteorological information transmission from radio-probes to the meteorological-aircraft or ship. This probe-retransmitter is ejected from the SC together with radio-probes and retransmits their signals to the aircraft (meteorological), ship or communication satellite. The analogous system of information collection would be used in the sounding of "ozone holes" at regions which are relatively accessible for the aviation, ground and floating means of information collection.

When the Antarctic ozone anomaly should be sounded it is necessary to take into account both the great remoteness of investigated region and the severe nature environment (especially during a polar night). They stipulate a necessity to use the SC which has delivered the radio-probes also for a collection of the ozone-aerological information from them. In this case the complex is functioning by the following way (see the Fig. 2). After the separation of complete set of RCs from the SC the on-board retransmitter (BR) is put in the working condition and the orientation

of SC in position of the BR's antenna directed to the Earth is performed.

At the second turn of SC's orbital flight during the SC passing over the region of landing radio-probes the collection of information from memory devices of radio-probes is performed by the command from BR and this information is brought in the memory device of SC's BR.

When the SC approaches to the latitude of 70 degree South the SC is oriented in position of BR's antenna directed to the geostationary "Stationar-4" communication satellite (in the longitude of 14 deg West) and begins the transmission of information from it's BR via the satellite to the on-ground measuring points (GMPs). After the transmission of complete information from memory device of SC's BR at the third turn of orbital flight approximately in 12000 seconds of flight the SC is oriented and the braking impulse is performed on purpose to lead away the SC from the orbit and to sink it in the World Ocean area at the approximate coordinates of 56 degree South and 143 degree East. In the case of using of the polar stations (PS) during the experiment implementation the transmission of parameters for their receiving by the radio-means of PSs is carried out simultaneously with a recording them into the memory devices radio-probes which are in radio visibility of PSs.

A determination of current local situation for radio-probes when they carry out the meteorological measurements can be performed by a using of the "Navstar" ("Glonass") global navigation systems. The components of wind velocity by whole required range are determined in the radio-probe by the "Glonass" and/or "Navstar" system.

#### Conclusion

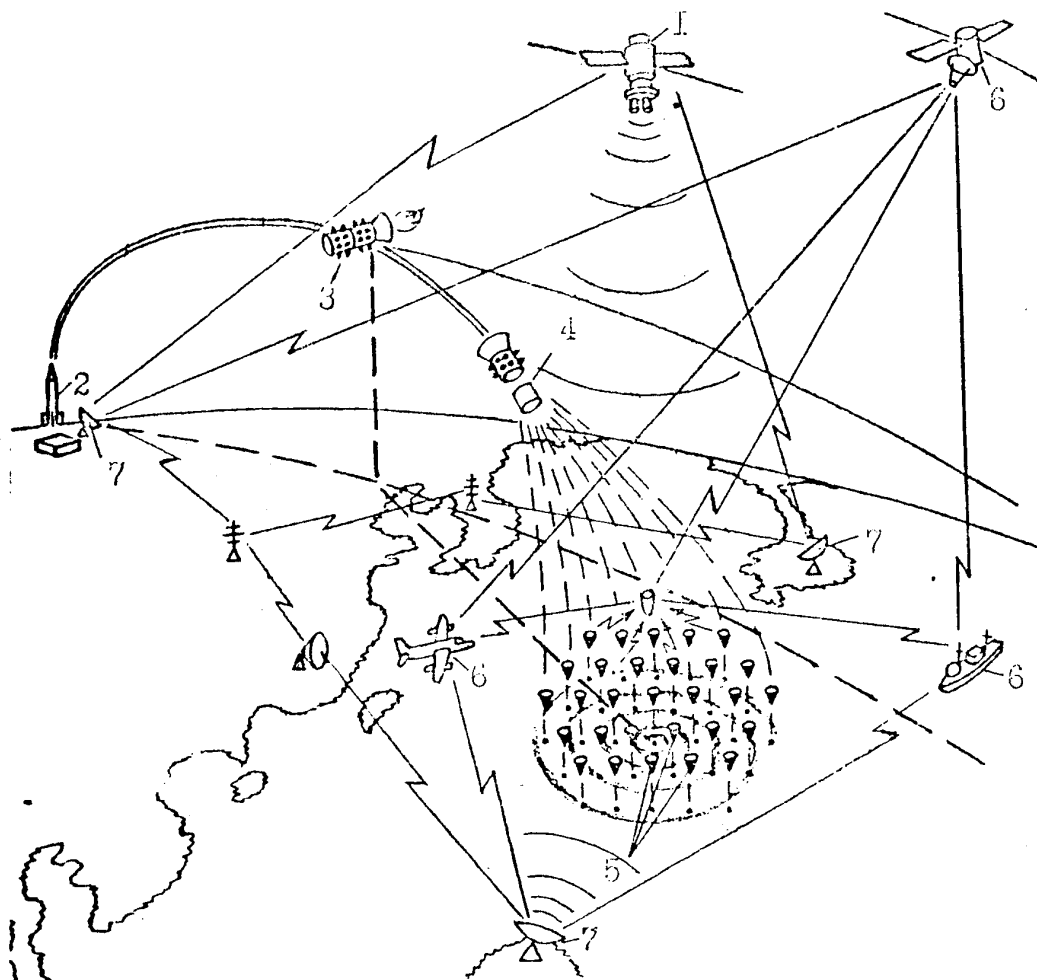
1. The analysis of currently used technical means and methods for experimental investigations of tropical cyclones and ozone layer showed that these means and methods (satellite remote measurements, a using of aircrafts-meteorological laboratories, ozone-measuring meteo-probes) do not provide a receiving of detail three-dimensional representation for the investigated phenomena with required discrepancy and efficiency which are necessary for a practical using in development of the measures on decrease the damage caused by these large-scale atmospheric phenomena.

2. The conception for creation of the space-rocket complex intended for investigations of large-scale natural phenomena in any region of the globe by the method of remote sounding with efficient transmitting of measurement results in the interested consumers is developed on base of the conversed space-rocket technology means.

3. The carrying out of experimental investigation of TC by the space-rocket complex (SRC) will allow to receive the unique science-capacious information on dynamics of large-scale vertical processes which occur along whole volume of this natural phenomena; to form the data bank on three-dimensional structure of TC; to improve significantly the forecast of TCs intensity and trajectory of its movement.

4. The using of SRC for contact sounding of Antarctic ozone anomaly in time of its

## THE SCHEME OF "TYPHOON" SRC FUNCTIONING



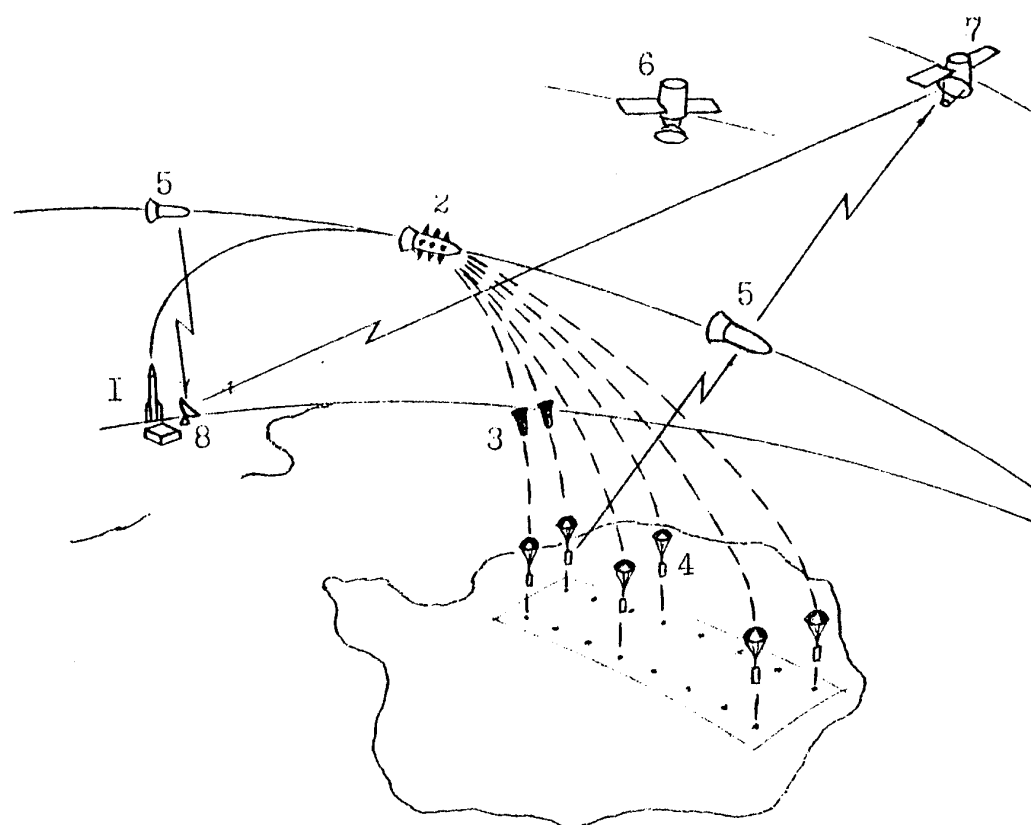
1. Tropical cyclone (TC) detection by satellite.
2. Rocket launching.
3. Deorbiting of space nose section with reentry capsules and probe - retransmitter.
4. Reentry capsules and probe-retransmitter separation and opening them in space according to the defined law for tropical cyclone covering area.
5. Radio-probe and probe-retransmitter parachute breaking out descent.
6. Tropical cyclones area atmosphere parameters measuring by radio probes through descent and transmission to probe-retransmitter.
7. Data transmission by probe-retransmitter to aircraft-based meteorological laboratory, ship, communications satellite or ground receiving facilities.

## The "Typhoon" SRC specifications

Specification	Value
Number of delivered radio-probes	up to 50
Probe mass, kg	up to 2
Reentry capsule mass, rg	up to 12
Diameter of sounded area, km	up to 500
Sounded altitudes, km	35...0
Measured atmosphere parameters:	
- pressure, mbar	1050...100
- relative humidity, %	40...95
- temperature, deg.	-50...+60
- components of wind velocity, m/s	2...100

Fig.1

# THE SCHEME OF "OZONE" SPACE-ROCKET COMPLEX FUNCTIONING



1-launch vehicle; 2-spacecraft; 3-reentry capsule; 4-radio-probe; 5-on-board retransmitter; 6-"Glonass" satellite; 7-"Stationar-4" geostationary satellite; 8-on-ground measuring point.

## The "Ozone" space-rocket complex specifications

Specification	Value
Number of delivered radio-probes	up to 25
Probe mass, kg	up to 2
Reentry capsule mass, kg	up to 12
Length of sounded area, km	up to 5000
Width of sounded area, km	500
Sounded altitudes, km	40...0
Measured atmosphere parameters:	
- pressure, mbar	1050...100
- relative humidity, %	40...95
- temperature, deg. C	-50...+60
- ozone concentration, %	0...100
- components of wind velocity, m/s	2...100

Fig. 2



intensification during period of polar night will allow to develop the models of ozone anomalies dynamics and to determine the ways for effective technical solution of the ozone layer preservation problem.

5. The conducted investigations and project developments have shown a technical feasibility for the SRC of efficient multi-parametrical contact sounding of large-scale atmospheric phenomenas which should be based on the "Rockot" LV and for the elements of "Scut" ("Orbita") system drawn for a collection and transmitting of the parametrical information from meteo-probes and the elements of

"Navstar"("Glonass") system drawn for a navigational determination of received information.

6. The importance of proposed SRC using together with other technical means of monitoring for a solving of problems on the World's commonwealth protection against such terrible natural phenomenas as TC's and ozone anomalies make a development of that SRC as the expedient action which would be financed from the funds of GEOWARN International Organization which is founded as the UNO specialized Agency on development of calamity seach and warning global system.

## COMMERCIAL USAGE OF NAVY COMPONENTS DEVELOPED AND MANUFACTURED BY CRI "DELFIN"

Novgorodski A.V.  
Chichinadze M.V.

CRI "Delphin", 42 Ozernaja street  
Moscow, 119361 Russian Federation

### Summary

Parameters of gyro systems (accuracy, size, power consumption, reliability, etc.) are determined by parameters of the elements of which the gyro unit consists. The elements developed for military equipment meet the utmost requirements. Over the past ten years the "Delphin" Central Research Institute developed a whole number of elements including a gyro, an accelerometer, a torquer, a slip-ring assembly, etc. to provide a basis for designing gyro systems for military purposes. The conversion made it possible to use these elements in commercial gyro systems. The present paper deals with such elements and systems created on their basis and used for commercial purposes.

\*\*\*

The "Delphin" Central Research Institute was set up in Moscow in 1966. The Institute specializes in the field of marine navigation and oceanographic shipboard equipment. The equipment includes precision electromechanical gyro devices and electronic control units. The Institute is a leading enterprise in research and development of gyrocompasses in Russia. It comprises research and development departments, test stands and a production plant equipped with new-type machinery and other up-date equipment for manufacture of gyro and electronic devices.

Over the past ten years up-date elements of the gyro devices were developed at the Institute for a new generation of navigation equipment. These components are to provide the creation of a precise small-size gyro system with low power consumption and high reliability.

Due to the reduction of military orders from the Navy, the Institute had to cut down research and development as well as serial production for the Defence Ministry. That accounts for the conversion process started at the enterprise in order to survive and use our considerable scientific, technological and production potential. The Institute has started development and production of equipment and instruments for oil and gas prospecting, extraction and transportation. Our products are also widely used in commercial shipbuilding. The new direction in our work allow the Institute to get financing, keep its know-how and prevent losing qualified personnel.

The following main miniature components formed the basis for development of gyro systems which are used for military and commercial purposes:

- dynamically tuned gyro (DTG);
- quartz accelerometer (QA);
- torquer (stabilization motor);
- slip-ring assembly;
- angular sensor;

- electronic power supply units;
- printed circuit boards (PCBs).

### Dynamically Tuned Gyro

DTG is a miniature two-degree-of-freedom gyro with a flexible suspension. The rotor of DTG is fastened to the gyromotor's driving shaft by means of a special suspension. The suspension is a flexible element made of one piece of alloyed steel by electroerosion technology.

It consists of four parts (fig.1): a shaft of suspension, two cardan rings and an outer rim to which the massive rotor is stuck. The rotor is bound to two cardan rings by means of two mutually perpendicular pairs of flexible crosspieces. The shaft of suspension is stuck to the gyromotor's driving shaft. The rotor's turning in relation to the suspension shaft causes flexible torques proportional to the small angles of the turn. These torques get balanced by inertial torques of the cardan rings when the DTG is tuned. Under this condition the mechanical bound between the rotor and the driving shaft seems to disappear and the rotor becomes a free gyro.

The dynamical tuning is made by changing inertia moments of the cardan rings when two pairs of screws are moved in opposite directions parallel to the driving shaft.

The measurement of the rotor's turn around the two axes of sensitivity is provided by two angular pick-offs. The output signal is an analogue one. Its frequency is 19.2 kHz, voltage is proportional to the angle. The phase corresponds to the direction of rotation. Two torquers are used to control the gyro. The torquers's rotor is fastened to the gyro's rotor. It comprises permanent magnets. The torquers' stator is installed in the housing of the DTG. It consists of a couple of air-core coils connected in series and located opposite each other.

Rotation of the gyro rotor is restricted by the angles of  $\pm 15^\circ$  by means of a stop which excludes any damage or deformation of the flexible crosspieces. The DTG's housing is filled with hydrogen. Two heaters warm up the DTG while starting and operating.

### Specifications

Limiting drift rate, deg/h	0.05
Speed up time, not more than, s	30
Speed of rotation, rpm	12,000
Power consumption, W:	
gyromotor	2
pick-ups and torquers	5
heaters	100
Power supply, V, Hz	20, 400
Weight, gr	350

### Miniature Accelerometer

The accelerometer is a single-axis pendulous accelerometer with quartz torsion-bar suspension of trial mass. The small quartz frame is a trial mass. It is suspended with two quartz torsion-bars (fig.2). While accelerating along the axis of sensitivity, the frame turns and a photoelectric sensor (light-emitting diode-photodiode) transduces an angle into electric signals which go to the amplifier's input. The output current of the amplifier flows into the metallized quartz frame and torsion-bars, interacts with the field of the permanent magnets built in the housing, and puts a moment on the frame, which compensates the inertial moment. The current and its direction are proportional to acceleration and its direction. The output signal, as a voltage, is picked up from the resistor. The housing is filled with damping liquid.

#### Specifications

Limiting error, g	2x10 <sup>-5</sup>
Measured acceleration range, g	+/-2
Scale factor, V/g	5
Power consumption, W	0.45
Weight, gr	115

### Torquer

The torquer is a commutator machine of direct current without shaft bearings. It consists of a stator with permanent magnets, a rotor with winding and a commutator with brushes. The permanent magnets are soldered into the permalloy stator. The rotor's core is assembled from stamped permalloy plates. The commutator is mounted on the front part of the rotor. The brush holder is installed on the stator. Two brushes are connected parallel to increase reliability.

#### Specifications

Max. moment, gcm	1,350
Max. power consumption, W	25
Weight, gr	250

### Slip-Ring Assembly

The slip-ring assembly provides transmission of an electric signal to the platform having an unlimited angle of turn (about the azimuth shaft). It is a set of thirty co-axial gold rings and thirty pairs of silver brushes.

#### Specifications

Length, mm	28
Diameter, mm	16
Max. current, A	5
Weight, gr	80

Beside the above mentioned components, the following elements are developed: a flat sine-cosine transformer used as a transducer in a follow-up system, a thermo-relay used in thermo-stabilization systems, electronic boards for the control of torquers, power supply units, etc.

The given components were used as a basis for the development of various types of inertial units providing primary information on angular speed and linear acceleration of the inertial unit. This information is processed by a computer for obtaining final parameters of attitude and position of the moving object on which the inertial unit is mounted. The inertial units have different numbers of gyros (1 or 2), accelerometers (2 or 3)

They also differ in methods of installation on the object:

- by means of a gimbal;
- strap-down inertial system.

Now we shall consider two navigation systems where the first method of installation is applied.

### Miniature Gyrocompass

The gyrocompass consists of a master compass, electronic, control and transmission units. The basis of the gyrocompass is a gyroplatform with one DTG (the spin axis is directed to the North) and two accelerometers ("North" and "East").

The rotation axis of the gyroplatform (fig. 3) is orthogonal to the gyro's spin axes and lies in the plane of the ship's deck. The platform rotates relatively to the outer gimbal frame having an axis of rotation perpendicular to the deck's plane.

The two gyro's pick-offs produce output signals when there is misalignment of the gyro's rotor with its housing in two mutually orthogonal directions. These signals are amplified and supplied to the stabilization motors of the gyroplatform and outer gimbal frame which stabilize the platform in space. The gyro's attitude is controlled by the DTG's torquers in accordance with the signals of the computer.

The "North" accelerometer produces an output signal proportional to the rotation angle of the gyroplatform relative to the horizontal plane in the meridional one.

The "East" accelerometer measures the tilt of the gyroplatform in the East-West plane. The signals of the accelerometers go to the computer.

#### Specifications

Limiting dynamic error, deg	0.6 sec lat
Settling time, min	60
Latitude of navigation, deg	up to 75
Vessel's speed, kn	up to 60
Weight (including transmission unit), kg	29.5
Power consumption (without repeaters), W	30
Supply voltage, VDC	24
Interface:	
- Sperry step data	up to 8 repeaters
- digital code as per NMEA 0183	up to 4 receivers

The gyrocompass complies with the Russian Register of Shipping, IMO Resolution A.424(XI) of 1979 and ISO International Standard 8728 of 1987.

### Small-Size Navigation, Heading and Attitude System

The system consists of a master unit, a transmission unit, a control unit and a power supply unit. The master unit includes gyro and electronic units.

The basis of the system is a gyroplatform with two DTGs and two accelerometers. The spin axis of the first gyro is directed to the North, the spin axis of the second one is orthogonal to the first gyro. One of the accelerometers measures the Northern acceleration, the other one - the Eastern acceleration of the ship.

The platform has a vertical axis of rotation in relation to the inner gimbal frame. The inner and outer gimbal frames have horizontal orthogonal axes. Each of the three axes is controlled by a torquer. Torquers' control is ensured in the same way as in the miniature gyrocompass. The fourth pick-off of the gyro provides perpendicularity of the spin axis of the Eastern gyro to the Northern one.

The gyro's attitude is controlled by the DTG's torquers from the signal of the computer. The computer processes the signals from the accelerometers and velocity and latitude data.

The system has several operating modes:

- integrated navigation system using information from a log and GPS;
- inertial navigation system providing short-term storage of navigation parameters without log and GPS inputs;
- stabilized gyrocompass producing heading, roll and pitch angles, calculating latitude and longitude on the basis of a log output;
- stabilized directional gyro storing data on heading and other navigational information, taking into account a log input.

#### Specifications

Limiting errors (integrated mode)	
- positioning, m	30
- heading (at latitudes up to 70), arc-min	6
- roll and pitch, arc-min	3
Limiting heading storage, deg/h	0.1
Settling time, h	
- fast (heading error up to 1 degree)	0.5
- full	4.0
Power consumption, kVA	0.9
Weight, kg	
- system	222
- master unit	95

#### No-Gyro Sensor of Roll, Angular Rate and Angular Acceleration

The simplest of strap-down inertial systems is a no-gyro sensor of roll, angular rate and angular acceleration for the ship's roll stabilizer (fig. 4).

The sensor consists of two miniature accelerometers with parallel sensitive axes. It is mounted on the hull of a ship, so that the sensitive axes are situated in the plane of the bulkhead. The accelerometers' pick-off signals are connected opposite each other. As there is a distance between the accelerometers in the plane perpendicular to the deck, the sensor's pick-off signal is proportional to roll acceleration.

An angular rate signal is produced by means of integration of the roll acceleration signal. The smoothed out pick-off from one of the accelerometers is proportional to the tilt of a ship.

#### Specifications

Limiting error, %	5
Distance between accelerometers, mm	300
Measured parameters	
- roll, deg	+/-30
- angular rate, deg/s	+/-25
- angular acceleration, deg/s <sup>2</sup>	+/-32
Weight, kg	4
Power consumption, W	4.5
Power supply, VDC	+/-15

#### Gyro Inclinometer

The unified gyro inclinometer measures geometrical parameters of oil and gas bore-holes with complex profile. The inclinometer acts as a sensor to detect its own direction and therefore, the direction of the bore-hole's axis. The inclinometer's output information is the azimuth and inclination of the well's axis.

The inclinometer (fig. 5) consists of two parts connected by a cable:

- downhole package (gyro unit, computer, power supply unit);
- surface equipment (computer, control unit, power supply unit, check-out stand).

The inclinometer has two modes of operation:

- measurement while drilling, MWD;
- measurement while stopping, MWS.

The accuracy in the second mode is higher.

The strap-down inertial system is used in the tool because the downhole package has minimum dimensions and can be placed inside pipes of the well.

The sensors of the inertial unit are two DTGs and three quartz accelerometers. The gyros are fixed inside the downhole package so that their spin axes are orthogonal to each other. The spin axis of one of the DTGs is parallel to the axis of the pipe. The sensitive axes of the two accelerometers are parallel to the gyro's spin axes.

The DTGs are used in the mode of two-axes angular rate sensors. In the given mode the output signals of the two gyros are amplified and supplied to the two DTGs' torquers, forming the follow-up system. The current on the torquer is proportional to the component's angular rate of the inertial unit around the axis of the gyro's pick-off.

Three components of angular rate and three components of acceleration which depend on their attitude towards gravity acceleration are fed into the computer where the azimuth and inclination are calculated. These parameters are transmitted via the cable to the surface equipment.

Prior to operation, the tool is calibrated on the laboratory check-out stand by monitoring preset attitudes as well as temperatures.

#### Specifications

Limiting error, deg	
- MWD mode	
azimuth	1.0
inclination	0.15
- MWS mode	
azimuth	0.5
inclination	0.1
Speed of lowering (raising), m/h	3,000
Temperature, °C	0-100
Diameter of housing, mm	90
Length of housing, m	4.5

#### Navigation System for Checking Gas Trunks with a Moving Projectile

The instrument measures a magnitude of bend of a gas trunk in horizontal and vertical planes to locate sections with increased deformation. The system (fig. 6) measures the actual heading and tilt of a gas trunk using a projectile, and compares the received parameters with the

estimated geodesic ones. The difference between them shows deformation of the trunk. Besides, the system determines position of measured values along the trunk axis to spot sections with increased deformation. The system consists of an inertial unit, a computer and a recorder installed on the projectile, as well as surface equipment designed for the system's preparation and analysis of recorded information.

The on-board equipment represents a strap-down inertial system which is similar in its structure and principles of operation to the strap-down system of the gyro's inclinometer though is different in design. The output information is recorded during the movement of the projectile from one station of the gas trunk to another to be decoded afterwards by the surface equipment.

### Specifications

Limiting errors	
- heading, deg	0.5
- tilt, deg	0.5
- positioning, km	1.0
Diameter of gas pipe, m	0.7-1.4
Speed of projectile, km/h	up to 25
Operating time, h	up to 5

\*\*\*

At present, the "Delphin" Institute keeps perfecting the technology of production of the gyro elements and extending their usage. For instance, a stabilization platform has been worked out for the marine gravimetric system on the basis of the DTG and accelerometers. The miniature gyrocompass is being updated to improve design of its control panel and combine all the devices in a whole unit.

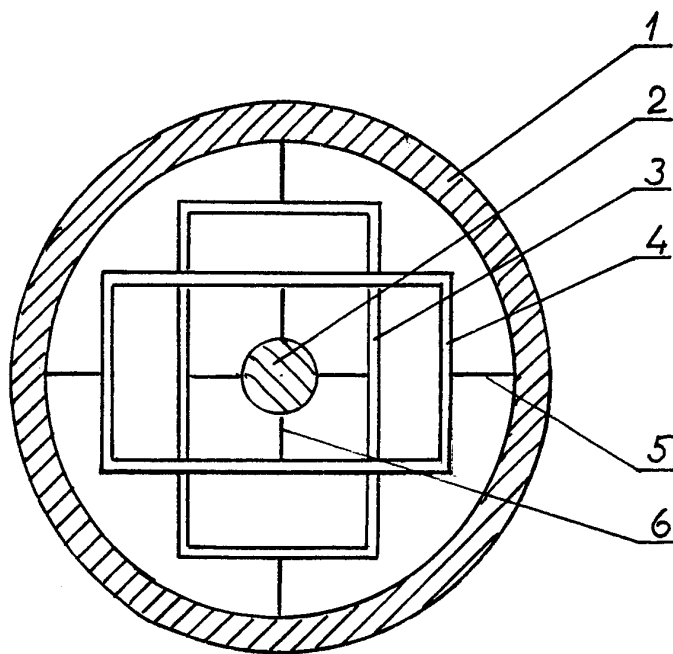


FIG.1.

### DTG SUSPENSION

- 1 - OUTER RIM
- 2 - SHAFT OF SUSPENSION
- 3,4 - CARDAN RINGS
- 5,6 - FLEXIBLE CROSSPIECES

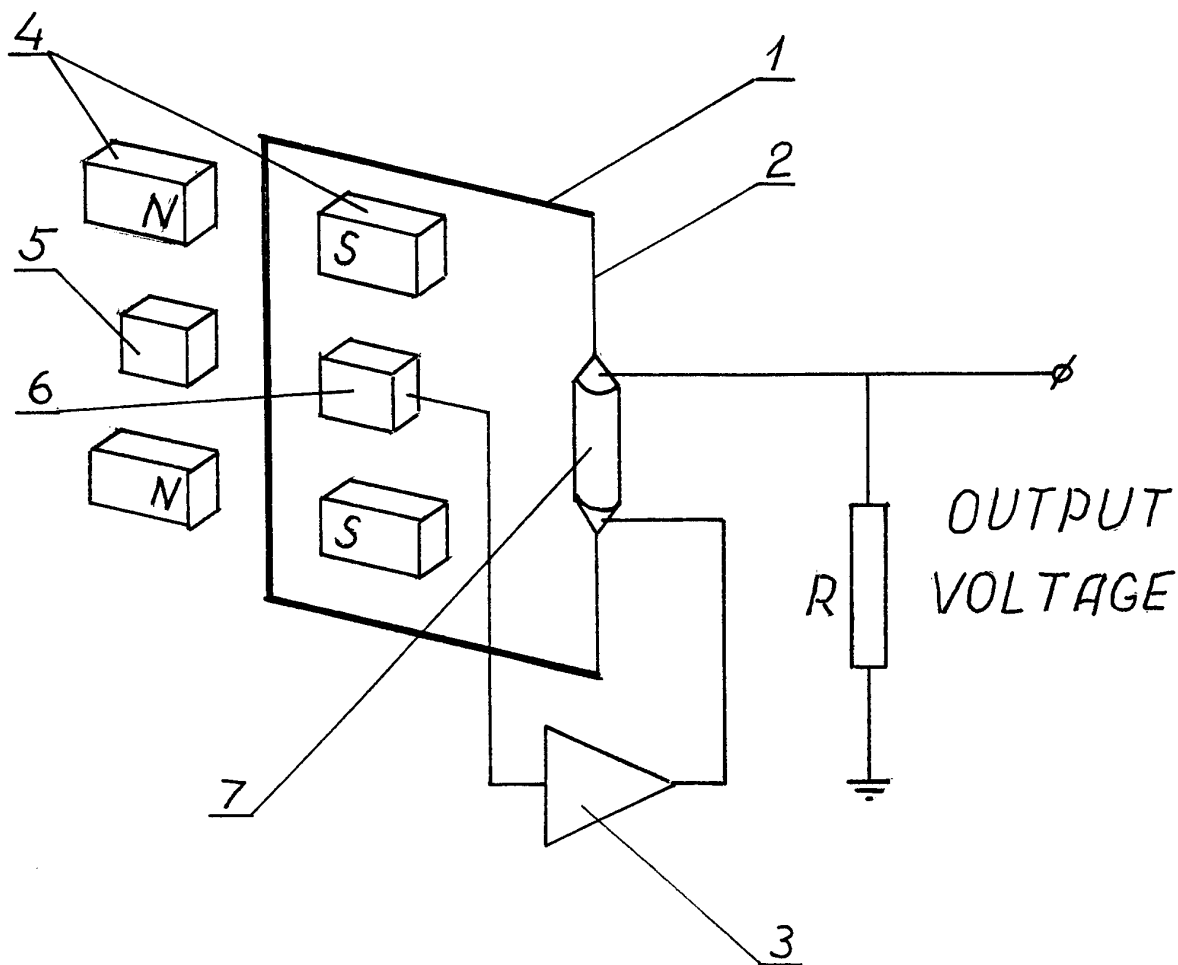


FIG. 2.

MINIATURE ACCELEROMETER

- 1 - METALLIZED QUARTS FRAME
- 2 - METALLIZED TORSION BAR
- 3 - AMPLIFIER
- 4 - PERMANENT MAGNETS
- 5 - LID
- 6 - PHOTODIODE
- 7 - STEM WITH METALLIZED FACE PLATE

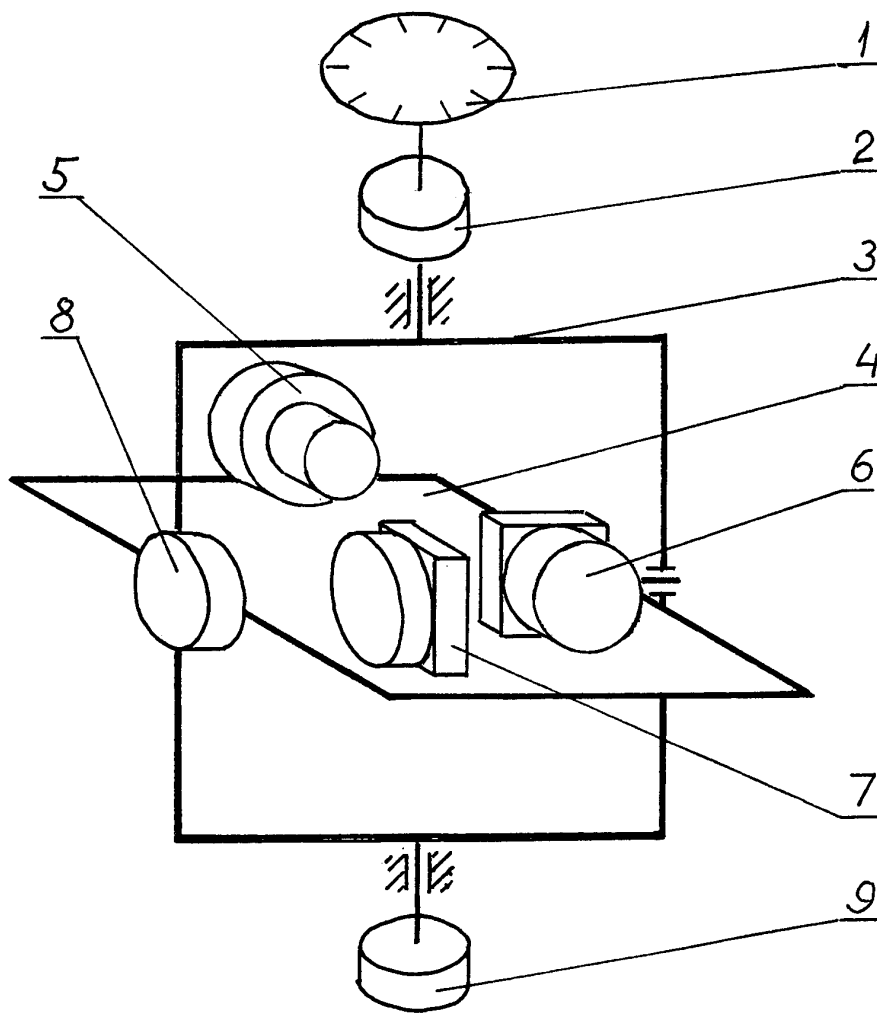
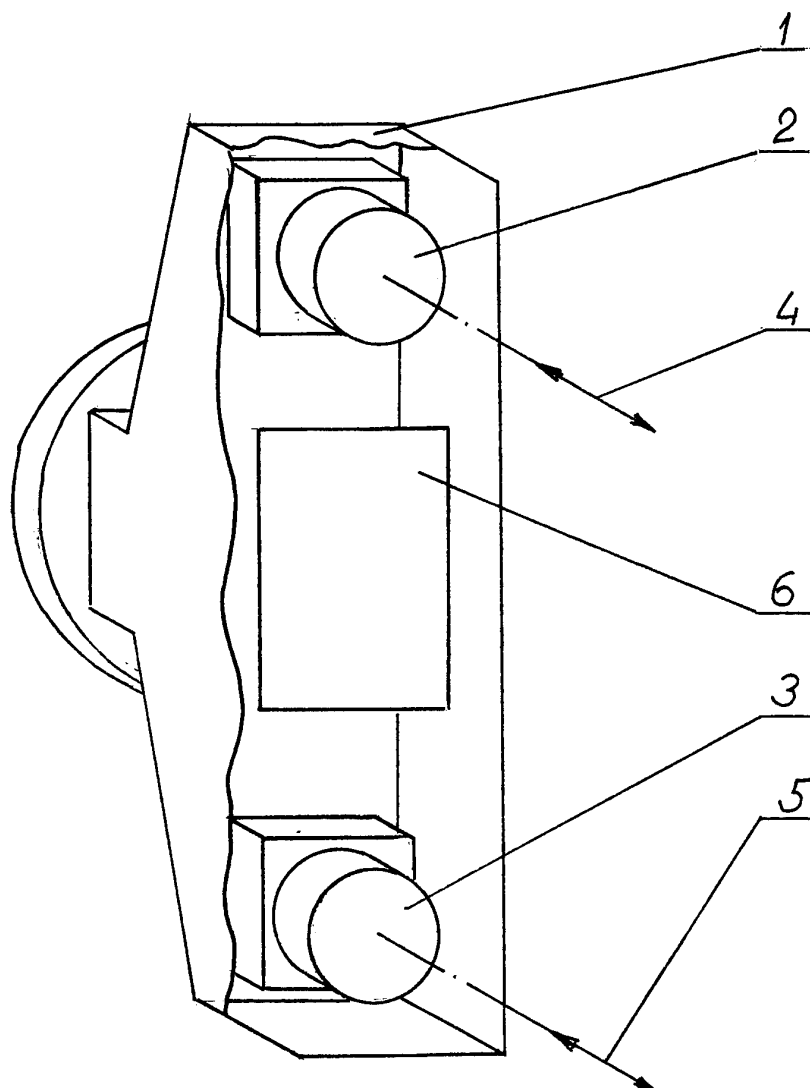


FIG. 3. MINIATURE GYROCOMPASS

- 1 - SCALE
- 2 - HEADING
- 3 - OUTER GIMBAL
- 4 - GYRO PLATFORM
- 5 - DTG
- 6 - NORTH ACCELEROMETER
- 7 - EAST ACCELEROMETER
- 8 - PLATFORM TORQUER
- 9 - OUTER GIMBAL TORQUER



**FIG. 4.** NO-GYRO SENSOR OF ROLL, ANGULAR RATE AND ANGULAR ACCERATION.

- 1 - HOUSING
- 2,3 - ACCELEROMETERS
- 4,5 - SENSITIVE AXES
- 6 - PRINTED CIRCUIT BOARD



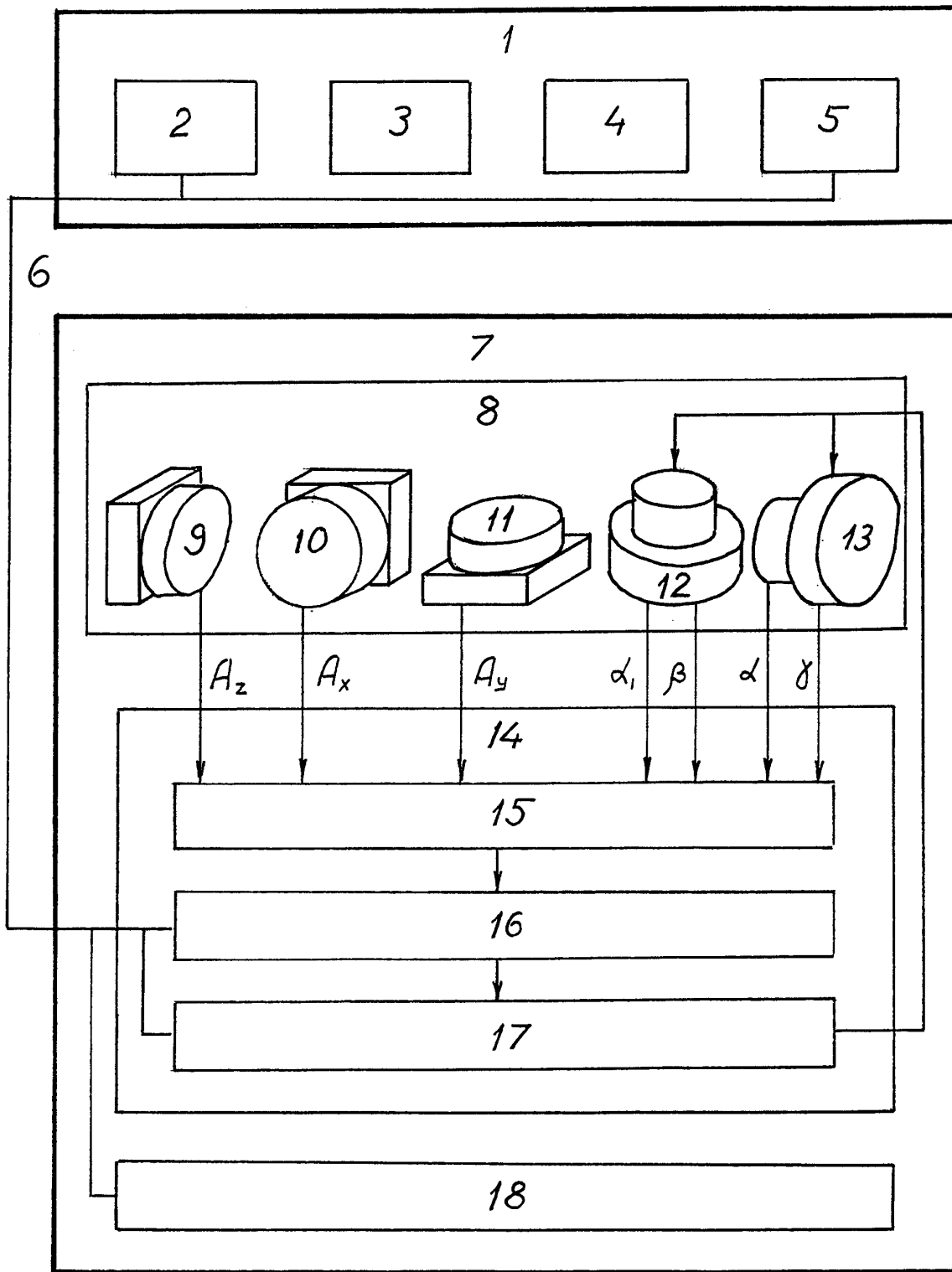


FIG. 5. GYRO INCLINOMETER

1 - SURFACE EQUIPMENT, 2 - INTERFACE, 3 - CONTROL AND DISPLAY DEVICE, 4 - CHECK-OUT STAND, 5 - POWER SUPPLY UNIT, 6 - CABLE, 7 - DOWNHOLE PACKAGE, 8 - GYRO UNIT, 9, 10, 11 - ACCELEROMETERS, 12, 13 - DTGs, 14 - COMPUTER, 15 - VOLTAGE-CODE CONVERTER, 16 - DIGITAL COMPUTER, 17 - CODE-VOLTAGE CONVERTER, 18 - POWER SUPPLY UNIT,  $A_x, A_y, A_z$  - SIGNALS OF ACCELERATION,  $\alpha, \alpha_1, \beta, \gamma$  - SIGNALS OF GYRO PICK-OFFS

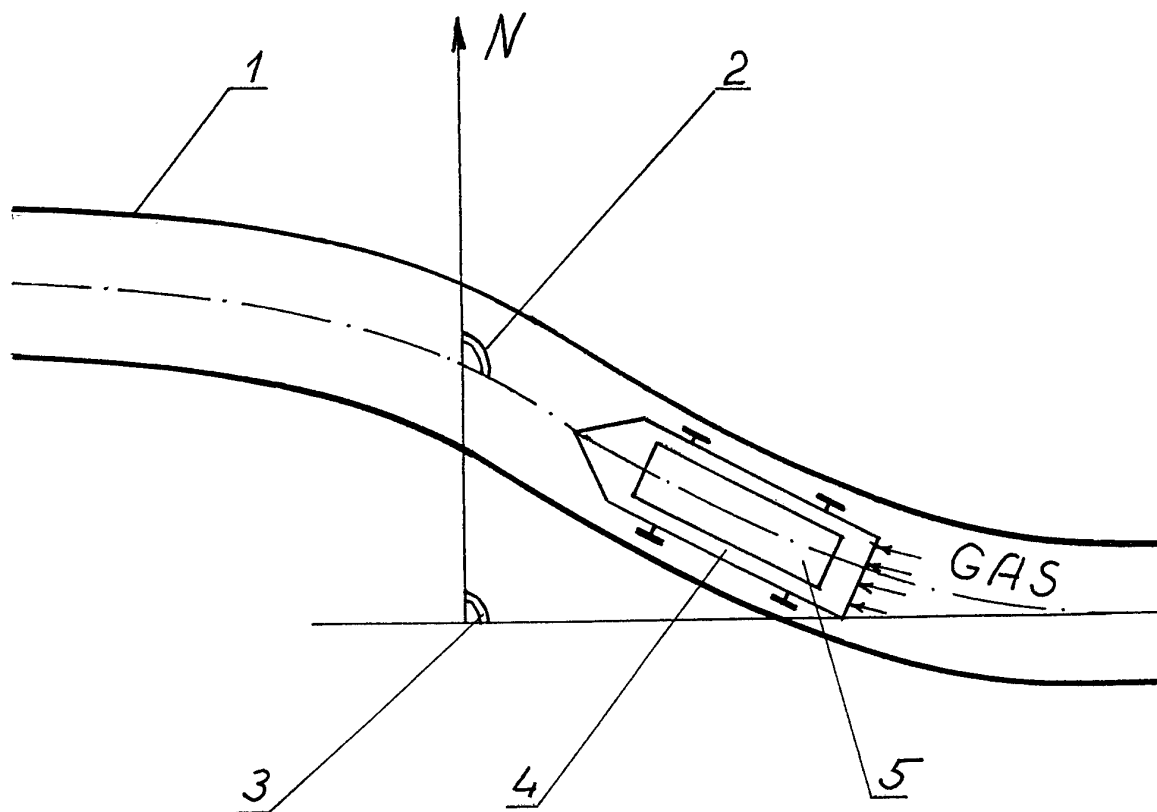


FIG. 6. NAVIGATION SYSTEM FOR CHECKING GAS TRUNKS WITH A MOVING PROJECTILE.

- 1 - TRUNK
- 2 - ACTUAL HEADING
- 3 - ESTIMATED GEODESIC HEADING
- 4 - PROJECTILE
- 5 - STRAP-DOWN INERTIAL SYSTEM

# SOME RESULTS OF INTERNATIONAL COOPERATION IN MILITARY TO COMMERCIAL CONVERSION OF LASER GYRO TECHNOLOGY

Yu.V.Filatov  
D.P.Loukianov  
A.V.Mochalov

St.Petersburg State Electrotechnical University (SPEU), Russia

R. Probst

Physikalisch-Technische Bundesanstalt (PTB), Braunschweig, Germany

R. Rodloff

B. Stieler

Institut für Flugführung, DLR, Braunschweig, Germany

## SUMMARY

The results of military to commercial conversion in the field of laser gyro technology are considered. Laser gyro systems were developed in Russia for military purposes. After some modifications within an international cooperation they are used nowadays also for civil applications as track surveying, deformation measurements of long objects and precision angle and angular rate measurements and angle calibration.

## 1.INTRODUCTION

Laser gyro technology, as one of the modern science branches, was borne in the war industrial complex in the 60-ies. Now it is looking not only for ways of survival but also as a way of more intensive development with support of high technology and intellectual potential.

Last decade's changes in the world allowed the international contacts in the field which was closed in the previous years. At the same time these changes initiated conversional processes not only in the former Warsaw pact countries but in the NATO countries too. Analysis of conversion strategy and tactics directions shows that the best way is the dual usage of military technical components for solving civil problems in various countries (e.g. Russia, Germany) within the framework of international co-operation. So in this report some problems in the field of laser gyro dual usage and their solution are discussed.

## 2.TRACK SURVEYING

The experience of the laser gyro (LG) usage in inertial strapdown systems turned out very useful in the system concept for railway and underground track surveying.

In Fig.1 the block-diagram of a simple system concept for measuring the inclination between both tracks is presented.

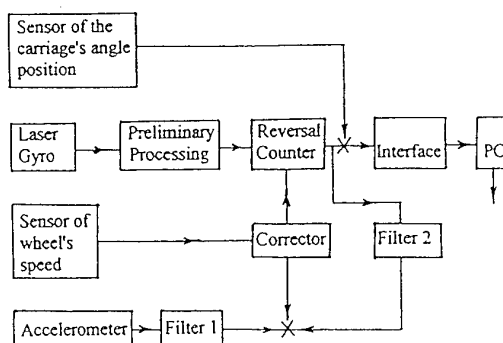


Fig. 1 System Concept for Measuring the Inclination between Railway Tracks

Such measuring system modification provides average accuracy of measurement what is sufficient for underground requirements. In the system the LG with dithering (angle vibration to avoid lock-in effect) is set in the carriage in such a way that its measuring axis is aligned with the direction of the tracks. The LG output signal is fed to a counter. The carriage angle position with respect to the wheels is measured by an electromechanical sensor. Its output signal is subtracted from that of the LG resulting in the inclination of both tracks. The accelerometer is mounted with its input axis perpendicular to the gyro axis in the carriage surface

plane and measures the carriage inclination about the track direction, too. It is used for compensating the LG drifts and earth rotation at the LG output. During the turns of carriage the correction is switched off automatically.

Preliminary results for St. Petersburg metro track measurements are shown in Fig. 2.

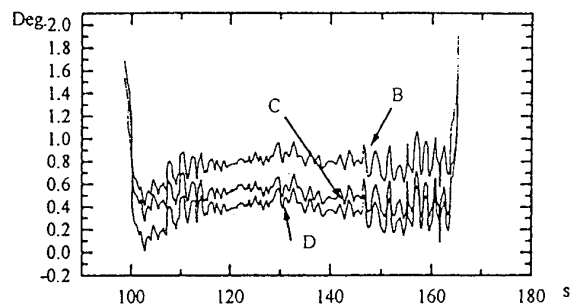


Fig. 2 Results of St. Petersburg Metro Track Surveying

B - Laser gyro; C - Accelerometer,  
D - Output signal after correction.

They were taken at a speed of about 80 km/h and confirm that an accuracy of about 1 mm for the top of one rail with respect to the other (cross profile) can be achieved.

The system can be simplified considerably by mounting the inertial sensors directly to the housing of the wheel bearing.

With the increase of the requirements to measurement accuracy up to 0,1 mm the system should be completed with an additional LG and accelerometer. In this case the complexity of the algorithms of signal processing come closed to the gyroorientator algorithms of strapdown navigation system.

Also there are some joint investigation in this field with the test facility of the German Railway in Minden.

### 3. LONG OBJECT DEFORMATION MEASUREMENTS

A special 6-axis LG block developed for space applications is now used by SPEU in a system for measuring deformations long object such as tankers, huge aircraft and others.

During their movement these objects are under the influence of the significant static and dynamic deformation that can bring them to crash which often is accompanied with human casualties and large ecological consequences.

The deformation measurement method and its realisation were developed on the basis of results obtained earlier for the increase of marine weapon accuracy. To realise the method it is necessary to mount two 3-axis LG blocks in two different points of the object. Comparison of their readings allows to determine parameters of their mutual angles and angular rates about three orthogonal axes.

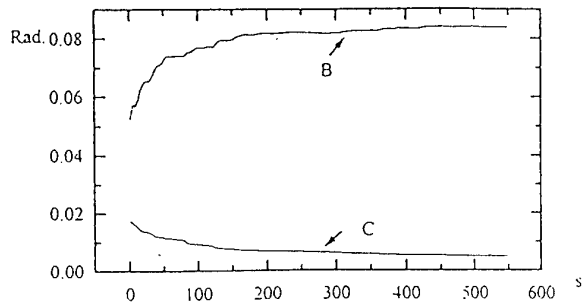
The application of optimal Kalman filtering allows to increase the measurement accuracy and to distinguish between static and dynamic deformations.

Simulations of marine object deformation measurements due to rolling showed that dynamic components of deformation about three axis can be estimated with an error of about 10-29 arc sec within 1 to 2 minutes. Similar results can be obtained for static measurement within 3 to 5 minutes.

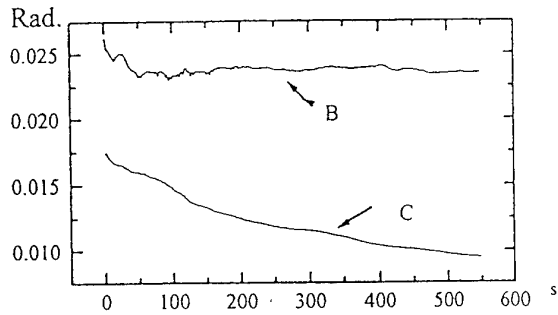
During the simulation it was found out that the cross correlation between the oscillating motion and the deformation has rather big influence on the observability and the estimation accuracy.

A measurement system was developed and tested by SPEU. The investigations and testings that were carried out on special stands, and allowed to determine the system accuracy and to refine the error models of the sensors. In 1992 and 1993 marine testings of the system in Baltic Sea on hydrographic ship were carried out in cooperation with scientists of the Institute of Earth Magnetism. The first aim of the test was the determination of the angle orientation of the 3-axis magnetometer fixed in different points of the ship with respect to the inertial navigation system (INS). One vector of the ship angle rate was obtained by means of differentiation of the angles of roll, pitch and heading provided by the INS and by means of taking into account earth rate. Another vector was provided by the LG block that was rigidly fixed to the magnetometer. The mutual angular misalignment between INS and magnetometer was determined by Kalman filtering. The magnetometer orientation with respect to the geographic frame and the drifts of laser gyros were estimated also.

In Fig.3 the angular misalignment estimations are presented in two cases: a) for the longitudinal plane of the ship; b) for the cross plane of the ship. The standard deviation of the estimations are presented in the figures also. In Fig.4 the form of the two real signals from INS and LG block in a during of marine ship measurements is shown for roll angle.



a)



b)

Fig. 3 Estimation of Misalignment between INS and LG

Block

a) for longitudinal plane of the ship

b) for cross section the ship

B - estimation

C - RMS of estimation

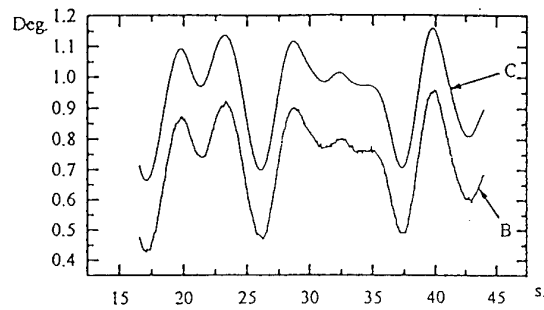


Fig. 4. Measurements by the INS (B) and the LG block (C) for Roll Angle

The example of 3-axis ( $\alpha$ ,  $\beta$ ,  $\gamma$ ) angular misalignment determination is presented in the Table.

The testings showed the measuring system capability of working under real conditions on marine objects. The random component of the angular misalignment estimation is equal to 0,32; 0,15; 0,23 the all in degree for the roll, pitch and heading angles  $\alpha$ ,  $\beta$ ,  $\gamma$  accordingly. The analysis indicated the necessity of adding a vertical reference to the system based on accelerometers.

Two Sets of Measurements for Angle Misalignment

Realisation number	Angular misalignment estimation (degree)			Estimation error (degree)		
	$\alpha$	$\beta$	$\gamma$	$\alpha$	$\beta$	$\gamma$
1	3,48	1,78	-0,29	0,57	0,64	0,53
2	3,73	1,76	-0,33	0,54	0,51	0,44

#### 4. HIGH PRECISION ANGLE MEASUREMENTS

On the basis of a LG a high precision dynamic angular measuring system was developed. Such a system allowed to estimate the drift of gyro platforms for various types of ballistic rockets in an extremely short time. The principles of the laser goniometer are shown in Fig. 5. The LG and an optical polygon (OP) are mounted on a common rotating axis. The laser beam from the null indicator (NI) comes to the polygon face and reflects consecutively from the two mirrors, the reference mirror (RM) fixed on the base and the control mirror (CM) which is on the platform. The LG pulses between these two events are counted and define the angle between both mirrors..

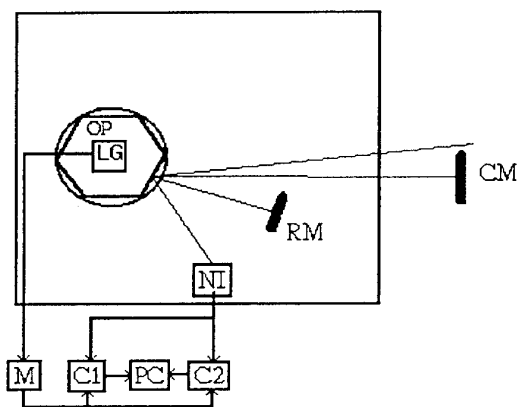


Fig.5. The Scheme of the Laser Goniometric System (LGS) for the Measurement of the Object Angular Position.

M multiplier of LG output signal frequency  
C1, C2 counters  
PC personal computer

The described laser goniometric system (LGS) was developed and successfully used for the estimation of the navigation systems accuracy. In the same time the comprehension appeared that the developed LGS is a system with more wide range of capabilities. This system is similar to the photoelectric autocollimator, but its range is with 30 deg. almost hundred times as much as the maximum range of known photoelectric autocollimators, Elcomate-2000, for instance. At the same time the accuracy of the LGS is on the level of the best photoelectric autocollimators. In Fig.6 the results of investigations are presented which were obtained in the angle measurement laboratory of PTB, Braunschweig, Germany. During the measurements the LGS was set on the standard turn table and was turned from 0 to 30 degrees in 1 degree steps. The error of the standard

turn table was not more than 0,1 arcs. During the measurements the LGS was mounted on the turn table and the CM was fixed on the stationary base. From Fig.6

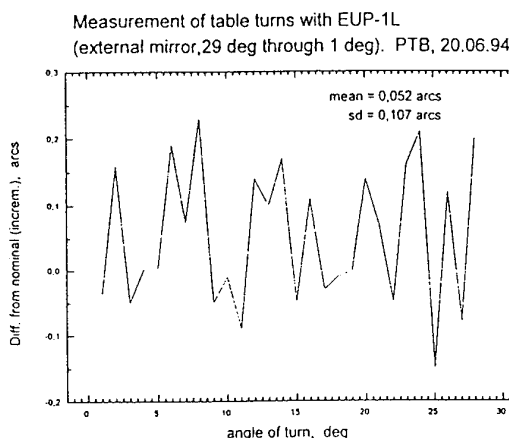


Fig. 6. Measurement of Turn Table Angle Position by LGS.

it is possible to see that the LGS measurements differ from the nominal values of the turn angle with the systematic component of about 0,05 arcs and the random component (standard deviation) - 0,11 arcs in the whole measurement range.

Another efficient application of the LGS is the certification of various angle transducers. After some modification it was used for certification of optical encoders of Heidenhain. In Fig.7 the results of several series of measurements for the optical encoder RON 255 (18000 scale marks) are presented.

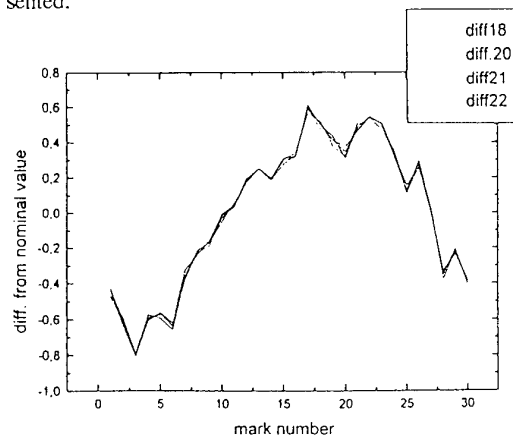


Fig. 7. Repeatability of Measurements by LGS.

Due to electronic limits the output signal frequency of the RON255 was divided by a factor of 300 during the measurements. After this division 30 angle intervals of the encoder were certified (one interval - 12 deg.). The estimation of the random component of the error obtained from 25 series of measurements was about to 0.02 arcs.

#### CONCLUSION

Laser gyro technology developed primarily for military application can fairly well be converted to civil ones. Russian examples for such conversions are in the field of track surveying, the measurement of the deformation of

long objects (tankers, huge aircraft) and the high precision angular and angular rate measurements. These examples are discussed and measurement results are presented.

In Russia and in Germany research in the field of high precision goniometry with laser gyro technology goes back to the time before perestroika. A very fruitful cooperation was initiated after that time between SPEU, DLR and PTB with support of DLR and of the German Ministry for Research and Development (BMFT). Contacts with industries were initiated by this cooperation, too. Problems of track surveying are other example for a fruitful international cooperation. The Deutsche Bahn AG is the German partner of SPEU in this field.

## NAVIGATIONAL TECHNOLOGY OF DUAL USAGE

V.G. Peshekhonov  
I.M. Okon  
L.P. Nesenjuk  
Yu.P. Belous

State Scientific Centre of the Russian Federation - Central R&D Institute "Elektropribor"  
(30, Malaya Posadskaya St., Saint Petersburg, 197046, Russia)

### SUMMARY

Under the new conditions of defence production conversion and basing on high technologies that were developed for the production of military navigation technology the Central R&D Institute "Elektropribor" has been developing and starts manufacturing products for civil application. Part of the project is dual usage technology. Three trends of the research are considered in this paper: 1) a gimbaled-type inertial system used to inspect railway tracks and in inertial geodesy; 2) gyro-stabilized gravity meter for geological prospecting of oil and gas from ships and planes; 3) shipborne integrated chartgraphic navigation-controlling system.

### 1 INTRODUCTION

Unprecedented scales of reduction of orders for military technology in Russia (in 1993 the output of military production accounted for around 30% of 1991 level) forced development engineers and manufacturers of weapons to look urgently for commercial applications of their designs and technologies.

The approach to this problem and the first results obtained in solving it are set forth in the present paper - the Central R&D Institute "Elektropribor" (St. Petersburg, Russia) will be taken as an example.

Since 1994 the institute has the status of the State Scientific Centre of the Russian Federation and is the leading Russian enterprise in the field of precise gyro technology, marine navigation and marine gravimetry. The institute carries out the full cycle of works on the new techniques creation - from theoretical investigations to production of industrial specimens, it being the usual practice in Russia for such institutes.

Before the reduction of the Defence Ministry order more than 90% of the institute developments were carried out by the orders of that Ministry. The institute has developed inertial systems and navigation complexes, which are being exploited in navy, all shipborne systems of gyroscopic stabilization, all marine gravimeters for oceanographic service, many of shipborne automatic control systems.

At present the defence order of the institute is less than 50% of the total volume of work, and the tendency to its reduction remains. The institute seeks and finds the new spheres of efforts application. At this we are guided by the following criteria:

- \* a new development, independent of its sphere of application, should be based on advanced technologies the institute possesses;
- \* as a rule, the institute undertakes to design and manufacture the production which was not earlier produced in Russia or has important advantages in

comparison with the one in the market.

By now 20 new designs, which meet these criteria are being completed. Part of them is the equipment of dual usage. Three of such developments are considered in this paper.

### 2 UNIVERSAL INERTIAL SYSTEM

Marine inertial navigation systems (INS) is the most important type of the institute production. The reduction of their development and manufacture is one of the most painful consequences of defence order curtailment. At the same time at present INS are more often used for new functions, mainly for construction of non-disturbable reference coordinate system of moving vehicle, in which the parameters of motion are being measured (accelerations, velocities, displacements).

In this direction it was possible to solve new commercial problems, two of them are discussed below.

*Railway track monitoring system on the base of INS.*  
Gyroscopic facilities have been used for railway track monitoring for more than 30 years. In the country with large extension of the railways, such as Russia, this way of monitoring is of special significance. Dozens of track-testing cars-laboratories have been constructed and are widely operated; their equipment includes short-period gyroscopic pendulums, which are used to determine the relative height of rails.

However the accuracy of gyroscopic pendulum disturbed by accelerations is not sufficient. Besides, the measurements are only possible on the base, determined by the design of a car-laboratory (of the order of 20 m), whereas with the increased velocities of the train motion the role of errors with large period (of the order of 100 m) grows.

It is necessary to use non-disturbable gyroscopic platform. The analysis of the requirements to the non-disturbable (inertial) system of a car-laboratory [1] showed that to measure the mutual height of rails to error of the order of 1 mm, the measurement accuracy of INS supporting platform turning angle relative to the longitudinal axis must be no worse than 2 arc min. For measuring the vertical alignment of a road to the accuracy of 2 mm it is necessary to measure the angles of pitch to the accuracy no worse than 0,2 arc min.

These accuracies should be provided under vibrations within the range of 1 - 50 Hz with amplitude up to 1 g, single shocks with peak value up to 3 g and car vibrations with frequency 0,1 - 5 Hz.

The shipborne INS on the base of floated gyros, which prototype was manufactured in 1991, completely meets the indicated requirements. It was intended for new navy ships, but was not claimed



for by the customer. In this connection there appeared the idea to use the INS prototype as the pre-image of the railway gyroplatform.

This prototype testings carried out on the special railway proving ground near Moscow in 1994 (the route represents the regular circle by radius, equal 955 m), showed that INS provides determination of track profile irregularities with error no worse than 4 mm for 200 m of a route. The error in determining irregularities in a plan ran to 1 - 4 mm for 100 m of a route, that of the testing circle coordinate centre - 2 m, of the circle radius - 1 m.

So, the full-scale testings of the prototype verified the potentialities of INS application for estimation of long-period track irregularities.

At present the specialized INS "Marshrut" has been manufactured and is being adjusted. It is smaller and lighter and less expensive in comparison with the tested prototype, at the same time, its accuracy characteristics are higher.

Semi-analytic type INS "Marshrut" is based on floated gyroscopes with random gyro drift no worse than  $5 \cdot 10^{-3}$  deg/hr, accelerometer zero drift no more than 10 arc sec, angular error of gyro mounting no more than 20 arc sec, control circuit gain error - 10-2%. The circuit with integral correction with damping of oscillation from external velocity source (odometer) is used.

To exclude the growth of dispersion of INS output data there used the information from external position sensor-receiver of satellite navigation GPS system, operating in differential mode.

The mode of forced rotation of stabilization platform relative to the azimuth axis is used, enabling continuous calibration mode during INS operation at which the systematic components of gyro drift, accelerometer zero drift, angles of gyro nonadjustment and errors of gyro control coefficient are continuously estimated by information from external position sources (GPS receiver and odometer).

The INS devices, main specifications and mass-dimension parameters are shown in fig.1. We should notice that the overall dimensions and the mass of a specialized computer units may be considerably reduced provided western electronics element base is used.

The system "Marshrut" will be completed in 1995, the deliveries to customers will begin from the second half of 1996.

*Inertial geodetic system.* In parallel with the development of the INS "Marshrut" considered above the possibilities of its other applications, not connected with railway transport, were analyzed.

In the modern complicated economical conditions it is difficult to rely upon commercial success of the new INS production, unless its application is provided at least in two-three spheres of engineering.

The use of the INS "Marshrut" in geodesy seems very prospective. It is known that the inertial geodesy is a quickly developing new trend of INS usage. The geodetic INS, created by the present time, showed the possibility of increasing the geodetic survey efficiency in comparison with traditional geodetic methods on roads with extension of the order of 100 km, when the vehicle - INS carrier moves by intervals of several minutes and stops of the order of 1 min.

As a rule, the laser strapdown INS (SINS) are used to

solve problems of inertial geodesy. The obvious advantages of SINS are small readiness time, immunity to external actions, relatively low cost. However, the SINS disadvantage - low accuracy - is also obvious. INS "Marshrut" has several times higher accuracy characteristics.

Detailed investigation of mathematical error model of INS "Marshrut" shows that this system can find its application in inertial geodesy providing the accuracy of coordinate determination is no worse than 1 m on the distance up to 100 km.

The testings of the INS "Marshrut" on the geodetic proving ground are planned for the middle of 1995.

### 3 UNIVERSAL GYROSTABILIZED GRAVIMETER

Gravimetry themes of the institute, which had been earlier oriented to the needs of oceanographic service of the Ministry of Defence for more than 20 years, proved to be in no less difficult situation, than inertial ones. Using the experience of creation of marine automatized gravity systems, providing gravimetric surveying with error less than 1 m Gal all over the World Ocean when rolling and pitching are considerable and intervals between calls at a port are long (more than 1 month), the institute started the development of gravity meter for geologic prospecting on the sea. The analysis of gravitational prospecting potentialities from geologic ships and airplanes in searching for mineral resources, oil and gas, in particular, determined new requirements to gravimetry systems.

So, for searching of gas and oil containing zones on shelf the marine gravity meter must provide the detection of anomalies of less than 0,5 mGal of amplitude and less than 1 km in length, that considerably rises the requirements for resolution and operating speed of gravity sensor. Such qualities as compactness, low cost, simplicity of mounting, dismounting and transporting become very essential too.

At the same time the requirements for accuracy of zero drift accounting, for accuracy of scale factor in large measurement range and for reliability during long time functioning are more lenient than for gravity meters designed to use all over the World Ocean.

Considering the new requirements in 1990-1993 on the base of modern gravity meter, ordered by Oceanographic Service, the modified gravimetry system "Chekan" intended for usage on geologic ships and aircrafts has been designed and tested [2, 3].

The component parts and main specifications of the system "Chekan-M" are shown in fig.2.

System "Chekan" and its components were tested on Institute's test bench and during two years of its exploitation on the geologic prospecting vessel. Preliminary testings were also carried out on airplanes.

In summer 1993 the system "Chekan" jointly with other home produced gravity meters was used for carrying out the gravimetric prospecting on a shelf in Barents Sea region. This work was intended for research of gravimetric survey efficiency by comparing its results with seismic prospecting data, and also for comparison of survey accuracy by different gravity meter types. The important feature of conducted works was the fact that for the first time in home practice the receiver of satellite navigation system GPS operating in code differential mode was used for survey coordinating. The coordinating error did not exceed 10 m. By the present time the final data processing is not completed, but according to

preliminary estimations the results of gravimetric survey agree with seismic prospecting results. Also the high accuracy of gravity meter system "Chekan" was confirmed.

The systems random error determined by cross points was 0,3 mGal, that allowed to make a map of Free Air Anomaly field in isolines with section 0,5 mGal.

If the results of sea tests of system "Chekan" were expected to a great extent, taking into account large experience of development and operation of sea gravity meter systems, then the first testings of the system on the airplanes AH-12 and AH-30 in the region of Ladoga lake performed in 1992 and 1993 are our entrance into new sphere that demands thorough check of previously gained experience of development and quick adaptation to new conditions.

The airplanes were equipped with the receiver A-734 of satellite navigation system GLONASS, airborne inertial navigation system and radio altimeter. The average flight altitude was 1000 m and velocity - 100 m/s. During the testing we made sure of normal functioning of all system components, verified the basic opportunity to use gravimeter "Chekan" for air survey and defined the trends of further work on air gravity meter creation.

The main source of errors of airborne gravity meter were vertical accelerations caused by flight altitude variation with amplitude about 1 m and with prevalent period about 40 s. To reduce the survey error to 1 mGal, that meets the modern requirements, it is necessary to provide the measurement of flight altitude variation with error of order about 1 cm. According to the data of "Carson Services, Inc." firm, this problem may be solved by means of satellite navigation systems GPS and GLONASS, operating in phase differential mode. The works in this direction are planned with the geological enterprises of Russia and Braunschweig technical university (Germany) for the next year.

#### 4 ELECTRONIC CHART DISPLAY INFORMATION SYSTEM (ECDIS)

In contrast to two preceding directions of the Institute work this trend, formed at the end of the 80-ies, was from the beginning oriented on the development of the dual usage equipment. Practically simultaneously the elaboration of the system for naval and civil ships was started.

The block-diagram of ECDIS is given in Fig. 3. The central component is a marinized personal computer of the standard configuration. Through standard ports RS232 the computer interfaces:

- with sensors of information about the coordinates of the position, heading, relative velocity and depth under the keel of the ship and also the measured bearing distances and distances of the radar reference points.
- with any types of autopilots, having an interface according to IEC 1162 standard.

The system provides the solution of the three groups of tasks: CHART, NAVIGATION and CONTROL.

The group of tasks, named CHART includes:

- synthesis of electronic navigation chart (ENC), representation, scale changing, off-centering, change of palette (day/night) and variation of ENC load, the output of information references on ENC and its objects, forming, representation and correction of the available ENC catalogue, mapping of the ship's sign and silhouette, the electronic magnifying glass and the protractor;

- ENC correction;
- ENC selection for the given point, area and route.

The group of tasks, named NAVIGATION, includes:

- preliminary plotting of the route with application and correction (with the check up for navigational safety) of the route points;
- dead reckoning of the ship route with estimation of accuracy;
- positional correction of the system by data from both GPS, LORAN (DECCA) and also automatic radar plotting system, working-out information about ranges and bearings of reference points and also about distances up to the shore line in the direction of the set bearings;
- elaboration of the direct vector, route angle and absolute velocity;
- automatic continuous control of navigational sailing safety with calculation and representation of the dangerous headings sectors and safety zones, indication of navigational table and also the traces and vectors of the targets, tracked by the automatic radar plotting system;
- ship motion control on the given way line or in the given motion strap with the output of warning signals;
- memorizing and indication of the ship trajectory during the last 8 hours.

The group of CONTROL tasks includes:

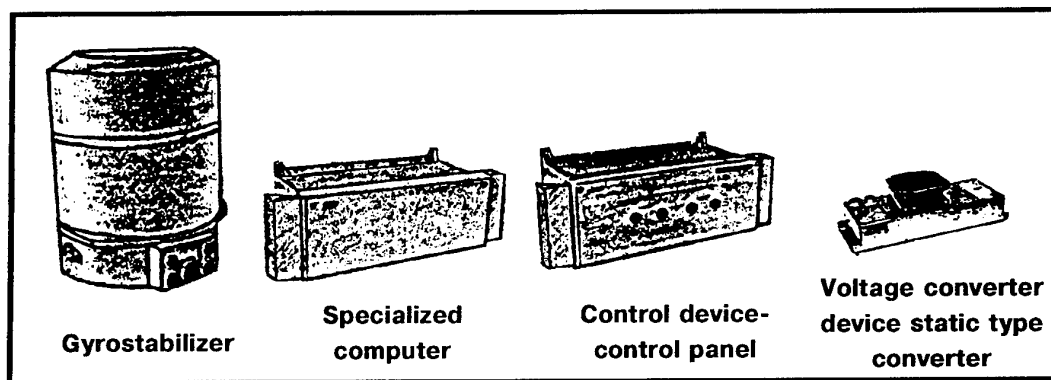
- identification of parameters of the controlled ship;
- stabilization of ship motion on the given way line in the given motion strap with the generation of the control signals by the rudder blade.

In 1993 the testbed and marine trials of the prototype with ENC were carried out. They allowed, among other aims, to form the conception of the integrated navigational system and ship motion control with ENC for raising safety of sailing and economic efficiency of different ships operation, first of all transport, when sailing by the given routes.

In 1994 the development of the ENC prototype must be completed and the expanded testbed trials must be carried out. The deliveries of ECDIS are planned to begin from the second half of 1995.

#### REFERENCES

- 1 Okon I.M., Vaysgant I.B., Tupyev V.A., "Inertial goniometrical system for high-speed railway International Conference on Gyroscopic track-testing car", in "First Saint Petersburg Technology", S.Petersburg: CSRI "Elektropribor", 1994, pp. 110 - 119.
- 2 Nesenjuk L.P., Peshekhonov V.G., Elinson L.S., "Marine Gravity System", in "First Annual Workshop
- 3 Blazhnov B.A., Elinson L.S., Nesenjuk L.P., Peshekhonov V.G., "Marine and Airborne Gyrostabilized Gravimeters which are Developed in CSRI "Elektropribor", in "First Saint Petersburg International Conference on Gyroscopic Technology", S.Petersburg: CSRI "Elektropribor", 1994. - P. 126 - 312.



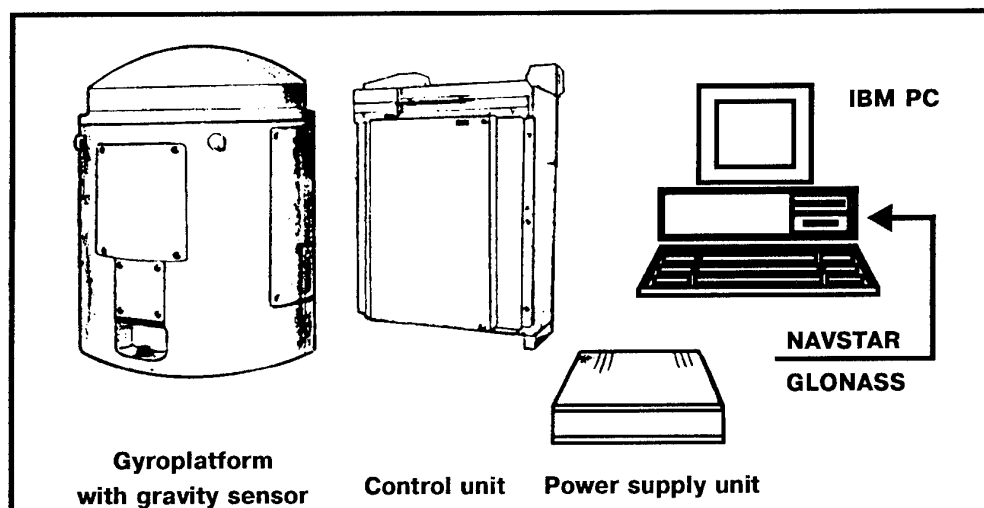
## COMPOSITION

	Dimensions, mm	Weight, kg
Gyrostabilizer	390x480x390	65
Specialized computer	945x480x325	65
Control device - control panel	785x480x325	55
Voltage converter device static type converter	400x150x100	10

## SPECIFICATIONS

Tilt angles measurement accuracy, arc min	0,2
Heading working-out accuracy, arc min	3 (for 60° latitude)
Instantaneous linear velocity components measurement accuracy, mm/s	0,2
Power supply	380/220 V A.C. 50/60 Hz (3 phases) or 27 V D.C. in the case of VCD absence
Power consumed, VA	less than 1000
Speed of the track-testing van, km/h	up to 250 when latitude changing up to +85°
Permissible maximum acceleration during turns, m/sec <sup>2</sup>	2,2
Permissible vibration in the frequency range 1-50 Hz	with acceleration up to 1 g
Permissible individual shocks	with acceleration up to 3 g
Format of the output information	digital with 1 kHz frequency
Assigned resource	30000 hours
Readiness time when parking, min	less than 15

**Fig. 1**  
**Composition and specifications of precise inertial measuring system**  
**"Marshrut"**



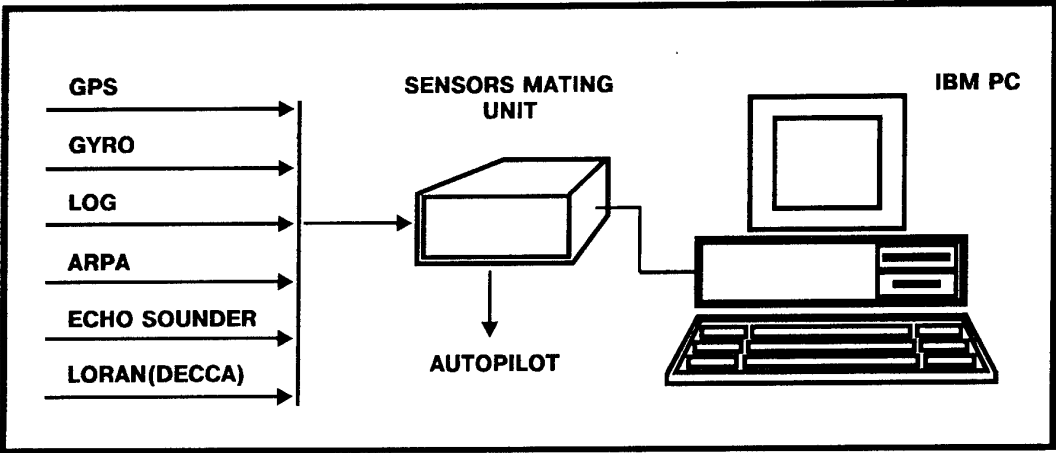
## COMPOSITION

	Dimensions, mm	Weight, kg
Gyroplatform with gravity sensor	Ø590x750	170
Control unit	568x842x530	120
Power supply unit	150x150x800	12
Personal computer compatible with IBM PC		<50

## SPECIFICATIONS

Root-mean-square survey error (if oscillating accelerations do not exceed 100 Gal)	no more than 0,5 mGal
Scale division unit	0,01 mGal
Error of drift rate estimations:	
prior no more than	0,05 mGal per 24 h
posterior	0,002 mGal per 24 h
Error caused by oscillating accelerations (cross-coupling effect)	practically absent
Systematic error caused by scale factor estimation uncertainty on the manufacturing enterprise test bed (for gravity change range +3 Gal)	no more than 1 mGal
GP systematic error	no more than 30 arc sec
GP dynamic error (if rolling and pitching angles do not exceed 15°)	no more than 15 arc sec
Operating life	60000 h
Power supply	400 Hz 3x220 V 300 W (1000 W when starting) 50 Hz 220 V 200 W

**Fig. 2**  
**Composition and specifications**  
**of Gravity Meter "Chekan-M"**



COMPOSITION

	Dimensions, mm	Weight, kg
Sensors mating unit	330x210x160	3,5
Personal computer compatible with IBM PC		< 50

SPECIFICATIONS

Total error in mapping coordinates	no worse than 1 mm
Bearing measurement errors	no worse than 0,5°
Distance measurement errors	no worse than 0,7°
Service life	60000 h
Power supply	50 Hz 220 V
Power consumption	no more than 250 W

**Fig. 3**  
**Composition and specifications of integrated electronic cartographic navigation-controlling system**

## DUAL-USE MICROMECHANICAL INERTIAL SENSORS

**John M. Elwell Jr.**

The Charles Stark Draper Laboratory, Inc.  
555 Technology Square  
Cambridge, Massachusetts, U.S.A.  
02139-3563

### SUMMARY

A new industry, which will provide low-cost silicon-based inertial sensors to the commercial and military markets, is being created. Inertial measurement units are used extensively in military systems, and new versions are expected to find their way into commercial products, such as automobiles, as production costs fall as technology advances. An automotive inertial measurement unit can be expected to perform a complete range of control, diagnostic, and navigation functions. These functions are expected to provide significant active safety, performance, comfort, convenience, and fuel economy advantages to the automotive consumer. An inertial measurement unit applicable to the automobile industry would meet many of the performance requirements for the military in important areas, such as antenna and image stabilization, autopilot control, and the guidance of smart weapons. Such a new industrial base will significantly reduce the acquisition cost of many future tactical weapons systems. An alliance, consisting of the Charles Stark Draper Laboratory and Rockwell International, has been created to develop inertial products for this new industry.

### INTRODUCTION

A new industry that has the potential to become the next Silicon Valley is being created. This new industrial base will also significantly reduce the acquisition cost of many future tactical weapons systems. An alliance, consisting of the Charles Stark Draper Laboratory and Rockwell International, has been created to develop inertial products for this new industry.

This major new industry is in the currently evolving technology of silicon micromachining, estimated to have a yearly market potential on the order of \$8 billion. The single largest portion, representing approximately one half, of this market is expected to be in the automobile inertial sensor area. Yearly worldwide sales of automobiles, trucks, and busses currently runs at about 50 million units.

Inertial measurement units (IMUs), consisting of several orthogonal gyroscopes and accelerometers along with associated processing electronics, are used extensively in military systems. An IMU for the automobile industry would meet many of the performance requirements for the military in important areas, such as antenna and image stabilization, autopilot control, and the guidance of smart weapons. In addition, miniature low-cost IMU availability is expected to result in new military weapons concepts that would not have been practical with older technology. For example, this technology will allow precision guidance of many munitions, including bombs, artillery shells, and mortars. Such

new capability, in addition to enhancing the force structure, is expected to reduce procurement buys compared to conventional munitions, and to simplify logistics, resulting in less manpower needed to support an equivalent number of troops in the field. Force projections for the year 2000 and beyond anticipate yearly procurements of perhaps 200,000 units in this low-cost precision munitions area alone. The availability of active manufacturing facilities, producing silicon micromachined IMUs at comparable performance levels, will significantly reduce the acquisition costs for these and many other tactical weapons systems.

Draper has been actively developing silicon micromechanical inertial sensor and IMU technology for the past eight years. We have brought this basic technology to the point where the required level of performance and manufacturability indicates commercial viability, and we have formed an alliance with Rockwell International to productize and manufacture micromechanical inertial instruments for the marketplace. This relationship was formed in 1993, and extensive investments have been made by both organizations in this new inertial technology and in preparing it for eventual production. Our silicon micromachining technology is expected to result in the lowest cost product.

### THE TECHNOLOGY

The process of anisotropic etching of boron-diffused silicon provides for the manufacture of micron-sized mechanical structures. Draper has been developing many different silicon micromachined inertial sensor designs employing both single-crystal and polysilicon technologies. An example of one of our single-crystal rebalanced gyroscope designs is shown in Figure 1 next to an ant for comparison. This micromechanical gyro is a double gimbal design with an oscillating vertical mass mounted on the inner gimbal in order to store momentum. This device is about 300 by 600  $\mu\text{m}$  in size. Recently, this gyro has been redesigned using a planar tuning fork construction, which is more optimal for micromechanical fabrication. For a 1-mm silicon tuning fork gyroscope design, the eventual projected performance is 1 deg/h bias and a performance of 28 deg/h has already been demonstrated.

### THE FABRICATION PROCESS

Micromachining of single-crystal silicon using a "dissolved wafer process" has been selected as the fabrication method for this program's inertial sensors. Three to ten thousand sensors, gyroscopes or accelerometers can be fabricated from a single five-inch wafer of silicon. It is this attribute that results in the low cost associated with any IMU developed from this technology. The potential cost savings over conventional gyroscopes and



Figure 1. Silicon micromechanical gyro size comparison.

accelerometers assembled from piece parts is two to three orders of magnitude.

Micromachining of single-crystal silicon using a "dissolved wafer process" as shown in Figure 2 contains the fewest number of process steps and leads to the simplest process. Undercutting of the silicon crystal, used in other processes, involves many more steps, is harder to control, and is more expensive. Polysilicon as an alternative has more steps, and the mechanical characteristics of the structures are not yet fully understood. In production, wafer scale bonding and etching of silicon and Pyrex will be done. Wafer-level testing and trim-

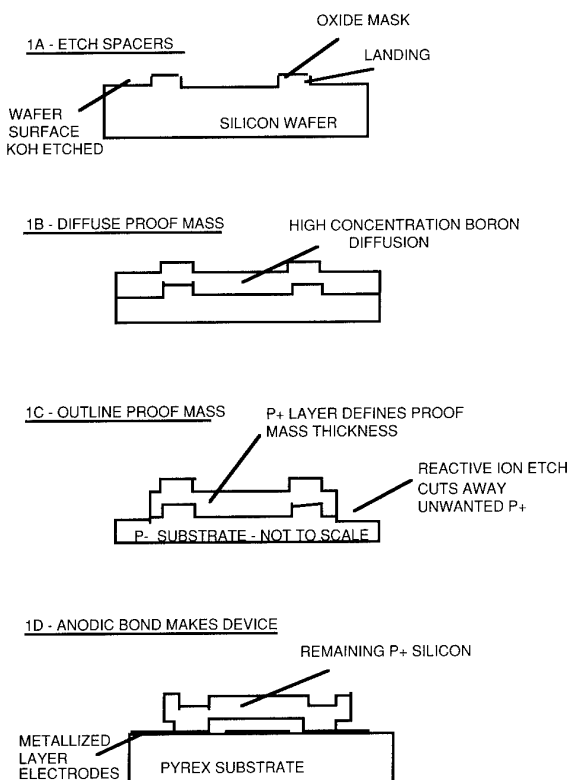


Figure 2. Dissolved wafer process.

ming, if necessary, are also envisioned to minimize costs.

The process begins with protrusions or "landings" that determine the electrode to proof mass spacing gap, and are first created by photomasking and KOH etching the surface of the wafer. Next, the proof mass thickness is determined by a very deep, high-concentration boron diffusion into the lightly doped silicon substrate. The outline geometry of the device is then defined by a second photomasking step and a reactive ion etching process that cuts vertically through the P+ diffusion. At this point, the silicon half of the wafer is complete and is ready for bonding to the Pyrex wafer. The Pyrex substrate has been patterned, etched, and metallized in preparation for bonding to the silicon wafer. After bonding, the Pyrex/silicon assembly is then etched in an Ethylene Diamine Pyrochatechol, or EDP, solution. The solution selectively etches away the undoped silicon, leaving the free-standing gyro structure bonded to the Pyrex.

## GYROSCOPE

A comb drive tuning fork design was selected for the gyro. A photograph of one of our silicon micromachined tuning fork gyroscopes fabricated using our dissolved wafer process is shown in Figure 3. Tuning fork tines are driven by electrostatic combs that are excited in opposite directions so that forces are generated that do not depend on the lateral position of the masses. The resulting large amplitude vibrations yield high gyro sensitivity. Rotations in the plane of the silicon substrate result in Coriolis forces that lift one mass up and the other down. The output motion is detected, amplified by the preamplifiers, and processed by the signal processing electronics. The resulting rebalance signal is proportional to the true inertial angle rate.

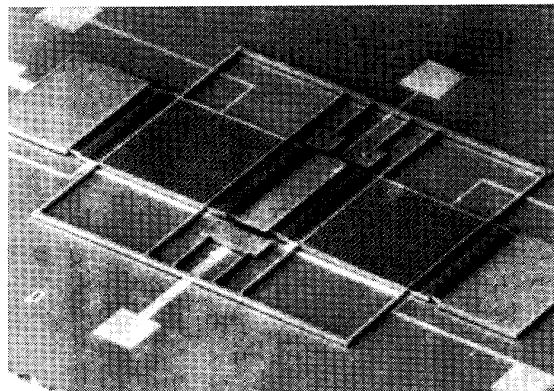


Figure 3. Micromachined comb drive tuning fork gyro.

For gyroscopes whose active elements are roughly 1 mm in dimension, projected performance is 1 deg/h. Bandwidth resolution is limited by input voltage noise in the preamplifier, which senses proof mass displacements along the input axis and instrument gain. Performance at the 28 deg/h level has already been demonstrated.

## ACCELEROMETER

Current micromechanical accelerometer design concepts feature a gimbaled pendulous proof mass supported by torsional flexure that rotates about the flexures under input-axis acceleration. The proof mass rotation angle is proportional to acceleration and is measured by a pair of capacitive electrode signal generators. The accelerometer may be rebalanced via electrodes to provide improved dynamic range. When used in a rebalance mode, the signal is integrated and fed back to a torque generator. The torque generator output is applied to the torquing electrodes to rebalance the proof mass to obtain an output null. The output of the integrator is a measure of the acceleration being sensed.

Using the dissolved wafer process, the flexures of the accelerometer are connected to both the proof mass and the landings, which are the only part of the silicon structure to make physical contact with the glass substrate. The proof mass and torsion parts of the flexures are suspended over the electrode pattern on the glass. A photograph of an actual accelerometer sensor fabricated at Draper Laboratory is shown in Figure 4. The proof mass dimensions are  $170 \times 180 \mu\text{m}$  and the proof mass extends an additional  $55 \mu\text{m}$  on one side to provide the asymmetry required to sense acceleration.

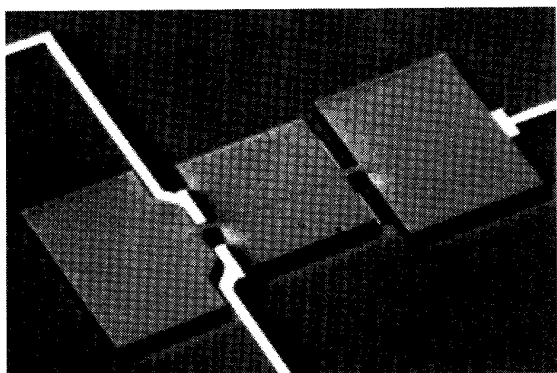


Figure 4. Micromechanical accelerometer.

## INERTIAL MEASUREMENT UNIT ARCHITECTURE

Because the micromechanical sensors, which are the heart of the IMU, are produced in quantities of 3,000 to 10,000 per 5-inch silicon wafer, they do not represent a significant factor in the overall IMU cost. The cost of the IMU will be driven primarily by the packaging, testing, and electronics approaches that are employed.

For a full-up IMU that has six degrees of freedom (three rate, three acceleration), a cost goal is to concentrate on minimizing the electronics, that is, reduce the amount of silicon area and also the number of discrete components that can add to the complexity of the packaging design. Figure 5 is an overall block diagram of the IMU architecture. It consists of three major elements: the sensor assembly, the conversion assembly, and the processor assembly. Perhaps the ultimate goal toward

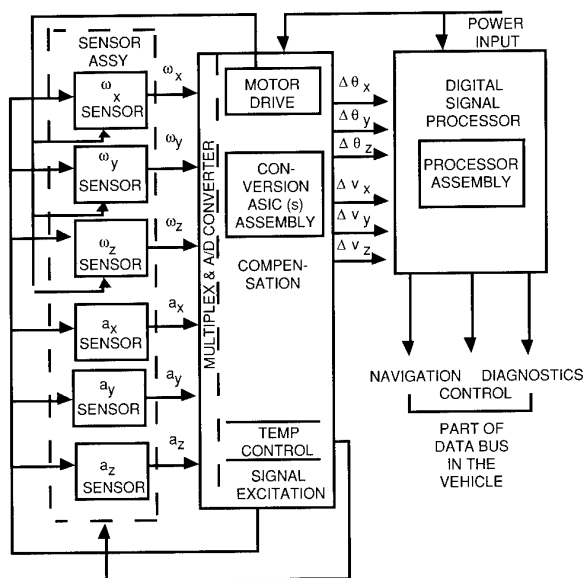


Figure 5. Inertial measurement unit architecture.

reducing cost is to have all functions implemented on a single silicon chip. Current state-of-the-art in micromachined sensors probably puts such an approach beyond the year 2000, however, it does represent the ultimate technical goal and is clearly the means to obtain the lowest cost product. A nearer term approach is to have each sensor with its own application-specific integrated circuit (ASIC) generating an input for the microprocessor. This approach is well within the current state of the art. This approach leads to a system with six integrated circuits for conversion, a sensor assembly, a processor chip, and miscellaneous discrete components.

The sensor assembly will consist of multiple inertial sensors, along with their associated buffer amplifiers, which must be located as close to the sensor as possible in order to minimize stray capacitance. One approach for achieving three orthogonal sensor axes is to mount the six inertial instruments on the face of a cube. An alternative approach is to have two forms of gyro and accelerometer sensing, that is, "in-plane" and "out-of-plane" designs that can be mounted on a single plane. Ultimately, all six sensors can then be fabricated on a single chip. The inertial sensors must be fabricated with a vacuum cap over the gyro and a hermetic seal cap over the accelerometer in order to meet their performance requirements. This protects the moving elements from contamination, since particles can affect performance.

## TRANSITION TO PRODUCTION

Figure 6 depicts those steps involved in the Alliance transition process and uses as a model, the transition of very-large-scale integrated circuit (VLSI) products from the experimental stage to volume production.

The design and development activities are led by Draper. Micromechanical inertial sensor and IMU technology are then transitioned to Rockwell, and this



TECHNOLOGY	DESIGN	DEVELOPMENT	PROTOTYPES	LOW RATE PROD.	VOLUME PRODUCTION
TRANSITION THE "EXPERIMENTAL" TO "STATE-OF-THE-ART"	ESTABLISH & IMPLEMENT REQUIREMENTS: SI PROCESS, PHOTO MASKS, DESIGN RULES, AND EQUIPMENT	PRODUCT DEVELOPMENT, MFG. PROCESS QUAL., PACKAGING QUAL., CAD TOOLS, MARKETING & SALES	PRODUCT QUAL., CUSTOMER SAMPLES, MTBF, FFU, APPLICATION ENG. SUPPORT	PROCESS CONTROLS, YIELD IMPROVEMENT, COST REDUCTIONS, MARKET ACCEPTANCE	MARKET SHARE DOMINANCE  PRODUCT MIGRATIONS

Figure 6. The transition process.

process is facilitated by the duplication and/or adaptation of the Draper developmental designs and processes. Rockwell will integrate the process technology, device design, packaging, test, and the product requirements in order to achieve necessary production levels.

### MARKET PROJECTIONS

The dual-use performance flowchart for this automotive technology is shown in Figure 7. Automotive applications for IMUs are shown at the top of this figure, and it can be seen that the range of possible requirements runs from about 3600 deg/h to close to 100 deg/h for bias stability performance. Accelerometer requirements scale comparably to the gyro performance requirements. Corresponding to each range of automotive performance requirements are a set of military requirements. It is seen that many military requirements are covered within the same general performance range as the automotive IMU.

### COMMERCIAL MARKETPLACE

Commercial applications for low-cost inertial sensors have already been identified in the areas of general aviation, camcorders, binoculars, telescopes, cameras,

robotics, industrial automation, medical electronics, PC mouse, virtual reality, and toys, in addition to the aforementioned automobile area. Actual gyro performance provided will be a function of the level of sophistication of the sensor electronics selected and the sensor mass balancing required for each application. These process steps are the primary determinants of unit product cost. An analysis of the product and market have resulted in the relationship shown in Figure 8. In this figure, we have plotted expected per-axis gyro price with respect to corresponding performance available. The range of uncertainty in this analysis is represented by the breadth of the line.

Today, the automobile industry is evaluating the utility of gyroscope and accelerometer assemblies in concept cars. Initially, inertial requirements are being determined for a relatively simple, low-performance gyro intended only to provide for a range of automotive control functions, such as four-wheel steering and automatic braking.

The ultimate objective is to use a full-up inertial measurement unit that will be able to perform the complete range of required control, diagnostic, and navigation functions planned for the automobile of the future. Some of these functions are shown in Table 1, and their

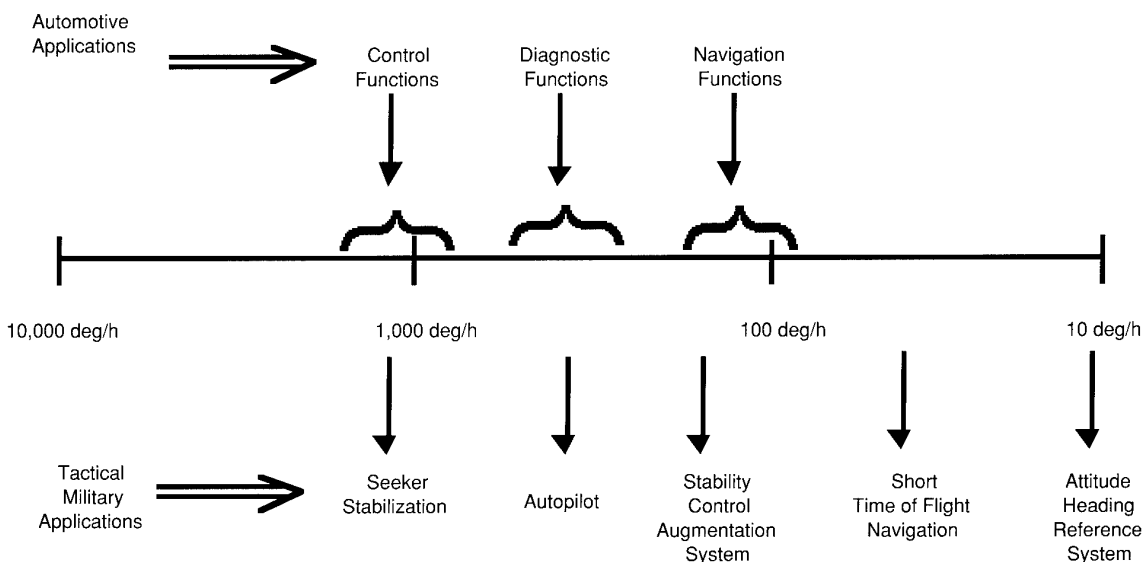


Figure 7. Dual-use technology.

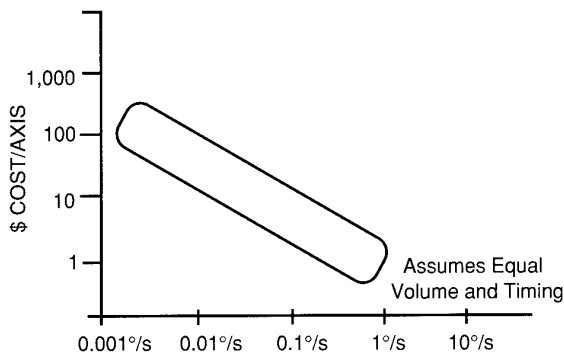


Figure 8. Market potential as a function of price.

Table 1. Automotive functions.

Control	Diagnostics	Navigation
Skid detector	Suspension System	Integrated highway systems sensor
ABS system	Engine response	GPS/inertial systems integration
Active suspension	Brake system	Collision avoidance component
Air bag backup	Crash recording component	
Four-wheel/all-wheel steering		

use is expected to provide significant active safety, performance, comfort, convenience, and fuel economy advantages to the automotive consumer.

Clearly, auto market size will be a significant function of the product selling price. Approximately 50 million autos, light trucks, heavy trucks, and busses are built every year worldwide. This turns out to be the dominating market sector within the silicon micromachined inertial market.

## MILITARY MARKETPLACE

The military uses both individual inertial sensors and IMUs in numerous weapon systems and will benefit significantly from commercial development. The largest consumption of inertial sensors, at a technical performance level, which is commensurate with the automotive industries needs, occurs in the tactical weapons area. Commercialization will result in a significant reduction in tactical system acquisition costs for the military. We have identified three broad classes of inertial applications for this technology. Table 2 presents examples of military applications for micromachined IMUs or sensors.

"New systems, capabilities, and concepts" applications are those that, while technically feasible prior to this point, may not have been justified on the basis of cost, but now become feasible given the low cost associated with micromechanical technology. Thus, new military capabilities will be created that never existed before. "New methods for solving old problems," represents those applications where inertial sensors are currently employed successfully, but which can be enhanced through the use of micromechanical technology. Use of this new technology can result in, for example, better packaging options, often reducing overall weapons system size and weight. "Technology insertion in current systems" represents P<sup>3</sup>I to systems currently under development such as BAT, JDAM, and JSOW. A lower cost IMU means that more missiles can be procured for the military with the same number of dollars.

Table 2. Military applications.

New Systems, Concepts, and Capabilities	New Methods of Solving Old Problems	Technology Insertion in Current Systems
Miniature guided projectiles	Tactical seeker stabilization	JDAM
Smart skins and structures	Autopilots	JSOW
Personal navigation	Short time of flight missiles	BAT
Guided bombs and artillery shells	Low cost compass attitude heading reference systems	

Since the fall of the former Soviet Union, the actual number of weapons systems that will be procured in the future by the Government is uncertain. However, the general trend is clearly away from large strategic systems toward smaller tactical systems, as was illustrated during the Gulf War. Predictions for the future size of the military market have been made independently and the largest portion of this new military market forecast is expected to be in munitions and projectiles, at an eventual rate of 200,000 per year.

## CONCLUSIONS

The entire silicon micromechanical market has been estimated at \$8 billion per year. Our alliance has independently estimated the size of the inertial sensor market, which is a subset to this overall market. Inertial sensors represent approximately one half of the overall market, and this submarket is primarily dominated by automobile industry needs.

Our analysis of the overall market size is summarized in Table 3.

Table 3. Inertial marketplace summary.

Applications	Price Per Axis	Number of Products Produced	Potential Market Volume
Cameras, camcorders, inertial mouse, other consumer items	\$1-15	$10^7$ - $10^8$ /year	\$100M
Automotive, marine, industrial, etc.	\$5-100	$10^5$ - $10^8$ /year	\$4,000M
Munitions, fusing, etc.	\$100-500	$10^4$ - $10^7$ /year	\$500M
Autopilot, stabilization, rate packages	\$100-1000	$10^4$ - $10^5$ /year	\$10M

This product is an ideal match to the definition of dual use, supporting closely coupled commercial and military applications. While the immediate product under discussion is to be an automotive IMU, individual inertial sensor products and other spinoffs of this technology are eventually expected to find their way into general aviation, camcorders, binoculars, telescopes, cameras, robotics, industrial automation, medical electronics, virtual reality, and toys.

## LASER GYROSCOPY TENDENCIES AND THEIR ANALYSIS OF DEVELOPMENT IN UKRAINE

ALEXANDER DOVBESHKO

Scientific - research institute of mechanics problem "Ritm",  
37, Peremogu aven., 4030 - "Ritm", Kiev, 252056, Ukraine.

## I. SUMMARY

The papers deal with the theoretical and experimental data analysis, approached accuracy and characteristics of laser gyroscopes obtained by Ukrainian firms.

Theoretical model of physical phenomena in ring laser with 4 mirrors resonator are created. Ring lasers are considered as continuous, nonlinear self-excited oscillatory system, that contain a number of limited and spatial nonuniform elements (active medium, diaphragms, mirrors). Model of laser generation that considers effect of more than 40 resonator and amplifying medium parameters on output laser characteristics (intensity, frequencies difference, locking zone, etc) was created. We have investigated the mechanism that determine a mode selection and backscattering light from mirrors and diaphragms influence on intensity and frequency difference of the traveling-wave in ring laser. The mode formation mechanism (caustic or guide, or guide-caustic type) that depends on resonator type and mirrors dimension, radius of curvature oneself and the channel shape and it's linear dimensions would be achieved in laser. It is shown, that the connection of the counter waves has diffractive as well as interference nature and is defined by parameters of the resonator mirrors and diaphragms as well as by their disposition as to the amplifying medium.

Using the latter, the methods and the devices that allow to decrease the influence of the static zone of the waves lock in on the output characteristics in 10-20 times have been created. Proceeding from the created mathematical model the methods of optimization element composition and parameters of optical-physical scheme of the ring laser and the systems of stabilization and control of the laser generation regime of the laser gyroscope have been worked out.

The microprocessor systems for laser gyroscope generation regime support and stabilization its parameters during exploitation were fulfilled. It is shown experimentally that laser gyroscope with such systems has a null drift 0.005 degree/hour and a random walk 0.003 degree/sqrt (hour).

## 1. INTRODUCTION.

The basis of all the modern inertial and navigation systems (NS) and the guidance systems (GS) for the aircraft, ships and other objects is the inertial measuring unit. The inertial block consists of 3 gyroscopes - to measure velocity of rotation around three orthogonal axes. The requirements to the gyroscope blocks (GB) of GS and NS are very high: resolving ability and null drift (ND) is 0,05 - 0,001 deg/hour (d/h), instability of scale coefficient (SC) is  $10^{-4}$  -  $10^{-5}$ , and dynamic range is  $10^{-6}$  -  $10^{-7}$ . Gyroscopes are also used as angle rate sensors in the systems of antennae control, aircraft flaps, robototechnics. They should provide dynamic range of  $10^{-4}$  -  $10^{-6}$ , ND of 1 - 0,05 deg/hour, stability of SC not worse than  $10^{-3}$  -  $10^{-4}$ .

For the both directions of gyroscopes application it is extremely necessary to provide low power consumption (2 - 20 Wt), volume (0,5 - 5 dm<sup>3</sup>), weight (0,5 - 8 kg), output time on the measuring regime (0,1 - 1 sec), performance of gyroscopes in the conditions of intensive knock strength (up to 200 g), vibrational (up to 10 g) overloading, when the temperature of environment varies at range of -60 C - +60 C.

That is why in the last ten years the designers of navigation and control systems take great interest in laser gyroscopes (LG). The devices of the mentioned types are based on the application of the Sagnac effect (electrodynamical analogue of the law of momentum conservation of photon flow propagating in the limited non-inertial space). The Sagnac effect was discovered in 1913. But only on the modern stage of development of quantum electronics elementary basis, after the development and introduction of a number of new

ideas about the maintenance of maximum effect display, it became possible to apply it to technics.

A sensitive element of laser gyroscope is the laser with ring resonator, where two counter-rotated moving waves are generated. Ring laser (RL) is a continuous, self-excited oscillatory non-linear structure, that consists of a number of dielectric mirrors, which provide propagation of waves on a limited circuit, placed between them space-limited diaphragms and sections with nonlinear amplifying medium. Imperfect conditions of ring laser elements, instability of their characteristics in time, essentially influences the frequential, amplitude-phase, polarization characteristics of generated waves. Considering the latter and the fact, that RL are being exploited in imperfect conditions (under different temperatures of environment, intensive vibrational and knock exposures, exposures of exterior electromagnetic, static and variable fields, etc), it is possible to conclude that to maintain all the abovementioned requirements to the output characteristics of RL is extremely difficult.

The problem of increasing stability of the RL output characteristics becomes more complicated because of the fact that at low angle rotation rate frequencies of counter waves will be locked in and the information about object rotation will be lost. To measure in the sphere of low angle rates, additional nonreciprocity for counter waves is created in RL. Instabilities of systems, that create an additional frequencies shift, introduce a direct error into the results of measurements. As the result, the process of forming of output characteristics of waves, generated in RL, is accompanied by a great number of physical phenomena of different origin, but by virtue of the fact that they are small and are closely interconnected, they lead to almost identical change of beat frequency and other laser parameters. In this connection it is extremely difficult to select physical mechanisms effecting accuracy characteristics of the concrete real gyroscope. For this you need to know a large collection of laser parameters, that are unknown to the moment of investigation.

The investigation of the concrete physical mechanisms is advantageous to conduct through the complex experimental and theoretical modeling, when the concrete physical phenomenon or the group of phenomena are displayed at maximum.

With the assumption of the abovementioned, in this article the following questions are considered.

In the second chapter the summary of physical-technical principles of the precise laser gyroscopes construction, developed by the leading Ukrainian firms.

In the third chapter the analysis of the mathematical models of processes of the output characteristics forming in the ring laser is being conducted. It is shown that the existing theoretical models of processes in the ring laser make difficult the explanation of peculiarities of forming of waves characteristics in small-sized ring lasers with the space-anisotropic resonator. The mathematical model of forming of waves characteristics in the one-mode ring laser with the resonator formed by anisotropic, disaligned mirrors that contains space-limited non-linear structure, placed between plane (spheric) mirrors, "thin" diaphragm, placed between spheric (plane) mirrors. With the help of the averaging method, the system of the shortened equations that describe transformation of vector waves in non-linear space-limited amplifying medium, has been received. The task of stability of one and two-mode generation in the RL has been solved. The connection of these conditions with the value of amplitude anisotropy of resonator mirrors and with other laser parameters has been shown. While analysing the effectiveness of higher TEM modes selection by the resonator diaphragm it is necessary to consider the change of the modes strengthening coefficient with the growth of their transverse index. Selection coefficient here will depend on discharge current, channel diameter, filled by the amplifying medium.

In the fourth section the theoretico-experimental investigation of possibility of counter waves connection control in the LG has been shown. The mathematical model of counter waves connection forming in the ring laser that contains distributed sources of waves scattering has been suggested. It is shown, that at a certain choice of the RL resonator parameters the influence of synchronization zone of waves frequency on the LG output characteristics can be essentially decreased. Minimization and stabilization methods of counter waves connection has been suggested.

## 2. COMPARATIVE ANALYSIS OF EXISTING LG.

At present 3 Ukrainian enterprises (Central Design Department (CDD) "Arsenal", Scientific-Research Institute of Mechanics Problem (SRI MP) "Ritm", Industrial Enterprise (IE) "Zavod Arsenal", Kiev) are engaged in development and manufacturing of laser gyroscopes.

For the first time in the world the series manufacturing of LG was implemented in 1974 by CDD, IE "Zavod Arsenal". After this more than 10 types of LG have been developed and manufactured. On the peculiarities of their characteristics we shall dwell later. The LG had "null" instability of 3-10 d/h, instability of SC 0.0005. Resonators of the LG was executed on the four (five) mirrors scheme. The Faraday nonreciprocal element, assembled according to the special optical scheme has been placed inside the resonator. The laser gyroscope GS-1L has been developed and issued in series by these enterprises. Its ND is not more than 1 d/h, instability of SC is  $10^{-3}$ . The angle-measuring device GS-1L that has measurements error better than 0.1 angle/sec, has been manufactured based on LG GS-1L. The subsequent investigation showed that such a high null instability is connected with the change of characteristics usage of the systems of preliminary frequency shift, (SPFS) based on the Faraday nonreciprocal element in the first case and the RL rotation around its sensitivity axis in the second, inappropriate high level of resonator mirrors quality (scattering coefficient in the semi-sphere is  $(1-2) \cdot 10^{-4}$ ) and the monoblock material (CTLE  $1-2 \cdot 10^{-7}$  1/degree C) and others.

The CDD "Arsenal" the three-axes LG BLG-56 with alternative magnetic Faraday SPFS (ND 0.1-0.3 degrees per hour, instability of SC 0.0002) and then the LG "LGTm" (ND 0.1 - 0.05 d/h, instability of SC  $5 \cdot 10^{-5}$ ) where vibrational SPFS was realized, had been development and manufactured on the IE "Zavod Arsenal". The LG passed stand mechanical, climate tests and proved the perspective of the LG usage in the NS.

From the 1987 to create perspective LG for the guidance and control systems the following works in SRI MP "Ritm" have been done:

- The mathematical model of waves forming processes in the LG with the four mirrors resonator has been worked out, and on its basis a packet of application programs on modeling (optimization) of LG characteristics (parameters) with the help of computer has been created.
- The analysis of the main measurements errors has been done and physico-technical methods of their decreasing have been developed.
- The optimization of composition and parameters of elements of laser gyroscope optico-physical scheme (mirror curvature radiuses; radius, length and position of diaphragm and of amplifying medium in resonator; position of piezocorrectors; allowance on the monoblock manufacturing, channels and diaphragms, etc.) has been carried out.

In 1993 the LG "Ritm-1" with the following characteristics was created:

- the threshold generation current on the main mode is 0.6mA;
- the threshold current of generation appearance on the higher modes is 2.5 mA;
- to increase in 5-10 times the accuracy of perimeter and discharge current stabilization;
- to increase the speed of response of the perimeter stabilization systems at the LG output in the working regime and when passing from one longitudinal mode to the other in the processes of LG performance to 0.1 mc (it was 1 mc).
- measurements accuracy is 0.01 d/h;
- the random zero drift is 0,005 d/sqrt(h).

The analysis shows that the majority of the developed LG satisfy the requirements of NS, imposed for sensors at the range of the measured angle rates, for the times of measurement and averaging power

consumption and in the number of cases provide the error of the angle rate measurements and instability of SC of the LG.

It is extremely difficult to realise the accuracy characteristics of the LG at variation of the environment temperature at range - 60 C - +60 C, at vibrational (more than 10 g) and knock exposures (more than 200 g). It has appeared, that it is extremely difficult to bring into coincidence the high requirements, imposed for the measurements accuracy and dimensions-weight gyroscopes indexes. With the existing element basis it is difficult to expect the achievement of accuracy of 0.001 d/h in dimensions of three-axes GB 1-2 dm<sup>3</sup>. The latter is connected with the fact, that the quantity of the waves connection, stipulated by the waves scattering, laser dimensions and the ultimate measurements accuracy are closely interconnected. The less are the sensor dimensions, the worse is the accuracy measurements.

The further increase of the accuracy, decrease of dimensions and of power consumption is possible with the optimizing of the RL optico-physical scheme (reducing to a minimum allowed level of discharge current of amplifying medium; with the help of selection of active medium composition and cathode material to decrease the voltage of discharge combustion), increasing of transformers performance coefficient (for this it is advantageous to move on from the usual transformers scheme to the piezotransformer with the performance coefficient of 70 - 80%), optimizing of composition and structure of electronic systems of performance maintenance and control of LG generation regime (through transfer of their tasks to the microprocessor), increasing of the influence of reverse scattering on the output characteristics of LG.

## SECTION 3.

### MATHEMATICAL MODEL OF RING LASER GENERATION WITH THE SPACE DISTRIBUTED HETEROGENIOUS ANISOTROPIC RESONATOR.

A great number of works is devoted to the theoretical analysis of physical phenomena, observed in the RL. The results of these works are generalised in [1,3,7]. The advantages and deficiencies of mathematical models, used in these works, were discussed in [8]. Special attention is given to the fact, that at receiving of the shortened equations for amplitudes (intensities) and generated waves phases, the suppositions are originally made, the final result of which can be estimated only by building of consecutive theory of processes.

There are several examples of this:

- approximation of the specified field [3,4,5,7];
- replacement of the boundary conditions by effective [3-5,7];
- the independence of space and polarization characteristics of waves [7,10-13];
- the model of the active medium thin layer [10].

To what extent are these simplifications competent? The answer to this question is important from the point of view of laser gyroscopy practice, that uses received by the theory relations for the counter waves frequency difference and other characteristics at laser gyroscopes designing and forecasting of their characteristics in the process of their exploitation, as well as from the point of view of deepening of the insight into the physics of processes that follow in lasers.

To define energetic, frequential and space-polarizational waves characteristics steadiest in the ring laser resonator (RL) in the process of generation, it is necessary to solve

the wave equation for the vector of intensity  $E$  of the field [3-6]

$$\frac{\epsilon \mu}{c^2} \frac{\partial^2 \vec{E}}{\partial t^2} + \frac{4\pi\mu\sigma}{c^2} \frac{\partial \vec{E}}{\partial t} - \left( \frac{\partial^2 \vec{E}}{\partial x^2} + \frac{\partial^2 \vec{E}}{\partial y^2} + \frac{\partial^2 \vec{E}}{\partial z^2} \right) - \frac{2}{c} \left( \vec{\nabla} \text{grad} \right) \frac{\partial \vec{E}}{\partial t} = - \frac{4\pi\mu}{c^2} \frac{\partial^2 \vec{P}}{\partial t^2}, \quad (1)$$

with the boundary conditions, that define incomplete waves reflection by the resonator mirrors and their transformation on space-distributed diaphragms and volume boundaries, occupied by the active medium. Found solutions have to satisfy the conditions of Sommerfeld emission and Meixner conditions on the element edges. Here

$\sigma$  - ohmic conduction of this medium,  $c$  - light velocity.

$\vec{\omega} = [\vec{\nabla} \times \vec{r}]$  - linear rotation rate in a point, radius vector of which is

$\vec{r}$ , and  $\vec{\theta}$  - angle rate vector,

$\hat{\epsilon}$  and  $\hat{\mu}$  - tensors of dielectric and magnetic perviousness of mediums filling the resonator,  $\vec{P}$  - non-linear polarization (average dipole moment of the volume unit) of inverse transition of active medium, that maintain waves generation [6].

In case when active medium consists of two isotopes, emission line of which is heterogeneously widened, the polarized vector is defined by the expression [5,15].

$$\vec{P} = N \sum_{j=a,b} \int_{-\infty}^{+\infty} d\mathbf{v} W_j(\mathbf{v}) \vec{\mu}_j(\vec{r}, t, \mathbf{v}) \quad (2)$$

Here N is a density of the number of active atoms;  $W(\mathbf{v})$  - function of distribution of atoms on speeds. For the Maxwell distribution

$$W_j(\mathbf{v}) = \frac{1}{\sqrt{\pi} u_j} \exp \left\{ - \left( \frac{\mathbf{v}}{u_j} \right)^2 \right\}$$

$u_j$  - the average heat velocity of atoms motion,  $\mu_j$  - average dipole moment of atom of j- isotope, that have proection of motion velocity on a direction of the wave ( $\mathbf{v}$ ) propagation.

From the equation for the density matrix [5,15] for  $\vec{\mu}_j$ ; it is not difficult to obtain the following system of equations

$$\begin{aligned} \frac{\partial \vec{\mu}_j}{\partial t} + \mathbf{v} \frac{\partial \vec{\mu}_j}{\partial z} + \vec{\mu}_j \gamma_{ab}^{(j)} &= i \omega_{ab}^{(j)} \vec{R}_j \\ \frac{\partial \vec{R}_j}{\partial t} + \mathbf{v} \frac{\partial \vec{R}_j}{\partial z} + \vec{R}_j \gamma_{ab}^{(j)} &= i \omega_{ab}^{(j)} \vec{\mu}_j - \frac{2i}{\hbar} |\mu_{ab}^{(j)}|^2 \vec{E} (\rho_b^{(j)} - \rho_a^{(j)}) \\ \frac{\partial \rho_a^{(j)}}{\partial t} + \mathbf{v} \frac{\partial \rho_a^{(j)}}{\partial z} + \gamma_a^{(j)} (\rho_a^{(j)} - \rho_a^{(j,0)}) &= \frac{i}{\hbar} \vec{R}_j \vec{E} \\ \frac{\partial \rho_b^{(j)}}{\partial t} + \mathbf{v} \frac{\partial \rho_b^{(j)}}{\partial z} + \gamma_b^{(j)} (\rho_b^{(j)} - \rho_b^{(j,0)}) &= -\frac{i}{\hbar} \vec{R}_j \vec{E} \end{aligned} \quad (3)$$

where  $\omega_{ab}^{(j)}$  - the central frequency of atomic transition of j-isotope;  $\gamma_a^{(j)}, \gamma_b^{(j)}$  - relaxation constants of the working levels;  $\gamma_{ab}^{(j)}$  - the constant of transverse relaxation;  $|\mu_{ab}^{(j)}|$  - matrix element of dipole transition moment,  $\hbar$  - Planck constant.

In the further accounts it is suggested, that characteristics of  $\gamma_a^{(j)}, \gamma_b^{(j)}, \gamma_{ab}^{(j)}, \gamma_a^{(j,0)}, \gamma_b^{(j,0)}$  transitions for the both isotopes are the same.

In case of homogeneously-widened line, equations (3) change to equations, obtained in [22].

Considering that medium relaxation constants are much less than the central transition frequency, in the generation process the oscillation regime, close to the harmonic, will be set. The frequencies of this process will be close to the central transition frequency, waves vectors - to the wave vector of the longitudinal model with the index q, intrinsic for this resonance structure, and amplitudes will be slowly-changing functions of coordinates and time.

For the two-frequency process let it be;

$$\vec{E} = \epsilon_q^+ (\vec{r}, t) e^{i(\omega_q^+ t - K_q z)} + \epsilon_q^- e^{i(\omega_q^- t + K_q z)} + KC \quad (4)$$

Let's substitute (4) into (1.3) and average them over the

high frequency time period  $\frac{2\pi}{\omega} \left( \omega = \frac{\omega_q^+ + \omega_q^-}{2} \right)$  and then over

the space period  $\frac{2\pi}{K_q}$  of the waves changing. As the result we will

obtain the following equation system for the slowly changing complex waves amplitude.

$$\begin{aligned} i \left( \frac{\partial^2 \vec{E}_q^\pm}{\partial x^2} + \frac{\partial^2 \vec{E}_q^\pm}{\partial y^2} \right) \pm 2K_q \frac{\partial \vec{E}_q^\pm}{\partial z} + 2 \frac{\epsilon \mu}{c^2} \omega_q^\pm \frac{\partial \vec{E}_q^\pm}{\partial t} + \\ \left\{ \epsilon \mu \left( \frac{\omega_q^\pm}{c} \right)^2 \pm K_q \omega_q^\pm \frac{2V_z}{c^2} - K_q^2 \right\} + \omega_q^\pm \frac{4\pi\mu\sigma}{c^2} \vec{E}_q^\pm = \end{aligned} \quad (5)$$

$$= \alpha_0 \sum_j \int_{-\infty}^{+\infty} d\alpha e^{-i(\eta\alpha)^2} \left\{ \vec{A}_{\pm j} + \frac{\vec{A}_{\pm j}}{2(\vec{A}_{\pm j}^* \vec{A}_{\mp j}) f_{\mp}} [D - |\vec{A}_{\pm j}|^2 - |\vec{A}_{-j}|^2 - 1] D^{-1} \right\}$$

$$\text{where } \vec{E}_q^\pm = \beta \vec{e}_q^\pm; \vec{A}_{\pm j} = \vec{E}_q^\pm \left[ 1 + i(\Delta_{1,2}^{(j)} \mp \alpha) \right]^{-1};$$

$$\Delta_{1,2}^q = \frac{\omega_q^\pm - \omega_{ab}^{(j)}}{\gamma_{ab}};$$

$$D = \left[ 1 + |\vec{A}_{+j}|^2 + |\vec{A}_{-j}|^2 - 4(\vec{A}_{+j} \vec{A}_{-j}) \times (\vec{A}_{+j}^* \vec{A}_{-j}) f_{+} f_{-} \right]^{1/2}$$

$$\alpha_0 = \frac{4\pi\mu(\omega_q^\pm)^2}{2c^2} N \frac{|\mu_{ab}|^2 (\rho_a^{(0)} - \rho_b^{(0)})}{3\hbar K u};$$

$$\beta^2 = \frac{2}{3} \frac{|\mu_{ab}|^2 (\gamma_a + \gamma_b)}{\gamma_{ab} \gamma_a \gamma_b};$$

$$f_{\pm} = \frac{\left[ 1 \mp 4i \left( \frac{\Delta\omega - \gamma_{ab}\alpha}{\gamma_a + \gamma_b} \right) \right] \left[ 1 \mp i \left( \frac{\Delta\omega - \gamma_{ab}\alpha}{\gamma_{ab}} \right) \right]}{\left[ 1 \mp 2i \left( \frac{\Delta\omega - \gamma_{ab}\alpha}{\gamma_a} \right) \right] \left[ 1 \mp 2i \left( \frac{\Delta\omega - \gamma_{ab}\alpha}{\gamma_{ab}} \right) \right]};$$

$$\Delta\omega = 0.5(\omega_q^+ - \omega_q^-); \eta = \gamma_{ab}/K u.$$

For homogeneously-widened line, when  $\Delta\omega=0$  equations (5) coincide with the equations, obtained in [22].

In the approximation of the weak field  $\beta^2 |\vec{e}_q^\pm|^2 \ll 1$  equations (5)

will become

$$\begin{aligned} i \left( \frac{\partial \vec{E}_q^\pm}{\partial x^2} + \frac{\partial^2 \vec{E}_q^\pm}{\partial y^2} \right) + 2 \frac{\epsilon \mu}{c^2} \omega_q^\pm \frac{\partial \vec{E}_q^\pm}{\partial t} \pm 2K_q \frac{\partial \vec{E}_q^\pm}{\partial z} + \\ + \left\{ i \left[ \epsilon \mu \left( \frac{\omega_q^\pm}{c} \right)^2 \pm K_q \omega_q^\pm \frac{2V_z}{c^2} - K_q^2 \right] + \omega_q^\pm \frac{4\pi\mu\sigma}{c^2} \right\} \vec{E}_q^\pm = \\ = \alpha_0 \int_{-\infty}^{+\infty} d\alpha e^{-i(\eta\alpha)^2} \sum_j \left\{ \frac{\vec{E}_q^\pm}{1 + i(\Delta_{1,2}^{(j)} \mp \alpha)} \left[ 1 - \frac{|\vec{E}_q^\pm|^2}{1 + (\Delta_{1,2}^{(j)} - \alpha)^2} - \frac{|\vec{E}_q^\pm|^2}{1 + (\Delta_{2,1}^{(j)} + \alpha)^2} - \frac{\vec{E}_q^\pm (\vec{E}_q^\pm)^* f_{\mp}}{[1 + i(\Delta_{1,2}^{(j)} \mp \alpha)]} \right] \right\} = \\ = \frac{4\pi\mu\omega_q^\pm}{c^2} \vec{P}_q^\pm; \vec{P}_q^\pm = \chi_{\pm}(\vec{E}_q^+ \vec{E}_q^-) * \vec{E}_q^\pm \end{aligned} \quad (6)$$

Their difference from the famous in the theory ring lasers [3-7] shows up in the last component of the right part, that considers the influence of space inversion modulation of population in active medium with the counter waves.

The further calculations are carried out in based on the RL scheme, shown on the pic.1

To the equations systems (9)-(11) it is necessary to add boundary conditions that consider transformation of amplitude - polarization waves characteristics by the resonator mirrors and by the channels with the amplifying medium.

The channel of the monoblock with the amplifying medium will be represented as the cylinder section with the initial coordination in Cartesian basis  $x_n, y_n, z_n^\pm$  and the final  $x_k, y_k, z_k^\pm$ . The inside cavity has the radius  $d_{ac}$  and the cylinder  $Z_k^\pm$  axis does not



obligatory coincide with the axis of self-matched optical contour, laying in the cylinder field created by the system of disaligned mirrors  $M_1 \dots M_4$ . The dielectrical perviousness of the amplifying medium, filling this cavity, equals to  $\epsilon_1 + \chi_{\pm}(\vec{E}_q^+, \vec{E}_q^-)$ .

The dielectrical perviousness of the rest of cylinder equals to  $\epsilon_2$  and is not limited in the radial plane.

The electromagnetic field at the output of the amplifying medium

$\vec{E}_q^{\pm}(x_k y_k z_k^{\pm}, t)$  is connected with the field  $\vec{E}_q^{\pm}(x_h y_h z_h^{\pm}, t)$  at its input as applied to the resonator scheme shown at the picture N 1

$$\begin{aligned} \vec{E}_q^{\pm}(x_h y_h z_h^{\pm}) = & \hat{G}_{4h}^{\pm} \hat{M}_{44}^{\pm} \hat{G}_{3g}^{\pm} \hat{T}_1^{\pm} \hat{G}_{2g}^{\pm} \hat{M}_{22}^{\pm} \hat{G}_{12}^{\pm} \hat{M}_{11}^{\pm} \hat{G}_{k1}^{\pm} \\ & \vec{E}_q^{\pm}(x_k y_k z_k^{\pm}) e^{iK_q \ell_{AS}} + \\ & \left\{ \hat{G}_{h1}^{\pm} \hat{R}_1^{\pm} \hat{G}_{1k}^{\pm} \vec{E}_q^{\mp}(x_k y_k z_k^{\mp}) + \hat{G}_{h1}^{\pm} \hat{M}_{11}^{\pm} \hat{G}_{12}^{\pm} \right. \\ & \hat{R}_{21}^{\mp} \hat{G}_{21}^{\pm} \hat{M}_{11}^{\mp} \vec{E}_q^{\mp}(x_k y_k z_k^{\mp}) + \\ & \hat{G}_{h1}^{\pm} \hat{M}_{11}^{\pm} \hat{G}_{12}^{\pm} \hat{M}_{22}^{\pm} \hat{G}_{2g}^{\pm} \hat{R}_{2g}^{\mp} \hat{G}_{2q}^{\mp} \hat{M}_{21}^{\mp} \hat{G}_{11}^{\mp} \hat{G}_{1h}^{\mp} \\ & \vec{E}_q^{\mp}(x_k y_k z_k^{\mp}) \\ & + \hat{G}_{h1}^{\pm} \hat{M}_{11}^{\pm} \hat{G}_{12}^{\pm} \hat{M}_{22}^{\pm} \hat{G}_{2g}^{\pm} \hat{T}_g^{\mp} \hat{G}_{g3}^{\mp} \hat{R}_{33}^{\mp} \hat{G}_{3g}^{\mp} \\ & \hat{T}_g^{\mp} \hat{G}_{2g}^{\mp} \hat{M}_{21}^{\mp} \hat{M}_{11}^{\mp} \hat{G}_{1h}^{\mp} \vec{E}_q^{\mp}(x_k y_k z_k^{\mp}) + \\ & + \hat{G}_{h1}^{\pm} \hat{M}_{11}^{\pm} \hat{G}_{12}^{\pm} \hat{M}_{22}^{\pm} \hat{G}_{2g}^{\pm} \hat{T}_g^{\mp} \hat{G}_{g3}^{\mp} \hat{M}_{33}^{\mp} \hat{G}_{34}^{\mp} \hat{R}_{43}^{\mp} \hat{G}_{43}^{\mp} \times \\ & \hat{M}_{33}^{\mp} \hat{G}_{3g}^{\mp} \hat{T}_g^{\mp} \hat{G}_{2g}^{\mp} \hat{R}_{2g}^{\mp} \hat{G}_{21}^{\mp} \hat{M}_{11}^{\mp} \hat{G}_{1h}^{\mp} \vec{E}_q^{\mp}(x_k y_k z_k^{\mp}) \times \\ & + \hat{G}_{h1}^{\pm} \hat{M}_{11}^{\pm} \hat{G}_{12}^{\pm} \hat{M}_{22}^{\pm} \hat{G}_{2g}^{\pm} \hat{T}_g^{\mp} \hat{G}_{g3}^{\mp} \hat{M}_{33}^{\mp} \times \\ & \left. \hat{M}_{33}^{\mp} \hat{G}_{3g}^{\mp} \hat{T}_g^{\mp} \hat{G}_{2g}^{\mp} \hat{M}_{22}^{\mp} \hat{G}_{21}^{\mp} \hat{M}_{11}^{\mp} \hat{G}_{1h}^{\mp} \vec{E}_q^{\mp}(x_k y_k z_k^{\mp}) \right\} \times \\ & e^{i(\omega_q^{\pm} - \omega_q^{\mp})t \pm iK_q(z_k^{\pm} + z_k^{\mp} \pm L)} \quad (7) \end{aligned}$$

Here  $\hat{G}_{ij}^{\pm}$  - the integral operator defining the waves propagation

clockwise (+) or counterclockwise (-) between i- and j-elements of ring resonator respectively [14];  $\hat{M}_j^{\pm}$ ,  $\hat{R}_j^{\pm}$  - operator matrices 4\*4 in size that

characterize the reflection and scattering features of j-mirrors at the dropping of waves, propagating clockwise (+) and (-) for the counter [21];

$T_g$  - matrix operator 4\*4 in size, defining the diaphragm characteristics [14];

L - resonator perimeter.

$\ell_{AS}$  - length of the amplifying medium.

Resonance characteristics of the elements systems that make the resonator are described by the condition of periodicity [22].

$$\vec{E}_q^{\pm}(x, y, z^{\pm}, t) = \vec{E}_q^{\pm}(x, y, z^{\pm} \pm L, t) \exp(2\pi q) \quad (8)$$

where q - integer number.

Differential equation (6), together with the conditions of waves characteristics transformation (7) and with the condition of periodicity (8) comprise the closed equations system, describing the field in the ring laser with anisotropic elements and space distributed amplifying medium and the sources of the back scattering from one of the directions of propagation to the counter.

### 3.1 Shortened equations of generation in the one-mode case.

Using (6), the equations system, defining the change of waves

characteristics at their propagating in the channel of the monoblock filled with amplifying medium, will be obtained.

The solution of the equations system (6) can be represented as following:

$$\vec{E}_q^{\pm} = \sum_{v, \alpha} \vec{A}_{v\alpha}^{\pm} \Psi_{v\alpha}^{\pm} \quad (9)$$

where  $\Psi_{\mu\beta}^{\pm}$  satisfy the equation

$$\frac{\partial \Psi_{\mu\beta}^{\pm}}{\partial x^2} + \frac{\partial^2 \Psi_{\mu\beta}^{\pm}}{\partial y^2} \mp 2iK_q \frac{\partial \Psi_{\mu\beta}^{\pm}}{\partial z} = 0 \quad (10)$$

and the conditions of ortonormalization

$$\int_{-\infty}^{+\infty} dx dy \Psi_{v\alpha}^{\pm}(x, y, z) (\Psi_{\mu\beta}^{\pm}(x, y, z))^* = \delta_{vm} \delta_{\alpha\beta} \quad (11)$$

The wave vector  $K_q$  is connected with the frequency  $\omega_q^{\pm}$  by the following dispersion ratio:

$$\epsilon_1 \mu \left( \frac{\omega_q^{\pm}}{c} \right)^2 \pm 2K_q \frac{\omega_q^{\pm} v_z}{c} - K_q^2 = 0 \quad (12)$$

The equation (10) is parabolic. Its solution in the Cartesian basis is expressed by the functions of Hermit- Gauss [18].

Let us substitute (9) to (6) and using (10)-(12), we will obtain the following system of differential equations for the dispersion coefficients definition  $\vec{A}_{\mu\beta}^{\pm}(z, t)$ .

$$\begin{aligned} \mp 2iK_q \frac{\partial \vec{A}_{\mu\beta}^{\pm}}{\partial z} - 2i \frac{\mu \omega_q^{\pm}}{c^2} \left[ (\epsilon_2 - \Delta \epsilon Q_{\mu\mu, \beta\beta}) \frac{\partial \vec{A}_{\mu\beta}^{\pm}}{\partial t} - \right. \\ \left. \Delta \epsilon \sum_{\substack{v\alpha \\ v \neq \mu \\ \alpha \neq \beta}} \frac{\partial \vec{A}_{v\alpha}^{\pm}}{\partial t} Q_{v\mu, \alpha\beta} \right] + \Delta \epsilon \mu \left( \frac{\omega_q^{\pm}}{c} \right)^2 \times \end{aligned} \quad (13)$$

$$\left[ \vec{A}_{\mu\beta}^{\pm} (1 - Q_{\mu\mu, \beta\beta}^{\pm}) - \sum_{\substack{v\alpha \\ v \neq \mu \\ \alpha \neq \beta}} \vec{A}_{v\alpha}^{\pm} Q_{v\mu, \alpha\beta}^{\pm} \right] = \frac{4\pi\mu(\omega_q^{\pm})^2}{c^2} \times$$

$$\sum_{v\alpha} \iint_{S_{AS}} \vec{P}_{v\alpha}^{\pm} \Psi_{v\alpha}^{\pm} (\Psi_{\mu\beta}^{\pm})^* dx dy$$

$$\text{Here } \Delta \epsilon = \epsilon_2 - \epsilon_1, Q_{v\mu, \alpha\beta} = \iint_{S_{AS}} \Psi_{v\alpha} \Psi_{\mu\beta}^* dx dy$$

To make further transformations (13), let us use the approach [15].

According to it let us integrate (13) on z and considering that

$$\vec{A}_{\mu\beta}^{\pm}(z, t) \approx \vec{A}_{\mu\beta}^{\pm}(t), \text{ after the substitution (7), (8) in the one-mode it is}$$

not difficult to obtain the following equation system for modulus  $A_{\mu\beta, i}^{\pm}$

and phase  $\varphi_{\mu\beta, i}^{\pm}$ , i-component of  $\vec{A}_{\mu\beta, i}^{\pm}$  vector to the orthes of the

Cartesian orthogonal basis ( $i = \{x, y\}$ ).

$$A_{\mu\beta, j}^{\pm} = a_{\mu\beta, i}^{\pm} \exp(i\varphi_{\mu\beta, i}^{\pm}) \quad (14)$$

$$\begin{aligned} \frac{da_{\mu\beta, i}^{\pm}}{dt} = & (\tilde{\sigma}_{\mu\beta, i}^{\pm} - \Pi_{\mu\beta, i}^{\pm}) a_{\mu\beta, i}^{\pm} \\ & + r_{\mu\beta, i}^{\mp} a_{\mu\beta, i}^{\mp} \cos(\Psi_{\mu\beta, i}^{\pm} \pm \epsilon_{\mu\beta, i}^{\pm}) \end{aligned} \quad (15)$$

$$\frac{d\varphi_{\mu\beta, i}^{\pm}}{dt} = \sigma_{\mu\beta, i}^{\pm} + \Delta_{\mu\beta, i}^{\pm} \mp \frac{A_{\mu\beta, i}^{\mp}}{A_{\mu\beta, i}^{\pm}} r_{\mu\beta, i}^{\pm} \sin(\Psi_{\mu\beta, i}^{\pm} \pm \epsilon_{\mu\beta, i}^{\pm}) \quad (16)$$



in the equations (15), (16) the following unit symbols are accepted:

$$\sigma_{\mu\beta,i}^{\pm} + i\tilde{\sigma}_{\mu\beta,i}^{\pm} = \mp \frac{2\pi\omega^{\pm}}{\ell_{AC}\epsilon_2} \int_{Z_h^{\pm}}^{\tilde{Z}_k^{\pm}} dz \iint_{S_{AC}} \chi_{\pm} \psi_{\mu\beta}^{\pm} (\psi_{\mu\beta}^{\pm})^* dx dy ;$$

$$\Pi_{\mu\beta,j}^{\pm} = \frac{V_{\mu\beta}^{\pm} \left(1 \pm \frac{V_z}{\sqrt{\epsilon_2 \mu_0}}\right)}{\ell_{AC} \sqrt{\epsilon_2 \mu_0}} \left[1 - R_{\mu\beta,j}^{\pm}\right] +$$

$$\frac{V_{\mu\beta}^{\pm}}{\ell_{AC}} \left[ \frac{\Delta\epsilon}{2} \left(1 - \tilde{F}_{\mu\beta,\mu\beta}^{\pm}\right) - \frac{\Delta\epsilon}{2} F_{\mu\beta,\mu\beta}^{\pm} \right] \sqrt{\frac{\mu}{\epsilon}} +$$

$$+ \frac{2\pi\sigma_0 F_{\mu\beta,\mu\beta}}{c\epsilon_2 \ell_{AC} \mu_{\mu\beta}} ;$$

$$\epsilon_2 = \epsilon_2 + i\tilde{\epsilon}_2 ;$$

$$\frac{\Delta\epsilon}{\epsilon_2} = \frac{\Delta\epsilon + i\Delta\tilde{\epsilon}}{\epsilon_2} ; F_{\mu\beta,\mu\beta} = F_{\mu\beta,\mu\beta} + i\tilde{F}_{\mu\beta,\mu\beta} ;$$

$$r_{\mu\beta,j}^{\pm} = \rho_{j,\phi}^{\pm} |S_{\mu\mu,\beta\beta}^{\pm}| ; \epsilon_{\mu\beta,j}^{\pm} = \varphi_{\phi}^{\pm} + \arg \{S_{\mu\mu,\beta\beta}^{\pm}\} ;$$

$$V_{\mu\beta}^{\pm} + i\tilde{V}_{\mu\beta}^{\pm} = \frac{c}{\sqrt{\epsilon_2 \mu}} q_{\mu\beta} ; \psi_{\mu\beta,j} = \varphi_{\mu\beta,j}^{\pm} - \varphi_{\mu\beta}^{\pm} ;$$

$$\Delta_{\mu\beta}^{\pm} = \frac{V_{\mu\beta}}{2\epsilon_2 \ell_{AC}} \left\{ \Delta\epsilon \left[1 - F_{\mu\beta,\mu\beta}^{\pm}\right] + \frac{\Delta\epsilon}{2} \tilde{F}_{\mu\beta,\mu\beta}^{\pm} \right\}$$

$$+ \frac{2\pi\sigma_0}{c} \frac{V_{\mu\beta}}{\ell_{AC}} \tilde{F}_{\mu\beta,\mu\beta}^{\pm} + \left\{ \omega_{\pm}^q - \omega_{\pm}^q \right\} \frac{1}{2} ;$$

$$R_{\mu\beta,j}^{\pm} = R_j^{\pm} \operatorname{Re} \left\{ Z_{\mu\mu\beta\beta}^{\pm} \right\} ; R_j^{\pm} = R_{j,1}^{\pm} R_{j,2}^{\pm} R_{j,3}^{\pm} R_{j,4}^{\pm}$$

$$q_{\mu\beta} = \left(1 - \frac{\Delta\epsilon}{\ell_{AC} \epsilon_2} F_{\mu\beta,\mu\beta}^{\pm}\right) ; F_{\mu\nu,\beta\alpha}^{\pm} = \int_{Z_h^{\pm}}^{\tilde{Z}_k^{\pm}} Q_{\mu\nu,\beta\alpha}^{\pm} dz ;$$

$$Z_{\mu\nu,\beta\alpha}^{\pm} = \int_{-\infty}^{+\infty} \left( \psi_{\mu\beta}^{\pm} \right)^* \hat{Q}_{hk}^{\pm} \psi_{\nu\alpha}^{\pm} dx dy_h$$

(17)

$$\rho_{x,\phi}^{\pm} = 0,25 \left( \rho_{x,1}^{\pm} + \rho_{x,2}^{\pm} + \rho_{x,3}^{\pm} + \rho_{x,4}^{\pm} \right) ;$$

$$\rho_{y,\phi}^{\pm} \Rightarrow \rho_{x,\phi}^{\pm} (x \rightarrow y)$$

$$\varphi_{\phi}^{\pm} = 0,25 \left( \varphi_1^{\pm} + \varphi_2^{\pm} + \varphi_3^{\pm} + \varphi_4^{\pm} \right) ;$$

$$S_{\mu\nu,\beta\alpha}^{\pm} = \int_{-\infty}^{+\infty} \left( \psi_{\mu\beta}^{\pm} \right)^* \hat{R}_{int}^{\pm} \psi_{\nu\alpha}^{\pm} ;$$

$$\hat{R}_{int}^{\pm} = \hat{G}_{h1}^{\pm} R_{h1}^{\pm} \hat{G}_{1k}^{\pm} + \hat{G}_{h1}^{\pm} \hat{G}_{12}^{\pm} R_{2k}^{\pm} \hat{G}_{21}^{\pm} \hat{G}_{1k}^{\pm} + \dots$$

$$R_g^{\pm} = \begin{cases} \rho_{x,j}^{\pm} / \rho_{x\phi}^{\pm} e^{i(\varphi_j^{\pm} - \varphi_{\phi}^{\pm})} & \text{at } (x,y) \in S_j \\ 0 & \text{at } (x,y) \notin S_j \end{cases}$$

$$\rho_{x1}^{\pm} = r_{x1}^{\pm} ; \rho_{x2}^{\pm} = R_{x1}^{\pm} R_{x1}^{\mp} r_{x2}^{\pm} ;$$

$$\rho_{x3}^{\pm} = R_{x1}^{\pm} R_{x2}^{\pm} R_{x2}^{\mp} R_{x1}^{\mp} r_{x3}^{\pm} ;$$

$$\rho_{x4}^{\pm} = R_{x1}^{\pm} R_{x2}^{\pm} R_{x3}^{\pm} R_{x3}^{\mp} R_{x2}^{\mp} R_{x1}^{\mp} r_{x4}^{\pm} ;$$

$$T_g^{\pm} = \begin{cases} 1 & \text{at } (x,y) \in S_i \\ 0 & \text{at } (x,y) \notin S_i \end{cases}$$

$$\hat{Q}_{hk}^{\pm} = \hat{G}_{4k}^{\pm} T_4^{\pm} \hat{G}_{43}^{\pm} T_3^{\pm} \hat{G}_{3g}^{\pm} T_g^{\pm} \hat{G}_{g2}^{\pm} T_2^{\pm} \hat{G}_{21}^{\pm} T_1^{\pm} \hat{G}_{1h}^{\pm} \ln$$

expressions (17) the following unit symbols are accepted.

$R_{x,j}^{\pm} ; R_{y,j}^{\pm} ; (r_{x,j}^{\pm}, r_{y,j}^{\pm}) ; \psi_j^{\pm}(\varphi_j^{\pm})$  - reflection coefficients (scattering in XOZ and YOZ and the quantity of the phase anisotropy (the wave phase shift at scattering) from the j-resonator mirror, respectively.  $Z_h^{\pm}, Z_k^{\pm}$  - lengthwise coordinates of the initial and final volume surfaces with the amplifying medium.

$S_{ac}, S_j, S_g$  - the square of amplifying medium section, j-mirror and diaphragm, respectively.

q - integer number.

Signs + or - above the corresponding variables shows the direction of the wave propagation.

When obtaining equations (15), (16), the phase condition of modes generation was considered [15]. According to them the least losses in resonator belong to the mode with the wave vector  $K_q$ , that satisfies the equation.

$$K_q L - \psi - \delta_{\mu\beta}^{\pm} = 2\pi q$$

$$\text{Here } \psi = \psi_1 + \psi_2 + \psi_3 + \psi_4 -$$

the summarized mode phase running on, stipulated by their anisotropy

$$\delta_{\mu\beta}^{\pm} = \frac{\operatorname{Im} Z_{\mu\mu,\beta\beta}^{\pm}}{\operatorname{Re} Z_{\mu\mu,\beta\beta}^{\pm}} - \text{additive to the phase of } \mu, \beta \text{ resonator}$$

mode connected with the final dimensions and the resonator mirrors curvature, their mutual disposition.

Expression for  $\Pi_{\mu\beta,j}^{\pm}$  defines the energetic attenuation coefficient of the j-component of the  $\mu, \beta$  wave mode, propagating clockwise (+) or counterclockwise (-) in resonator. The first component in  $\Pi_{\mu\beta,j}^{\pm}$  is stipulated by the energy losses because of the finity of dimensions and mirrors and resonator diaphragm transmission. The second component characterizes the wave losses on the border of amplifying medium and monoblock channel. The third component defines the influence of the amplifying medium conduction on the waves output characteristics. The estimations of losses components in resonator show that depending on the curvature radius, transverse dimensions of the reflecting coating of mirrors, resonator dimensions and the length, radius of volume with the amplifying medium in the ring laser, the process of generation will have either caustic or waveguide character.

Coefficients  $\tilde{\sigma}_{\mu\beta,j}^{\pm}, \tilde{\sigma}_{\mu\beta,j}^{\pm}$ , give the saturated with the generated waves, coefficients of amplification and the medium dispersive characteristics. Expressions for them and connection with the amplifying medium parameters can be easily obtained from (6). The only difference between them is that the quantity depends on the space position of the volume with the amplifying medium inside the resonator.

Expression  $\Delta_{\mu\beta}^{\pm}$  is defined by the additive to the emission frequency, caused by the imaginary and actual components of the medium dielectrical perviousness that surrounds the amplifying medium (the first and the second component), the amplifying medium conduction finity (the third) and the rotation of the ring laser in the inertial space (the fourth).

Coefficients  $r_{\mu\beta,j}^{\pm}$  and  $\epsilon_{\mu\beta,j}^{\pm}$  gives the influence of amplitude and phase of waves back scattering from the resonator elements on the laser output characteristics. Their peculiarity is in the fact that within the frames of the accepted methods their diffractive as well as their interference component is considered. And this leads, as it will be shown below, to the opportunity to create systems that will allow to minimize and stabilize the connection of waves in the ring laser.

The equations (15) and (16) coincide in shape with the similar, obtained in many works [1,3-7]. Their difference is that they specify the dependance from the structure and resonator elements and amplifying medium parameters. The difference is that the coefficients describing the linear and non-linear waves interactions in the amplifying medium, depend on the structure and composition of ring resonator and on the amplifying medium position in it.

The further consideration will be made for the main mode TEM<sub>00q</sub> ( $\mu = 0, \beta = 0$ ), linearly polarized in the XOZ (i=x) plane and that is why indexes  $\mu, \beta, i$  will be omitted below.

### 3.2. Peculiarities of the competition of main and cross modes in the ring resonator with the weak-anisotropic resonator.

Resonator of ring lasers are weakly anisotropic, and the results, obtained earlier can not be applicable here. The modes competition in such lasers, as it for the first time shown in the works [16,20,42-44], has its own peculiarities, connected with the parameters of the amplifying medium. (transition type, the character of the energetic level degeneration, relaxation characteristics of levels), and with the value and character of radial heterogeneity.

The stability condition of the higher modes generation with the orthogonal polarization or parallel polarization of the main mode at resonator and amplifying medium parameters changing, is shown as:

$$\mathbf{D}_B^{(1)} = \frac{\Theta_{AB} \mu_{AB}}{\Theta_B \mu_B} < \frac{\alpha_A}{\alpha_B} < \frac{\Theta_A \mu_A}{\Theta_{BA} \mu_{BA}} \equiv \mathbf{D}_B^{(2)} \quad (18)$$

where  $\Theta_{A(B)}, \Theta_{AB(BA)}$  - the imaginative part of coefficients of self- and cross-saturation, contour of amplification by waves, generating modes; (A - index of the main mode, B=(P,K), P - index of the higher mode with the collinear polarization, K - with the plane of polarization of orthogonal polarization plane of the main mode),  $\alpha_A, \alpha_B$  - the increase of amplification under the losses for the main and the higher mode;  $\mu_{A(B)}, \mu_{AB(BA)}$  - the real part of the coefficients of space overlap of generating modes [32]. B(1) parameters are defined by the transition type, the degree of energetic level degeneration, general pressure of the amplifying medium, frequencies disadjustments, generating modes as to the central transition frequency and to each other, space characteristics of generated modes [42].

At occurrence at the generation spectrum of the higher mode  $\alpha_A/\alpha_B > 1$ . For the transition  $3S_2 - 2P_4$  of He-Ne mixture ( $\lambda=0,633$  mkm)  $\mathbf{D}_P^{(1)}, \mathbf{D}_K^{(1)} < 1$  at the whole range of the pressure change, disalignment of the generated modes. That means that the left sign of inequalities is always fulfilled. This condition of existence and stability of the linearly polarization mode of TEM<sub>00q</sub>.

With the increase of the discharge current the value of  $\alpha_A/\alpha_B$  decreases and from the certain  $i_{\Pi}^{(B)}$  the rightsign in (18) starts to fulfil - at the generation spectrum a stable higher mode occurs. Supposing  $\Delta i_{\Pi}^{(A)} = i_{\Pi}^{(B)}$ , where  $i_{\Pi}^{(A)}, i_{\Pi}^{(B)}$  - the threshold current of the generation occurrence on the TEM<sub>00q</sub> (TEM<sub>mnq</sub>)

$$\Delta i_{\Pi}^{(B)} = \left( \frac{r_B}{\alpha_B} - \frac{r_A}{\alpha_A} \right) \left[ 1 - \frac{\alpha_A}{\alpha_B \cdot \mathbf{D}_B^{(2)}} \right]^{-1} \quad (19)$$

where  $r_{A(B)}$  - the full losses for the i-mode at resonator passing by;

$\alpha_{A(B)}$  - the slope of change of the amplification coefficient of main and higher mode with the change of the discharge current. The analysis showed that for the transition 3S<sub>2</sub>-2P<sub>4</sub> of the mixture at the whole range of parameters changes of the proportion  $\mathbf{D}_K^{(2)} / \mathbf{D}_P^{(2)} > 1$ .

From that according to (18), when

$$\left( \frac{r_K - r_P}{r_K - (r_A \alpha_K) / \alpha_A} \right) < 0.7 \quad (20)$$

follows  $\Delta i_{nor}^{(K)} / \Delta i_{nor}^{(P)} < 1$ . So the discharge current of the generation occurrence on the mode TEM<sub>00q</sub> is less than for the same mode with polarization coinciding it the direction of the main.

In the works [43] carried out to investigate this phenomenon, it was shown that at discharge current more than 6,5 mA in the generation spectrum the mode TEM<sub>10q</sub> has occurred, with the polarization plane orthogonal to the main mode, when the occurrence threshold of the main mode comprised 4,5 mA. The further increase of discharge current up to  $i_P \approx 13,5$  mA did not lead to the change of generation spectrum and only at this value it was possible to observe distinctly the deformation of the spot of generated emission on the monitor screen. Estimations, carried out on (19), and using the estimation of losses and amplification of the main and higher modes. The results presented in chapter 3 gave the value  $i_{\Pi}^A = 2,7$  mA, when  $\Delta i_{\Pi}^{(K)} = 3,9$  mA. So the threshold of occurrence of the TEM<sub>10q</sub> mode, the polarization plane of which is orthogonal to the polarization plane of the mode TEM<sub>00q</sub> would have been 6,6 mA. A small difference of the calculated value  $i_{\Pi}^{(K)}$  from the experimentally found in connected with the inaccuracy of the summarized losses in the laser (error  $\pm 5\%$ ), on which in (2) coefficient  $\alpha_A$ .

There were researched the dependence of the threshold discharge current (mA) of occurrence in the generation of the main mode TEM<sub>00q</sub> and the threshold discharge current (mA) of occurrence in the mode TEM<sub>00q</sub> generation spectrum at changing of the diaphragm diameter from 1,4mm to 1,8mm for the radiuses of the spheric mirrors 6m, 8m, 10m and diameters of the channel with the amplifying medium

The summing pressure  $^{20}\text{Ne}$  and  $^{22}\text{Ne}$  in the active medium equaled to 0.2 tors, and the proportion of the components  $^3\text{He} / (^{20}\text{Ne} + ^{22}\text{Ne})$  equal to 16,5. Amplification coefficient on the axis according to [23] equals to  $5,62 \cdot 10^{-3} \text{ mm}^2/\text{mA}$ . Calculations were made according to the formulas (18,19) on the IBM PC/AT. It is clear that the threshold of the higher mode appearance TEM<sub>10q</sub> with the polarisation, orthogonal to the main mode on 0,6 -

1,6 mA is lower, that at TEM<sub>10</sub> mode, the polarization vector of which is parallel to the main mode.

The analysis of the calculations results showed, that the threshold current of the mode TEM<sub>01</sub> occurrence equals to the double threshold current of the mode TEM<sub>00</sub> occurrence for RL, shown at fig.1, at the active medium diameter 2,7 mm and radiiuses of the spheric mirrors 6 m, 8 m, 10 m if the diameter of the diaphragm equals, respectively, 1,64 mm, 1,78 mm, 1,8 mm.

At one and the same volume of the AM diameter the difference of the thresholds of the higher modes occurance with the parallel and perpendicular to the main mode polarization, increases with the growth of the mirror curvature radius, diaphragm diameter the value of losses difference on transmission in p- and s-planes of waves fall on the resonator mirrors.

At 
$$\frac{(r_K - r_P)}{[r_K - (r_A \alpha_K) / \alpha_A]} < 0.7$$
 the threshold

discharge current, at which the TEM mode starts to generate with polarization, parallel to the polarization of the main mode, on 0,6-1,6mA more, than the threshold current of mode occurrence with the polarization, orthogonal to the main.

The analysis of iniquity (18) showed, that in resonator while defining the conditions of the higher modes occurance in the laser emission it is necessary to conduct the account of the transition type, levels of degradation and relaxation characteristics of the energetic levels, proportions of diffractive and polarizational losses for TEM<sub>00</sub> and TEM<sub>mn</sub>. And if the difference of polarizational losses is less than the difference of diffractive losses, the threshold of the higher mode TEM<sub>mn</sub> occurrence, polarized orthogonally to the polarization plane of the main mode is less than of the same mode with the polarization plane parallel to the main. Because of this, the upper boundary of the field of discharge currents, within the limits of which the generation on the main mode TEM<sub>00</sub> is carried out and it has to be defined on occurrence of the orthogonally polarized higher mode TEM<sub>mn</sub>. It will be observed in the cross distribution of the generation field in the far zone when placed between laser output mirror and the polarization screen, the axes of anisotropy of which is perpendicular to the polarization plane of the main mode.

Obtained proportions (18-20) allow to choose parameters of resonator and of active medium of the gaseous laser (composition, pressure of the active medium, channel diameter, mirror radius, resonator length), the one-mode generation regime at the whole range of discharge currents changes and the disalignments of the generation frequency is provided.

#### 4. RESEARCH OF THE OPPORTUNITY OF BACKSCATTERING CONTROL IN THE RING LASER GYRO.

##### 4.1. The review of the methods of the backscattering influence decrease on the RLG accuracy

For decrease of the backscattering influence on RLG accuracy two basic methods are proposed.

The first method assumes the use of the system of backscattering minimization and stabilization. This system changes the geometry of resonator and as result of this its optical legs reorganize. The change of geometry of resonator is executed with the help of slow controlled

180 degree out of phase movements of mirrors, such, that the perimeter of axial contour remains constant value. The mirrors can make linear and angular movements [24-27,45].

The best variant of backscattering minimization and stabilization system is developed by the firm "Honeywell Inc." and also in the Scientific Research Institute of problems of mechanic "Ritm" (the realizations are different). The system observes parameters and calculates the

function 
$$F = \sqrt{a_1^2 + b_1^2 + 2a_1b_1 \cos(V_1 - V_2)}$$
 and with the help of change of resonator geometry minimizes its value. This function F most completely characterizes the RLG backscattering and in the first order contain information about lock-in threshold of the RLG.

The second basic method of backscattering influence decrease on the RLG accuracy assumes the use of the 180 degree out of phase vibrations of two RLG mirrors with equal amplitudes. (In the literature this procedure is called "mirror dithering"). The perimeter of axial contour in this case remains constant value. The amplitudes of mirror vibrations are specially preselected. This way is described in literature [28] and is protected by many patents (see, for example, [29-36]). The advantage of this method is the absence in the RLG of moving mechanical parts.

The development of the second method is the sharing of mirror vibrations and modulations of differences of currents in gas discharge shoulders [37, 38].

There is also patent [39] on sharing mechanical dithering and mirror dithering. In summary we note the one more method of struggle with the back-scattering in the RLG. This method assumes the use of modulation of difference of currents in gas discharge shoulders [40].

##### 4.2. The influence of waves connections on the LG output characteristics.

The solution of equations system (15,16) beyond the sphere of counter waves frequency synchronization will be represented as the following:

$$I_1 = a_0 + a_1 \sin(\psi + V_1) \quad (21)$$

$$I_2 = b_0 + b_1 \sin(\psi + V_2);$$

$$(I_1 = (a_{0,x}^+)^2);$$

$I_1$  and  $I_2$  are the dimensionless intensities of the counter waves.

Here:  $a_0, b_0, a, b, V_1, V_2$  are constant components, amplitudes and phases of modulation components of the counter waves intensities, respectively;

$\psi$  - momentary phases difference between the counter waves.

Quantities  $a_0, b_0, a, b, V_1, V_2$  usually can be controlled in the process of experiment.

Substituting (21) into the (15,16) and considering that modulus and phases of the back scattering coefficients, beat frequency and the lock in zones of counter waves are the sought quantities, in supposition that  $a_0 \gg a_1 \approx r_1; b_0 \gg b_1 \approx r_2$ ; (approximation of weak connection [3,6]), it is not difficult to obtain for the average value of beat frequency  $\Omega_B = [\Omega_{ab}^2 - \Omega_{L\alpha\alpha}^2]$  and the lock-in zone  $\Omega_{L\alpha\alpha}$

the following expressions:

$$\Omega_{L\alpha\alpha} = [A_1^2 + A_2^2 - 2A_1A_2 \cos(\varphi_1 - \varphi_2)]^{1/2} \quad (22)$$

$$\begin{aligned}
\text{Here } A_1^2 &= b_1^2 (\rho_2 - \tau_{12})^2 + a_1^2 (\rho_1 - \tau_{21})^2 - \\
&\quad - 2a_1 b_1 (\rho_1 - \tau_{12})(\rho_2 - \tau_{21}) \cos(V_2 - V_1) \\
A_2^2 &= \frac{1}{4} \left( \frac{\partial \Psi}{\partial t} \right)^2 \left[ \left( \frac{b_1}{b_0} \right)^2 + \left( \frac{a_1}{a_0} \right)^2 + 2 \frac{a_1 b_1}{a_0 b_0} \cos(V_1 - V_2) \right] \\
&\quad + \beta_2^2 b_1^2 + b_1 a_1^2 + 2\beta_1 \beta_2 a_1 b_1 \cos(V_1 - V_2) + \\
&\quad \theta_{21}^2 a_1^2 + a_{12}^2 b_1^2 + 2\theta_{12} \theta_{21} a_1 b_1 \cos(V_1 - V_2) + \\
&\quad 2\beta_1 \theta_{12} (a_1^2 + a_1 b_1 \cos(V_1 - V_2)) \quad (23) \\
&\quad + 2\beta_2 \theta_{21} (b_1^2 + a_1 b_1 \cos(V_1 - V_2)) + \\
&\quad a_1 b_1 \left( \frac{d\Psi}{dt} \right) \sin(V_1 - V_2) \times \left[ \left( \frac{\theta_{21}}{b_0} - \frac{\theta_{12}}{a_0} \right) + \left( \frac{\beta_1}{b_0} - \frac{\beta_2}{a_0} \right) \right]
\end{aligned}$$

Expressions for  $\text{tg } \varphi_1$  and  $\text{tg } \varphi_2$  are too awkward to be shown here.

In the expressions (23) the following unit symbols are introduced:

$\beta_{1,2}$  - parameters, characterizing the waves self-saturation;

$\theta_{12}, \theta_{21}$  - parameters, defining the waves mutual saturation

$\rho_1, \rho_2, \tau_{12}, \tau_{21}$  - parameters, characterizing the auto- and cross-"ejection" of counter waves frequency.

From (6) it is not difficult to define their concrete value within the accepted model of the ring laser processes.

We do not show them here, because we will not need them further. For the further calculations let us stop at the case, when the frequency of laser generation is adjusted to the center of the summarizes contour of amplification.

In this case, considering the fact that the frequency and the losses difference for the waves is small, like in [6] it is possible to consider

$$\beta_1 \approx \beta_2 = \beta; \quad \theta_{12} \approx \theta_{21} = \theta; \quad \rho_1 \approx \rho_2 = \rho;$$

$$\tau_{12} \approx \tau_{21} = \tau; \quad a_0 \approx b_0 = a$$

$$\text{So } A_1 = (\rho - \tau) \left[ a_1^2 + b_1^2 - 2a_1 b_1 \cos(V_1 - V_2) \right]^{1/2} \quad (24)$$

$$A_1 = \left[ \frac{1}{4a^2} \left( \frac{d\Psi}{dt} \right)^2 + (\beta + \theta)^2 \right]^{1/2}$$

$$\left[ a_1^2 + b_1^2 + 2a_1 b_1 \cos(V_1 - V_2) \right]^{1/2}$$

$$\text{Because } (\rho - \tau) \ll \left[ \frac{1}{4a^2} \left( \frac{d\Psi}{dt} \right)^2 + (\beta + \theta)^2 \right], \text{ the minimum}$$

of the synchronization zone of counter waves will be realized under the following conditions:

$$a_1 = b_1, \cos(V_1 - V_2) = \pi \quad (25)$$

While fulfilling of this condition (25), as it comes from (24), the minimum of the additive to the frequency beat, stipulated by the waves scattering from the one direction of propagation to the counter.

Coefficient  $A_1$  depends on the  $(\rho - \tau)$  parameter. The estimations show that it is close to the null at the adjustment of the generation

frequency on the summarized contour of the amplification coefficient of two-isotopes He-Ne<sup>20</sup>-Ne<sup>22</sup> mixture.

Thus, to decrease the influence of the waves scattering on the resonator elements on the output characteristics it is necessary to minimize and stabilize the functional

$W(a_1, b_1, V_1 - V_2) = \sqrt{a_1^2 + b_1^2 + 2a_1 b_1 \cos(V_1 - V_2)}$  and to support the generation frequency in the centre of the amplification line.

#### 4.3. Minimization and stabilization of the counter waves.

Investigation, carried out in [41] showed, that within the model of the back scattering, formed in the given work integral coefficients of the counter waves back scattering are connected with the counter phase travel of the two neighbouring mirrors of the square resonator in the following proportion:

$$\hat{r}_1 = \text{const} * \exp\left(\pi\sqrt{2} \frac{W}{\lambda}\right) = r_1 e^{i\epsilon_1} \quad (26)$$

$$\hat{r}_2 = \hat{r}_1$$

As considering (26) the expression  $\Omega_L$  will be shown as

$$\Omega_L \cong \text{const} * \cos\left(2\pi\sqrt{2} \frac{W}{\lambda}\right)$$

(27)

As it is clear from (36), linear counter phase travel of the resonator flat mirrorson w quantity lead to the harmonic low of lock in zone changes and the functional of  $w(a_1, b_1, V_1, V_2)$  minimization. To follow their behaviour on the one period, in the square resonator it is necessary to move counter phasely two neighbouring mirrors with the

help of the piezoelement to the distance of  $w = \frac{\lambda}{\sqrt{2}}$ .

In MSRI of Mechanics problems RITM the microprocessor system of minimization and stabilization of the counter waves connection (MSMAS), that realizes the specified principle has been worked out and then created.

The experimental device was designed for observation of the ring laser null drift with the switched on as well as with the switched off MSMAS of the counter waves connection.

According to the scheme, piezocorrectors (PC) of the ring laser with the switched on vibrational supporting system are controlled from the two independent subsystems:

- 1) system of perimeter stabilization and
- 2) system of minimization and stabilization of the counter waves connection.

The results of the multi-hour realization of the null drift of the laser gyroscope without the MSMAS show that null of the LG drifts during the operating time of 8-9 hours on the quantity not more than 0,1 degrees/hour.

The results of the null drift measurements of the ring laser with the operating MSMAS show that the value of the null drift comprised 0,005 degrees /hour.

Here it is necessary to mention that in the both cases the discharge current in the amplifying medium was the same, and the parameters, defining the character of the supporting system "noisiness", were also identical.

## CONCLUSIONS.

Within this work the analysis of the LG, developed and created here in Ukraine, is being carried out.

The mathematical model of waves characteristics forming in the ring laser, that contains space-distributed, limited volumes with the amplifying medium of the diaphragm and the sources of waves scattering is suggested.

The experimental investigations of the methods of stabilization and minimization of the counter waves connections in the four mirrors resonator, enclosed in the controllable change of the ring laser configuration by feeding of the additional counter phase voltage on the piezoconverter of the resonator mirrors that minimize and stabilize the functional, are suggested and the results are stated below:

$$W(a_1, b_1, V_1 - V_2) = \sqrt{a_1^2 + b_1^2 + 2a_1b_1 \cos(V_1 - V_2)}, \text{ where}$$

$a_1, b_1$  - quantities, proportional to the amplitudes of the modulation components of the counter waves intensities, and  $V_1 - V_2$  - , phases difference between them, here the quantity of the resonator perimeter remains unchanged.

It is shown , that in case when the resonator mirrors has similar scattering coefficients, the quantity of the lock in zone can be essentially decreased. It has been stated that the appliance of the system of minimization and stabilization of the counter waves connection allowed to maintain the null drift at actuation within the limits of 0,005 d/h, occasional component of the drift 0.005 d/√h.

The LG in standard regime had null drift within the limits of 0,1 d/h, the occasional drift component 0.07 d/√h

The achievement of the results, attained by the leading American and Russian companies, is possible in Ukraine, because SRI MP "Ritm" as well as CDD "Arsenal" possess scientific and technical potential and a number of technologies and IE "Zavod Arsenal" has all necessary equipment and developed technological processes, that are necessary for the LG manufacturing and their production in quantity for the various NS.

## EPILOGUE

The author expresses his sincere gratefulness to the academicians of the Ukrainian Academy of Technological sciences M.A.Pavlovsky and Y.A.Karpachev for their efforts to solve all the questions of laser gyroscopy development in Ukrainian , doctor V.A. Kanchenko (Kiev, Ukraine) , doctor B.V.Yefimov ( Moscow, Russia), professor G.S. Kruglik (Minsk,Belarus), doctor V.I. Kuzmenko (Kiev, Ukraine) for the fruitful discussions, that helped to formulate and solve stated within this work problems and also to the staff of the laboratory of the sensitive elements of MSRI MP RITM (Kiev, Ukraine), whose contribution to the realization of the specified approaches and laser gyroscope creation is really great.

## Bibliography

1. Statz, H., Dorschein, T.A., Holtz, M., Smith, I.W., "The multi-oscillator - ring laser gyroscope," Laser Handbook, vol IV. Ed. by Stieh and M.Bass, N.Y., Academic Press, 1985, pp 229-332.
2. Solomin, A.V., "Electromagnetic field of ring resonators in non-inertially moving reference systems", dissertation for the obtaining of the scientific degree of the Candidate of the physical-mathematical sciences, Kiev , Kiev State University, 1979.
3. Menegosi, L.M., Lamb, W.E., "Theory of ring laser", Physical Review A, General Physics, v.8, N 7, Jule 1973, pp 2103-2125.
4. Aronowitz, F., "Theory of a traveling wave optical masers", Phys.Rev., V.139, 1965, pp 635-647.
5. Landa, P.C., Investigation of the dynamic and statistic characteristics of optical quantum generators and amplifiers. Doctoral dissertation, Mocsow, Moscow State University, 1972.
6. Waves and fluctuation processes in lasers, articles edited by Y.L.Klimantovich, Moscow, Nauka, 1974, 245 p.
7. Fradkin, E.Ye. Waves processes in gas lasers of the current wave. dissertation for the obtaining of the scientific degree of the Doctor of the physical-mathematical sciences LSU, 1975, 396 p.
8. Birman, A. YA., Saushkin, A.F., Toropkin, Ye. N., Tzigurow N.G. About legitimacy of the Slatter method in the theory of the open resonator, Opt. and spectrum, vol.47, v.4, 1979, p.739-744.
9. Ananyev, YU.A., Anikichev, s.G. About expansion into series on own functions of open resonator equations., Opt and spectroscopy, vol.61, v.4., 1982, p. 856-860.
10. Birman, A. YA., Saushkin, A.F., Solomatin, V.A., Toropkin, Ye.N. Approximation of weak diffraction in the theory of ring laser with Gauss diaphragm., Opt. and spectrum, vol.9, N 6, 1982, p. 1238-1245.
11. Birman, A. YA., Saushkin, A.F. Theory of the diffractive phenomena in ring laser., Opt. and spectrum, vol.37, v.2, 1974, p.317-321.
12. Birman, A. YA., Saushkin, A.F., To the theory of ring laser with the heterogenous resonator., Opt. and spectrum., vol.38, v.3, 1975, p.615-619.
13. Birman, A. YA., Saushkin, A.F., Toropkin, Ye. Diffractive split of frequencies of counter waves in the ring resonator with two-scales corrector. Opt. and spectrum., vol. 50, v.4., 1980, p. 750-754.
14. Vinogradova, M.B., Rudenko, O.V., Suhorukov, A.P., Waves theory., Moscow, Nauka., GRFML, 1979, 383.
15. Apanasevich, P.A., Foundation of the theory of interaction between light and substance., Minsk, Nauka i tehnica., 1977, p. 496.
16. Ramasanova, G.S., Experimental and theoretical research of resonators, containing medium with the complex transverse optical heterogeneity. Dissert. for Candidate of technical Scinces., Moscow., 1977, p.174.

17. Ilyinski, A. S., Slepian, G.Y.A., Oscillation of waves in electrodynamic systems with losses., Moscow, Publishing house of Moscow State University, 1983, p.242.
18. Yariv A., Introduction to the optical electronics., Moscow., Vysshaya shkola., p. 398.
19. Papulis A., Theory of the systems and transformations in optics., Moscow., Mir., 1971, p. 495.
20. Gulin, A.V., Ramasanova G.S. Investigation of selection of the transverse modes of the resonator with the Gauss diaphragms., in the book "Mezhvuzonski tematicheski sbornik", "Applied physical optics", N 60, Moscow, Moscow Energetical Institute, 1985, 117-124 p.
21. Tiunov, Ye. A., "Non-linear interaction of elliptically polarized current waves in the ring laser with the magnetic field" Candidate dissertation, Leningrad, Leningrad State University, 1979, p.199.
22. Fain, V.M., Hanin Ya.I., Quantum Radiophysics., Moscow, Sovetskoye Radio., 1965, 397, p. 28. Voitovich, A.P., Magnetic optics of gas lasers., Minsk, Nauka i tehnika., 1984, p.208.
23. Spor, S., Latimer, I.D., "On accurate determination of the radial distribution of gain at 633 nm in small bore helium - neon discharges", J.Phys. Appl Phys, v. 17, N 8, 1984, pp 1607-1615.
24. Aronovits, F., "Laser gyroscopes", in the book "Appliance of lasers", edited by V.P. Tychinski., Moscow, Mir, 1974.
25. Rodloff, R., "A laser gyro with optimized resonator geometry", IEEE J.Quantum Electronics, V 23, N 4, 1987, pp 438-451.
26. Patent of the USA N 4, 473, 297 from 25.09.84.
27. Patent of the USA N 4, 526, 469 from 02.07.85.
28. Patterson, R.A., Ljung, B. and Smith, D.A., "Reduction of beam coupling in a ring laser gyro by Doppler shifting of scattered light", SPIE, V. 487, 1984, pp 78-84.
29. Patent of the USA N 4, 410, 274 from 11.10.83.
30. Patent of the USA N 4, 410, 276 from 18.10.83.
31. Patent of the USA N 4, 281, 930 from 04.08.81.
32. Patent of the FRG N 3, 320, 345 from 06.12.84.
33. Patent of France N 2, 557, 970 from 12.07.85.
34. Patent of the FRG N 3, 500, 044 from 18.07.85.
35. Patent of the UK N 2, 143, 367 from 06.02.85.
36. Patent of the UK N 2, 143, 366 from 06.02.85.
37. Patent of France N 462 548 from 03.08.84.
38. Patent of the UK N 2, 136 630 from 19.09.84.
39. Patent of France N 578 133 from 15.08.85.
40. Patent of the UK N 2, 143 638 from 06.02.85.
41. Bondarenko, Ye.A., "Calculations of the optical lengths of shoulders of disaligned ring resonator" Quantum electronics v.19, 1992, p.171-174.
42. Dovbeshko, A.A., Kanchenko, V.A., Conditions of appearance of the transverse modes in the spectrum of gas lasers generation with the quasitropic resonator. Mechanics of gyroscope systems. Edited by M.A.Pavlovsky. Kiev, 1989, issue 6, P.87-92.
43. Dovbeshko, A.A., Kanchenko, V.A., Kutovoi, N.G. Space-polarizational phenomena in He-Ne lasers with quasitropic resonator. Shkola-87, vol.2., Ostashkov, 1989, p.75-81.
44. Dovbeshko, A.A., Kanchenko, V.A., Kutovoi, N.G. About one method of definition of space distribution of field, generated by ring laser. Dep. manuscript. CSIII, 1989, bibliographic references. Series 1, n 2. Certificate of deponing N 3188/27.
45. Dovbeshko, A.A., Kanchenko, V.A., Strelets, I.A. Anomalies in behaviour of ring laser amplitude characteristics. Dep. manuscript. CSIII, 1989, bibliographic references. Series 1, n 2. Certificate of deponing N 3191/28.

## Effects of the Specific Military Aspects of Satellite Navigation on the Civil Use of GPS/GLONASS

**Dipl.-Ing Detlef Kayser**  
 Institut für Flugführung  
 - Prof. Dr.-Ing. Gunther Schänzer -  
 Technische Universität Braunschweig  
 Hans-Sommer-Str. 66  
 38106 Braunschweig  
 Germany

### Summary

Satellite Navigation is one of today's most promising and prospering infrastructure technologies. The performance improvement of this technology in comparison to the "conventional" terrestrial navigation systems can be seen in almost every aspect, e.g.:

- accuracy (decimeter level)
- coverage (worldwide)
- availability (24 hrs)
- dimension (4 dimensional navigation (space and time))
- system capacity (unlimited number of users)

This led to a widespread application of satellite navigation and an according fast growing figure of satellite navigation equipment in the civil market. Up to now however, the final breakthrough in a lot of commercial applications, like in the aviation industry and in the maritime business, has not been reached. Beside some still unsolved technical aspects, like the integrity problem, the fact that GPS and GLONASS are military systems is one of the main hurdles. This institutional aspect however, is not only an obstacle from the political point of view, but the military background of GPS/GLONASS led to a lot of design features of the system, that have a strong influence on the use of the system in civil applications. This paper will describe details on the different areas in which the military design limits the use of the system.

### Historical Background and Status of Satellite Navigation

The very fundamental basis of satellite navigation goes back as far as to the beginning of this century. At that time there was available mainly one satellite, which was the moon. The geodesist's community used the observation of the moon's ephemeris to determine the shape of the earth. Later in the century, when the first satellites were launched, these procedures were further developed and in 1958 it was observed that the DOPPLER shift measured on the Sputnik satellite could be used to determine its orbit and furthermore that these techniques could also be reversed to give an information about the observer himself. Therefore already in 1958 a navigation system was proposed which finally led to the development of the TRANSIT system. The first TRANSIT space vehicle was launched only two years later, in 1960, and a number of almost 30 satellites were to follow.

The background of TRANSIT was a military one, because it was first of all designed to help updating the inertial platforms of Navy vessels and submarines. It was specifically designed for this purpose as can be seen by the applied update intervals of a few hours, which is sufficient for marine applications, but makes the technique more or less unusable for aviation purposes. The achievable accuracy with TRANSIT is very much dependent on the user's velocity and therefore is heavily degraded in a high dynamic environment like in an airplane. This demonstrates that already with TRANSIT the specific military background of the system prevented a wide application of the technique for civil users.

Single channel receivers gained an accuracy of approx. 250m, dual channel receivers could provide up to 50m position accuracy in low dynamics.

At the moment there are 12 TRANSIT satellites in orbit, from which only eight are operated at the same time. According to the Federal Radionavigation Plan (FRP) the system will be switched off in 1996 because of the superiority of GPS. There is also a russian counterpart to TRANSIT, TSICADA, which has an unknown future and is very much comparable from the technical point of view (which is quite the same situation as with GLONASS and GPS).

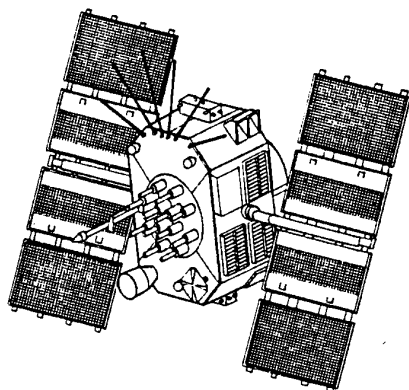


**Figure 1:** GPS Space Vehicle

The beginning of the development of GPS goes back to the year 1973, when the US Secretary of Defense merged the Navy's TIMATION programme with the Air Force 621B project to form the Navigation Technology Programme. The 621B programme used an „inverted range“ technique whereby satellite-type signals were generated by ground stations to provide ranging signals for aircraft positioning, while the Navy actually launched satellites.

As the name says, the TIMATION programme was mainly based on the usage of precise time references in space. In 1967 the first TIMATION satellite was launched into a 500 mile orbit, using a high quality quartz frequency standard. Timing accuracy for the time transfers was accurate to within one microsecond. The Timation II space vehicle was very much comparable to Timation I, whereas Timation III/NTS-1 had significant changes: the altitude was lifted from a low earth orbit up to 7500 nm to reduce atmospheric drag and in addition to the UHF frequencies of the earlier satellites an L-band Pseudo Random Noise Signal (PRN) at the same frequency as that of the later GPS satellites was added. The most significant change however was the usage of two rubidium

clocks, which offered a stability of  $10^{12}$  per day.

Finally NTS-2 was the first satellite completely designed and built under the sponsorship of the NAVSTAR GPS programme. The orbit was already the final GPS orbit with an altitude of 10980nm and instead of rubidium time standards two cesium clocks with a stability of 1-2 parts in  $10^{13}$  per day were used.

It is interesting to note that the inclination of the NTS-2 and the following NTS-3 (launch 1981) satellites were approx.  $63^\circ$ . This goes along with all of the first GPS space vehicles (Block I) that were launched in 1978 and had an inclination of just that  $63^\circ$ . Later this was changed to a far less inclination of approx.  $55^\circ$ , which is still used today (see chapter on space segment layout).

Today (autumn 1994) GPS has gained its IOC (initial operational capability) status and all planned 24 space vehicles are in orbit. The lifetime of most space vehicles launched up to now has by far exceeded the expected lifetime. A severe error in the space segment has only been reported from one satellite (SV 19) which had problem with the PRN-code. The new generation of space vehicles (Block II-r) is already under construction. The average launch rate is 2 satellites a year. Even though there are a lot of agreements between the military GPS command and the civil authorities (Department of Defense/Department of Transportation) the final control over the system remains in the hands of the Pentagon. A change of this status, e.g. transferring the system into the hands of a civil body with international participation, can not be expected for the foreseeable future.

One of the main problems with GLONASS is the reliability of the space vehicles. A lot of GLONASS satellites failed in a rather short time.

**Table 1:** GPS/GLONASS System Parameters

Parameter	GLONASS	GPS
geodetic coordinate system	SGS 85	WGS 84
number of satellites in full operational system	21+3	21+3
duration of almanac transmission	2.5 min	12.5 min
number of orbital planes	3	6
inclination	$64.8^\circ$	$55^\circ$
altitude	19100km	20180km
satellite signal division	frequency	code
frequency band	1602.56 - 1615.5 + 0.5 Mhz	1575.42 + 1 MHz



The main reason seems to be the frequency standards on board. Nevertheless there are 14 GLONASS satellites in orbit and Russia is continuing to launch the further satellites as pronounced (6 satellites in 1994, one however failed to reach its orbit). After a very restricted information policy on GLONASS, Russia is now seeking for a close cooperation with western partners. This year western observers had access to the Russian GLONASS Control Center in Moskau for the first time. The Table 1 shows the most important system parameters of GPS and GLONASS:

### **Specific Military Aspects of the GPS and GLONASS Technology**

#### *Restricted Accuracy / Selective Availability Policy*

One of the military features of GPS that has the strongest influence on the civil use of the system is the so called selective availability (SA) technique. This technique was introduced to the GPS system in March 1990, with the launch and operation of the BLOCK II satellites. Up to that point GPS could be used by the civil users with almost the same precision like the military P-code users.

SA is a technique that has the aim to allow only authorized users to gain the full accuracy of GPS. This policy goes back to the year 1982, when an interagency study panel, composed of representatives from the Office of the Secretary of Defense, the military services, the Office of the Joint Chiefs of Staff, intelligent agencies and the Defense mapping agency recommended to allow a Standard Precision Service (SPS) of only 100m accuracy for the civil users.

SA is implemented by either broadcasting wrong ephemeris data or degrading the timing information of GPS. The SA effect can be varied very strongly and there are clear statements that in the case of a military threat by an enemy to the US the president may order a significant increase in the level of SA.

The background of SA is the fear of the US Department of Defense (DoD) that the GPS technology could be used by hostile nations against the USA with the highest precision available. This level is now only available to special authorized PPS (Precision Position Service) users, who have to use special PPS-hardware. There are two main cases of a potential threat for the US:

- the first is a conflict like the Gulf War, in which GPS was widely used by the military for the first time. The fear was that for example the Iraq could position and launch its Scud rockets with the help of

GPS with the highest precision using standard civil GPS equipment of the shelf.

- the second type of threat are terrorists, who for example could fire missiles into the White House, guided by GPS.

When the SA technique was put into operation a fierce discussion started within the GPS-user community. The main argument of the SA opponents was that in the case of a war it does not matter if a Scud missile is precise to within 10m or 100m, because that precision is of the same level like the accuracy of most missiles themselves. This is probably true for the majority of applications of satellite navigation in the military environment. It is also very interesting to note that in the Gulf War the SA technique was switched off. The reason behind this was that the US military had not enough PPS capable GPS receivers and therefore had its troops equipped with standard SPS receiver hardware (and maybe also driven by the fact that PPS receivers need the CA code to lock in quickly). There are no reports about any military actions by the enemy in this war that could have been prevented if SA had been switched on. (It is also an interesting side effect that as a civil user one can foresee in the home office at what time a military crisis for the US will start by simply looking at the level of SA on GPS.)

The argument of terrorist's threats is turned down by the SA opponents with a hint to the fact that a terrorist could very easily built up a differential station (see differential technique later on) close to his target and then gain the highest precision again. A van, parking close to the White House, having a GPS antenna and a small telemetry antenna on top would not be noticed by anyone and would cost the terrorist only a few hundred dollars (This option can also be used in wartime by enemies but could be encountered by jamming, which is not true for single peacetime terrorist action).

It was suggested that the SA technique should only be put into effect in the case of a crisis and that in peacetime the full precision of GPS should be made available. This was turned down by the US military with the remark that the users of GPS (esp. the military) must get used to SA and be aware of this effect all the time.

Meanwhile the discussion about SA has gained a new aspect by the upcoming of GLONASS. GLONASS has no degradation on its broadcast message at all and therefore the civil GLONASS code is almost as good as the GPS P-code. As can be seen in Figure 2 there is only an offset in the output of GPS and GLONASS resulting out of the different coordinate system that are used. The Russians have declared that they will not put any

SA like effect onto GLONASS and most probably the system is not even capable of this technique because GLONASS was never meant to be used by civilians.

Today several companies sell GLONASS receivers on the open market and even hybrid GPS/GLONASS receivers are produced by western (American) companies. The question arises who will prevent an enemy or a terrorist from buying GLONASS instead of GPS?

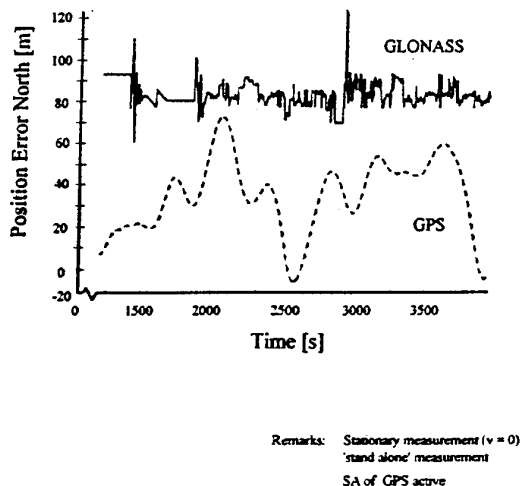


**Figure 2:** Selective Availability with GPS compared to GLONASS Accuracy

The European civil users look at the SA policy with some kind of confusion. On one side it is strange to see that the American tax payer is first giving his money to build up a satellite system, then spending extra money to design technologies that can artificially degrade the accuracy of the system and then finally pay again money for services that compensate this artificial degradation (differential services). On the other side SA is the most obvious effect of the main deficiency of GPS for a civil user and that is its military control. If the GPS is offered with a 95% guarantee what is happening in the more than 15 days a year when the SA level is much higher than 100m? What happens if the US president decides to increase the level of SA because of a US national crisis (Grenada, Haiti etc.)?

These difficulties on the other hand forced the Europeans at a very early stage to develop techniques that counter the effect of SA. This is the

main reason why Europe has such a profound background in differential techniques and could therefore catch up in the application of satellite navigation with the owner and designer of the system. From today's viewpoint it was more beneficial than a drawback for Europe that the US DoD applied SA to GPS.

This is especially true for the very high precision applications that soon arose mainly in the field of aviation. To gain the accuracies needed for precision landings the differential technique is a must in any way, even if SA would not be in effect, to compensate atmospheric disturbances and inaccuracies of the ephemerides data. That is one reason why for example the first fully automatic landing based on GPS was not performed in the US but in Germany (in 1989 in Braunschweig, by the Institute for Flight Guidance and Control).

However with the upcoming application of the satellite technology in fields like car navigation, SA must be seen again in another light. The land navigation market will be the biggest commercial market for satellite technology (estimated 70% share in 1996) and at the same time the market in which every dollar in production costs makes a significant difference in competition. The accuracy requirements for the land navigation field are in many cases just in the area of GPS without SA (20m) as a variety of user surveys have shown. This means that a satellite navigation system without SA would make additional equipment in the car for the differential data transmission obsolete and therefore would have a significant cost reduction effect. In Europe with its 120 million cars, and especially in Germany with 50 million cars alone, there is a strong requirements for a satellite navigation system that is not degraded. In Germany an expected major pusher for the application of satellite navigation in cars is the planned road pricing policy of the Ministry of Transportation. One of the best candidates to form an intelligent toll system is based on GPS and is now in a test phase. If this system can demonstrate its technical feasibility there will still be the question if a nation can base a fee collecting system that is operated by the military of a foreign nation. It can not be imagined that the tax income in Germany depends on the activities of the US army in some far away part of the world (the same applies to maritime navigation, see Figure 3). Therefore the military background of GPS forces countries like Germany to plan independent civil systems, even though this leads to redundancy, that is not needed from the technical point of view.



**Figure 3:** SA-Effect to Maritime Applications

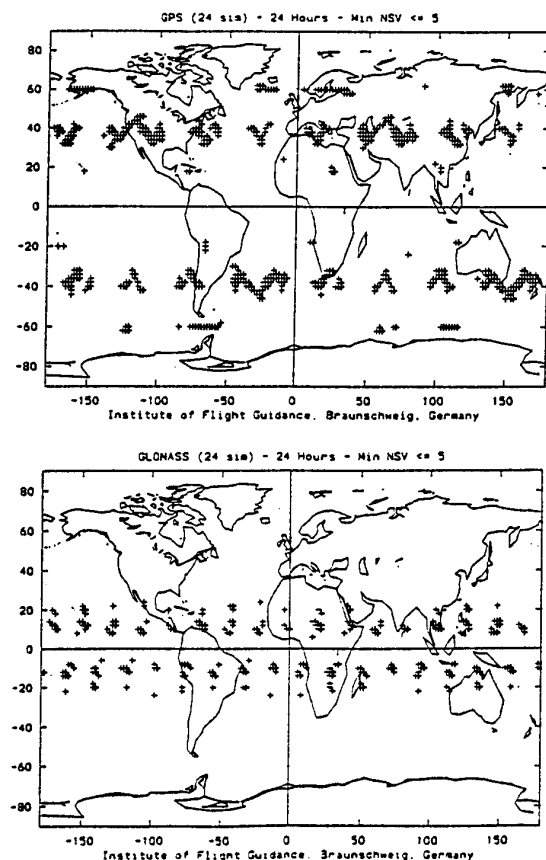


**Figure 4:** Coverage Gaps with GPS and GLONASS

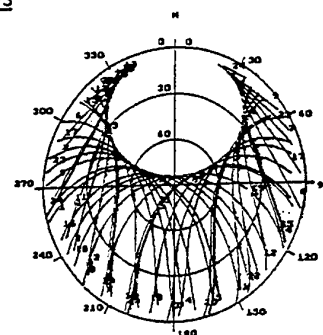
### Restricted Availability- the Coverage of GPS and GLONASS

Both systems GPS and GLONASS are designed to provide a worldwide coverage. This means that at every time at any place on the globe one can see at least 4 space vehicle at a time. In the full constellation that requirement is fulfilled by both systems and often 6 to 8 satellites are visible. To gain the best performance of the systems it is of course also important in which constellation the satellites can be seen. That means the more homogeneous the satellites are distributed over the sky the better will be the geometrical performance, which often is expressed in terms of DOP (Dilution of Position) values. In general it can be stated that the more satellites a user can see the better the navigation performance will be (and a better redundancy in the case of a faulty satellites is provided).

The way the globe is covered by a satellite system depends among other factors predominantly on the altitude of the orbits and the inclination of the orbital planes. It is very interesting to analyze GPS and GLONASS under this respect, because both have approx. the same altitude but differ significantly in terms of inclination. Figure 4a and Figure 4b show in which areas of the earth only five or less satellites can be seen from the GPS and from the GLONASS space segment.

12. 4.1994  
Lat 50.00143  
Long 0.00143  
H 50.01m3  
MinElev 5.0443  
Copyright Inet.  
FUR Flugführung  
TU Braunschweig  
Time 0 h 0 m  
000P3 000P2  
2.14 1.23  
SV Elev Azim  
3 1.0 163.3  
4 34.8 47.2  
7 0.9 77.3  
11 28.3 284.4  
12 12.8 229.4  
13 30.8 309.3  
18 73.7 90.0  
19 30.2 77.4  
23 74.1 214.9

#### GPS



12. 4.1994  
Lat 50.00143  
Long 0.00143  
H 50.01m3  
MinElev 5.0443  
Copyright Inet.  
FUR Flugführung  
TU Braunschweig  
Time 0 h 0 m  
000P3 000P2  
1.87 1.08  
SV Elev Azim  
6 0.2 282.4  
7 11.2 359.4  
10 0.7 17.3  
12 23.2 132.4  
13 77.1 112.7  
14 44.3 312.0  
15 90.3 189.4  
19 30.3 37.9

#### GLONASS

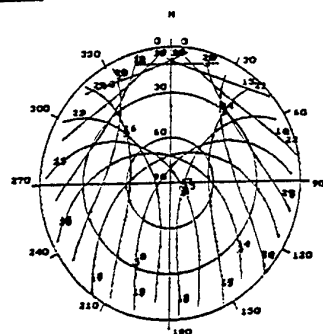


**Figure 5:** Sky Plots for GPS and GLONASS at 50° North, showing a Gap for GPS in the North

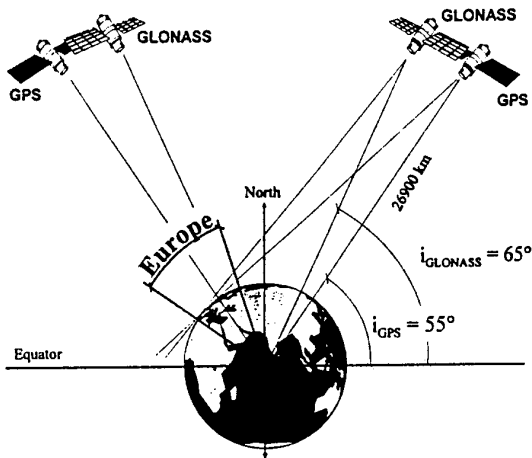


**Figure 6:** Geometry of GPS/GLONASS

It is remarkable that GPS has significant deficiencies in the middle latitudes that means also in the area of CONUS (Continental US), while GLONASS has a worse coverage around the equator. The reason for this lies in the fact that the GLONASS satellites can look far more over the poles than GPS due to the higher inclination. That is shown in Figure 6 which explains that the coverage of the polar regions is absolutely no problem for satellite systems with altitudes of approx. 20.000km and high inclinations.

From the viewpoint of satellite visibility GLONASS is therefore much more favourable for Europeans (and Americans) than GPS. This is also true if one does not just look at the number of satellites visible but also analyzes the geometrical distribution in detail. The according optimal DOP values are gained if the satellites are distributed evenly along a circle close to the horizon and a satellites in the zenith. This on the other hand assumes that there are satellites visible also in the north (or south for the southern hemisphere respectively). In Figure 5 so called sky plots are shown for a latitude of 50° north. These plots show the track of the satellites in terms of azimuth and elevation. It can be seen that GLONASS is much better also in the geometrical performance, because it has no coverage gap in the north like GPS.

As a final proof of this fact Table 2 gives the RAIM-performance of GPS and GLONASS. RAIM, which stands for Receiver Autonomous Integrity Monitoring, is a technique that uses sub-

sets of all visible satellites, to check the integrity of the satellite system by analyzing the redundant information from all those subsets. The RAIM capability is an essential feature for the civil use of satellite navigation in safety critical applications. It can be seen that GLONASS is favourable to GPS.

**Table 2:** Raim Non-Availability per Day

System	Area	Phase of Flight		
		Enroute [%]	Terminal [%]	NPA [%]
GPS	world	2.8	2.8	11.1
	Europe	2.8	2.8	9.7
	N-Am.	2.78	2.78	9.72
GLONASS	world	6.9	8.3	33.3
	Europe	0.0	0.0	2.8
	N-Am.	0.0	0.0	2.78
GPS & GLONASS	world	0.0	0.0	0.0
	Europe	0.0	0.0	0.0
	N-Am.	0.0	0.0	0.0

The question that arises is, why GPS and GLONASS were designed in such ways by the military. First of all it seems to be obvious that GPS was not designed for the civil use in the area of CONUS. The best performance of GPS and GLONASS is gained in Central-Europe which during the cold war was always thought to be the battlefield of the next military confrontation between East and West. The navigation systems were of course optimized to guide for example missiles very precisely into the battlefield. While the East probably also held the area of CONUS as a potential aim for missiles in mind, for the West Europe and the USSR were an almost identical target area, having the same latitude band. From today's viewpoint this background of the two systems is very frightening but today Europe has the advantage to be the area for which both satellite systems were optimized. While GPS certainly has advantages in the latitude bands close to the equator (areas which probably are also thought of as being possible candidates for conflict situations) the GLONASS space segment is much better designed for civil applications in those areas of the world with the highest demands for precision navigation.

As stated above in the beginning of GPS the GPS Block I satellites had a higher inclination of 63°. The reason why the orbits were changed later on is not exactly known to the author but several possibilities can be considered. One is that the planned number of space vehicles changed several times during the development of the system: from 18 satellites to 24 satellites back to 21 satellites. From the orbit mechanical standpoint the GPS orbits belong to the class of so called DELTA patterns. A 24 satellite 6 orbit pattern is one of those configurations that WALKER, who made very detailed analysis studies of Delta patterns over more than

20 years, selected as being among the optimal choices. Walker however focused his orbit selection on n-coverage communication purposes and took not into account the DOP criteria for best geometrical performance. WALKER suggests an approx.  $55^\circ$  inclination for the 24/3 Delta patterns, so that GPS seems to have been optimized by his kind of evaluation. The same is true for GLONASS, because WALKER suggests for a  $65^\circ$  inclination a 24 satellite configuration in eight orbits, which is exactly the GLONASS space segment layout.

Another point is the transport vehicle that is used to launch GPS space vehicles: it was planned to use the Space Shuttle carrier but after difficulties with the Shuttle's launch schedules and then finally after the Challenger accident the GPS space vehicles were all launched by rockets. The capacity of the Space Shuttle would however have restricted the GPS orbits in their inclination and maybe this also led to the  $55^\circ$  GPS inclination.

The altitude of approx. 20000km for both GPS and GLONASS leads to an orbital period of 12hrs. for the two systems. It is not absolutely clear, why exactly that altitude was chosen for the systems. As will be shown later the cost optimized altitude for a navigation system is significantly lower. The systems also need a higher power level to gain the same signal to noise ratio like in the lower altitudes. Even though it is favourable to have an orbital period that is an even factor of the 24hr revolution period of the earth (for ground communications etc.), this is also true for 8hr or 6hr orbits. There may be two reasons for the high altitude of GPS and GLONASS from the military point of view. One is that a 12hr orbit is high enough to counter possible attacks of so called „killer satellites“. If such a satellite would be launched to destroy a GPS space vehicle it would take several hours to reach the 20000km altitude and the GPS Command Control could start counter measures (shift orbits etc.). The other one is that the GPS space vehicles were also designed to carry atomic explosion detection sensors that may have a need for a certain field of view.

### Commercial Aspects

At the first sight there seems to be no connection between the military background of GPS and GLONASS and their civil use concerning costs. A lot of users are especially fond of the satellite technology because they only have to pay for the receiver hardware and not for the service itself. However, even though GPS as well as GLONASS are free of charge, they are definitely not free of costs, at least not for Europeans. The reason for this lies in the fact, that during the development of GPS the US DoD gave a lot of contracts to the American electronic industry for the development

of receiver equipment. There are statements from GPS officials that 5 to 6 billion \$US were spend for this purpose. This gave the US electronic industry a big advantage in the civil receiver market. Even today almost all high value receiver hardware is manufactured in North America and there are only two European manufacturers (Japan is mainly designing low cost, low performance receivers). With an expected multi billion dollar market for the US the GPS investment has certainly paid off (see Figure 7), while there is a big danger that this whole new market will be lost for Europe.

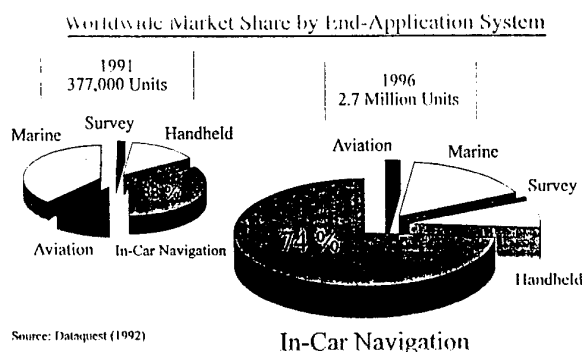


**Figure 7:** Market Development for Satellite Navigation

By offering GPS free for every civil user the US DoD created a de facto standard and a monopoly at the same time. Most of the users did and do not see the need to think about alternative systems, even though their national industry loses significant market shares by this. That is even more true, when the estimated figures for the costs of satellite navigation systems are discussed. The US DoD quotes about 10 to 12 billion \$US for the development of GPS. This seems to be a very high figure and is often brought forward as an argument against the development of a complete new, civil satellite navigation system (GNSS II, second generation Global Navigation Satellite System). The high development costs for GPS are however to a very great extent driven by its military background and a GNSS II is believed to be much cheaper. The cost reduction is mainly due to the following aspects:

1. The receiver development must not be repeated. It is commonly agreed that a GNSS II will at least be GPS downwards compatible, so that only minor receiver modifications will be nec-

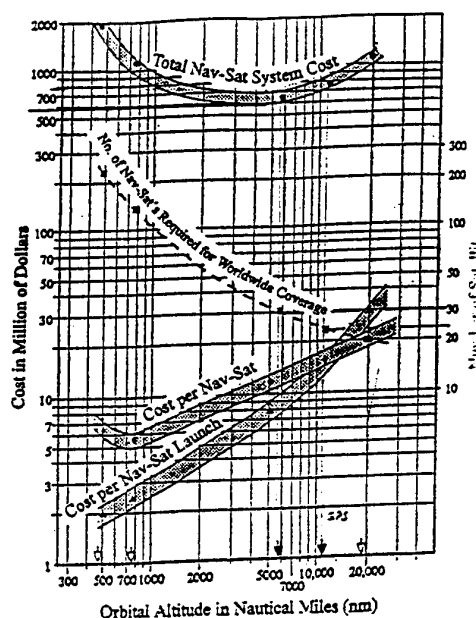


**Figure 8: Costs for a Satellite Navigation System (INMARSAT Econsat Concept)**

essary. This reduces the figure of 10 billion \$US by approx. 50%.

1. As shown in the previous chapter the orbital layout is not cost optimized. With a different space segment the launch costs will be significantly lower as can be seen in Figure 8.
2. The following military GPS features are also not needed in a civil GNSS II:

- selective availability technology
- P-code or encryption (Anti Spoofing)
- long term memory support
- cross link communication or ranging (autonomous navigation)
- triple cross-strapped redundancy
- nuclear radiation hardening
- high frequency standard stability requirement

Taking all this into account a figure of 1 to 2 billion \$US seems to be a realistic order of magnitude for a GNSS II. INMARSAT even proposed its ECONSAT concept for a price as low as 600 million \$US. These are investments in the order of cellular phone networks, that even the private

industry could afford and today big electronic companies (like Siemens) are already considering this in their long term strategies.

### **Institutional Aspects and Future Developments**

From the very first beginning of satellite navigation aviation has played the role of the main driver of the new technology. This is also true for the civil application of GNSS even though land navigation will offer the biggest commercial potential for the technology. The reason for this is the high demand from the aviation community for worldwide, whole earth, wheather independent radionavigation aids of very high precision.

In addition to that the requirement levels, especially concerning integrity, of the aviation applications are extremely high and therefore have been subject of intensive research all around the world. Even though it has been proven that GPS and GLONASS offer the capability even for high precision landings down to Category III, the certification of avionics based on satellite navigation is still an unsolved problem.

This is first of all of course a political problem. The commercial aviation can not rely on a system that in the case of a crisis is degraded possibly up to a level were it is not usable any more. If the only solution for this problem would be to still have the existing systems like ILS as a backup in the airplane, the technology is not of interest for the airlines because it does not offer a cost reduction. This might be a solution for a transition phase from one technology to the other but cannot be the final goal.

The only way for GPS and GLONASS to serve as a sole means navigation tool for aviation would be the transition from a military command structure to an internationally controlled, civil body that has the full control over the systems, or commitments of the DoD's that every nation that uses the system is asked if the system can be degraded or not. Both options are very unlikely and therefore the only practicle solution seems to be the development of a complete new, civil GNSS, to make the technology acceptable for safety critical applications like aviation.

As stated already earlier in this paper a downward compatability to GPS of this future GNSS is a must. It will however most probably differ in the design of the space vehicles and in the layout of the orbital configuration. The development in the airborne application of GNSS has shown that integrity is the biggest problem to solve. This is a completely new requirement for the existing systems, because GPS and GLONASS were not designed to meet any civil integrity requirements at all. For a military system it is not necessary to offer an integrity level of up to  $10^{-10}$  as it is required for Category III precision landings in civil aviation. Today studies show that 24 satellites are probably not

enough to offer an acceptable level of redundancy for RAIM algorithms while a combination of GPS and GLONASS (with more than 40 satellites) offers a significant improvement for RAIM. A future GNSS II will therefore consist of more than 24 satellites, which are sufficient for the military requirements.

Another way to get around the integrity problem of GPS and GLONASS is known under the term of Geostationary Overlay or GNSS I. The geostationary overlay is planned as an augmentation to GPS and GLONASS in the form of 4 geostationary satellites with navigation transponders. Besides a GPS-compatible navigation message the satellites will broadcast an integrity message, giving the user data on the integrity status of the whole satellite navigation segment. At the moment this technology is discussed in a very controversial way, because it has some severe drawbacks that will most probably not allow to make it an operational system. One reason is that the coverage of geostationary satellites is not very good for higher latitudes (pole routes, alternate airports for North America flights) and when taking into account the allowed bank angle limits for civil aviation the system can not be certified for the use in latitudes down to 45° (the latitude of Turin). On the other hand the integrity channel can only offer information about the satellite status, while the biggest part of the integrity problem will happen on the way of the signal from the satellites to the user (shadowing, multipath, jamming etc.). And finally, most important of all, the basic system is still GPS (and/or GLONASS) and therefore all the institutional problems described above are still unsolved. Therefore the GNSS I approach must be looked at as an interim phase for Europe in which some experience with the operational aspects of satellite navigation can be gathered. The final goal must however be GNSS II.

Today the integrity information offered by GPS and GLONASS via the „health status information“ in the navigation message is only very rudimentary and shows again, that both systems were not designed to meet civil requirements. A problem with the „health status information“ is that the time delay (up to several hours) is several orders of magnitude too high for civil applications. Especially GLONASS has the problem, that there are too few ground stations to monitor the system „on-line“. In addition the ground stations are only on the territory of the former USSR out of military reasons so that an error in a space vehicle can be unnoticed by more than 10 hours.

#### *Future Developments*

In Europe the European Union, ESA and Eurocontrol have decided to look at GNSS as a key element of the so called transeuropean networks and therefore as an important part of the future international

infrastructure. As a first step it was decided to support the development of a civil GNSS, by launching a GNSS I / GNSS II programme. At the moment ESA evaluates proposals for the according mission analysis studies in the frame of its ARTES Element 9 activities. In the first phase a budget of up to 100 million ECU's is planned.

The cornerstones of the future system are already laid down. Besides the already mentioned GPS compatibility it is very likely that there will be a multi frequency service for civil use, to allow the user for compensation of atmospheric delays in the signal transmission (like with P-code service today). There is also the demand for a communication capability, so that a user can transmit his navigation data. To increase the navigation performance of today's systems, GNSS II might work with higher „chip rates“ and an improved navigation message.

It must however be stated, that from the technical point of view, GPS and GLONASS are performing very well and that all technical improvements will only have a minor effect on the overall performance of satellite navigation.

#### **Conclusion**

For the commercial success of the satellite navigation technology the military background seems to become a hurdle that can not be overcome with the present systems, at least not in the foreseeable future. It is very likely, however, that without the military background of GPS and GLONASS the technology would not have developed in such an explosive way as it did, or may even not be available up to day at all.

The civil applications are so wide spread that only imagination is the limit and the number of civil users outnumbers the military ones by far. The following short list is meant to give an impression of the potential of the technology, by describing some special commercial application systems that integrate satellite navigation and additional sensors for highest precision:

- Flight Inspection Systems: integrated systems are used to measure the performance of the radionavigation aids of bigger airports (instrument landing systems (ILS)) and therefore has to be more accurate than these systems.
- Air data measurements: integrated GPS-based systems are used to measure very precisely the tracks along which air data are collected. If combined with very precise aerodynamic sensors (5 hole probes etc.) the difference of the track speed and the air speed is the wind in the atmosphere. In Germany this technique is for example used in a tethered measurement system underneath a helicopter to do polar re-

search and is also used to perform air pollution measurements.

- Van Carrier Location System: a precise GPS-positioning system is used in container terminals to track single containers. This helps to minimise the loss of containers, a problem in big harbours like Hamburg. The system has paid off in less than half a year.

A big field of application are also all search and rescue purposes. Already today a lot of firebrigades and ambulance car fleets all around the world are using GPS to save time and thereby numerous lives.

As a summary it can be stated that GPS and GLONASS are dual use technologies with unprecedented benefit for the civil world. The billions of dollars that have been spent by the US and the Soviet military for the development and operations have most probably already paid off from the economical point of view and definitely have launched a technology that will be an explosively growing, multi billion dollar civil market in the future.

#### References.

/Jacob/

Integrated System using Differential GPS and Inertial Measurement Unit, in: Schwarz, K.P. and Lachapelle, G. (eds.): Kinematic Systems in Geodesy, Surveying and Remote Sensing, Springer Verlag, New York, 1991

/Jacob/

Beitrag zur Präzisionserkennung von dynamisch bewegten Fahrzeugen, Thesis, Technical University Braunschweig 1992, ZLR-Forschungsbericht 92-03

/Jacobsen, Len/

The Need for Selective Availability  
GPS WORLD, May 1991  
Volume 2, Number 5

/Redeker/

Computer-Aided Flight Testing of an Digital Autopilot on Board a Research Aircraft, ICAS Conference Proceedings 14th International Congress, September 9-14, 1984, Toulouse

/Schänzer/

Flight Test Results of a Complex Precise Digital Flight Control System, AGARD Conference Proceedings 452 "Flight Test Techniques", 17.-20. Oktober 1988, Edwards Air Force Base, California

/DGPS '91/

First International Symposium: real Time Differential Applications of the Global Positioning System, Deutsche Gesellschaft für Ortung und Navigation, TÜV Rheinland, 1991, Braunschweig

/Easton, R.L./

The Navigation Technology Program  
Papers published in NAVIGATION  
Volume 1, 1980

/McDonald, Keith/

ECONSATS  
GPS WORLD, September 1993  
Volume 4, Number 9

/Bennet, Verne/

GPS Forum: No Need for Peacetime Selective Availability  
GPS World, September 1991  
Volume 2, Number 8

/Lindemann, Haverland/

AeroNav, an Integrated Navigation System for Special Mission Aircraft, Conference Proceedings DGPS '91, Braunschweig, Germany.

/Haverland, Redeker/

The Use of Differential GPS as Position Reference for Flight Inspection purposes, Conference proceedings 16th International Flight Inspection Symposium, 1990, Washington D.C., USA

/Schänzer/

Satellite - Navigation; State of the Art and Future Potential; an European View, ESA / Euro-space Symposium, Brüssel 1993

/Gu, Tiemeyer/

High Precision Navigation with Wide Area DGPS, DSNS '93 Symposium, Amsterdam, 1993

/Vieweg, Tiemeyer/

Modelling and Calibration of DSNS and Inertial Sensors in an Integrated Navigation System, DSNS '93 Symposium, Amsterdam, 1993

/BMVg-Studie/

Study for the German Ministry of Defense/  
Experimental Study on the Performance of different GPS-Receiver Types in the Application of Integrity Monitoring Techniques, 1993  
(subcontract for the Avionik Centre Braunschweig)

/Kayser/

The Satellite Navigation Space Segment from the European Point of View DSNS '94, London



# THE DLR RESEARCH PROGRAMME ON AN INTEGRATED MULTI SENSOR SYSTEM FOR SURFACE MOVEMENT GUIDANCE AND CONTROL

Dipl. Ing. Kurt Klein  
DLR  
German Aerospace Research Establishment  
Institute of Flight Guidance  
Lilienthalplatz 7  
D-38108 Braunschweig  
Germany

## 1 SUMMARY

Based on the long-term experience in the field of Navigation and Air Traffic Control the Institute of Flight Guidance within the German Aerospace Research Establishment (DLR) is conducting a major effort to develop new solutions, system components and procedures for an integrated Surface Movement Guidance and Control System (SMGCS). In addition to and derived from the work on operational procedures, planning tools and HMI in our institute we are focusing our work on an integrated sensor concept to meet the requirements. SMGCS is to be regarded as an integrated concept that has a clearly defined modular approach to meet the particular requirements of a specific aerodrome.

After outlining the conception several years ago a solution for the realisation was evaluated in close co-operation with the DFS and the national industry. The objective of DLR research is

- to analyse the characteristics and to optimise as far as necessary the sensor candidates (e.g. DGPS, SSR Mode S Multilateration),
- to evaluate the sensor information integration including data fusion algorithms,
- to find solutions for the specific SMGCS data exchange problems via RF link,
- to optimise the whole system loop in order to avoid interference by implementing modules into the system,
- to solve airfield operating problems by finding new functions within the SMGCS sensor domain.

Although the main goal is the improvement of civil airport traffic the work meets as well military operation problems. Besides that a lot of knowledge gained in military applications have to be considered.

The research activities are funded by the DLR itself. To extend the theoretical and laboratory work to more realistic analysis an Experimental SMGCS is build up at the Braunschweig airport. This ESMGCS has the advantage to be very flexible with respect to the implementation of various subsystems and to tests in a real environment. Braunschweig airport is very suitable for experiments like this due to low traffic density and the available research infrastructure. Part of the ESMGCS will be a test environment that is based on the experiences gained during the MLS competition as well as during the development of the Avionics Flight Test System. Main part of the test environment is a measurement system for computing a reference situation assessment.

The backbone of the ESMGCS is a high speed data network on fibre cable basis that connects the peripheral stations around the airfield to the master station. Different sensor subsystems or parts of these will be installed in the peripheral stations.

The data fusion and the situation analysis are software processes within the master station. The derived situation information can be handed over to planning tools and to the tower simulator available in the DLR Institute of Flight Guidance.

## 2 INTRODUCTION

ICAO coined the term SMGCS for a new concept of an integrated airport surface movement management system. Several aviation bodies recognise that the development of such a system is required in order to cope with the projected aviation growth in the near future and, for improved ground movement safety and efficiency.

Today ground control systems are made up of loosely coupled functions that provide advisory information to the co-operative tasks of the ground Air Traffic Controller and the Pilot. The primary controlling functions are human related - voice communication, visual situation awareness and planning by knowledge. With technology most of these functions can be improved, integrated and automated, so that SMGCS will enhance efficiency by reducing human workloads, and by maintaining safety levels with an increase in airport capacity.

To avoid new bottlenecks at airports that cause flow management problems due to weather, capacity, communication and slot management inadequacies the concept SMGCS has to fit into a higher degree of a common technological solution.

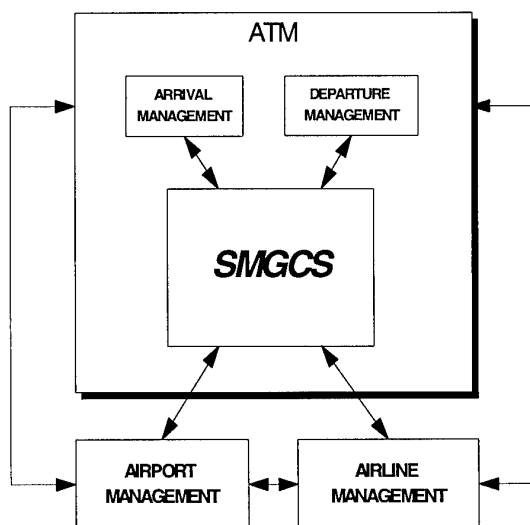


Fig. 1: SMGCS ENVIRONMENT

SMGCS will be one element of the Air Traffic Management and it will interchange information to other functional elements (Arrival and Departure Management). To get the whole benefit of existing information the exchange of data between Airport Management as well as Airline Management and the SMGCS is necessary.

Analysing the present day ground movement on a high level of abstraction without regarding the realisation in a human mind or in a machine the functional loop may be described by four fundamental function domains:

- Situation Assessment
- Situation Monitoring
- Planning
- Guidance.

The controlled object, whether aircraft or vehicle, must be detected, identified and its attitude determined and predicted. Other objects on runways and taxiways have to be detected and classified. Regardless of visibility conditions this will be done by the use of sensors. Combining and comparing sensor data with the knowledge of the airport, with plans, etc. can be done much more precise and faster by automatic situation monitoring. Planning functions and the guidance functions complete the loop.

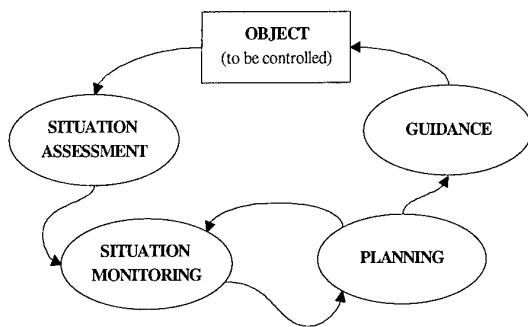


Fig. 2: SMGCS Functional Architecture

After the definition of the functions within the domains it is necessary to represent them by a system outline. Designing the SMGCS the present day working relationship between pilot, controller and electronics is adopted, but the authority of certain procedures and methodologies will be changed in the future. Electronics will play a much larger role. Although some of the international bodies discussing the airport ground management technology are labelling the future system as A-SMGCS (Advanced-SMGCS) in this paper SMGCS is used as a general term.

### 3 THE CNS PART OF THE DLR SMGCS CONCEPT TARMAC

#### 3.1 The SMGCS Concept of DLR

The Institute of Flight Guidance within the German Aerospace Research Establishment (DLR) has a long-term research experience in the field of Navigation as well as in Air Traffic Control. As a consequence the development of new solutions, system components and procedures for an integrated Surface Movement Guidance and Control System is one of the important work areas.

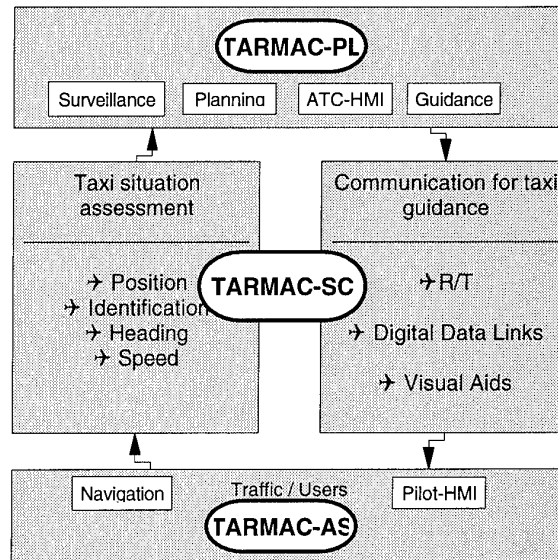


Fig. 3: SMGCS System Loop

Several years ago the DLR started in close co-operation with the German ATC Authority (BFS, now: DFS) the analysis of the present situation on large airports. The derived frame concept **TARMAC (Taxiway And Ramp Management and Control)** identified the lack of planning tools and conflict detection tools, the need for better co-ordination systems for the departure and arrival management and better human machine interfaces. The results and proceedings are documented in [Di94].

In addition to and derived from the operational procedures, planning tools and HMI the DLR is focusing the work also on an integrated sensor concept to meet the requirements of ATC, Airports and Airlines. Considering this 'Top Down Approach' the system loop has to be completed by adequate subsystems for the surveillance and guidance functions. This part - contributing hardware elements - is called **TARMAC-SC** (SC = Surveillance and Communication).

#### 3.2 TARMAC-SC

In the manoeuvring area of an airport various types of vehicles partly equipped with modern electronic, and non controllable objects are present. Considering this traffic both types of sensor subsystems have to be implemented into a SMGCS:

- co-operative sensor subsystems and
- non-co-operative sensor subsystems.

Co-operative sensors need onboard installation (e.g.: SSR Mode S transponder, ADS transmitter) and non-co-operative sensors are for example inductive loops, radar systems. The aircraft related co-operative sensor subsystems have to meet the standards for onboard equipment.

The use of at least two different types of sensors implies the sensor data fusion function in the system. This function will be implemented as a software process within the SMGCS computer facilities. This function has to provide an unambiguous traffic situation to the other function domains (situation monitoring, planning, guidance). For each object on the manoeuvring area a reliable data set including position, speed, etc. is necessary. The benefit of including more than the

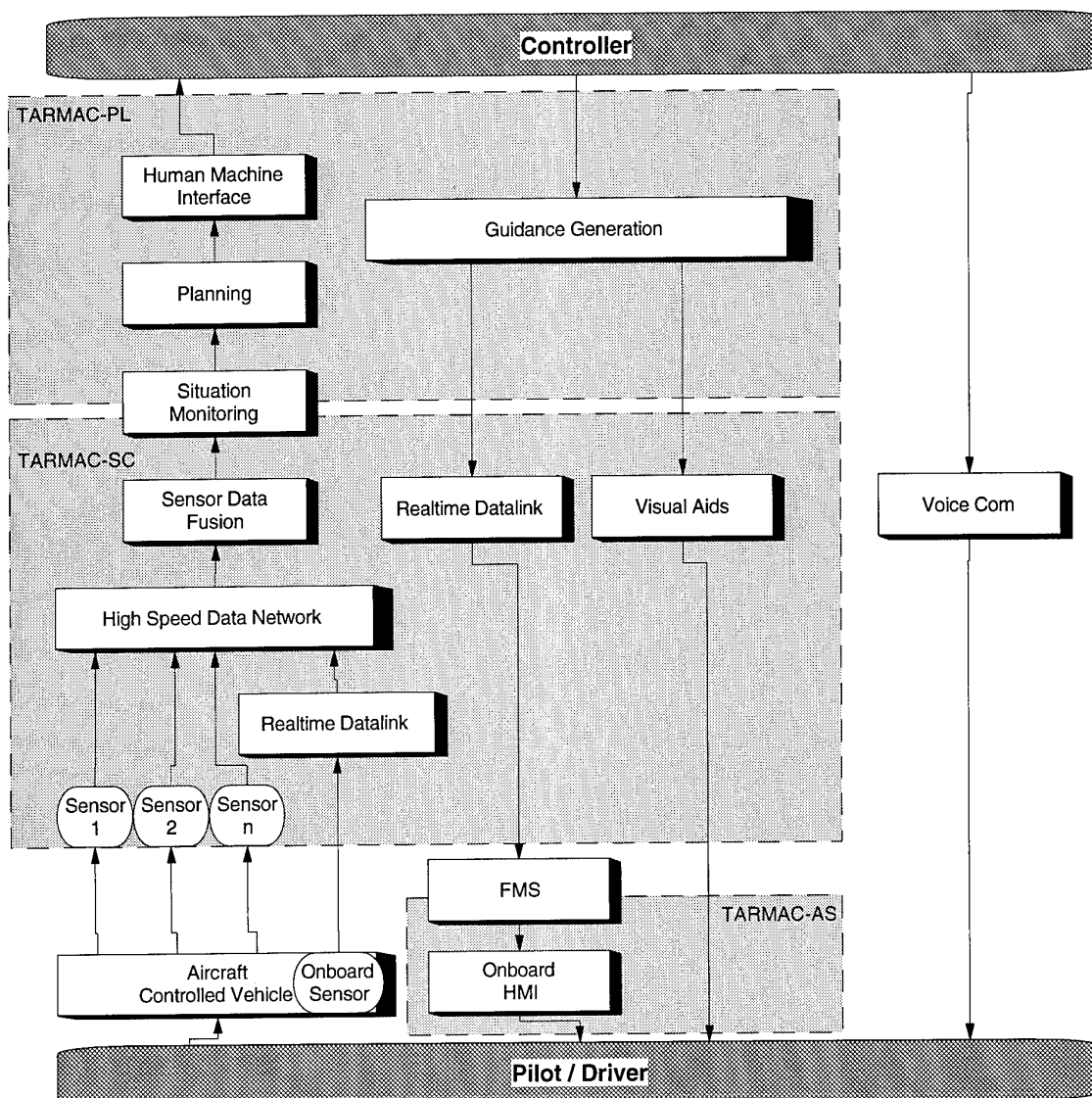


Fig. 4: DLR SMGCS System Structure

minimum of two sensor subsystems will be the increase of the performance of the total system.

One of the most interesting onboard sensors is the GPS receiver. As the civil available C/A Code does not fulfil the SMGCS requirements differential techniques have to be used.

The use of onboard navigation equipment for SMGCS implies the use of data links to transmit position, speed, etc. to the ground. In addition the opposite RF link is needed to transmit reference data for differential GPS. Near real time data transportation is needed for these system internal links.

The guidance functions are presently realised in most cases by voice communication or by traffic lights. In the future a digital data link will improve this function enormously. Due to standards these SMGCS data links have to meet the principles of ATN (Aeronautical Telecommunication Network) and of on-board installations. Several RF links will be available but the overhead of the ATN is not applicable for the ground movement application.

Separate RF links are available for the data communication with ground vehicles. As this equipment may vary from country to country or even between airports. Different techniques have to be taken into consideration in designing the concept.

So, SMGCS is to be regarded as an integrated concept that includes several subsystems. It has a clearly defined modular approach to meet the particular requirements of a specific aerodrome. Systems may vary from very simple surveillance and guidance tools to sophisticated multi-sensor systems due to very different needs of the airports.

DLR approached the problem by dealing with the combination of sensors concerning safety and commercial aspects as well as the aim to come to a systematic concept that can be approved by all type of users. The structure of the advantageous open system is designed in that way that any type of sensor subsystem or guidance subsystem can be adopted. But to get the most benefit of specific combinations the technical characteristics as well as commercial aspects of each subsystem have to be analysed carefully.

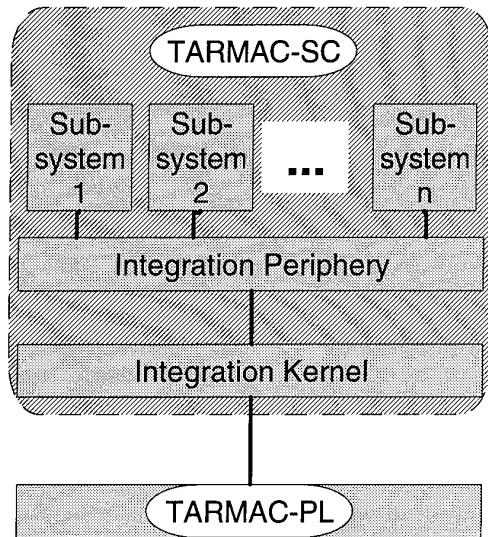


Fig. 5: TARMAC-SC System Location Areas

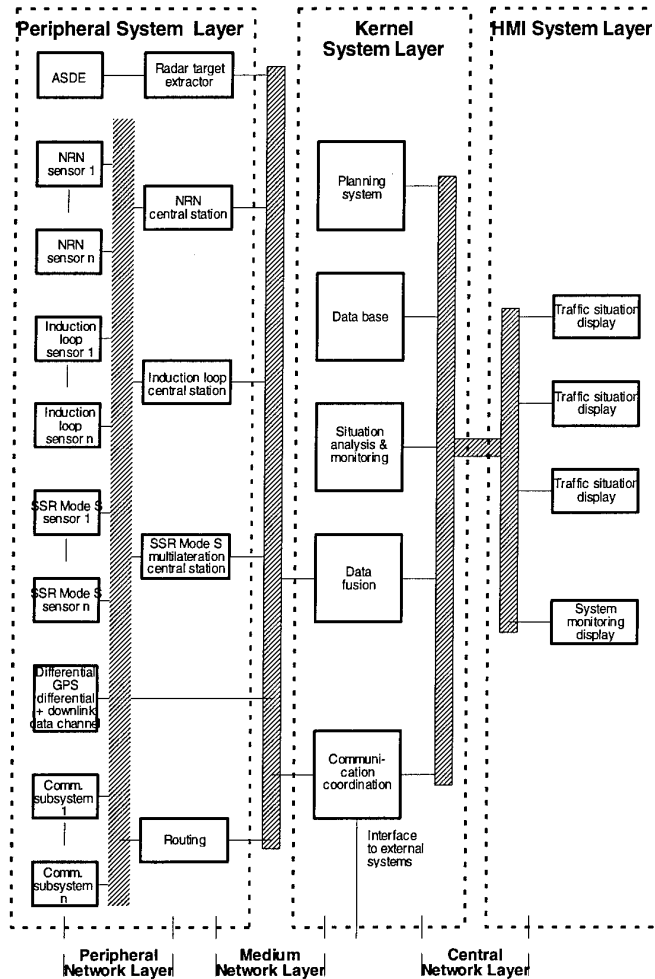


Fig. 6: DLR System Architecture of the SMGCS

Another view on such a complex system like TARMAC highlights the subsystem local distribution. As sensor subsystems and RF transmitters and receivers have to be located around the airport's surface and the main computers will be concentrated, whereas the controller working position will stay in the tower a powerful data distribution subsystem (a data network) is necessary.

The time limitation of all system internal data transportation and data processing are of major importance. The human display and manual interface have to be in a direct correspondence to the real physical effects. This means that the whole system has to be a real time system in the main data processing line. The trade off between delay time and any data prediction has to be done carefully. The resulting update rate has to be at least once per second.

So the DLR concept includes a high speed data network on the airport. The task of this integration periphery is to interconnect modules of the system or subsystem modules. Considering the available and well-tested technology this will be a powerful computer network. But the DLR research lead to the result that a specific adaptation to the application is needed.

#### 4 DLR RESEARCH AREAS WITHIN TARMAC-SC

As outlined in the previous chapter DLR work is a stringent top down approach, and so the general architecture from the function level down to system design and subsystem integration aspects is one of the major tasks. Especially new subsystems have to be analysed and characteristics - if not available - are estimated to evaluate the possibilities and the criteria for integration into the whole system.

A new Near-Range Radar Network (NRN) as a supplemental subsystem is developed within DLR by our colleagues in the Institute for Radiofrequency Technology and is presented in [Sc94].

The ground based interconnection via data network and the methods and algorithms for fusing sensor data are kernel elements of the SMGCS. Conception work is done in the field of real-time radio data link systems and the routing. Further studies include new functions for future implementation to put more cognitive processes into machines in order to reduce human workload. Appropriate interfacing the TARMAC-SC part to the planning system and to the HMI is as well an important item.

#### 5 COMMUNICATION WITHIN TARMAC-SC

As already mentioned the time critical transportation of data within the integrated system is one of the major problems to be solved. Therefore the highspeed data network installed on the airport surface and in the buildings has to fulfil hard specifications. To avoid interference only fibre optical media are applicable for future systems. The requirements for a SMGCS LAN differ from networking office computers. Therefore the evaluation of the specification needs more investigation. It is already clear that the top state of the art (FDDI or ATM technique) has to be used.

Concerning the position reports for vehicles (similar to enroute ADS functions) a powerful RF downlink is necessary with near real-time requirements.

A separate problem is the communication between board and ground. For guidance RF data links will

replace the presently used voice communication on VHF (or UHF for military links) in the normal ATC business. The voice link will still be used for backup and in emergency cases. In the aeronautical area digital data links are a necessity in the future. But the specific requirements in the SMGCS are not yet met by available certified technique.

As it is unrealistic to rely on radio frequencies not yet used for aeronautical purposes the already installed or discussed data links have to be the starting point for the SMGCS data link discussion. These candidates are:

- ATN under standardisation
- SSR Mode S under standardisation
- AMSS (SATCOM) specified by service provider
- ACARS specified by service provider
- AVPAC specified by service provider
- VDL under standardisation
- Gatelink under standardisation
- Special VHF solutions not standardised  
(e.g. „Swedavia System“)
- MLS Frequencies standardised, to be adapted

The use of the ATN for this purpose as it is outlined seems not very appropriate as the delay times are too long. Moreover it is not efficient to fill up the ATN with small area related data. The use of one of the specified ATN subsystems (Satellite, Mode S, VHF) has to be studied further but the satellite link delays are also very long.

Mode S is one of the most promising subsystems as it is already discussed to implement real time data transmissions on a low level of the OSI model. Simultaneously the Mode S may be used as a sensor by using Multilateration techniques. ACARS and AVPAC are commercial systems that do not meet the technical SMGCS requirements. The VDL standardisation

process may be influenced in that way that the specific real time requirements can be implemented similar to the Mode S design.

But undoubtedly special solutions using time division multiple access technology - well known in the commercial mobile telephone world - has the most promising potential to solve SMGCS data link problems. A lot of further research and development work are necessary to meet aeronautical requirements.

## 6 THE ESMGCS

The SMGCS concept has to be demonstrated and an experimental environment for further development is needed. Besides that tested components have to be implemented in a phased approach in a representative airport for operational evaluation. To extend the theoretical and laboratory work to more realistic analysis an Experimental SMGCS is build up at the Braunschweig airport, funded by DLR. This ESMGCS has the advantage to be very flexible with respect to the implementation of various subsystems and to tests in a real environment. Braunschweig airport is very suitable for experiments like this due to low traffic density and the available research infrastructure.

In the following table (Fig. 7) the criteria to be tested within the ESMGCS are outlined in horizontal direction but only a part of these is scheduled yet due to budget limits. As the SMGCS may be a very complex system it is necessary to evaluate the possibilities of each subsystem to match into the whole system and to check whether interference problems arise by implementing the component. The overview refers to the DLR plans regarding industry products already tested. So the interoperability test is the main goal.

Part of the DLR installation will be a test environment (see Fig. 8) that is based on the experiences gained during the MLS competition as well as during the development of the Avionics Flight Test System. Main part of the test environment is a measurement system for computing a reference situation assessment. Although this test environment will be the main tool for the mentioned TARMAC-SC research work it is

		Function	Modularity	Integrity	Reliability	Specifica- tions	Interference Resistance	Matching	Basics
Sensors	SSR Mode S					☒		☒	
	DGNSS					☒	☒	☒	☒
	NRN	☒				☒	☒	☒	☒
	ASDE							☒	
	VHF- Transponder					☒	☒	☒	
	Loops							☒	
	Others							☒	
Highspeed Data Network		☒	☒	☒	☒	☒	☒		
SDF		☒	☒	☒	☒	☒			☒
Situation Monitoring		☒	☒	☒	☒	☒			☒
System Monitor		☒				☒			
RF Data Link		☒				☒	☒		
TARMAC + HMI Interface		☒							
FMS and A/C HMI		☒				☒	☒		
System Integration		☒	☒	☒	☒	☒	☒		☒

Fig. 7: Items to be tested by DLR in the ESMGCS

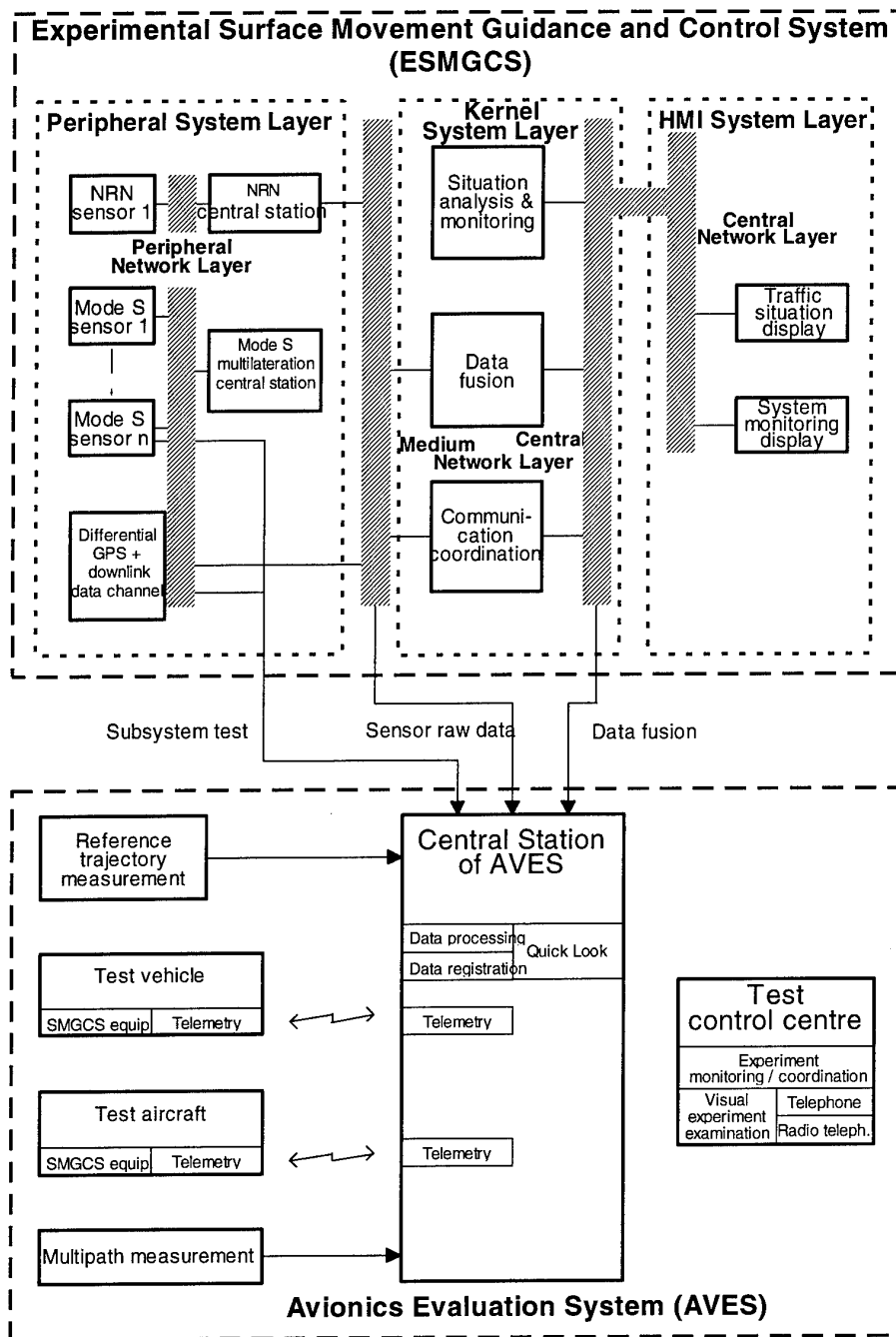


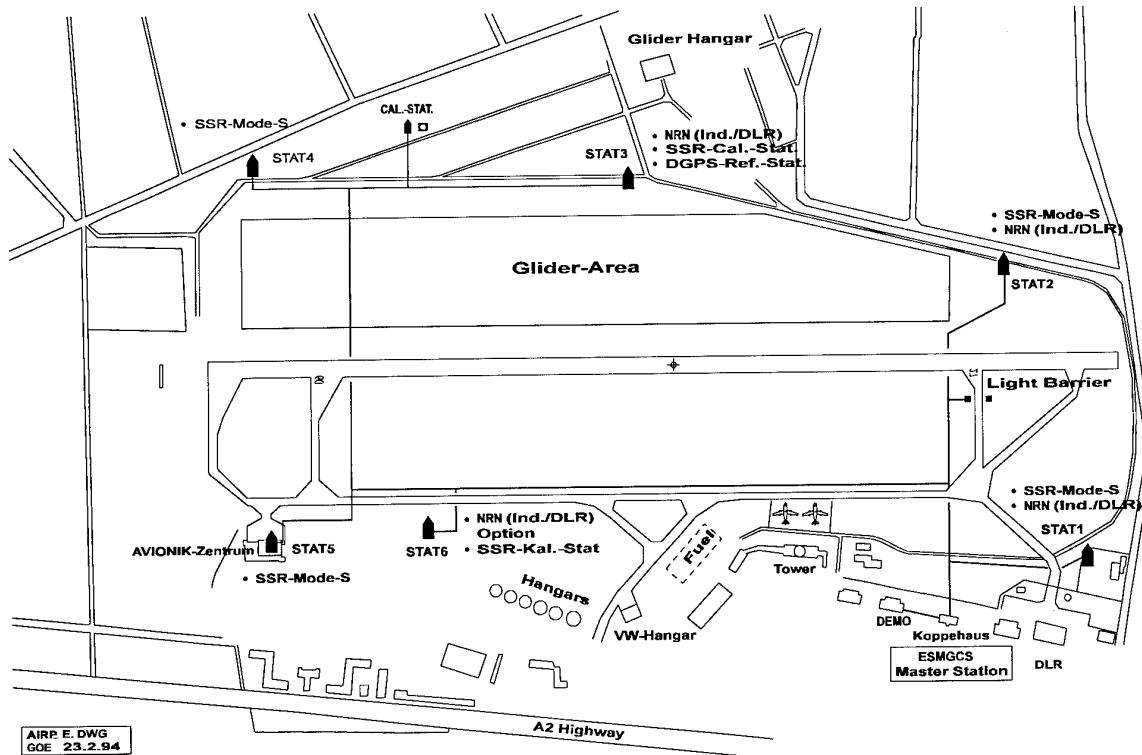
Fig. 8: ESGMCS with Avionics Evaluation System

tool for the mentioned TARMAC-SC research work it is possible to use it as well for additional evaluations in cooperation with other partners.

The peripheral stations of the ESGMCS around the airfield are connected to the master station by a high speed data network on fibre cable basis. Different sensor subsystems or parts of these will be installed in the peripheral stations. Within the master station the data fusion and the situation analysis are software processes. The derived situation information can be handed over to planning tools and to the tower simulator available in the DLR Institute of Flight Guidance.

Figure 9 gives an overview on the ESGMCS facilities at Braunschweig airport where one of the DLR research centres is located. The peripheral stations are located around the airfield. Most of the cables are routed through tubes to be flexible.

The main computer equipment and the displays are installed in DLR buildings south-east of the airfield. An easy interconnection will be done to the other DLR facilities like the research computer network and the Tower Simulator in the DLR Institute of Flight Guidance.



### ESMGCS Scenario at Braunschweig Airport

Fig. 9: The Test Location

#### 7 CIVIL AND MILITARY SUBSYSTEMS FOR SMGCS

First of all SMGCS and in general the ATM discussion and development is a civil problem. But the military traffic has to be taken into account.

More than that a lot of knowledge developed in military projects is applicable for SMGCS. So the use of sensor systems like GPS or sensor principles (Near Field Radars) and data fusion techniques seem to be very promising SMGCS elements.

The future managing functions within a SMGCS need reliable and precise surveillance information delivered by the data fusion subsystem. The DLR research for the situation assessment considers not only the sensor data and characteristics but as well additional knowledge of the airport and the traffic. For an optimised situation assessment a data fusion as outlined in Fig. 10 as an extension of the sensor data fusion will improve the function.

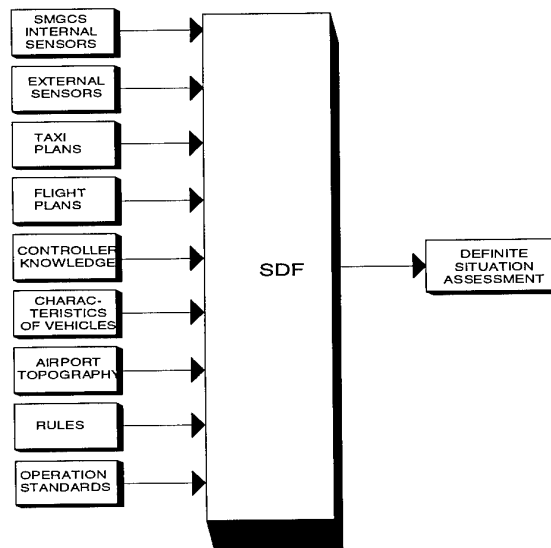


Fig. 10. The functional structure of the situation assessment including the sensor data fusion

#### 8 OUTLOOK

Further analysis of the SMGCS is necessary and depends on the technology available. A careful trade off between the human and machine processes is a basis for the system design.

After a European acceptance of guidelines for designing these functions there is as well a need for validation standards as the functions may be implemented in a variety of different system designs adapted to specific airports.

Several proposals discussed the system realisation of the surveillance and guidance functions but only the integrated view including planning and the controller working place will give the most benefit. Therefore further investigation is needed not only to get perfect elements but also to develop an optimised overall system. Now, the European Commission has implemented these actions in the 4th framework programme and several national activities will be preceded.

## 9 REFERENCES

- [Eu94] EUROCAE „SURFACE MOVEMENT GUIDANCE AND CONTROL SYSTEMS“ Volume I + II, EUROCAE Working Group 41 Report, ED-200A, February 1994, Paris
- [ES94] EUROCAE 1. Report of Subgroup 6 „SYSTEM INTEGRATION ASPECTS“, EUROCAE WG-41, January 1994, Paris
- [DG93] DGON Report „AERONAUTICAL DATA COMMUNICATION“, The German Institute of Navigation, 1. December 1993, Düsseldorf
- [DA91] DGON / ADV „GUIDANCE, CONTROL, AND TRAFFIC MANAGEMENT ON THE AIRPORT SURFACE“ Proceedings of the Symposium, 8 - 9. October 1991, Braunschweig
- [IC78] ICAO „MANUAL OF THE AERONAUTICAL TELECOMMUNICATION NETWORK (ATN)“, Doc 9578-AN/935, Montreal
- [Be91] Becker, Prof. Dr. A., et. al. „EXPERIMENTELLES INTEGRIERTES ÜBERWACHUNGS- UND KOMMUNIKATIONS-SYSTEM FÜR DEN ROLLENDEN VERKEHR AUF FLUGHÄFEN“, DLR Institut für Flugführung / Institut für Hochfrequenztechnik, IB 112-91/21, IB 551-91/4, März 1991, Braunschweig / Oberpfaffenhofen
- [Sc94] Schroth, Prof. Dr. A. „A NOVEL NEAR-RANGE RADAR NETWORK FOR SURVEILLANCE AND GUIDANCE OF AIRPORT GROUND TRAFFIC“, in ECAC APATSI / EC Workshop on SMGCS, Frankfurt, 6-8 April 1994
- [Di94] Dippe, D. „A PLANNING SYSTEM FOR AIRPORT SURFACE TRAFFIC MANAGEMENT“, in ECAC APATSI / EC Workshop on SMGCS, Frankfurt, 6-8 April 1994

## 10 ACRONYMS

A-SMGCS	Advanced Surface Movement Guidance and Control System
A/C	Aircraft
ACARS	ARINC Communications Addressing and Reporting System
ADS	Automatic Dependend Surveillance
ATC	Air Traffic Control
ATM	Air Traffic Management
ATN	Aeronautical Telecommunication Network
AVPAC	Aviation VHF Packet Communications
BFS	Bundesanstalt für FlugSicherung (former German ATC Authority, now privatised: DFS)
CNS	Communication Navigation Surveillance
DFS	Deutsche FlugSicherung GmbH (German ATC )
DGPS	Differential GPS
DLR	Deutsche Forschungsanstalt für Luft- und Raumfahrt (German Aerospace Research Establishment)
ESMGCS	Experimental Surface Movement Guidance and Control System
EUROCAE	The European Organisation for Civil Aviation Equipment
FDDI	Fibre Distributed Data Interface
GPS	Global Positioning System
HMI	Human Machine Interface
ICAO	International Civil Aviation Organisation
MLS	Microwave Landing System
OSI	Open System Interconnection
RF	Radio Frequency
RWY	Runway
SDF	Sensor Data Fusion
SMGCS	Surface Movement Guidance and Control System
SSR Mode S	Secondary Surveillance Radar Mode S
TARMAC	Taxi And Ramp Management And Control
TARMAC-SC	TARMAC Surveillance and Communication
UHF	Ultra High Frequency
VDL	VHF Digital Link (under ICAO standardisation)
VHF	Very High Frequency



# Low-level Data Fusion for Landing Runways Detection

Laure Sliwa, Xavier Briottet

Département d'Etudes et de Recherche en Optique

Centre d'Etudes et de Recherches de Toulouse

Office national d'Etudes et de Recherches en Aérospatiale

2, avenue Edouard Belin B.P. 4025 31055 Toulouse Cedex  
France

## 1. SUMMARY

Data fusion brings reliability and robustness to both military and commercial systems. Data fusion allows in fact to fully apprehend a situation by using multisensors data redundancy and/or complementarity.

The presented piece of work particularly concerns fusion of redundant data just outcoming from electro-optical sensors. The used methods are low-level fusion techniques, only preceeded by a calibration step. These fusion techniques take into account the radiometric -and not geometric- data content.

This paper is divided in two parts : the theoretical approach, and the guidance application of detecting a potential runway.

The theoretical approach, according to the proposed goal, raises two problems. The one of suiting the multisensors configuration to the mission. And the one of evaluating data at every step from ground reality to fusion. It appears necessary to define quality criteria to evaluate every sensor acquisition within the mission scope. The optimization of these criteria defines the weighted combination at the pixel level of the multispectral images.

A priori knowledge of road materials spectral signatures and definition of appropriate quality criteria are necessary to detect roads or runways by pixel fusion. They allow to define the appropriate configuration of spectral bands to merge so that the runway shows up clearly. This paper presents the obtained results from low-level fusion of five broad bands (approximately 100 nm wide).

The main advantage of pixel fusion is the saving of processing time. On one hand, the multispectral data process is quick. On the other hand, the landing runway can be detected at long range, in a large field of view.

## 2. INTRODUCTION

### 2. 1 Guidance interests in data fusion

Data fusion uses multisensors data complementarity and/or redundancy. In fact, by using for instance outcoming data from visual and acoustic sensors, or from sensors measuring the same physical quantity, fusion allows to better apprehend a situation. This approach makes the false alarm rate decrease, and a priori knowledge of the scene characteristics become less restricting. Data fusion brings reliability and robustness to both military systems (operations theatre surveillance for example), and commercial systems (ground-to-air and air-to-ground airport surveillance for instance).

Three data fusion levels exist, according to different data levels of abstraction. Combination of rough and redundant data is low-level data fusion. This fusion does require identical or comparable sensors. When a processing step, such as primitives research, preceeds information combination, we talk of numerical fusion. Concerning

symbolic data fusion, data of proposition model are combined.

This paper particularly concerns fusion of redundant data just coming from electro-optical sensors (visible and infra-red). Within the image processing context, these methods are called pixel fusion since the merged data are pixels. The used methods are low-level fusion techniques, only preceeded by an image calibration step. These fusion techniques take into account the radiometric -and not geometric- data content.

Guidance can resort to different levels of data fusion, specially in bad environmental conditions. Low-level data fusion can be used to detect a landing runway or an obstacle. Numerical fusion can classify runways according to their length or to their materials (1). Symbolic fusion will be used to identify an airport or an obstacle on a runway. This paper focuses on low-level data fusion for landing runways detection.

### 2. 2 Low-level data fusion purposes

Low-level data fusion does not require a previous processing step, but a unique geometric and radiometric inter-calibration. The whole useful information is available. Low-level data fusion principle lies in the rough data merging in accordance with the scene physical analysis (specially spectral analysis). The nearest to the sensors, the more efficient the fusion is. Therefore, this approach requires the scene a priori knowledge (reflectance, emissivity, atmospheric conditions, ...). The low-level data fusion purpose is to increase the contrast and/or the signal-to-noise ratio, specially in images with hidden or furtive targets. This approach followed by an adequate thresholding, can lead to target and background detection.

In the guidance context, the aim of this work is to detect a potential landing runway by optimizing multisensors data fusion. Radiometric signatures of runway materials are a priori known. Then, two problems have to be solved. Suiting the multisensors configuration to the mission, and merging and evaluating the resultant data.

### 2. 3 Low-level data fusion state of the art

Data fusion bibliography emphasizes the motivations and interests of an approach based on signal physics and combination of data straight after the sensors (2, 3, 4, 5). As far as data fusion motivations are concerned, the most meaningful one is the race to furtivity. It can also be noticed that the automatic target recognition has been paralysed because of disregard for the scene's physical characteristics (6).

The state of the art also raises the question : how to merge the data ? Nevertheless, few work has been realized, and few concrete answers given. The state of the art rather deals with the general classification of data fusion methods, than with the usable criteria definition. It is

rather general theory than solved examples of low-level data fusion. Let us give a general data fusion classification. Clark (2) divides all the methods in two classes : the weakly coupled methods and the strongly coupled ones. The methods are arranged according to the independence or dependence of the data to be combined. Harmon (6) bases his classification on the use of data evaluation criteria. This allows to combine data by weighting and averaging all of them. Or one of the data can be chosen to be the resultant one according to its evaluation. Criteria can also permit to guide the sensors to another spectral window of interest. However, neither of the authors gives a mathematical definition of the criteria. Therefore, that deficiency of the state of the art has to be fulfilled by : giving a definition of various quality criteria to evaluate data and fusion, evolving a low-level data fusion and optimizing the method.

In this aim, this paper is divided in two parts : the theoretical approach, and the guidance applications.

### 3. LOW-LEVEL DATA FUSION PRINCIPLE

#### 3.1 The framework

The theoretical approach, according to the proposed goals raises two problems : suiting the multisensors configuration to the mission, and merging and evaluating data.

To cope with these problems, low-level data fusion requires rather accurate physical reality models. Each sensor acquisition should be analyzed and formalized, by taking into account the target, the atmosphere and the sensor. Then, it becomes necessary to define quality criteria to evaluate each sensor acquisition within the mission scope. This allows to choose a multisensors configuration appropriate to the real situation.

The image from each chosen sensor is weighted and combined at the pixel level with the others. The weights are defined by optimizing the quality criterion appropriate to the mission.

#### 3.2 Analysis and formalism

The general framework, within low-level data fusion is here evolved, is the merging of redundant information from electro-optic sensors (visible and infrared). So, the measured physical quantity is spectral radiance. The upwelling radiance of the scene characterizes the target and its surrounding. It takes into account the atmospheric path from the scene to the sensor. In fact, the whole upwelling radiance arriving on the sensor can come from the target itself, but also from the surrounding background, and from various atmosphere constituents. Therefore, as part of the guidance program, a data base of landing runways spectral characteristics is necessary, and the atmospheric conditions are to be known. Then every pixel value in the image of the scene given by a chosen sensor can be predicted.

#### 3.3 The criterion choice

The sought criteria must allow inter-evaluation of the various fusion methods, and comparison between the resultant piece of information and the whole starting information. To achieve the objective of pixel fusion, the criteria have to be appropriate to contrast enhancement for detection missions, and to target classification for identification missions. In the first case, the target spatially covers several pixels, and its variance can be computed. Most of the classical quality criteria can then be used : contrast modulation, signal-to-noise ratio, Bhattacharyya distance, ... . In the other case, the target spatially cover less than a pixel, its variance cannot be

then computed. Among the first listed criteria, the only contrast is usable.

Coming back to the framework of a hidden target detection mission, the objective to achieve is the target-to-background contrast enhancement, and/or the target signal-to-noise ratio enhancement, too. After this mathematical processing, target and background should become separable, as the target surrounding histogram is roughly made of two classes. As far as image histogram quality is concerned, the meaningful quantities are the distance between the two classes (i.e. the target-to-background contrast), and each class width (i.e. the target and background variances).

Consequently, the chosen criteria are the contrast modulation and the signal-to-noise ratio, defined as follows :

$$C = \frac{|n_t - n_b|}{n_t + n_b} \quad \text{equation 1}$$

$$S/N = \frac{(n_t + n_b)/2}{\sqrt{s_t^2 + s_b^2}} \quad \text{equation 2}$$

where  $n_t$  and  $n_b$  stand respectively for the target and background levels in the image,  $\sigma_t$  and  $\sigma_b$  stand for the standard deviations.

In the mathematical state of the art, a criterion takes both contrast and signal-to-noise ratio into account : it is the Bhattacharyya distance.

$$Db = \frac{(n_t - n_b)^2}{4(\sigma_t^2 + \sigma_b^2)} + \frac{1}{2} \ln \left( \frac{\sigma_t^2 + \sigma_b^2}{2\sqrt{\sigma_t^2} \sqrt{\sigma_b^2}} \right) \quad \text{equation 3}$$

This distance appears as the square product of the contrast and the signal-to-noise ratio. The second expression takes differences of level distribution into account. It is often insignificant as the signal-to-noise ratio is greater than 10. This criterion will also be considered in the following work. one of the meaningful advantage of these three criteria is that they are independant of the image signal level. And we can either consider  $n_t$  and  $n_b$  as radiance levels or as grey levels.

#### 3.4 Low-level fusion methods

As it has been written in the first part of this paper, the state of the art suggests a general fusion methods classification. The low-level multispectral data fusion belongs to the weakly coupled fusion methods class. Each sensor gives an inaccurate piece of information that can be used on its own. The principle of the fusion is to weight and then to combine the multispectral information in the aim of reducing the inaccuracy in the resulting information. Some of the authors prefer to weight by the accuracy of each source of data (8). And so they do not link the fusion method with the mission goal. The aim of our work is more global. We are concerned by the fusion method optimization according to the mission. We are interested in better suiting the merged spectral bands to the scene characteristics.

Consequently, the fusion technique is chosen to exploit the spatial criterion in each spectral image, and its evolution over the data spectrum. Looked at from this point of view, a weighted average :

$$F^{xy} = \sum_{i=1}^n a_i L_i^{xy} \quad \text{equation 4}$$

and a weighted averages ratio have been chosen as information combinations:

$$F^{xy} = \frac{\sum_{i=1}^n a_i L_i^{xy}}{\sum_{i=1}^n b_i L_i^{xy}} \quad \text{equation 5}$$

where  $L_i^{xy}$  stands for the  $(x, y)$  pixel radiance in the image  $i$ ,

$$\sum_{i=1}^n |a_i| = 1 \text{ and } -1 \leq a_i \leq 1, \sum_{i=1}^n b_i = 1 \text{ and } 0 \leq b_i \leq 1.$$

A weighted average of the multispectral radiance data results in a radiance homogeneous quantity. This one is defined in front of the sensors, fluctuating with atmospheric conditions. That is why the choice of evaluation criteria that do not exploit radiance levels but relative radiance levels is important. They can consider relative radiance levels either between target and background, or either between different spectral bands.

From this point of view, the weighted average analyses the spatial criterion in the image. For instance, the highest spatial contrast images are selected, i.e. they are given meaningful weights. It is the low-level data fusion method that Harmon (6) and Clark (2) speak about. And the ratio takes the spectral evolution of the criterion into account, i.e. the difference between the target and background spectral evolutions. It is called spectral contrast. The interest of this technique is emphasized by the vegetation index used by the remote sensing community.

### 3.5 Optimization

The aim of optimizing is to find the  $a_i$  and  $b_i$  parameters that raise quality criteria to a maximum. Various mathematical techniques have been evolved to cope with this point (9).

Since the parameters  $a_1$  to  $a_n$  and  $b_1$  to  $b_n$  have to be defined, a multidimensional case has to be considered. And as we want to optimize a function (the criterion) of the fusion result, the optimization is not linear. Considering these two points, and the additional fact that it can be quite difficult to evaluate the derivative of that function, the Downhill Simplex Method, due to Nelder and Mead, was chosen to optimize both fusions (equations 3 and 4). This method just crawls downhill in a straightforward fashion, that makes almost no special assumptions about the function. This can be extremely slow, but it can also, in some cases, be extremely robust.

## 4. APPLICATIONS TO GUIDANCE

### 4.1 Data description

To conform the low-level data fusion method described above, multispectral data are necessary. The advantage of the AVIRIS data is that they have been acquired in narrow and contiguous spectral band. So, they can be combined either to create a wide band image, or either to merge the multispectral pixels and detect a target.

The Airborne Visible/Infrared Imaging Spectrometer (AVIRIS) is an Earth-observing imaging spectrometer. It acquires data for scientific investigations of the surface and atmosphere. It has been developed by the Jet Propulsion Laboratory (JPL) in 1987, under funding from the US National Aeronautics and Space Administration (NASA). It became operational in 1989. Since then it has

kept on improving to provide high quality image data (10, 11).

AVIRIS acquires data across the solar spectrum from 0.4  $\mu\text{m}$  to 2.5  $\mu\text{m}$ . The spectral sampling interval and response function for each channel is nominally 10 nm. Spatial images of 11 kms by 100 kms are acquired with approximately 20-by-20 m spatial resolution, at a chosen aircraft altitude.

AVIRIS is a scanning imaging spectrometer that acquires :  
- cross-track spatial elements through movement of a scan mirror,

- along-track elements by the forward motion of the aircraft platform.

AVIRIS measures the total upwelling radiance in 224 spectral channels. The photons falling on the detectors are converted to an analog electrical signal, amplified, and then recorded as digitized numbers (DNs) ranging from 0 to 1024 for each of the 224 spectral channels. AVIRIS data calibration allows a quantitative analysis of the measured radiance, and a comparison with data acquired over various sites and at various times. The shape of the obtained spectrum is predominantly a consequence of the upwelling radiance, the instrument radiometric response, and the additive instrument dark current. Dark-current spectra (DC) are measured by AVIRIS for each channel ( $c$ ), and each scan-line ( $l$ ). This  $DC_{c,l}$  is subtracted from the measured signal for each channel, line and sample (or pixel)  $DN_{c,l,s}$  to generate a spectrum with values proportional to the upwelling radiance  $DN'_{c,l,s}$ .

$$DN'_{c,l,s} = DN_{c,l,s} - \overline{DC}_{c,l} \quad \text{equation 6}$$

To transform this spectrum to units of radiance, the radiometric calibration coefficients  $RCC_c$  for each channel determined during the laboratory calibration are applied. These coefficients are in units of radiance per DN.

$$L_{c,l,s} = RCC_c \times DN'_{c,l,s} \quad \text{equation 7}$$

For AVIRIS spectra measured off-nadir, a small cross-track vignetting correction is required. These factors compensate for the greater optical path, and are called the vignetting correction factor  $VCF_{c,s}$  for each spectral channel and each cross-track sample. The vignetting corrected radiance is  $L'_{c,l,s}$ .

$$L'_{c,l,s} = VCF_{c,s} \times L_{c,l,s} \quad \text{equation 8}$$

The spectral position ( $\lambda_{1c}, \lambda_{2c}$ ) and spectral response function  $SRF_c$  for each of the 224 AVIRIS channels are determined in the laboratory prior to each period of data acquisition. And the radiance for each channel, for each along-track line and each cross-track sample, resulting from radiometric and spectral calibrations.

$$L_{c,l,s} = \frac{\int_{\lambda_1}^{\lambda_2} SRF_c(\lambda) \times L'_{c,l,s} d\lambda}{\int_{\lambda_1}^{\lambda_2} SRF_c(\lambda) d\lambda} \quad \text{equation 9}$$

With a wish to make it easier and more understandable, it has been decided that only a few wide spectral bands would be available for data fusion. These bands have been selected rather in the atmospheric windows, and not

astride two spectrometers. The way broad spectral band radiances ( $L_{wb, i, s}$ ) have been simulated is as follow. The radiance has been integrated over the width of the wide band (wb).

$$L_{wb, i, s} = \int_{\lambda_1}^{\lambda_2} L_{c, i, s} d\lambda = \sum_{i=1}^n L_{c= i, i, s} \Delta\lambda_i \quad \text{equation 10}$$

Table 1 shows the five different spectral bands characteristics over La Crau site (France), where we will try to enhance the road (wich can be a potential runway). And table 3 shows the five different spectral bands characteristics over Moffett Field site (USA), where we will try to enhance a runway. The central wavelenght and the spectral width of each band is mentioned. Since the target  $t$  is a road (or a runway), and the background  $b$  is bare soil (or runway surroundings), the spatial contrast is computed as shown in equation 1. Furthermore, the signal-to-noise ratio is computed, according to equation 2. For the road images, this signal-to-noise ratio is quite good and similar (around 12) over the five spectral bands, the greater is computed for the first band, and the smaller for band 2. On the other hand, for the runway, the signal-to-noise ratio is very bad over the five bands ( $S/N < 5$ ). Nevertheless, for both of the two set of images, the spatial contrast fluctuates a lot. For the road, it varies from 0.08 in band 1 to 0.22 in bands 4 and 5, band 3 having a mean value. For the runway, bands 3, 4 and 5 have very poor contrast ( $C < 0.05$ ). The Bhattacharyya distances are computed as shown in equation 3.

Figure 1 and figure 8 show the different corresponding images and histograms. In these latter, we can note the bare soil (or runway surroundings) pick characteristics : it is neither narrow, nor spreaded. The target and background mean levels are quite close, compared to image dynamics.

#### 4.2 Low-level Data Fusion Results

The main efforts have been concentrated on obtaining the various parameters ( $a_i$  and  $b_j$ ) of the low-level data fusion method in order to optimize one of two criteria. These were chosen to be the contrast modulation and the Bhattacharyya distance. The two fusion methods, weighted

average and weighted averages ratio, have been tested.

It is necessary to notice that as the chosen criteria are independant of the radiance level, the fusion parameters resulting of the optimization of these criteria are consequently also independant of the signal level.

For a good analysis of the results, we have to compare the different products  $a_i L_i^{xy}$

All the following results are summarized in table 2 for the road, and in table 4 for the runway.

##### 4.2.1 contrast optimization

The weighted average fusion technique wae done for both sites. It tries to separate the target mean level from the background one, regardless of the target and background pick spreading in the histogram.

The spectral images that have the most significant weights are the ones with good spectral contrasts : bands 4 and 5 for the first site, band 1 and 2 for the runway. For the road detection, the band 1 coefficient is not insignificant. It is even negative. This is due to the fact that this band allows to reduce the mean level of the fused image. By this way, it increases the contrast modulation. For the runway detection, the contrast is enhanced by the fact that the runway surroundings radiance level in band 1 and 2 are similar, when the runway radiance levels are differents. The parameters of the other bands are quite weak, because these spectral bands do not play a role in the fusion performance.

As for both resulting images and histograms (see figures 2 and 9), it can be observed that the distance between the two mean levels has increased. But the fusion spreads the picks. As the fusion increases the target and background variances, the signal-to-noise ratio in the fused image is worse than in the initial multispectral images.

The first test of the weighted averages ratio technique includes the constraint that all the  $a_i$  and  $b_j$  parameters are positive. It was done for La Crau site. The result of the optimization is the ratio between the best contrast image and the worst contrast image. Because  $a_i$  parameters cannot be negative, this ratio is another way to reduce the mean level in the best contrast image. Unfortunately, the resulting contrast is not very good, compared to the initial contrats. On the other hand, the signal-to-noise ratio is

n° of spectral bands	1	2	3	4	5
central wavelength $\mu\text{m}$	0.520	0.800	1.05	1.55	1.66
spectral width nm	105	104.5	105	114.5	114
spatial contrast	0.08	0.11	0.13	0.23	0.22
signal-to-noise ratio	14.80	10.65	12.14	10.70	12.73
bhattacharyya distance	1.34	1.41	2.43	5.95	7.78

table 1 : road multispectral images characteristics

n° of spectral bands	1	2	3	4	5
central wavelength $\mu\text{m}$	0.520	0.800	1.05	1.55	1.66
spectral width nm	110.4	98	98.7	106.1	107.5
spatial contrast	0.26	0.11	0.01	0.04	0.01
signal-to-noise ratio	3.43	4.09	5.18	4.52	4.64
bhattacharyya distance	1.58	0.36	0.01	0.06	0.01

table 3 : runway multispectral images characteristics

optimization of	C	C	Db	Db	$C^{\alpha} \cdot S/N^{1-\alpha}$ $\alpha=0.52$
fusion method	average	ratio	average	ratio	average
n° of spectral bands	4	5	2	5	2
spatial contrast	0.83	0.81	0.20	0.68	0.23
signal-to-noise ratio	2.97	1.22	17.02	3.79	14.97
bhattacharyya distance	6.19	1.33	11.83	6.61	11.70

table 2 : summary of low-level fusion results for the road detection

optimization of	C	C	Db	Db	$C^{\alpha} \cdot S/N^{1-\alpha}$ $\alpha=0.41$	$C^{\alpha} \cdot S/N^{1-\alpha}$ $\alpha=0.6$
fusion method	average	ratio	average	ratio	average	ratio
n° of spectral bands	2	2	4	4	5	4
spatial contrast	0.67	0.71	0.22	0.20	0.2	0.26
signal-to-noise ratio	1.56	1.37	4.01	6.87	4.94	5.05
bhattacharyya distance	1.28	1.06	1.74	1.82	1.20	1.79

table 4 : summary of low-level fusion results for the runway detection

better. That point is emphasized by the histogram in figure 3. As far as contrast modulation enhancement is considered, this result is disappointing.

Figure 4 and figure 10 also concerns a weighted average ratio as the chosen fusion technique for both images sets. That time, only the  $b_i$  parameters are constrained to be positive. Concerning the parameters values, it is roughly the same result as above. But, as negative  $a_i$  values are authorized, a good contrast in the fused image is achieved, regardless of the signal-to-noise ratio which results to be very bad.

For these fused images resulting from contrast optimization, Bhattacharyya distances can be computed. These latter are quite bad in comparison with the initial ones.

#### 4.2.2 Bhattacharyya distance optimization

The Bhattacharyya distance can stand for a compromise between contrast and signal-to-noise ratio since this latter is greater than 10. It is the case for La Crau site images. For Moffett Field site, the signal-to-noise ratios are so bad that this Bhattacharyya optimization is not well-appropriated and gives bad results (see figure 11).

Then, only the road case will be interpreted. Since the method is a weighted average, and the  $a_i$  can either be positive or negative, the fusion results roughly band 4 subtracted from band 5. Band 5 and band 4 the greatest Bhattacharyya distance. The various quality evaluations (spatial contrast, signal-to-noise ratio and Bhattacharyya distance) of the resulting image are quite encouraging. The distance is more than 50% higher than the band 5 distance. Although the goal is not the contrast optimization, this latter is nearly the same as the best initial contrast. To finish, the signal-to-noise ratio is nearly one third greater than the signal-to-noise ratios in the two combined bands. Figure 5 shows the resultant image. It is thresholded according to the histogram shape.

On the opposite, the ratio technique rather enhances the spatial contrast than the signal-to-noise ratio (see figure 6 and table 2). It can be concluded that the optimization of two terms product is not always the best way to reach a

compromise between the two terms.

## 5. CONCLUSION

The comparison between the results obtained shows that :

- if a spatial contrast enhancement is wanted, regardless of any other criterion, a weighted average of the multispectral data is the best fusion method.

- if a bi-modal histogram is looked after, which corresponds to a compromise between contrast and signal-to-noise, an another criterion must be chosen for the optimization. We worked on the optimization of the Bhattacharyya distance in the fused image, in the case of good original signal-to-noise ratios. It can be concluded that the Bhattacharyya distance optimization of the fusion gives a good compromise between the contrast and the signal-to-noise ratio, which are two of the most important criteria to define the quality of an image.

We also seek after a criterion that would reflect the best compromise between contrast and signal-to-noise ratio in

the fused image:  $(\text{contrast})^{\alpha} \cdot (\text{signal-to-noise ratio})^{1-\alpha}$ . First results are included in table 2 and 4, and the respective images and histograms are shown (figures 7, 12 and 13).

For the time being, special interest is given to the evaluation of the fusion robustness, depending on atmospheric conditions and a priori knowledge.

## 6. ACKNOWLEDGMENTS

The authors express their appreciation to R. O. Green from the Jet Propulsion Laboratory for providing AVIRIS images and information. They also thank Mr Rouchouze from the "Direction de la Recherche et de l'Enseignement Technique" and the "Ministère de l'Enseignement Supérieur et de la Recherche" for financing this work.

## 7. REFERENCES

1. Benquet L. : "Extraction automatique des aéroports dans les images SPOT", 14ième Colloque GRETSI sur le Traitement du Signal et des Images, Juan-les-Pins, France, Septembre 1993.

2. Clark J.J., Yuille A.L. : "Data Fusion for Sensory information processing Systems", Kluwer academic Publishers, 1990.
3. Durrant-White H.F. : "Sensor models and multisensor integration", Spatial reasoning and Multi-Sensor, 1987 Workshop, pp. 303-312.
4. Hall D.L. : "Mathematical Techniques in Multisensor data Fusion", Artech House, Boston-London, 1992
5. Hancock R.J., Antonik P., McKay J.A. : "Multispectral sensor simulation", Proceedings of the 1987 Summer Computer Simulation Conference, pp. 275-278, 1987."
6. Harmon S.Y., Bianchini G.L., Pinz B.E. : "Sensor data fusion through a distributed balckboard", IEEE, Proceedings of the International Conference on Robotics and Automation, pp. 1449-1454, vol.3, 1986.
7. Castro C. : "Automatic target recognition shows promise", Defense Electronics, vol.22, n°8, pp. 49-50, August 1990.
8. Wright F.L. : "The art of multisensor fusion and correlation in a tactical anvironment", IEEE-Proceedings of the Region 5 Conference and Exposition, Emerging Technology : A Bridge to the 21st Century, pp. 90-93, 1982.
9. Press W.H., Flannery B.P., Teukolsky S.A., Vetterling W.T. : "Numerical Recipes in C : The Art of Scientific Computing", Cambridge University Press, 1988, ISBN 0-521-35465-X.
10. Green R.O., Larson S.A., Novak H.I., "Calibration of Aviris Data", Proceedings of the Third Airborne Visible/Infrared Imaging Spectrometer Workshop, may 20 and 21, 1991, pp. 109-118, August 1991.
11. Green R.O., Vane G., Chrien T.C., Enmark H.T., Hanse E.G., Porter W.M. : "The Airborne Visible/Infrared Imaging Spectrometer, Special Issue of Airborne Imaging Spectrometry", vol. 44, n° 2/3, May/June 1993, pp. 127-143.
12. Serrot G., Sliwa L., "Perception : état de l'art en physique de la mesure", rapport final 1/6306-00 RO, Juillet 1993.

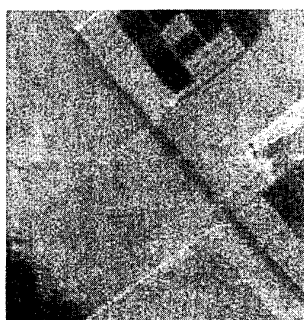
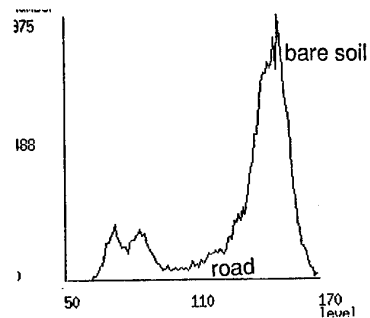
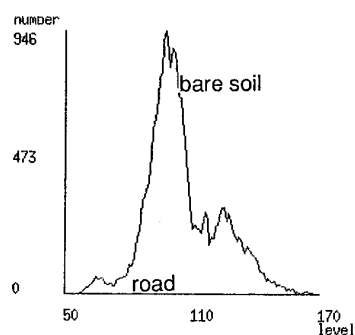
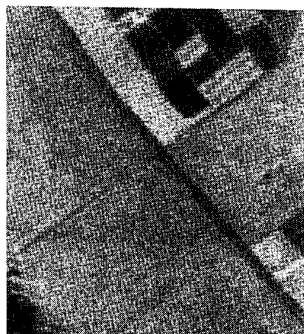
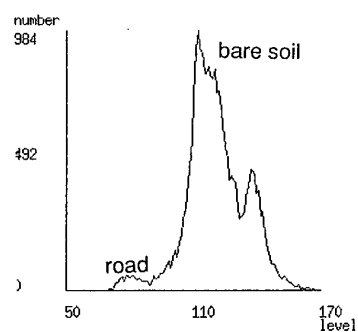
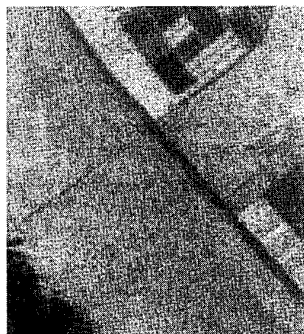
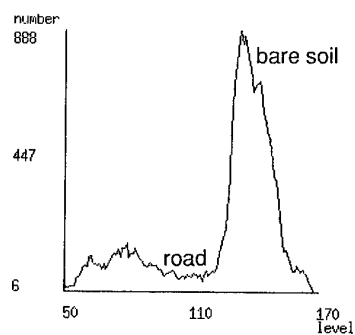
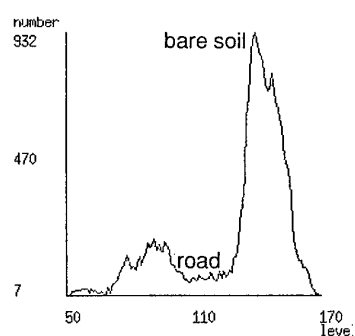
0.52 $\mu$ m0.8 $\mu$ m1.05 $\mu$ m1.55 $\mu$ m1.66 $\mu$ m

figure 1 : 5 multispectral images and histograms

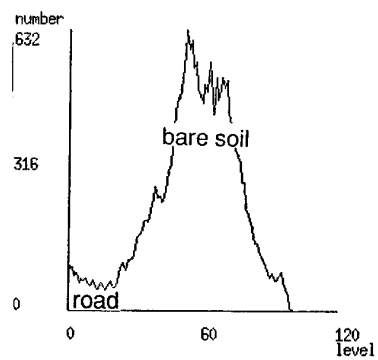


figure 2 : weighted average fusion

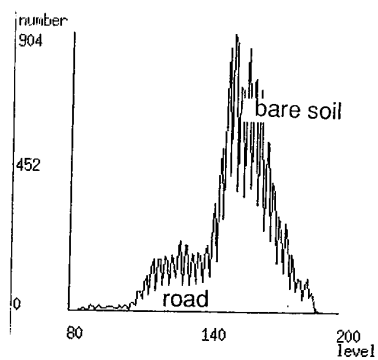
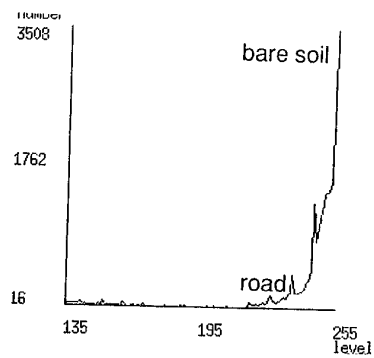


figure 3 : weighted averages ratio fusion (positive parameters)

figure 4 : weighted averages ratio fusion (positive  $b_j$  parameters)



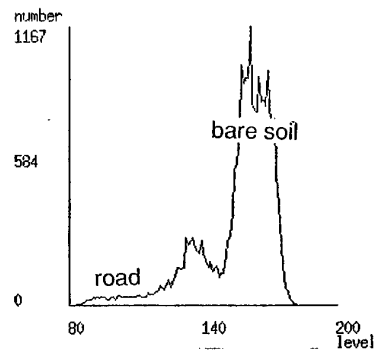
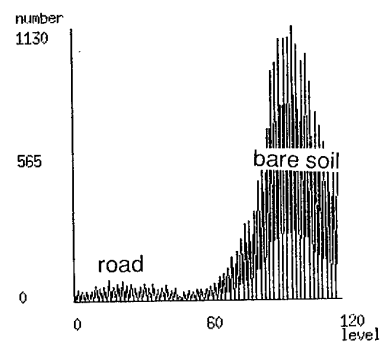
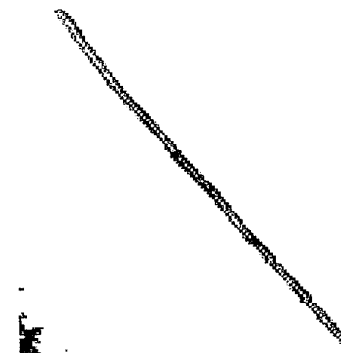


figure 5 : weighted average fusion

figure 6 : weighted averages ratio fusion (positive  $b_j$  parameters)

Optimization of  $(\text{contrast})^\alpha \cdot (S/N)^{1-\alpha}$



$(\alpha=0.52)$

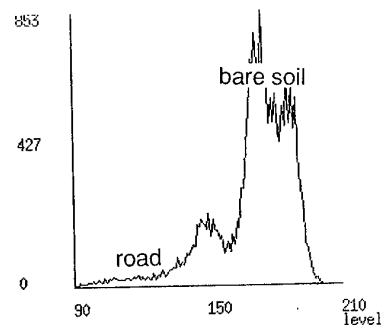
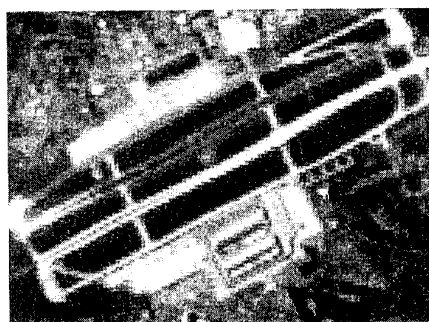
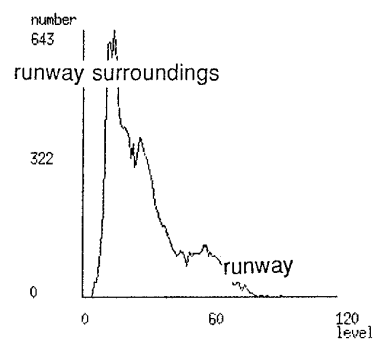


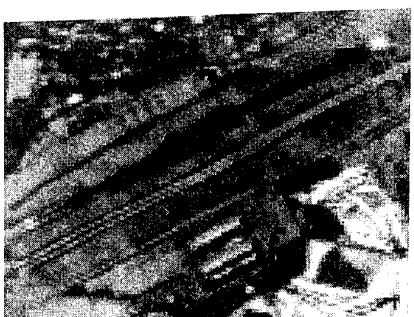
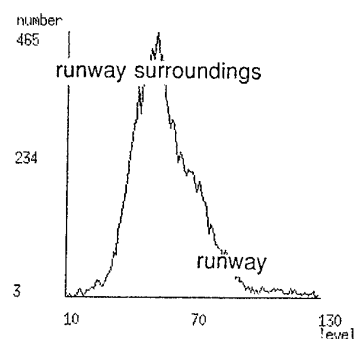
figure 7 : weighted average fusion



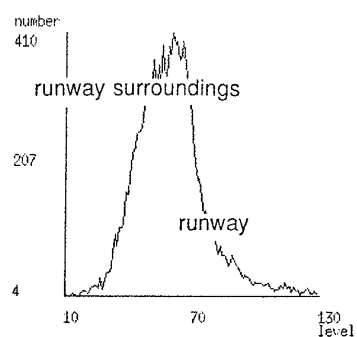
0.52μm



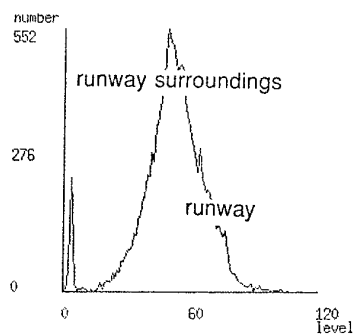
0.8μm



1.05μm



1.55μm



1.66μm

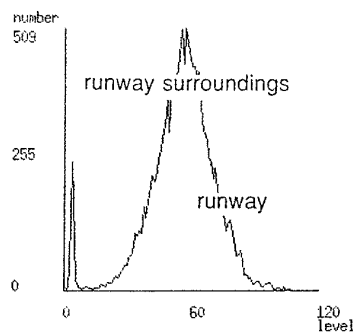


figure 8 : 5 multispectral images and histograms

## Contrast optimization

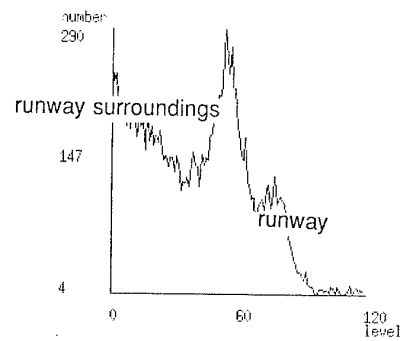


figure 9 : weighted average fusion

## Bhattacharyya optimization

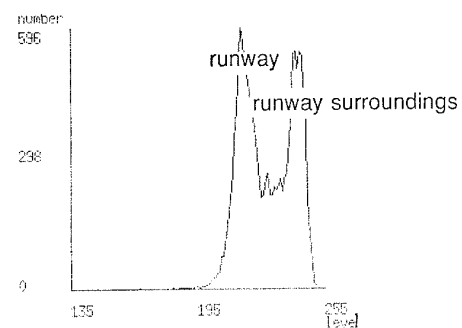
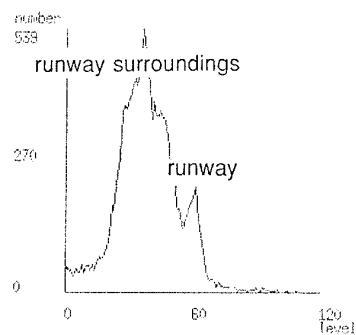
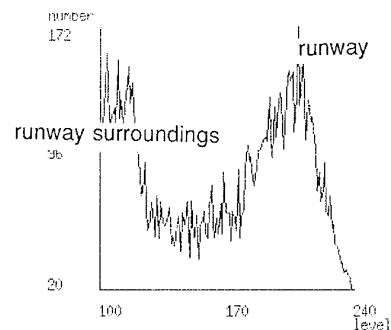
figure 10 : weighted averages ratio fusion (positive  $b_j$  parameters)Optimization of  $(\text{contrast})^\alpha \cdot (S/N)^{1-\alpha}$  $(\alpha=0.41)$ 

figure 11 : weighted average fusion

 $(\alpha=0.60)$ figure 12 : weighted averages ratio fusion (positive  $b_j$  parameters)

## HeliRadar - A Rotating Antenna Synthetic Aperture Radar for Helicopter Allweather Operations

W. Kreitmair-Steck

Eurocopter Deutschland GmbH, Dept. D/ET4,  
81663 Munich/Germany, Tel. +49 89 6000 2289

A.P. Wolframm

Deutsche Aerospace AG, Dept. RSX32,  
81663 Munich/Germany, Tel. +49 89 607 24658

### 1. SUMMARY

Today, available radar instruments cannot be applied for flight guidance purposes due to lack of resolution and ground elevation information. On the other side, optical sensors such as infrared systems provide an excellent resolution but are nearly blind at adverse weather conditions such as fog and rain. A new radar technology called ROSAR (Synthetic Aperture Radar based on ROTating antennas) promises to overcome the deficiencies of the traditional radar systems. On the basis of encouraging research work on ROSAR-technology and an investigation of the feasibility of a piloting system based on these ideas, Eurocopter Deutschland and Deutsche Aerospace started a development program called HeliRadar to develop a ROSAR-based piloting system. This device should be able to provide photolike images even under extreme visibility conditions.

Details on the investigation and the resulting concepts for synthetic vision based flight guidance at Eurocopter will be given. Following an introduction to the basics of ROSAR-technology, the technical concept of HeliRadar will be presented. The paper concludes with a discussion of the perspectives for civil and military applications.

### 2. INTRODUCTION

During the past years much effort has been taken to increase the effectiveness of helicopters for both civil and military mission tasks. Sensors and warning systems have been developed to increase safety during daytime missions and to enable helicopter operation during nighttime. Despite the big efforts undertaken, it is still dangerous to fly military missions during night, and it is still impossible to engage the helicopter at adverse weather situations except when using Instrument Flight Rules (IFR) procedures. Eurocopter's concept to overcome this deficiency is a synthetic vision based approach which could become applicable for civil as well as military helicopter operations. Since current sensor principles such as infrared or low light level sensors have its well known limits, a new radar-type sensor providing photolike images would be necessary to solve the problems. HeliRadar seems to have the potential for an overall solution of these problems.

### 3. THE CHALLENGE OF ALLWEATHER OPERATIONS

At present civil helicopter operation is dramatically restricted by weather conditions. The current limits are

well known: Cloud ceiling above 500 ft, flight visibility greater than 800 m and visual contact to the ground. While these limits have just *commercial* implications for operators, they have additional *social impact* if emergency medical services are concerned: traffic accidents happen to occur especially at poor weather conditions. As a result of helicopter accident investigations it is expected that in the near future for emergency operations in Europe these limits will even be extended to a flight visibility of 1500 m. But also the military operation of helicopters under bad visibility conditions is severely restricted: Weather minima dictate the operability and non-operability of helicopters.

Basically two types of approaches have been investigated in the past to allow for a flight guidance at reduced visibility conditions:

- (a) Flight guidance based on a digital terrain database in combination with precise navigation and an obstacle warning device.
- (b) Flight guidance based on imaging sensors that provide a photographic like outside view.

While being the best approach up to now, solution (a) suffers from a high degree of risk both for pilots and passengers, since it will always remain unclear how precise and how up-to-date the used onboard map really is. If there would be less risky alternatives, it seems to be advisable to rely on these alternative techniques.

Currently available imaging sensors such as low light level and infrared systems, though providing high resolution images, suffer from their short visibility ranges at poor weather conditions: Both are nearly blind during fog and rain. In addition, infrared systems face the problem of crossover phenomena at these weather conditions. On the other hand, conventional radar systems operating in a frequency range of up to 35 GHz which would allow for sensor ranges of 1 to 1.5 km suffer from low image resolution: A real aperture radar with an antenna of 50 cm length would have an angular resolution of  $1.0^\circ$  in azimuth which is a factor 5 more than would be required for a sensor based flight guidance. Thus, only some kind of synthetic aperture radar system which generates a virtually large antenna from the movement of a small one could solve this problem.

#### 4. SYNTHETIC VISION BASED FLIGHT GUIDANCE

Flight guidance based on synthetic vision is not only a matter of sensor technology but also of display technology and of man-machine interface techniques. While in the past most research has been focussed on sensor technology, it is now time to investigate the problems of synthetic vision based flight guidance in detail, especially:

- (a) the estimation of distances,
- (b) the estimation of object dimensions,
- (c) the correct positioning of the helicopter in relation to the sensor image,
- (d) the availability of important flight guidance information.

When moving in space the human being is used to have reference systems available that enable fairly exact "measurement" of spatial dimensions. Implicit comparison of unknown distances with intimately known distances or dimensions such as the length of its own arm or the typical size of known objects helps us to move ourselves in a secure way. If we drive vehicles according to sensor images, most of our typical reference mechanisms are missing and even perspectives and field of views are different from our experiences.

To overcome this problem of sensor based flight guidance a number of artificial means of reference have been studied at Eurocopter including distance markers and short distance color coding (cf. figure 1), artificial reference objects of defined dimensions at defined distances, and the projection of a "shadow" of the helicopter in the direction of the flight path. The last technique allows for a selective obstacle warning for relevant obstacles only.

Apart from the investigations of possible reference systems a number of problems paired with sensor based piloting have been studied:

- (a) Typically the field of view of the sensor is much smaller than the visual field of view.
- (b) The pilot's attention has to focus on a relatively small monitor (either head up or head down).
- (c) If a helmet mounted display is used for the sensor image, the pilot has to face the "walkman effect", i.e. nothing outside the artificial reality of the device is perceptible.
- (d) Dependent on the sensor type the images differ from ordinary TV-images.

The analysis of these problems at Eurocopter resulted in the following conceptual recommendations for the man-machine interface:

- The standard means of display should be a panoramic (i.e. 16:9) head-down-display with a resolution of 3 pixels/mm.
- The positioning of the head-down-display has to be as close as possible to the outside view.
- The azimuth field of view to be displayed head-down should be in the range of 60° to 80° - smaller angles would reduce helicopter manoeuvrability, larger values would cause unacceptable image distortions.
- For highly dynamic military applications, additionally a helmet mounted display and/or a head up display are recommended.
- The horizon has to be drawn at its actual position inside the image and supplemented with margins for the allowed roll angle.

Overlay of distance indication lines

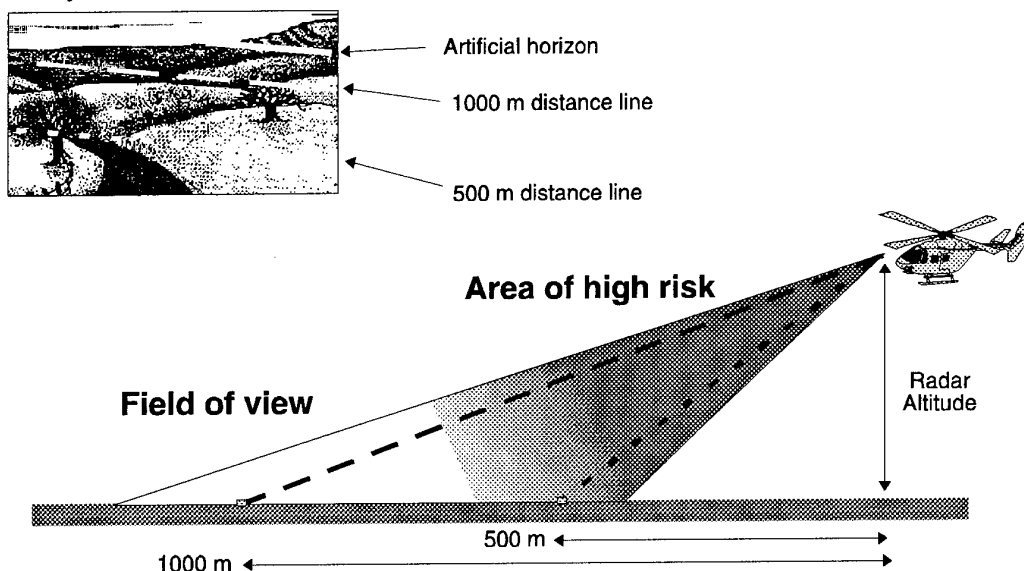


Figure 1: Concepts for the man-machine interface

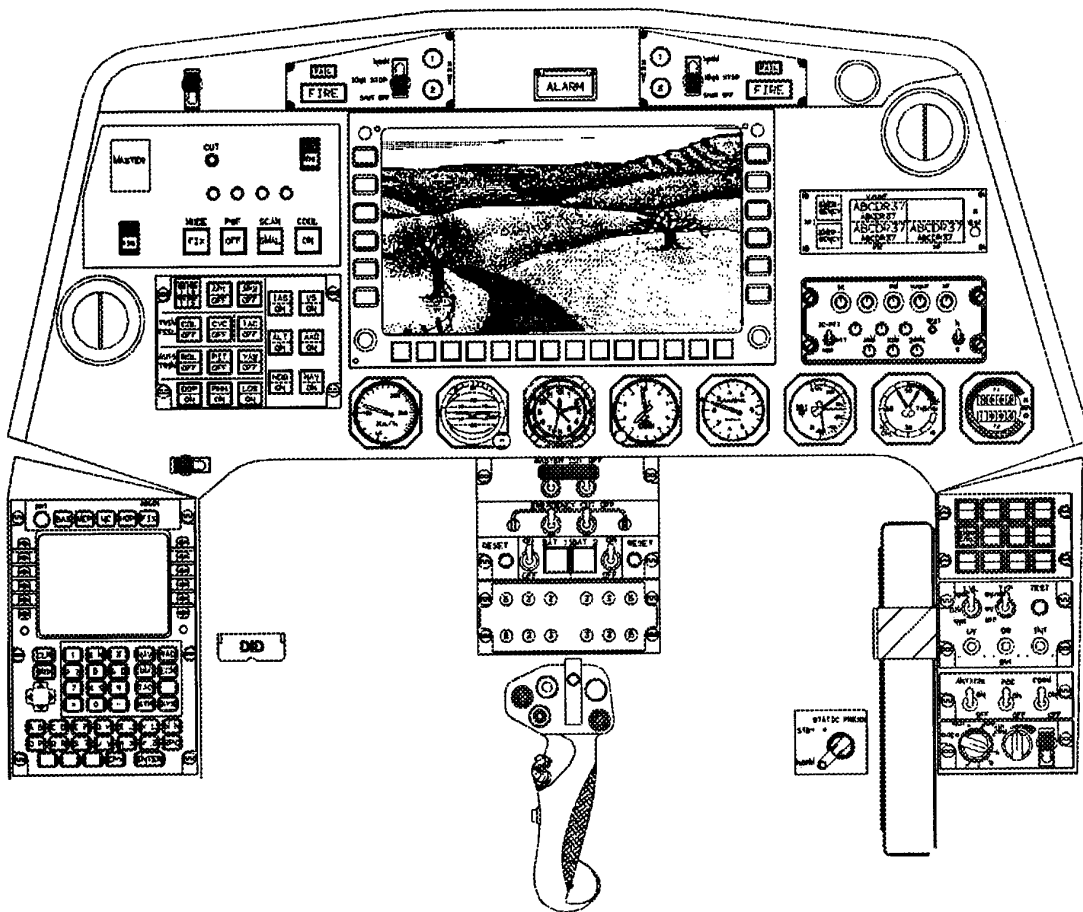


Figure 2: Tiger cockpit for allweather operation

- For backup purposes the most important flight instruments (Air speed indicator, Horizon, Altimeter, Climb rate indicator) should be positioned immediately below the head-down display.
- Important flight guidance informations have to overlay the sensor image in digital form supplemented by tendency indicators such as:
  - ◊ for "value is constant (within certain limits)"
  - ↓ / ↑ for "value is falling/rising"
  - ↘ / ↗ for "value is falling/rising fast"

Figure 2 shows a possible tiger cockpit design that satisfies the above stated requirements and figure 3 gives an example of a symbology overlay in conformance with these requirements.

In parallel with the investigations on display formats, optimal field of view for sensors, and overlay symbology for sensor images, Eurocopter has conducted research on necessary restrictions of the helicopter flight dynamics for sensor image based flight guidance and on specification parameters for the sensor itself. Especially the characteristics of two types of escape manoeuvres from obstacles have been analyzed: Lateral escape (see figure 4) and vertical escape (see figure 5).

Most of these results apply for all types of imaging sensors and could thus ameliorate current night operation performances significantly. However, allweather operation capability still seems to be dependent on a high resolution radar device such as the ROSAR-based HeliRadar.



Figure 3: Overlay symbology for sensor images

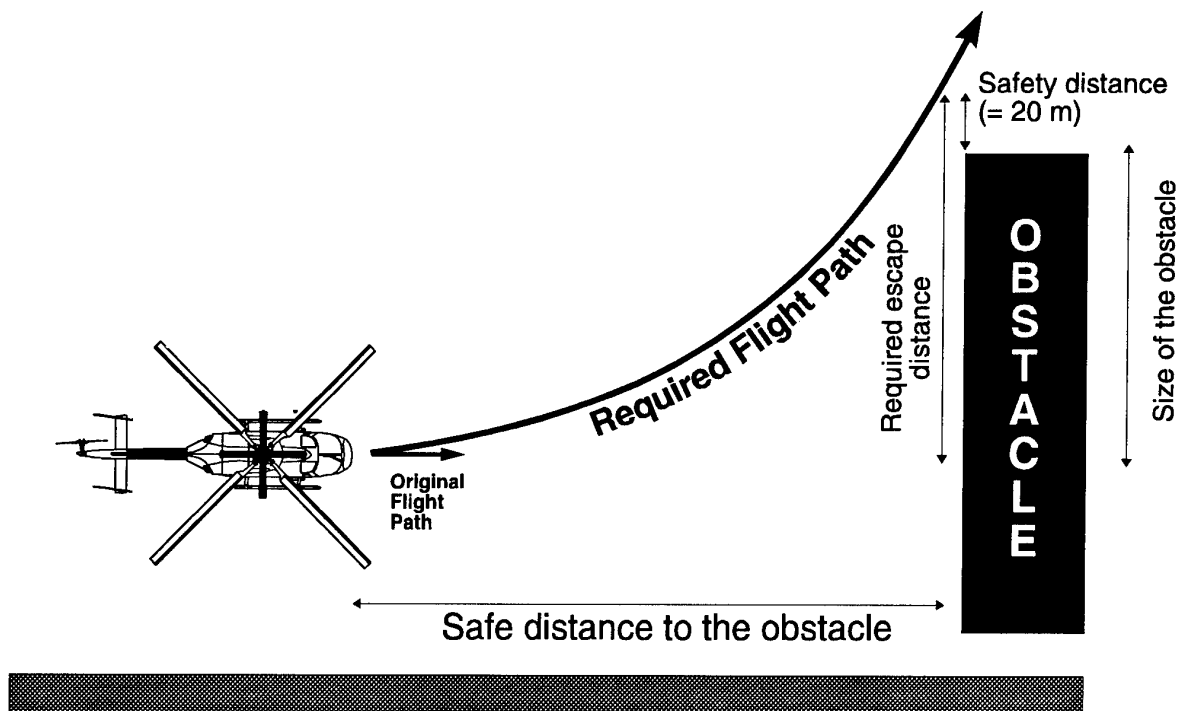


Figure 4: Lateral escape manoeuvre

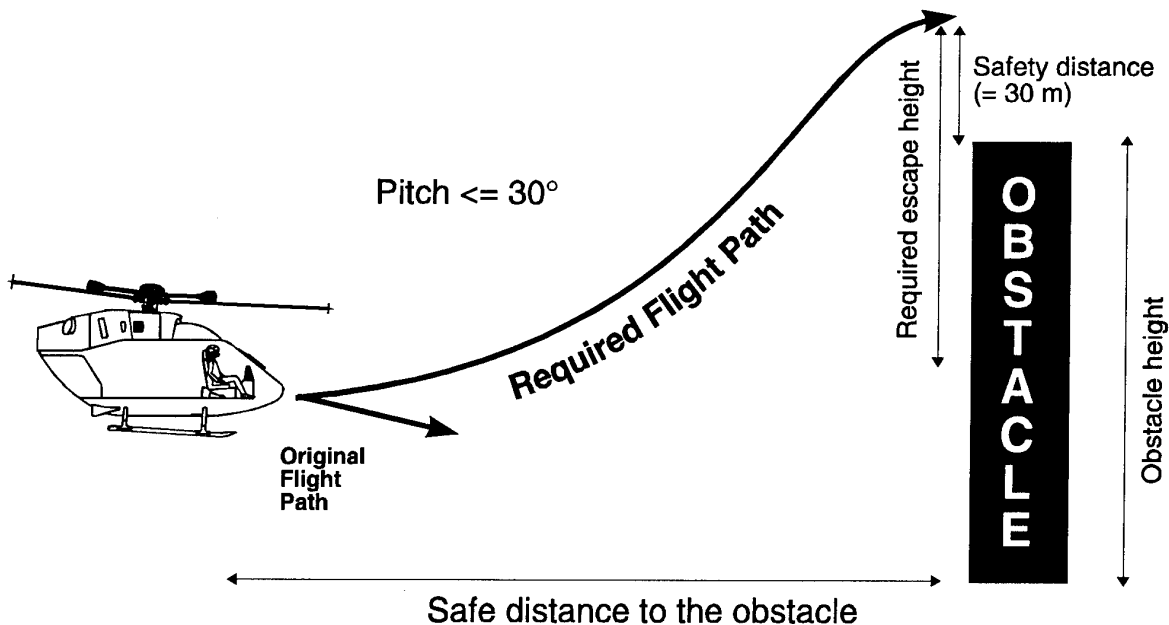


Figure 5: Vertical escape manoeuvre

## 5. BASICS OF ROSAR TECHNOLOGY

From an operational point of view the most important parameters of a radar system are its range at specified weather conditions and the size of the resolution cells. Since the dimension of the resolution cells should be not larger than 1/5th of the major dimension of the target object which has to be identified (ideally it should be 1/20th), the angular resolution for the identification of

vehicles and houses at a distance of 500m should be around  $0.2^\circ$ . While the radar range might be adjusted to the requirements by either frequency selection or transmitter power adaptation, the size of the 3-dimensional resolution cells (given a specific frequency) is dependent on the dimension of the radar antenna and the pulse bandwidth: For so-called real aperture radars the angular resolution is indirect proportional to the size of

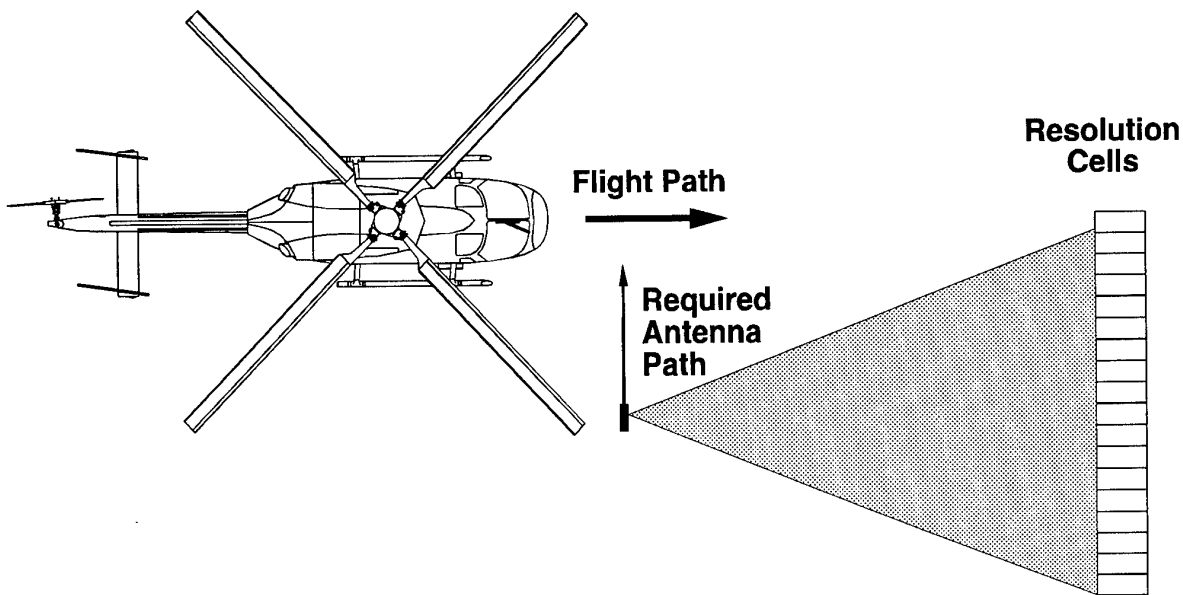


Figure 6: The dilemma of SAR systems for piloting

the radar antenna. As a consequence, to provide for the flight guidance tasks the desirable angular resolution with a 35 GHz radar, a bulky antenna of some 2.5 m diameter would be required.

In principle, SAR-technology would solve the problem to achieve high resolution with a small antenna: By moving the antenna along a linear path it is possible to produce by computation a fairly small angular resolution in the direction of the antenna path. Unfortunately this technique cannot be applied for a forward looking piloting aid, since it would require to move the SAR antenna with constant speed orthogonal to the flight path of the helicopter (cf. figure 6).

The only way to overcome this problem seems to be the ROSAR-principle: The antenna is mounted in such a way, that it radiates in radial direction and moves along a circular path. While rotating, the antenna scans the environment from various visual angles without assuming a movement of the platform itself (see figure 7). The high resolution is then computed by signal processing as a function of the rotation angle and the antenna movement along the circular path.

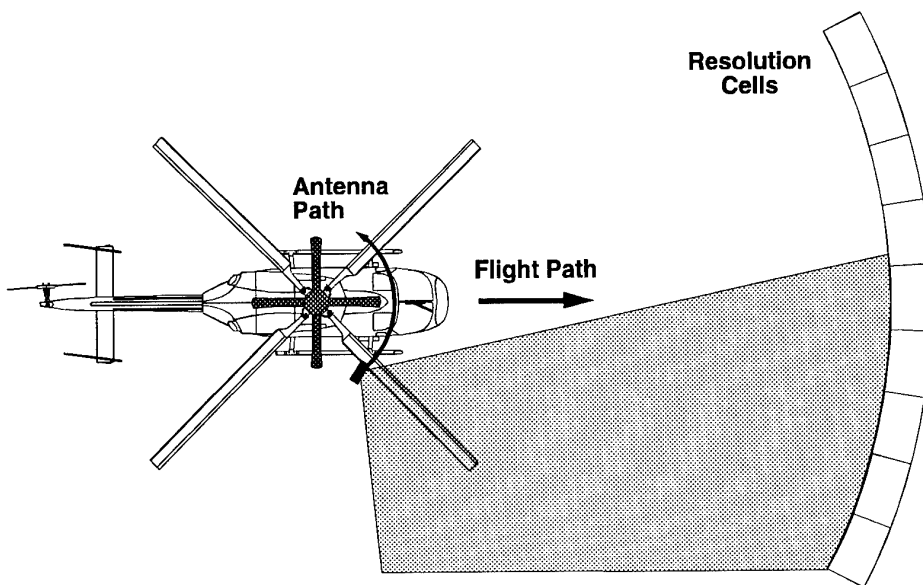


Figure 7: ROSAR-principle for helicopter flight guidance



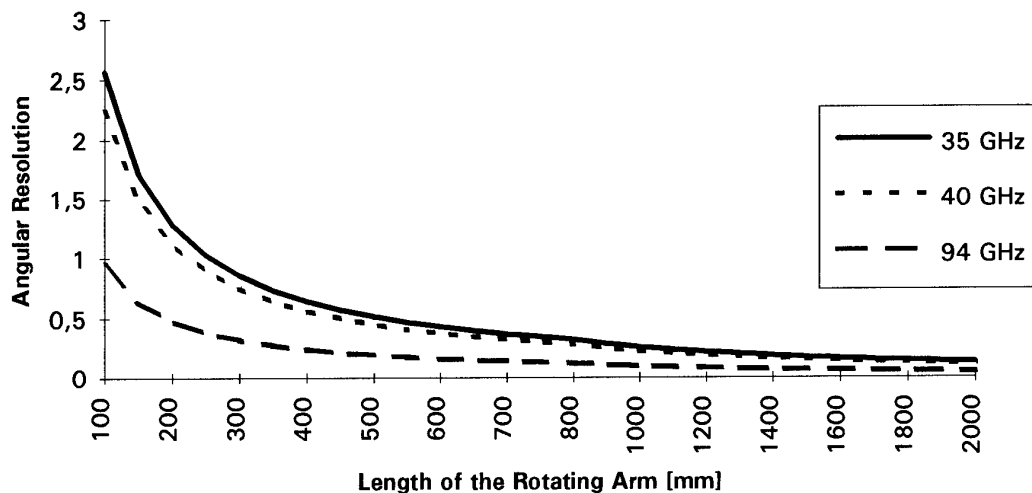


Figure 8: Azimuth Resolution of ROSAR Technology Radars

This ROSAR-theory has been worked out and validated by experiments in 1989 for an idealized circular movement of the transmitting and receiving antennas assuming constant angular velocity. The major challenge has been the special processing which requires a correlation of the received raw signals with internally generated or prestored reference functions, resulting in an angular compression that allows for a high angular resolution. For the experimental validation with a real rotating antenna, the angular velocity has been scaled down. The rotor consisted of an arm of 6m length and rotated at an angular velocity of  $0.2 \text{ s}^{-1}$ . The radar emitted signals with a frequency of 1.3 GHz and illuminated meadows, buildings, bushes, trees and four corner reflectors in a well known position.

The angular resolution in azimuth of ROSAR-systems is a function of the antenna beamwidth, the radius of the circular movement and the frequency of the radar signal. Assuming a beamwidth of  $45^\circ$  the azimuth resolution of ROSAR-technology based radars is shown in figure 8 for the frequencies 35 GHz, 45 GHz and 94 GHz.

In 1991 Eurocopter investigated the applicability of the ROSAR-technique for a high resolution imaging system for allweather operation of helicopters. A concept for landing approaches has been conceived and detailed requirements for an adequate synthetic vision system have been established. Later on, in a joint study with Deutsche Aerospace the technical feasibility of such a ROSAR-based piloting radar has been investigated. The

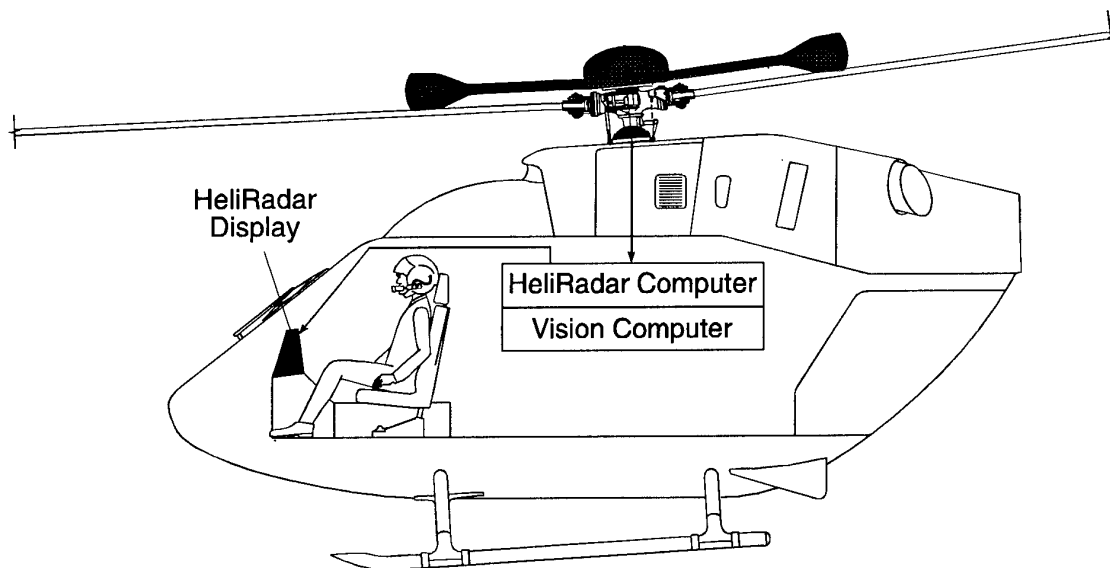


Figure 9: System Concept of HeliRadar

focus of this study was on three components of this piloting radar:

1. The concept of the rotating arms and their integration on top of the rotor head;
2. The analogue radar hardware;
3. The digital radar signal processor.

Since the outcome of this investigation was encouraging, Eurocopter and Deutsche Aerospace started a common development program called HeliRadar for such an experimental radar system. This experimental piloting radar shall have a large field of view of  $70^\circ \times 40^\circ$  and an image update rate of 6 Hz. The angular resolutions in azimuth and range will be better than  $0.2^\circ$  and  $2.5^\circ$  respectively.

## 6. TECHNICAL DETAILS OF HELIRADAR

The HeliRadar - as it is designed now - is a Frequency Modulated Continuous Wave (FMCW) Radar working in a frequency band around 35 GHz. The radar system consists of the usual transmitter unit, the receiver unit, the signal generation unit and a set of antennas. The complete transmitter/receiver/antenna system is fixed mounted on top of the rotating axis of the helicopter, as can be seen in figure 9.

The radar signals are transmitted and received through a number of antennas. They are mounted at the four ends of a cross and rotate at the same speed as the rotor. The antennas illuminate the area in front of the helicopter from a horizontal line down to a  $45^\circ$  depression angle. In order to secure a high enough isolation, the transmit path is separated from the receive path, i.e. the transmit signal is sent through a transmit antenna, whereas the receive signal enters via the receive antenna. As the system at the moment only illuminates the forward 90 degrees, only one transmitter/receiver system is used and switched from antenna arm to antenna arm via PIN diode switches.

### 6.1. The Analogue Part of HeliRadar

The FMCW signal is generated in the signal generator. The prime frequency source is a voltage controlled oscillator (VCO) working at 1 GHz. As the requirements in the linearity are fairly high at this high frequency, a linearisation network consisting of a digital processor with subsequent D/A-converters is included in the feed back network. The signal is then upconverted in two stages.

In this analogue part of the HeliRadar, the transmitter power amplifier is very challenging. Nevertheless, state of the art amplifiers can be used. The signal is at first amplified in a FET hybrid amplifier. The signal is then passed on to a GUNN oscillator amplifier. The last stage consists of combined IMPATT diodes. This last stage has a total power output of about 8 Watts.

The received signal is amplified in a low noise amplifier (LNA). A small portion of the transmitted signal is taken

from a directional coupler and then fed into a mixer, which therefore outputs a signal in the baseband. Sometimes this kind of receiver is also called deramp-on-receive and performs the first part of the required pulse compression. The last part of the pulse compression is then simply performed through a digital Fast Fourier Transform (FFT) in the digital signal processor (see later).

The received radar signals are converted from analog to digital. The digitized signal is transferred at a data rate of about 800Mbits/s via optical links through the center of the rotor axis down into the cabin of the helicopter, where it is then processed in the digital signal processor.

### 6.2. The Digital Part of HeliRadar

The design of the digital signal processor is one of the critical parts of the HeliRadar system. There are four main tasks of the processor: 2-dimensional pulse compression, motion compensation, image generation and obstacle detection. These vector oriented algorithms are computationally extremely challenging: By far the most demanding function is pulse compression; motion compensation though is important, otherwise the pulse compression does not focus the received signals correctly. The image generation task converts the slant range images into ground projected images. The functions are complemented by an obstacle detection and warning algorithm which detects obstacles like houses or power lines.

The HeliRadar processor is built up of modules mounted on motherboards. The DSP modules are connected through support chips to a network of links (see figure 10). The connection to the link network is programmable and therefore an arbitrary connection of different modules can be selected. This means that physically adjacent modules may not be connected to each other but may be logically connected to distant modules. Several motherboards are connected through a backplane, forming a possible generic logical structure. Using this structure, it is simple to perform matrix transpositions (i.e. corner turns).

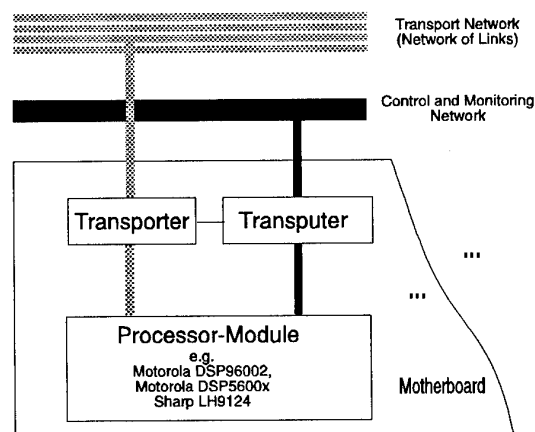


Figure 10: Communication structure for the processor

The distributed processor architecture provides an inherently high fault tolerant level. The system performance degrades gracefully and without interruption, in case of failure of transputer/DSP modules or their links. The chance of a catastrophic failure is low. On the other hand, the system detects defective modules through an extensive control, monitoring and error detection task. As there is a logical processing structure overlayed over the actual hardware structure, the processor can be dynamically reconfigured (by software) to circumvent defective transputer/DSP modules until their replacement.

The number of real operations (multiplications and additions) required are, depending on the final functionality of the radar instrument, in the order of around 10 billion per second (10 Giga FLOPS). The main challenge of this processor is the requirement for small volume and weight. The goal is to produce a processor in a box smaller than 50cm x 25cm x 25cm.

The output of the whole processing is a photographic like image but with somewhat lower resolution. This resolution though is sufficient enough to guide a pilot in an unknown area to the target destination. The radar image will distinguish between farming areas (fields), wooded areas, and roads or motorways. The second type of information the pilot can extract from the image are color-coded obstacles above the ground such as houses, individual trees and even power lines.

#### 7. CIVIL AND MILITARY APPLICATIONS

The HeliRadar mission system is designed in such a way, that the basic components might be applied both for civil and military NOE operations. While for civil operations the worst case resolution in elevation of 2.5° is considered to match the needs, for military operations a detailed mode with less than 1.0° resolution in elevation will be used for short range mapping. In addition, there will probably be different cockpit concepts for combat and transport helicopters:

- (a) Combat helicopters should have both head down and helmet mounted displays;
- (b) For transport helicopters a head down display could be sufficient.

According to the present time schedule such a military vision system for NOE-support could enter series production in 1999 if the required development budgets are available from the German FMOD.

On the civil side we intend to follow a two step approach for certification:

- (1) Certification of the system as a landing and takeoff aid, assuming that the rest of the mission is performed according to the instrument flight rules.
- (2) Extension of this certification to the complete flight under HeliRadar control.

To support the first step and to start as soon as possible discussions and demonstrations with civil aviation authorities, a helicopter simulator has been realized. As soon as the extensive flight tests have been performed and evaluated the second step could become feasible.

Additional military applications such as short range (10-20 km) reconnaissance tasks with a 360° field of view and missile guidance tasks with ranges of 6-8 km during fog and rain are possible extensions of the HeliRadar capability. Here the limiting factor is the capability of transmitter power amplifiers. As soon as the technology advances so that amplifiers at 35 GHz could yield a total power output of about 100 Watts, highly accurate long range adverse weather reconnaissance and missile guidance derivatives of HeliRadar will become reality.

#### 8. REFERENCES

1. Klausing, H., "Synthetic Aperture Radar with Rotating Antennas", in Proceedings of the "Military Microwaves Conference", 11th-13th July 1990, London.
2. Kreitmair-Steck, W., "Flugführung nach Sensordaten", in K.-P. Gärtner (ed.), Proceedings of the Conference on "Fortgeschrittene Anzeigesysteme für Flug-, Fahrzeug- und Prozeßführung", 24th-25th September 1991, Munich. DGLR-Report 92-02.
3. Kreitmair-Steck, W., H. Klausing, A.P. Wolframm, G. Weiss, "HeliRadar - a synthetic aperture radar with rotating antennas", in Proceedings of the "23rd European Microwave Conference 93", 6th-9th September 1993, Madrid.
4. Kreitmair-Steck, W., "All Weather Operations - The Radar Based Vision System", in Proceedings of the Intavox Technical Training Conference "Helicopter Survival 93", Intavox 1993, London.

# IDENTIFICATION OF TERRAIN IMAGERY WITH UNSTABLE REFLECTIVITY

Y.A.Kozko, Prof., D.Sc.  
V.V.Saveliev, Ph.D.

*Institute for Precise Instrumentation*  
1 Yurlovsky proezd, Moscow, 127490  
Russia

## 1. SUMMARY

This paper deals with a problem of two terrestrial images comparison: the observed one obtained with a known device and the reference one that is an idealized picture of a given object. The whole problem is formulated in terms of statistical object identification.

The SAR imagery main properties based on the analysis of experimental data are pointed out. A zonal SAR image model, encompassing signal fluctuation statistics, number of looks, S/N ratio and natural cover fragmentation of terrestrial surfaces is proposed.

Based on this model, the adaptive zonal recognition algorithms are built. Their efficiency has been confirmed experimentally in a wide range of zone contrasts and under various seasonal/weather conditions.

## 2. INTRODUCTION

Terrestrial surface images obtained by airborne or spaceborne remote sensing in various spectral ranges are widely used in many applications, including geophysics and ecological monitoring. A broad class of problems arising in the analysis of such imagery can be formulated in terms of object identification. Here are just a few examples.

*Geodetic registration of an image:* in the process of image formation in various devices --

optical, infrared, radar, etc. -- certain geometrical distortions usually arise. The kind of distortion depends on the particular imaging device, and can be both linear and nonlinear. In order to build a thematic map of a phenomenon investigated by means of image analysis, the images must be transformed into a standard map projection. This can be done by finding and identifying several objects shown on the map, measuring their coordinates in the image and calculating the parameters of the appropriate geometrical transformation.

*Mutual registration of two or more images:* for a joint analysis of several images of the same area obtained at different moments and/or with different sensors, a precise geometrical correspondence between the pixels of different images must be established, or else the images must be transformed into the same projection. This again requires that several reference objects are found in the images and their respective coordinates used for establishing the correspondence.

*Finding predetermined patterns:* image analysis often calls for a search for patterns of a given shape. For instance, tectonic fractures can be manifested in the form of linear patterns. In scene analysis, the image in question is described in high-level terms corresponding to the physical objects observed in the image. This description can be

AGARD has been unable to obtain an original copy of this paper, so its printed quality is not up to our normal standards.

built in a hierarchic way, beginning with elementary structural blocks such as lines or arcs and ending with such notions as "tectonic fracture", "oil-polluted area", etc. Thus the first stage of scene analysis is to identify all image fragments containing a given simple pattern.

The problem dealt with in the present report is formulated as follows. Compare two images, one of which -- the observed image -- has been obtained with a known device, and the other -- the reference image -- is an averaged or idealized picture of a given object. It is required to find their relative position, i.e., the coordinates of the reference object on the observed image.

This problem belongs to the field of pattern recognition, therefore the appropriate procedures are usually called recognition procedures. However, several other names for such procedures or algorithms are also in use: identification, classification, matching, and registration. We regard all these terms as synonyms. The pertinent procedures will be sometimes called classifiers.

Problems of this kind have been treated in a vast number of publications. However, the methods proposed earlier sometimes do not yield practically working algorithms. In the case of Earth surface images, this is due to several factors. One major factor is that the reflectivity of the same physical object at the surface can vary in a wide range, depending on the conditions of illumination, season, weather, etc. Another factor, most important in the case of SAR imagery, is the presence of random noise which makes the widely used contouring approach impracticable. The goal of the present report is to derive efficient recognition algorithms which

take into account the factors mentioned above.

### 3. IMAGE MODEL

A digital image  $I$  consisting of  $k \times l$  pixels can be represented as an  $n$ -vector

$$I = \{I_i\}, \quad i = 1, \dots, n,$$

where  $n=kl$ . The observed image will be denoted by  $z$  and the reference by  $a$ . We assume  $z$  to be a stochastic object, generated in the process of terrain observation under the action of noise and other distortions, while  $a$  is a deterministic picture of the same terrain. Ideally,  $a$  is the average of  $z$ :

$$a = \langle z \rangle. \quad (1)$$

Thus each pixel of the observed image is the corresponding reference pixel distorted by noise:

$$z_i = a_i \otimes \lambda_i. \quad (2)$$

Here  $\otimes$  is, in general, an arbitrary composition. In particular, it can be a sum (additive noise) or a product (multiplicative noise or clutter).

Additive noise is typical for optical, infrared, and other imagery obtained with incoherent illumination. The widely known Gaussian distribution is usually applicable in this case.

Clutter noise arises in images obtained with coherent systems, such as SAR or laser imaging systems. Additive noise is also present in SAR images but it enters them in an indirect manner. If  $z$  means the intensity of the received signal in a SAR image pixel, the statistical model for  $z$  is

$$z = a \cdot \lambda, \quad (3)$$

$$a^2 = r + \sigma^2, \quad (4)$$

where  $\sigma^2$  is the receiver additive noise variance and  $r$  is proportional to surface reflectivity. The clutter  $\lambda$  is distri-

buted as

$$f(\lambda) = \frac{L^L}{\Gamma(L)} \lambda^{L-1} \exp(-L\lambda). \quad (5)$$

Here  $L$  is the incoherent averaging factor (number of looks), the number of primary image pixels summed up to form an output pixel. The mean value of (5) is  $\langle \lambda \rangle = 1$ , as it should be according to the definition (1), and its variance is  $\sigma^2\{\lambda\} = 1/L$ .

For the additive model  $z = a + \lambda$ , one can assume  $a = r$  and  $\langle \lambda \rangle = 0$ . The noise variance  $\sigma^2$  is an independent parameter whose influence can be reduced by increasing receiver sensitivity, i.e., the signal-to-noise ratio  $SNR = r/\sigma^2$ . Contrary to this, in the multiplicative case, increasing receiver sensitivity or transmitter power does not reduce the clutter; its variance can be made smaller only by increasing the number of looks  $L$ , which can usually be achieved at the cost of a poorer resolution. This is why typical SAR images possess a grained, or speckled, fine structure. The impossibility of eliminating stochastic signal fluctuations necessitates the use of statistical methods for SAR image analysis.

Imaging devices are usually designed so that the noise can be assumed to be independent in different image pixels (at most, there may exist some correlation between immediate neighbors which can be disregarded without much loss of estimate accuracy). This greatly simplifies both the synthesis and the analysis of image processing algorithms.

#### 4. RECOGNITION ALGORITHMS

Somewhat refining the formulation of the previous section, it should be pointed out that the problem of identifying the observed and reference images is meaningful only if one image is

larger than the other, and, supposing that the smaller image is contained in the larger one, we have to determine their relative position. Thus the problem in question can be also regarded as the problem of measuring the vector shift parameter  $\tau = (x, y)$ .

Depending on the particular situation, both kinds of size relationship between the observed and reference images are possible: the first may be larger than the second and vice versa. We shall refer to the situation where the reference is larger than the observed image as the direct scheme of observation. The opposite situation will be called the inverse scheme. For definiteness, in what follows we shall mainly discuss the inverse scheme.

Let the dimensions of image  $I_1$  be  $M \times N$  pixels, those of  $I_2$   $m \times n$  pixels, with  $M > m$  and  $N > n$ . Then the number of possible positions of  $I_2$  on  $I_1$  is  $(M-m+1) \times (N-n+1)$ . The task of a recognition procedure is then to test each of the  $(M-m+1) \times (N-n+1)$  hypotheses concerning the value of the vector parameter  $\tau$  and select the one corresponding to the highest similarity between the respective image fragments. For the inverse scheme,  $I_1 = z$ ,  $I_2 = a$ , therefore the classifier must each time compare the reference image  $a$  with a fragment  $z(\tau)$  of the observed image  $z$ .

The general recognition procedure, understood as hypothesis testing, can be formulated as follows. Each of the  $(M-m+1) \times (N-n+1)$  hypotheses is analyzed sequentially. The corresponding image fragment  $z(\tau)$  is compared by a certain rule (algorithm) with the reference  $a$ . This comparison yields a value  $\Phi$  which is a measure of si-

milarity between the two images. After all the hypotheses have been tested, a two-dimensional field  $\Phi(\underline{z})$  is obtained. The global extremum of this field -- the point of highest similarity -- is used as the estimate of the true position.

We shall call  $\Phi(\underline{z})$  the decision function.

In the framework of the statistical approach, the decision function is constructed from the posterior probability  $P(\underline{z}|\underline{I})$

corresponding to the event that the fragment  $\underline{z}(\underline{I})$  is actually the reference  $\underline{a}$  affected by

noise. The statistics of noise is assumed to be known. This allows one to derive for each particular case a procedure which will select the most probable hypothesis with respect to noise statistics.

If the above assumption about noise independence in different pixels is valid, the multidimensional probability  $P(\underline{z}|\underline{I})$  be-

comes a product of one-dimensional functions:

$$P(\underline{z}|\underline{a}) = \prod_{\mu} p(z_{\mu}|a_{\mu}), \quad (6)$$

where  $z_{\mu}$ ,  $a_{\mu}$  are the brightness values in the  $\mu$ th pixel of the respective images. For the sake of computational convenience, (6) is usually replaced by its logarithm

$$\Phi(\underline{z}|\underline{a}) = \sum_{\mu} \varphi(z_{\mu}|a_{\mu}) = \ln P, \quad (7)$$

where  $\varphi = \ln p$ ,

reducing the procedure to the summation of independent contributions from all pixel pairs over the fragment. Such procedures will be called pixelwise classifiers.

Consider two particular cases

corresponding to the additive and multiplicative models.

Let the noise be additive and Gaussian. Then

$$p(z|a) = \frac{1}{\sigma\sqrt{2\pi}} \exp\left[-\frac{(z-a)^2}{2\sigma^2}\right], \quad (8)$$

and the logarithm is

$$\varphi(z|a) = -\ln\left[\sigma\sqrt{2\pi}\right] - \frac{(z-a)^2}{2\sigma^2}. \quad (9)$$

Omitting unimportant constants, we arrive at the following algorithm:

$$\Phi(\underline{z}|\underline{a}) = \sum_{\mu} (z_{i\mu} - a_{\mu})^2 = \min, \quad (10)$$

This is known as the "Minimum Squared Distance", or MSD, algorithm because it can be represented as  $\|\underline{z}_i - \underline{a}\|^2$  in the vector notation. Equivalently, (10) can be written as

$$\Phi(\underline{z}|\underline{a}) = 2 \sum_{\mu} z_{i\mu} a_{\mu} - \sum_{\mu} z_{i\mu}^2 = \max, \quad (11)$$

and if all the hypotheses have the same power (the second term in the right-hand side), then the algorithm is reduced to the scalar product of image vectors:

$$\Phi(\underline{z}|\underline{a}) = \sum_{\mu} z_{i\mu} a_{\mu} = \underline{z}_i^T \underline{a} = \max, \quad (12)$$

This is the well-known correlation algorithm. However, it can be seen from the above derivation that its validity depends on all the assumptions we have used. For incoherent-noise images, the assumptions of additivity and Gaussian distribution are usually satisfied. But the

condition of equal-power hypotheses, necessary for the transition from (11) to (12), is seldom valid: different parts of an image can have different levels of mean brightness, contrast, etc.

Let us now assume the noise to be multiplicative and distributed according to (5). The derivation of the appropriate algorithm for this case is quite similar. Instead of (8) and (9), we have

$$p(z|a) = \frac{L^L}{a \Gamma(L)} \left( \frac{z}{a} \right)^{L-1} \exp \left( -\frac{Lz}{a} \right), \quad (13)$$

$$\begin{aligned} \varphi(z|a) = & \ln \left( \frac{L^L}{\Gamma(L)} \right) + (L-1) \ln z - \\ & - L \left[ \ln a + \frac{z}{a} \right]. \end{aligned} \quad (14)$$

Again discarding unessential constants, the following algorithm is obtained:

$$\Phi(\underline{z}_I|a) = - \sum_{\mu} (z_{I\mu}/a_{\mu} + \ln a_{\mu}) = \max, \quad (15)$$

It should be stressed that the algorithm (15) is quite dissimilar in form from any modification of the correlation algorithm (10)--(12). This shows that the correlation method, used by many researchers without due analysis of the conditions of the particular problem, actually has a definitely limited scope of application, outside which other forms of mathematical processing may be necessary.

## 5. BRIGHTNESS-INVARIANT ALGORITHMS

The simple statistical models discussed above will adequately describe the actual situation --

and the ensuing algorithms will actually work -- only if other important factors acting during the observation of terrestrial surface are taken into account. The first of them is the overall gain. In practice, one seldom manages to calibrate the entire signal path in the imaging device so that the output signal could be exactly related to, say, the reflectivity of terrain surface. On the other hand, this is actually not necessary since all the information in an image is contained in brightness changes rather than the absolute values.

A standard technique to ensure invariance with respect to a parameter carrying no useful information is to transform the input image so that the parameter assumes a fixed standard value. One example is the two jointly used operations of image centering (subtraction of the average value) and normalization (division by the norm). The correlation procedure is frequently augmented with these operations to enhance its efficiency in real-life situations. It should be borne in mind, however, that such transformations influence the initial noise statistics. This can result in a formerly optimal procedure becoming sub-optimal (corresponding to an approximate model) or even heuristic (not based on any statistical model at all), with unpredictable loss of efficiency. The centered and normalized correlation can be regarded as suboptimal for additive noise. For SAR clutter, it is nothing but heuristic.

The next necessary extension is the so-called zonal model of a terrestrial image. Usually, terrain surface contains extended regions in which the surface reflectivity is approximately uniform. This is due to the same physical nature of surface cover in the region (grass, forest, open soil, water, etc.). Exactly



such regions are usually shown in maps, making it possible to use maps for preparing references. Such regions will be called homogeneous zones.

The zonal model can be written as

$$\begin{aligned} z &= \{z_k\}, \quad k = 1, \dots, N; \\ z_{k\mu} &= a_k \otimes \lambda_{k\mu}, \quad \mu = 1, \dots, n_k, \end{aligned} \quad (16)$$

Here  $k$  numbers the homogeneous zones,  $n_k$  is the volume (number of pixels) of the  $k$ th zone. The average brightness  $a_k$  for each zone is assumed to be the same throughout the zone, but initially unknown. Indeed, the surface reflectivity in a zone may vary with time in an unpredictable way due to the changes in its physical condition which can result from changing weather, season, illumination, etc. Such changes may be different in different zones. For instance, with the transition from summer to winter, the radar reflectivity usually becomes higher for water surfaces, diminishes for grassy areas, and remains about the same for forests. As a result, even the relative brightnesses (contrasts) of different zones will vary for different observation conditions. The zonal model actually assumes an individual unknown gain acting upon each separate zone.

The proposed approach to the design of recognition procedures under the assumptions of the zonal model is as follows. The reference image can no longer be constructed as a pattern of expected brightnesses; but, based on the known shape(s) of the reference object(s) -- taken from a map, for instance -- we can form a code pattern where each pixel contains a unique code attributing it to one of the homogeneous zones. This reference will divide the set of the ob-

served image pixels into  $N$  subsets corresponding to individual zones. For the true location, this division will be correct and each subset will contain random samples from the same statistical distribution (with the same value of  $a=a_k$ ). For all other locations, these pixel subsets will contain mixed distributions (with different values of  $a$ ).

A homogeneous zone usually consists of a large number of pixels. Therefore each subset  $\{z_{k\mu}\}$  is a random collection of many samples. Then the sample average

$$\hat{a}_k = n_k^{-1} \sum_{\mu} z_{k\mu}, \quad (17)$$

will be close to the actual mean  $a_k$ . This estimate exactly corresponds to the current condition of the observed terrain, compensating for all possible unpredictable factors which can be reduced to unknown gain. Its accuracy grows unlimitedly with the zone volume  $n_k$ .

If the estimates (17) are substituted into the general model (16) instead of the unknown true values, the resulting recognition procedures will be sub-optimal because they use approximate parameter values; however, they approach the respective optimal algorithms as the zone volumes increase. This class of recognition algorithms may be called adaptive since they estimate the necessary image parameters from the image itself.

Substituting (17) into the formulas describing the optimal procedures for the additive and multiplicative models, after some mathematical transformations we obtain instead of (10)

$$\Phi(\underline{z}_i|\underline{a}) = \sum_k n_k \hat{a}_k^2, \quad (18)$$

and instead of (15)

$$\Phi(\underline{z}_i|\underline{a}) = \sum_k n_k \ln \hat{a}_k, \quad (19)$$

respectively.

These classifiers have been tested on a large body of experimental material, including airborne and spaceborne remote sensing imagery of different Earth regions obtained under various observation conditions. The results confirm that the classifier given by (18) is indeed efficient for processing optical images, while that given by (19) works well with SAR data. Both classifiers remain efficient with inverted or partially inverted contrasts. Of

course, there is a lower threshold: if all the zone contrasts existing in the observed image are smaller than a certain admissible value, recognition efficiency rapidly degrades, the probability of anomalous errors reaching unacceptable levels. This threshold value is about 1.4--1.6 (say,  $a_2/a_1$ ) for typical SAR data.

As regards pixelwise classifiers which use brightness patterns for reference, they show acceptable performance only if no serious deviation of the actual contrasts from those in the reference image occurs. Otherwise, the decision function field usually becomes skewed so that a false peak may exceed the primary one, resulting in erroneous decision.

Development and application of the methods for pilot-aircraft system research  
to the manual control tasks of modern vehicles.

A.V.Efremov, A.V.Ogloblin

Simulators and pilot-vehicle lab, Moscow Aviation Institute (MAI),  
125422 Volokolamskoye sh. 4, Moscow, Russia

### Summary

There are discussed the influence of some typical for the modern vehicles features (high frequency phase delay and nonlinearities in flight control system (FCS)) and parameters of input spectral density corresponding to the real piloting tasks on pilot response characteristics. There are developed some new standard characteristics the optimal aircraft dynamics and discomfort frequency response, and demonstrated their efficiency for the several applied tasks in design of FCS and development of requirements to the handling qualities. There are discussed the ways for suppression of pilot limitation parameters and FCS nonlinear and phase delay effects.

### List of symbols.

$A_n$  - acceleration endured by pilot  
 $c(t)$  - operator output time function  
 $e(t)$  - error time function  
 $K_c$  - controlled element gain  
 $K_p$  - pilot gain  
 $\Delta L$  - gain margin  
 $H$  - altitude  
 $M_x = \frac{1}{J_y} \frac{\partial M}{\partial x}$ , where  $x = q, \alpha, \delta$   
 $N_z$  - normal acceleration  
 $\tau$  - pilot reaction time delay  
 $\tau_c$  - vehicle time delay  
 $\tau_e$  - time delay of crossover model  
 $T_L$  - pilot time constant  
 $Z_\alpha = \frac{1}{m} \frac{\partial Z}{\partial \alpha}$   
 $PR$  - pilot rating  
 $q$  - pitch rate  
 $S_{ii}(\omega)$  - input spectral density  
 $S_{dd}(\omega)$  - spectral density of disturbance  
 $S_{nne}(\omega)$  - remnant spectral density  
 $W_c(j\omega)$  - controlled element describing function

$W_{CL}(j\omega)$  - closed-loop describing function

$W_{OL}(j\omega)$  - open-loop describing function

$W_p(j\omega)$  - pilot describing function

$\varepsilon$  - angle of sight

$$\varepsilon = \theta + \arctg \frac{L}{H}$$

$L$  - distance between aircraft and aim

$\theta$  - pitch angle

$\sigma_e$  - standard deviation of error signal

$\xi_{sp}$  - short period damping ratio

$\omega_{sp}$  - short period undamped frequency

$\omega_{ie}$  - effective bandwidth,

$$\omega_{ie} = \frac{\int_0^\infty S_{ii}(\omega) d\omega}{\int_0^\infty (S_{ii}(\omega))^2 d\omega}$$

$\omega_{i,m}$  - parameters of  $\dot{S}_{ii}(\omega)$

$\omega_c$  - crossover frequency

### 1. Introduction

The high augmentation of the modern vehicles is the typical feature in their development. It is especially obvious in aviation, where the superaugmented aircraft appeared in the beginning of eighties. This new type of vehicle allows: to supply them with necessary flying qualities by the corresponding choice of flight control system (FCS); to synthesize practically any required information in any form on the display screen; to install the new types of manipulator with the different sizes and possibilities.

Except these positive features the superaugmented vehicles demonstrate and negative features such as:

- the increased high frequency phase delay;
- significant influence of surface rate and effectiveness limits on flying qualities;
- undesirable (in some cases) location of poles in trajectory motion and zeros in angular motion. (That is the typical for the Space Shuttle dynamics).

For realization of maximum augmentation possibilities there is necessary to understand which flying qualities has to be in each piloting task. New possibilities of augmentation and its side effects require to develop the new approaches for their realization or elimination. All that is impossible without the knowledge in regularities of control (pilot describing function  $W_p(j\omega)$  and remnant  $N_e(j\omega)$ ), psychophysiological ( $F$ ) and physiological ( $\Phi$ ) pilot response characteristics.

All these characteristics can be investigated by consideration of pilot-vehicle system (fig.1) which is one of man-machine systems such as driver-automobile, helmsmanship, etc. There is necessary to notice that regularities in pilot response characteristics and methods for the investigation are the general for many civil and military man-machine systems. The generalization is possible because of the existence of the main general features such as manual control regime and variables. The last are the following:

- task variable,  $T$  (controlled element, display and manipulator dynamics and their characteristics, parameters of input command  $i(t)$  or disturbance  $d(t)$  signals);
- environmental variables,  $\sigma$  (acceleration, vibration, temperature, etc.);
- procedural variables,  $\pi$  (motivation, pilot experience, the order of presentation, etc.);
- pilot-centered variables,  $\varepsilon$  (fatigue, training level, etc.).

The peculiarity of pilot-aircraft system, especially for military aviation, is the wide variety of tasks (landing, refueling, air-to-air tracking, terrain following and so on) and size of flight envelope (altitude  $H$ , velocity  $V$ , angle of attack  $\alpha$ ). All that comes to significant change in elements of vectors  $T$ ,  $\sigma$ ,  $\pi$ ,  $\varepsilon$ . As an example there are shown the set of input signal and controlled element dynamics for some piloting tasks (see fig. 2,3). As a consequence such variety comes to change of pilot responses and pilot-vehicle system characteristics.

These circumstances predetermined that the pilot-vehicle system was investigated more intensively. The more significant results here were received in USA by D.McRuer [Ref.1], S.Baron and W.Levison [Ref.2], L.Young [Ref.3], T.Sheridan [Ref.4] and other scientists. Systematic researches in this area were carried out and in Russia from the end of sixties-beginning of seventies. Basically, the results of these researches are discussed in Ref. [5].

In the present paper it was made the attempt to spread the knowledge about the pilot response characteristics and their application to

the different manual control tasks by generalization of researches carried out basically in Moscow aviation institute (MAI) during the last 20 years. Mainly there are discussed the regularities in pilot control response characteristics which are considered for single loop pilot-vehicle system because of the known limitation on the volume of paper.

## 2 Some new results in investigation of pilot response characteristics.

### The pilot control response characteristics ( $W_p(j\omega), S_{nene}(\omega)$ ).

These characteristics were investigated in many researches especially for singleloop system. In the majority of works the investigators used the oversimplified models of controlled element dynamics ( $W_c(s) = K_c / s$ ;  $K_c / s^2$ ) or models corresponding to simple models of conventional type of aircraft

$$(W_c = K_c / s(Ts + 1);$$

$$K_c(s - Z_a) / [s(s^2 + 2\xi_{sp}\omega_{sp}s + \omega_{sp}^2)]).$$

There were used basically rather wide bandwidth input signal in the majority researches. In many studies it had the rectangular spectral density form. These investigations allowed to define the pilot ability to adaptation to control element dynamics  $W_c(s)$  and input power spectral density in crossover frequency range. It was found that pilot tries to keep the invariant qualities of open-loop describing function  $W_{OL}(j\omega)$ . It was defined the widely used "crossover model"

$W_{OL} = \omega_c / j\omega \cdot e^{-j\omega\tau_e}$  with the parameters  $\omega_c$ ,  $\tau_e$  depended on  $W_c$  and equivalent frequency of input power spectra  $\omega_{ie}$ . These results allowed the authors to do the following conclusion widely used in many applied investigations: the controlled element dynamics of type  $W_c = K_c/s$  corresponds to the simplest type of human

operator behavior  $W_p = K_p \cdot e^{-s\tau}$  and therefore this dynamics has to be used as a standard in FCS and handling qualities design.

The main aspects in MAI's researches in human behavior for the single loop case carried out in the last period are the detailed investigations of influence of input signal characteristics and typical peculiarities for superaugmented vehicles.

As for the influence of input signal characteristics it was discovered the influence of input signal with low effective bandwidth ( $\omega_{ie} < 1$  1/sec) and form of its spectral density  $S_{ij}$  i.e.

parameters  $m$  and  $\omega_i$  of  $S_{ii} = k_i^2 / (\omega_i^2 + \omega^2)^m$ . The results demonstrated the specific influence of these parameters in crossover and low frequency ranges. As for crossover frequency range the well known recommendations (Ref.1) for the choice of  $\omega_c$  and  $\tau_e$  require more precise in cases when  $\omega_{ie} < 1$  1/sec and the spectral density of input signal has the flat form. In the low frequency range the experiments demonstrated that the decrease of frequency  $\omega_i$  (or  $\omega_{ie}$ ), especially for the sharp input spectral density form comes to appearance of additional pilot adaptation in the low frequency range (fig. 4). The pilot gain frequency response characteristic is increased in that frequency range and pilot behavior differs from the simplest type. Such additional adaptation especially noticed for the well-trained operator and in experiments with small side stick. All mentioned above results are not casual. The mathematical modeling demonstrates that they are defined pilot's aim to minimize an error signal.

As for typical supraaugmented peculiarities there are discussed two of them - increased phase delay in the high frequency range and significant influence of nonlinearities on aircraft dynamics.

The first peculiarity can be evaluated by time delay element,  $e^{-\tau_e s}$ . The research shown that the increase of  $\tau_e$  (up to 0.3-0.5 sec) comes to increase of positive slope in pilot gain frequency response up to 40-50 dB/dec in the frequency range 3-5 1/sec (fig.5). It comes to decrease of amplitude margin ( $\Delta L$ ) of open loop describing function up to 2-4 dB and decrease of the resonance peak ( $r$ ) of closed loop system up to 10-15 dB. Because of the frequency of resonance peak is practically equal to the frequency corresponding to  $\Delta L$  the equation for  $r$

is very simple  $r = \frac{|W_{OL}|}{1 - |W_{OL}|}$ . Analysis of

this equation shows that the decrease of  $\Delta L$  in the region of their small values comes to significant increase of resonance peak. It means that the random change of pilot gain coefficient can come to unstability of system for a time. The remnant power spectral density for that case has high level which demonstrates the high pilot gain coefficient variability and as a consequence the high probability of appearance of pilot induced oscillation (PIO) tendency.

There are different reasons for arising of nonlinear effects in manual control of modern vehicles. One of serious from them is connected with surface rate limit. This nonlinearity begins to show itself when the pilot begins to realize the

significant deflection of the stick. In that case the phase of controlled element dynamics deteriorates and it can come to unstability of the system. They used the different ways to eliminate arising unstability. One of them is the usage of nonlinear prefilter shown on fig.6 as a basic prefilter used for the Russian aerospace vehicle "Buran" [9]. In some conditions this prefilter begins to demonstrate its nonlinear effects also. It takes place under the transfer from significant to small deflections of the stick causing the decrease of  $\Delta L$  (fig. 6). In the case of high FCS time delay it comes to increase of resonance peak and PIO tendency.

#### The pilot physiological response characteristics.

The more interesting from the pilot physiological characteristics are generalized characteristics. One of them was received in [6] where it was investigated the pilot endurance to accelerations of different signs occurred during the flight in atmosphere turbulence and terrain following. The long duration of flight in such conditions decreases the capacity for work and accuracy of fulfillment of tracking task, arising the complex sensation of discomfort characterized by vestibular disturbances, changes in frequency of breath and pulse, sickness, the stable increase in diastolic and decrease in systolic blood pressure, headaches, pain in chest and decrease in keenness of vision. The careful investigation of these effects carried out on simulators and aircraft allowed to get the curve of maximum acceleration endured by pilot as a function of frequency [fig. 7]. This curve has 3 minimum each of them reflects the specific deterioration of comfort. The first lies in the frequency 0.5 Hz and reflects the effects of sickness. The second (3-5 Hz) - pain in the chest and inner organs. The third (8-9 Hz) - the decrease in keenness of vision.

All considered above regularities in control and physiological characteristics were widely used in decision of different applied tasks of manual control.

#### 3. The design of FCS and aircraft flying qualities based on the knowledge of pilot response characteristics.

The level of modern automatization allows to create practically any aircraft dynamic configuration. In depend on the piloting task there are different requirements to the controlled element because of the different standard dynamics configurations and criteria.

### 3.1 Development of new standard dynamics configurations and criteria.

For the modern level of FCS there is possible to require from a vehicle the maximum accuracy in each piloting task. The optimum

solution supplied this requirement  $-W_c^{\text{opt}}$  can

be achieved when the pilot behavior is the simplest and corresponds to the proportional type

( $W_p = K_p \cdot e^{-\tau s}$ ) in all frequency ranges. For that case the pilot behavior is characterized by the following psychophysiological limitations:

- the time delay  $\tau=0.15-0.2$  sec
- the remnant, having the simplest model of it power spectral density

$$S_{\text{nene}} = K_{ne} \cdot \sigma_e^2, (K_{ne} = 0.01).$$

In comparison with classical Wiener approach the considered task has two principal differences:

- the noise has the multiplicative nature, and its spectral density  $S_{\text{nene}}$  is a function of variance of error;
- the system has nonminimum phase element.

These peculiarities require to develop the special interactive procedure for the calculation of

the optimal dynamics parameters  $W_c^{\text{opt}}(j\omega)$  and to use the additional requirement - roughness of closed loop system. It means that the synthesizing part of the system wouldn't have the pools and zeros in the right half plane. The solution of this task can be found in Ref.5. The developed in MAI algorithm and software allow to get the

optimal dynamics  $W_c^{\text{opt}} = f(S_{\mu}(\omega), \tau, K_{ne})$  practically for any input power spectral density. There are shown on fig. 8 the optimal frequency

response characteristics  $W_c^{\text{opt}}(j\omega)$  for some

value of input spectral density parameter  $\omega_i$ . From this figure there is seen that in case of sharp spectral density form ( $m \geq 3$ ) the decrease of the input power spectral density bandwidth (decrease of  $\omega_i$ ) comes to increase of optimal dynamics

gain ( $W_c^{\text{opt}}(j\omega)$ ) in low frequency range. This increase is equivalent to the mentioned above additional adaptation induced by pilot in control when the controlled element has dynamics  $W_c = K_c / s$ . There were carried out the experimental tests for the comparison manual control results in cases when  $W_c = K_c / s$  and

$W_c^{\text{opt}}(j\omega)$  for the same input signal. These tests demonstrated that for the optimal dynamics the additional adaptation disappeared, time delay decreased, the accuracy increased in 2-2.5 times and variance of control deflection decreased up to 6-10 times.

The optimal aircraft dynamics was widely used for the design of different criteria for the following application to the different manual control tasks. One of them is a criteria required the maximum approach of controlled element dynamics  $W_c$  (its gain  $A$  and phase  $\varphi$ ) to the

optimal  $W_c^{\text{opt}}(j\omega)$  characterized by its own gain

$A_{\text{opt}}$  and  $\varphi_{\text{opt}}$ .

It has the following form :

$$J = \min_{a_i} \sum_{k=1}^m [\alpha_k (A_{\text{opt}} - A)^2 + \beta_k (\varphi_{\text{opt}} - \varphi)^2] \quad (1)$$

where  $k$  - number of frequency;  $a_i$  - aircraft or

FCS parameter;  $\alpha_k, \beta_k$  - weighting coefficients.

The second criteria used in the frame of "paper pilot technique" [ 7 ]. According to that technique there is necessary to have the criteria for the mathematical modeling of pilot-aircraft system, whose calculated value corresponds to predicted pilot rating (PR). The main difficulty here is the definition of weighting coefficients combining the partial criteria such as pilot lead time  $T_L$ , variance of error  $\sigma_e^2$  and others in created criteria. In Ref. 5 it was developed the technique for the determination of weighting coefficients based on the usage of aircraft optimal dynamics. For the pitch tracking task this criteria has the following equation:

$$PR = \alpha_1 \sigma_e^2 + \alpha_2 T_L \quad (2)$$

where  $\alpha_1 = 0.1 \frac{\text{rad}}{\text{sm}^2}$ ;  $\alpha_2 = 3 \frac{\text{rad}}{\text{sec}}$  for  $T_L \leq 0.75$  sec

and  $\alpha_2 = 1 \frac{\text{rad}}{\text{sec}}$  for  $T_L > 0.75$  sec

As for the research of flight dynamics in atmosphere turbulence they used often the minimum of variance of acceleration as a criteria

But it is well-known fact that for the aircraft of conventional configuration maximum effect in

decrease of  $\sigma_{\eta}^2$  is 25-30 % even in significant change of ride qualities supplied by very high values of FCS coefficients. That is reason why in Ref.7 the main goal for the flight in atmosphere

turbulence is declared the maximum increase of comfort conditions. For that purposes there is possible to use the curve of maximum acceleration endured by pilot  $A_n(\omega)$  (see fig. 7) to create so-called the discomfort frequency response:

$W_d(j\omega) = 1/A_n(\omega) = D/N_z$ . If the input signal, acceleration  $N_z$ , will be less  $A_n$ , then the output from discomfort frequency response,  $D$ , will be less 1. In the case when  $N_z \geq A_n$ ,  $D \geq 1$ . Because of the atmosphere turbulence is a random process, there is possible to form such criteria of discomfort as the variance or probability of the given level of discomfort  $P_d$ .

### 3.2 The usage of new standard dynamics configuration and criteria for the design.

There are demonstrated the application of the considered criteria and standard characteristics for some applied tasks.

Requirements to the handling qualities in air-to-air tracking task. In the table 3(fig.9) there are given the transfer functions and their parameters

$2\xi_{sp}\omega_{sp}$  and  $\omega_{sp}$  for the conventional and direct lift control (DLC) configurations of aircraft in air-to-air tracking task, where the aircraft output

is  $\varepsilon \cong \theta + H/L$ . For each set of  $\omega_{sp}$  and  $\xi_{sp}$  it can be calculated the value of criteria (1). On fig.9 there are shown the curves of equal values of  $J$  calculated for conventional type of aircraft. It is obvious that the motion in the shown direction (see the arrow on fig.9) comes to approaching to  $W_c^{opt}$ . On this figure there is drawn the curve corresponding to the equation (\*). For the specific value of  $M_q$  this curve touches the curve of constant value of  $J$  at point "A". For this point there is possible to find  $\xi_{sp}, \omega_{sp}$  and  $M_q$ . Suppose that curve  $J=0.35$  corresponds to the range of satisfactory handling qualities. The calculations demonstrate that for that case  $M_q = 36 \text{ rad/sec}$ . The same calculation can be carried out and for DLC configuration. It can be simplified because of  $J = f(M_q)$  only for that case. For  $J=0.35$  the pitch damping moment coefficient  $M_q$  is equal 16 rad/sec. So the DLC configuration does not require too high value of  $M_q$  to get the same results in comparison with the conventional configuration.

Requirements to the aircraft handling qualities or FCS parameters for the case of the existence of FCS time delay. This task was decided for the pitch tracking task by using "paper pilot technique" [Ref.5,7]. By using the equation (1) there is possible to calculate the curves of equal

$PR$  in the range  $\xi_{sp}, \omega_{sp}$  for the different time delay (see fig 10). Analysis of these curves shows that the aim to keep the constant  $PR$  in increase of time delay requires to increase the parameters

$\omega_{sp}$  and  $\xi_{sp}$ . It can be realized by the corresponding changes of aircraft or FCS parameters. But such way of time delay compensation has the limitation. For the case  $Z_\alpha$

$= 1 \text{ 1/sec}$ ,  $\omega_{sp} = 2.5 \text{ 1/sec}$ ,  $\xi_{sp} = 1$ , pilot time delay  $\tau = 0.19 \text{ sec}$  and input spectra

$$S_u = \frac{k_i^2}{(\omega_i^2 + \omega^2)}; \omega_i = 0.5 \frac{\text{rad}}{\text{sec}}, \quad \text{the}$$

maximum time delay which can be compensated by the change of  $\xi_{sp}, \omega_{sp}$  to keep  $PR=2.5$  is equal 0.15 sec.

The design of FCS filters. This task can be solved by the different ways. One of them based on usage the desired controlled element dynamics, (in particular aircraft optimal dynamics,  $W_c^{opt}$ ) is discussed below.

Let's suppose that the vehicle motion can be described with help of the following equation written in Laplace form

$$Sx = Ax + Bu$$

$x$  - phase vector

where  $u$  - is a vector of control surfaces deflections,

$S=sE$ , where  $s$ - Laplace operator,  $E$ - unit matrix,

$A$ - matrix of aircraft dynamic coefficients;

$B$ - matrix of control efficiency coefficients

$$u = W_c c - W_f x$$

Here  $W_c$  and  $W_f$  - command and feedback filters of FCS

$c$ - pilot output signal

By inducing the requirement that

$$x(s) = F(s)c(s)$$

where  $F(s)$  is a matrix of desired (standard) controlled element dynamics, there is easy to get the following equation for the definition of filters:

$$B W_c = (A + B W_f) F$$

Here  $A(s)$  is matrix,  $A = (S - A)$

In [ Ref.8] there is given the application of this equation to the design of command and feedback filters for the aircraft with DLC configuration supplied the desired (including the optimal) configuration for each phase coordinate.

The engineering technique for the single loop pitch tracking task for the unstable aircraft with the simplified dynamics

$$W_c = q/\delta = \frac{M_\delta}{S - M_q} \text{ is demonstrated below.}$$

For the input signal characterized by the first

order filter  $(S_{ii} = \frac{k_i^2}{(\omega^2 + \omega_i^2)})$  the aircraft optimal dynamics has the following form

$$W_c^{\text{opt}} = k_r \frac{(1 + \tau/2 \cdot s)}{\left(1 + \frac{1}{\omega_i} s\right) \left(1 + \frac{1}{\omega_r} s\right)}$$

where  $\omega_r = f(K_{n_r}, \tau, \omega_i)$

For  $\omega_i < 1$  rad / sec. It can be simplified by the following way

$$W_c^{\text{opt}} \cong K \frac{1 + \tau/2 \cdot s}{s \left(1 + \frac{1}{\omega_r} s\right)}$$

Using the filters (see fig. 11)

$$W_{f_2} = \frac{K_{f_2} \left(s + \frac{1}{T_{f_2}}\right)}{s}$$

and

$$W_{f_1} = \frac{1 + \tau/2 \cdot s}{1 + T_{f_1} \cdot s}$$

with parameters  $\frac{1}{T_{f_2}} = -M_q$ ,  $K_{f_2} M_\delta = \omega_r$ ,

$T_{f_1} < 0.05 \text{ sec}$  the tasks can be decided.

The requirements to the controlled element dynamics in flight in atmosphere turbulence. On fig. 12 there are shown the curves of equal values of discomfort probability  $P_d$  and probabilities of the given level of normal acceleration  $P_n$  in

coordinates  $\xi_{sp}$  and  $\omega_{sp}$ . The comparison of these curves demonstrates that the change of  $\omega_{sp}$  and

$\xi_{sp}$  allows to change  $P_d$  much more sufficiently than  $P_n$ . The efficiency in decreasing of discomfort is connected with the existence of some minimums in discomfort frequency response  $W_d(\omega)$ . The effect achieves with help of corresponding choice of FCS characteristics or aircraft parameters supplied the transformation of the maximums acceleration in the region of minimums of  $W_d(\omega)$ .

The design of FCS for suppression of shortcomings in pilot aircraft system.

There are two types of shortcomings depending on the different reasons: limitations on pilot possibilities and some negative side effects of controlled element dynamics. These both sources of shortcomings have to be investigated experimentally in conjunction with mathematical modeling technique. That is the single way to understand their reason for the following design of means for the suppression.

a. Suppression of limitation on pilot psychophysiological characteristics.

Even in the case when  $W_c = W_c^{\text{opt}}$  there are limitations on pilot ability in control: limitation on his psychophysiological parameters: delay in reaction and remnant. These shortcomings can be suppressed by additional automatic loop (fig. 13). Such way allows to decrease the noise and effective time delay even for the simple law in automatic loop ( $W_a = K_a$ ). Actually for that case the noise

$$N_e^* = N_e \frac{W_p}{W_p + K_a}$$

and effective pilot describing function

$$W_p^* = W_p + W_a \cong (K_p + K_a) \frac{1 + \tau/2 \frac{K_a - K_p}{K_a + K_p} s}{1 + \tau/2 s}$$

$$\text{Here } W_p = K_p e^{-sr} \cong K_p \frac{1 - \tau/2 s}{1 + \tau/2 s}$$

Experiment demonstrated that these conclusions are correct. Except it came to increase of the crossover frequency, bandwidth of closed loop



system. As for accuracy it increased up to 2-4 times in comparison with the experiments with  $W_c^{\text{opt}}$  when the system didn't have additional loop.

**b. The suppression of negative side effects of controlled element dynamics.**

There are discussed the ways in suppression of side effects which are typical for superaugmented aircraft: increased time delay and nonlinear effects.

**PIO suppressor.** It was shown above that the increased time delay increased the PIO tendency because of increase in pilot describing function slope. Mathematical modeling has demonstrated that the reason of this increase is explained by the active usage of pilot kinesthetic cues. So the source of PIO tendency is defined by the wrong organizing of pilot's inner feedbacks. This conclusion comes to idea to find the way allowed to suppress the kinesthetic feedback and to form the other information channel for improvement the closed-loop characteristics. For that purposes it was offered to use the information about additional forces realized by the change of stiffness of manipulator spring according to the signals from FCS. The example of such system is shown on fig. 14. Neglecting the servo dynamics, supposing that it generates the additional forces

$$\Delta P = F^c c_{sp}, \text{ and } W_f = \frac{1}{T_f s + 1}, \text{ there is}$$

possible to get the following transfer function of the change of stiffness:

$$\frac{F(s)}{C(s)} = F^c (1 - a) \frac{\frac{T_f}{1-a} \cdot s + 1}{T_f s + 1}$$

The gain frequency response of this transfer function is shown on fig. 15. By choosing the parameters "a" from 0-1 there is possible to find the appropriate law of change of stiffness in the frequency range 3-5 rad/sec. Experiments has shown that such additional information about forces was very useful for pilot. The slope of pilot describing function decreased and resonance peak in  $W_{cL}$  disappeared completely (fig. 15).

**The suppression of some nonlinear effects.** The absence of coordination between the pilot activity and FCS possibilities comes to appearance of nonlinear effects. The concrete solutions for such cases depend on the set of circumstances. The general recommendation can be formulated as a following requirement: to create of conditions which will decrease or even avoid the possibility of appearance the signal which would be equal or more that limit.

As for FCS of "Buran" it was offered the modified prefilter (fig. 6) whose gain coefficient was changed not to allow to reach the limit of nonlinear element. It was realized by the usage of special algorithm. After the decrease of input signal causing the decrease of gain coefficient it restored according to the special law. This modification allowed to decrease the effect of nonlinearity and "to linearize" it. The experiments demonstrated that the usage of such filter allows to decrease the resonance peak up to 30-35% and PIO tendency in comparison with the basic version.

## References

1. McRuer D. Krendel E., Mathematical models of human pilot AGARD AGD-188 1974, 72p.
2. Baron S. Kleinman D. Levison W. Application of optimal control theory to prediction of human performance in a complex task. Proceeding of the fifth NASA-university annual conference on manual control 1969, NASA - SP 215. pp. 367-387.
3. Young L. An adaptive manual control. Ergonomics, 1969, vol 2, N4, pp.635-675.
4. Sheridan T. Ferrel W. Man-machine systems. MIT Press, 1974, p.390.
5. Efremov A.V. Ogloblin A.V. et al Pilot as dynamic system. Mashinostroenie, Russia, 1992, p.331.
6. Aleksahin B.H. et al Experimental researches on influence of different signs of accelerations on pilot activity and passenger comfort. TSAGI, Scientific Notes, N3, 1972, pp.54-60.
7. Anderson R. A new approach to the specification and evaluation of flying qualities. AFFDL-TR-69-170, 1970
8. Efremov A.V. The synthesis of the flight control system based on standard aircraft dynamics. In the book "Dynamics of flight and aircraft control", MAI Press, Moscow, 1982, pp. 35-40.
9. Efremov A.V. Ogloblin A.V. Koshelenko A.V. Application of methods for pilot-vehicle research in the safety of flight tasks. Proceedings of international conference TSAGI-AGARD "Aircraft flight safety", pp.529-533, Zhykovsky, Russia, Sept. 1993.

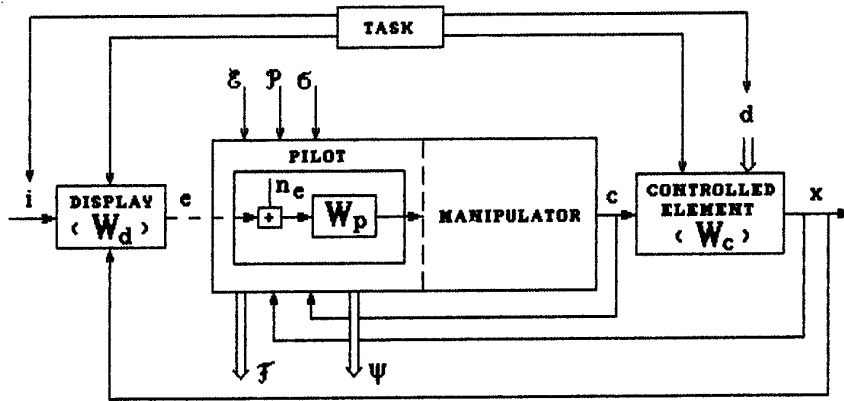


Fig.1. Pilot-vehicle system

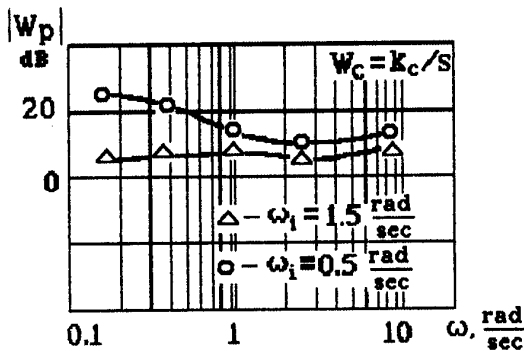
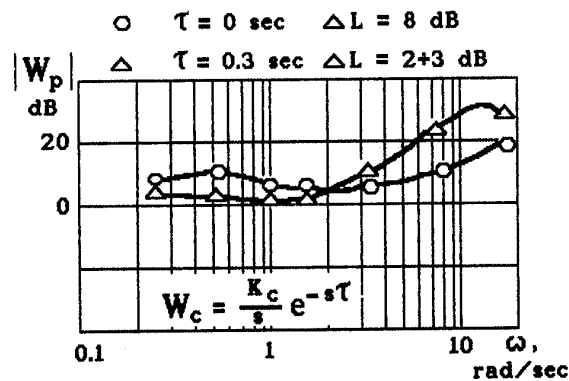
Table 1

Task	$S_{11}$	$S_{dd}$
pitch angle control	-	$\left  \frac{M_\alpha}{(j\omega^2) + 2\xi_{sp}\omega_{sp}j\omega + \omega_{sp}^2} \right ^2 S_{wg}$
terrain following	$\frac{k}{[\omega^2 + (0.12+0.16)^2]}$ $\sigma_h = 50+150 \text{ m } (H < 700 \text{ m})$	$\left  \frac{H}{W_g} \right ^2 S_{wg}$
air-to air combat	$\frac{k}{(\omega^2 + (0.33)^2)} \left  \frac{H_a}{n_a} \right ^2$	$\left  \frac{\epsilon_z}{W_g} \right ^2 S_{wg}$
glide tracking (longitudinal)	$\frac{(0.4)^2}{\omega^2 + (0.25)^2} \text{ [m}^2\text{]}$ ( $H = 30 \text{ m}$ )	$\left  \frac{d}{W_g} \right ^2 S_{wg}$

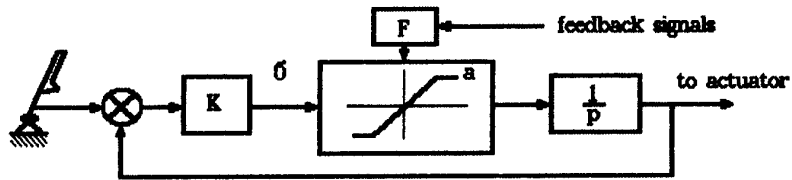
Fig.2. Input signals

Table 2

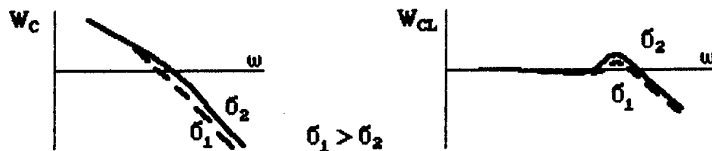
N	Output	$W_c$	Manual control task
1	$\theta$ pitch angle	$\frac{K_c(s - Z_\alpha) e^{-\tau s}}{s(s^2 + 2 \xi_{sp} \omega_{sp} s + \omega_{sp}^2)}$ $\frac{K_c}{s(s - M_q)}$	stabilization and control angular motion (conventional configuration)  aircraft with the DLC
2	$\epsilon_Z$ angle of sight	$\frac{K_c(s^2 - Z_\alpha s - Z_\alpha \frac{V}{L})}{s^2(s^2 + 2 \xi_{sp} \omega_{sp} s + \omega_{sp}^2)}$	taking aim $(\epsilon_Z = \vartheta + \arcsin \frac{H}{L})$
3	$\Delta H$ altitude	$\frac{K_c n_\alpha g}{s^2(s^2 + 2 \xi_{sp} \omega_{sp} s + \omega_{sp}^2)}$	formation flight, flare
4	$\gamma$ bank angle	$\frac{K_c}{s(s - L_p)}$	stabilization and control of angular motion

Fig. 3. Controlled element dynamics  $W_c$ Fig. 4. The influence of  $\omega_1$ Fig. 5. The influence of time delay  $\tau$

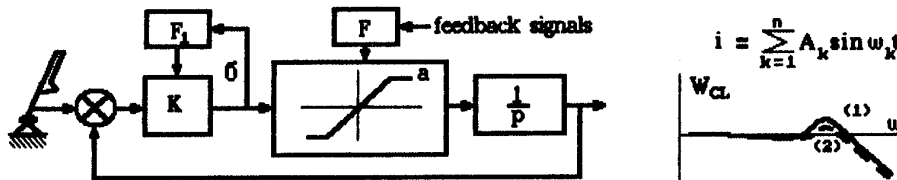
### 1. Basic prefilter



$$W = \frac{1}{Tj\omega + 1}, \quad T = \frac{1}{K \operatorname{erf}\left(\frac{a}{\sqrt{2}\sigma}\right)}$$



### 2. Modified prefilter



$$i = \sum_{k=1}^n A_k \sin \omega_k t$$

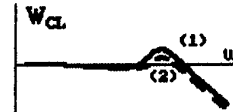


Fig.6. The influence of FCS nonlinearity and its suppression

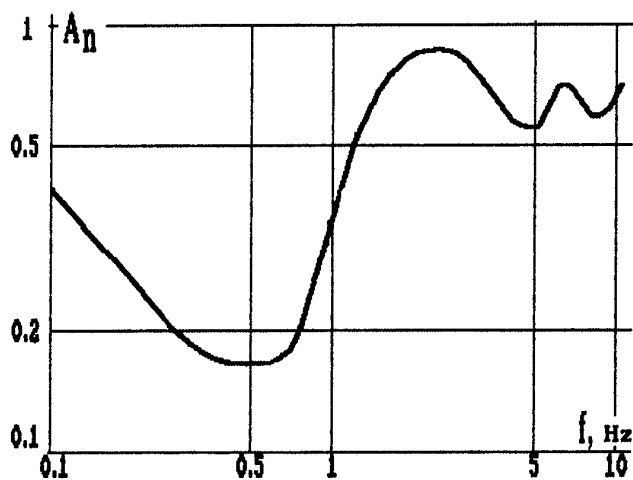


Fig.7. The accelerations endured by pilot

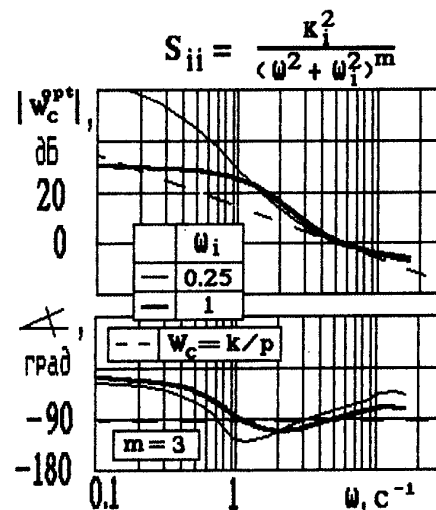


Fig.8. The optimal aircraft dynamics

Table 3

$$\varepsilon = \theta + \frac{H}{L}$$

	conventional configuration	DLC configuration
$W_C = \frac{\varepsilon}{C}$	$\frac{K_C(s^2 - Z_\alpha s - Z_\alpha \frac{V}{L})}{s^2(s^2 + 2\xi_{sp}\omega_{sp}s + \omega_{sp}^2)}$	$\frac{K_C(s + \frac{V}{L})(s - Z_\alpha)}{s^2(s^2 + 2\xi_{sp}\omega_{sp}s + \omega_{sp}^2)} = \frac{K_C(s + \frac{V}{L})}{s^2(s - M_q)}$
$2\xi_{sp}\omega_{sp}$	$-Z_\alpha - M_q$	
$\omega_{sp}^2$	$-M_\alpha + Z_\alpha M_q$	$Z_\alpha M_q$
$\omega_{sp}$	$\frac{-Z_\alpha - M_q}{2\xi_{sp}} (*)$	

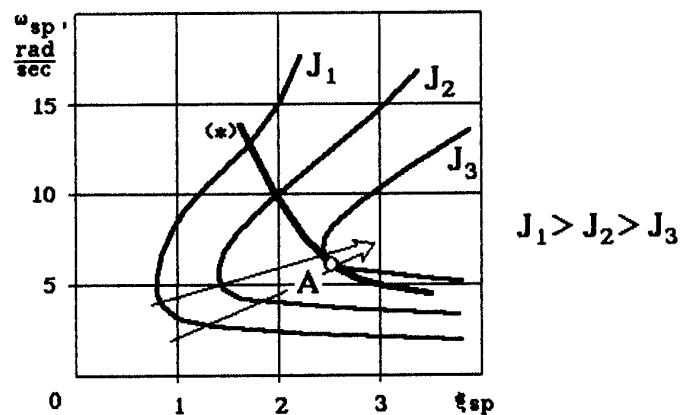


Fig.9. The requirements to the handling qualities in air-to-air task

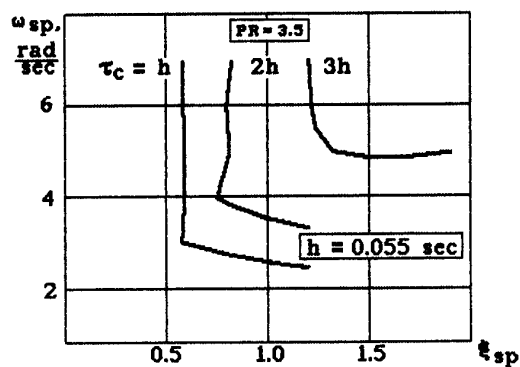


Fig.10. The compensation of time delay

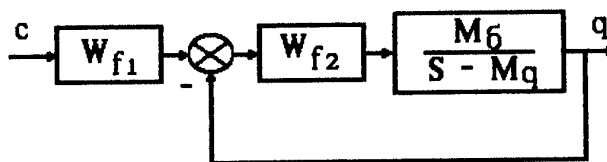


Fig.11. The design of standard dynamics by filters

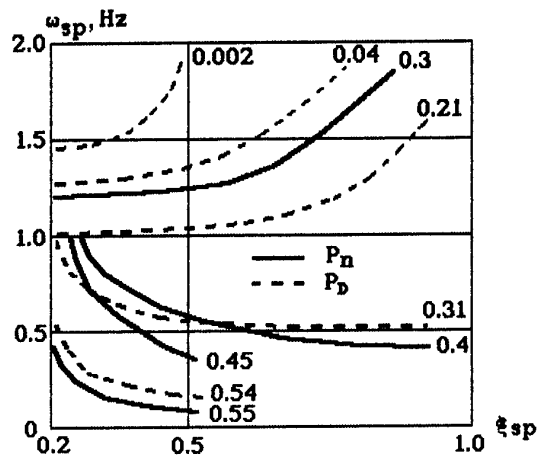
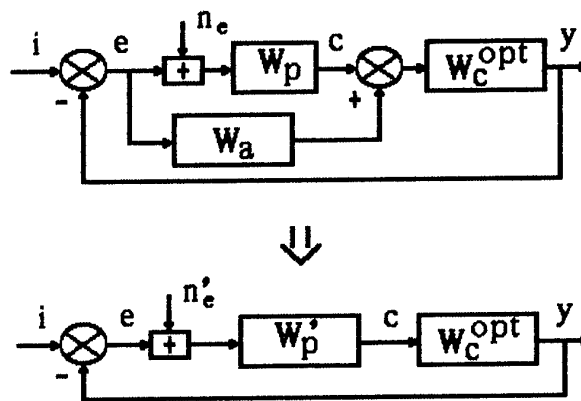
Fig.12. The probabilities of  $P_n$  and  $P_d$ 

Fig.13. The suppression of pilot limitations parameters

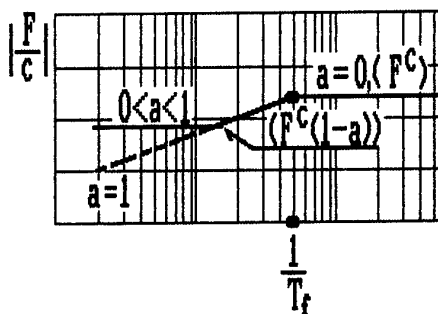
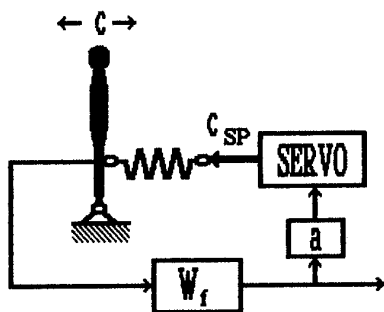
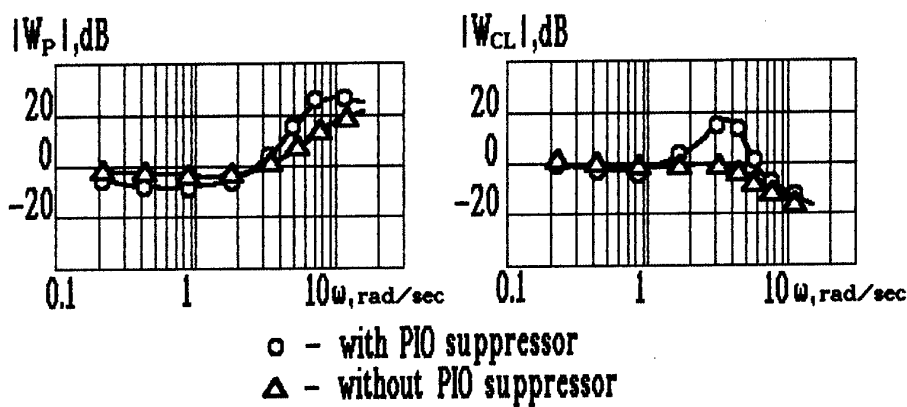
Fig 14. The manipulator with changable spring stiffness  
( PIO suppressor )

Fig.15. The effect of PIO suppressor

## APPLICATION OF ADVANCED SAFETY TECHNIQUE TO RING LASER GYRO INERTIAL NAVIGATION SYSTEM INTEGRATION

James Blaylock  
Lockheed Corporation  
Lockheed Fort Worth Company  
Fort Worth, Texas USA 76101-0748

Donald Swihart  
Wright Laboratory  
Wright Patterson Air Force Base  
Ohio USA 45433-7521

Captain Chuck Stribula  
Aeronautical Systems Center  
Wright Patterson Air Force Base  
Ohio USA 45433-7205

### SUMMARY

This paper documents the application of System-Wide Integrity Management (SWIM) to the integration of H-423 and LN-93 ring laser gyro (RLG) inertial navigation system (INS) units with the F-16 terrain following (TF) system. Safety modeling and mishap rate predictions are presented for F-16 TF with an RLG INS. This paper establishes that the H-423 and LN-93 RLG INS units are both safer for F-16 TF than the predecessor LN-39 gimbaled, mechanical-gyro INS.

The RLG INS design enhancements described are primarily built-in test (BIT) modifications that were developed as a result of the in-depth SWIM critical signal path analysis. These enhancements are low-cost design improvements to the RLG INS units because they were discovered prior to the manufacturer's final operational flight program (OFP) for the production units.

This paper discusses dual-use applications of the RLG INS to other military and civilian functions, with design enhancements resulting from the SWIM process. Other military applications include not only specialized control modes such as TF, but also all other phases of the military flight operations regime, since the INS is always active to provide current aircraft state information. Civilian uses can also benefit from the SWIM process improvement to the RLG INS because accurate, reliable, safe navigation with critical timing along congested air routes, in weather, and in dense traffic terminal areas is of paramount importance for passenger safety.

### BACKGROUND

Limited room in modern fighter aircraft for on-board equipment has led to the mechanization of advanced, flight-critical functions with nonredundant elements. For the F-16, such space limitations led to the mechanization of a terrain following (TF) system with multiple, nonredundant sensors and control processors. In spite of lacking redundancy in critical subsystems, flight safety concerns required that fault tolerance must be achieved in the overall TF system.

### Background Development

As a result of the TF fault tolerance requirement, F-16 TF system development was accomplished with an advanced flight safety enhancement technique – System-Wide Integrity Management (SWIM). SWIM is a new approach to both the design and use of in-flight built-in test (BIT) to detect otherwise undetectable malfunctions that could result in aircraft loss. SWIM was first developed by the Fort Worth Division of General Dynamics (renamed Lockheed Fort Worth Company after acquisition by Lockheed Corporation in March 1993) in its Advanced Fighter Technology Integration (AFTI) Program for the Automated Maneuvering Attack System (AMAS). SWIM was then applied to the F-16 TF system, which provides low-level vertical flight profile control during day, night, or adverse weather conditions. Flight is at a fixed offset over terrain while operating within aircraft and crew acceleration constraints. The F-16 TF operation is summarized in Figure 1 and its architecture is depicted in Figure 2. The TF subsystems are the combined altitude radar altimeter (CARA); low-altitude navigation and targeting infrared for night

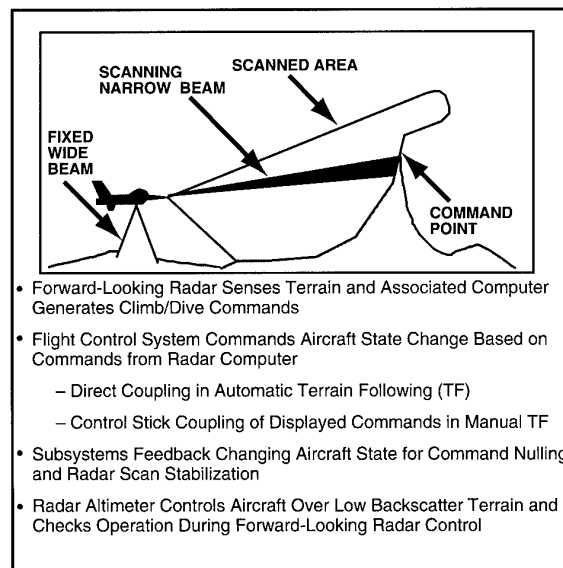


**Figure 1 Terrain Following Requires  
Integration of Multiple Subsystems**

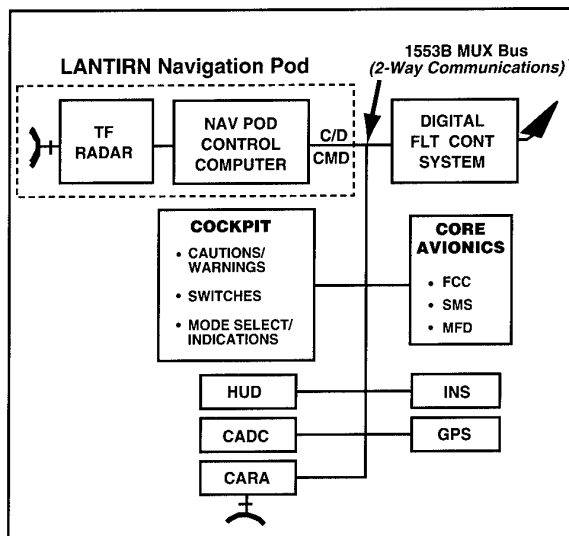


**Figure 2 F-16 TF System Architecture**

(LANTIRN) navigation pod, which contains the terrain-following radar (TFR) and navigation pod control computer, which generates the climb/dive (C/D) command; inertial navigation system (INS); central air data computer (CADC); head-up display (HUD); global positioning system (GPS); digital flight control system (DFLCS); and the core avionics that include the fire control computer (FCC), stores management set (SMS), multi-function display (MFD), and multiplex (MUX) bus connecting the subsystems. If SWIM detects flight-critical malfunctions, an automatic recovery maneuver is initiated, consisting of a roll to wings-level fly-up for the F-16 TF system.

The previously applied SWIM technique is defined briefly as self-test of a function, as opposed to traditional self-test of a single subsystem. Figure 3 illustrates the SWIM technique,

which is system-wide since it includes all individual subsystems and interfaces involved in that function (left circle). SWIM involves an independent monitor site (center circle), i.e., the F-16 TF DFLCS. The management aspect involves eliminating the safety impact associated with the failure rate of a particular subsystem through which a critical signal is routed when that subsystem has minimal involvement in the function (as in the right circle of Figure 3). SWIM management incorporates the SWIM monitor architecture designed to rely on an alternate route or bypass for the critical signal to ensure detection of failures in the subsystem that affect the critical signal. As a result, the safety impact of that particular subsystem is effectively bypassed.

The SWIM monitor host site has a requirement to preclude undetected, latent failures of SWIM monitors. This extreme dependability requirement resulted in the SWIM monitors being hosted in a fault-tolerant processing network, the F-16 DFLCS. Figure 4 is a diagram of the F-16 quad-redundant DFLCS.

As a result of the F-16 TF SWIM process, the 12 features or monitors listed in Figure 5 were added. SWIM drift and bias error features monitor the INS and LANTIRN navigation pod for attitude and inertial velocity corruption not detectable by subsystem self-tests. Using a DFLCS software attitude estimator, a GPS-based inertial velocity source, and a CARA-based, low-altitude check enables detection of such hazardous fly-low drift and bias conditions. Subsystem processor malfunction detection is provided by CARA status monitors, comparison of altitudes from the CARA receiver-transmitter

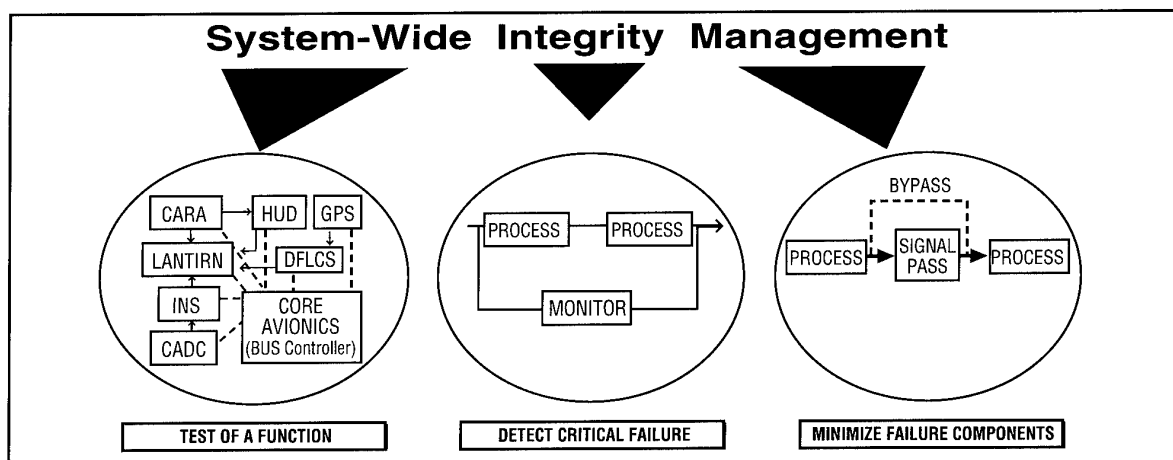


**Figure 3 System-Wide Integrity Management (SWIM)**



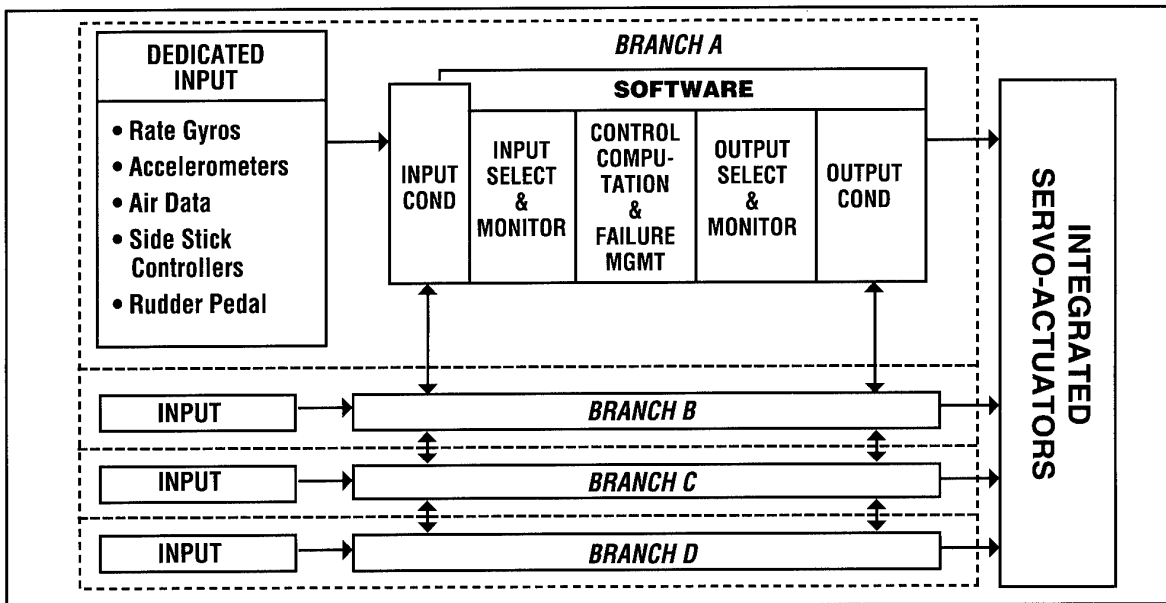


Figure 4 F-16 Digital Flight Control System

and the CARA signal data converter, and cyclic test problems in the LANTIRN navigation pod. These tests are all monitored in the DFLCS. The communication path loss features prevent undetected communication loss via (1) MUX terminal to MUX terminal transmission and receipt verification, (2) redundant status and integrity discretes that are provided independent of the MUX bus, and (3) an automatic TF (Auto-TF) engagement verification to prevent the pilot from relinquishing vertical clearance control to a TF system with Auto TF disengaged.

The SWIM safety improvements and the cost effectiveness of achieving those safety improvements noted in an earlier NATO AGARD paper (November 1988) are illustrated in Figures 6 and 7. Comparisons of the predicted mishap rate reductions of 14 percent for F-16 TF SWIM and 17 percent for traditional redundancy from Figure 6 with the costs of \$2 million for F-16 TF SWIM, \$100 million for traditional redundancy, and \$500 million for perfect TF, yield the Figure 7 cost effectiveness data. As indicated in Figure 7, SWIM mechanization for F-16 TF with its single-thread system is 47 times (140/3) more cost effective than traditional TF with its redundant INS and CARA.

### Background Chronology

Figure 8 is a graphic display of the background leading to the current paper on F-16 TF SWIM compatibility with an RLG INS. Though the SWIM concept originated in the AFTI F-16 AMAS Program, it was not until the F-16 TF Program, with its charter to implement a production system, that more stringent qualification and validation requirements had to be met than for the one-of-a-kind AFTI F-16 AMAS flight demonstration program. The first F-16 TF SWIM paper covered development of F-16 TF SWIM, the second paper focused on validation of F-16 TF SWIM using a laboratory ground test and flight test approach, and this paper establishes compatibility of the RLG INS for use with F-16 TF via the SWIM analysis process.

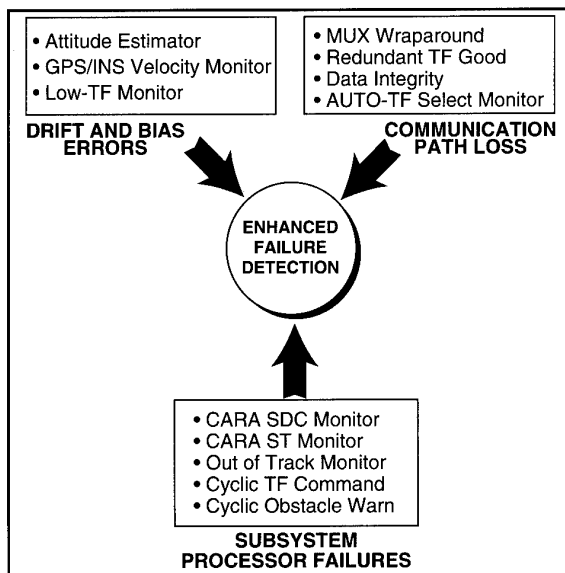


Figure 5 F-16 TF SWIM Features Cover Different Undetected Malfunctions

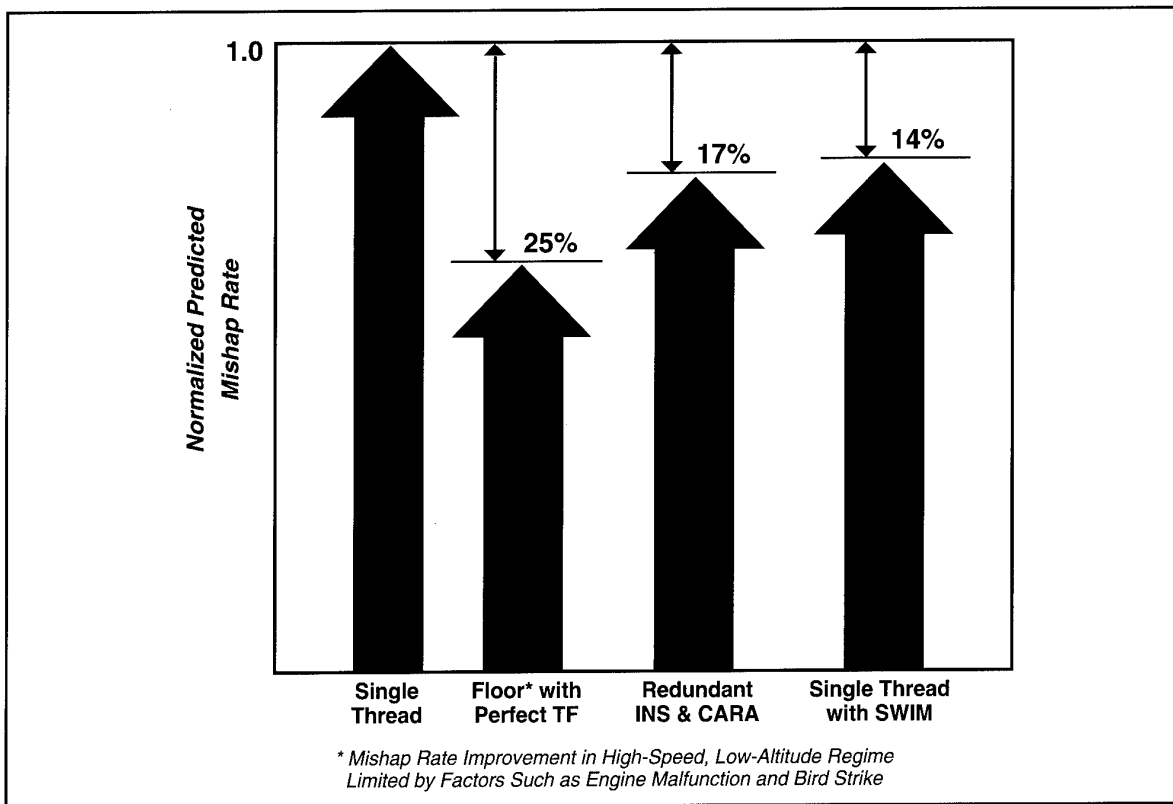


Figure 6 F-16 Predicted Mishap Rate Reduction

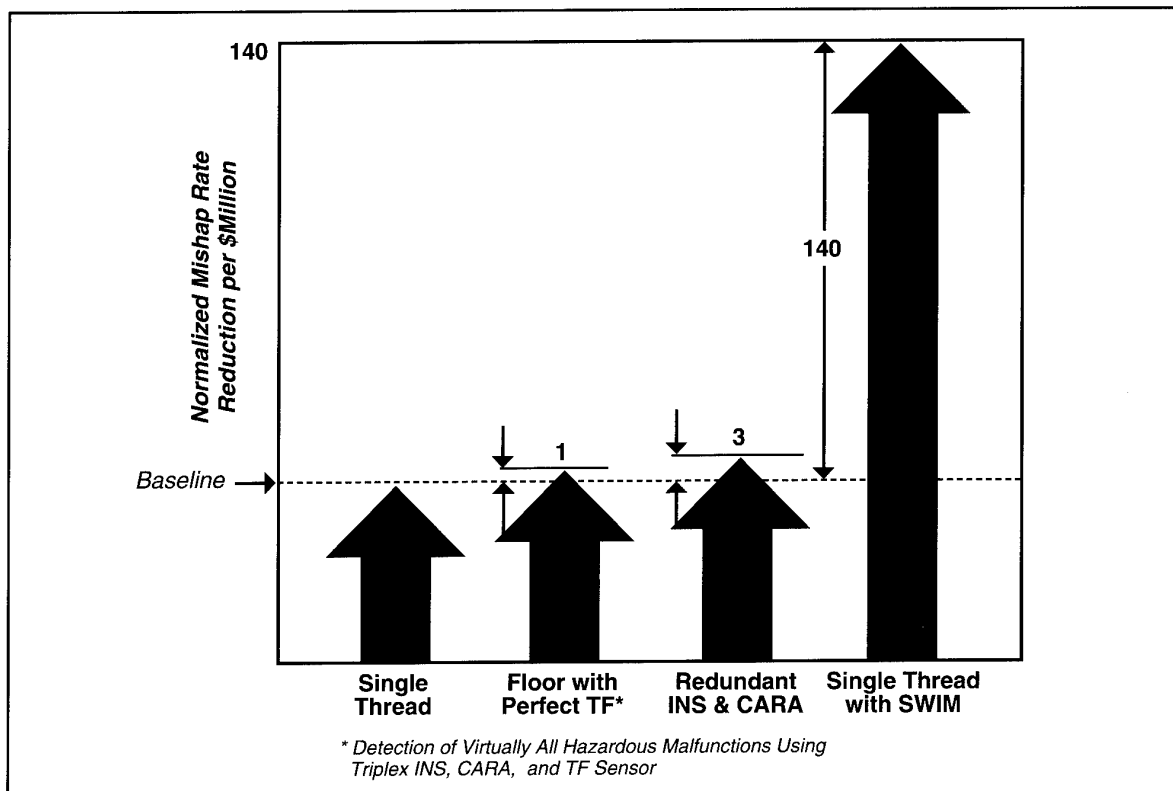


Figure 7 Alternate F-16 TF System Cost Effectiveness

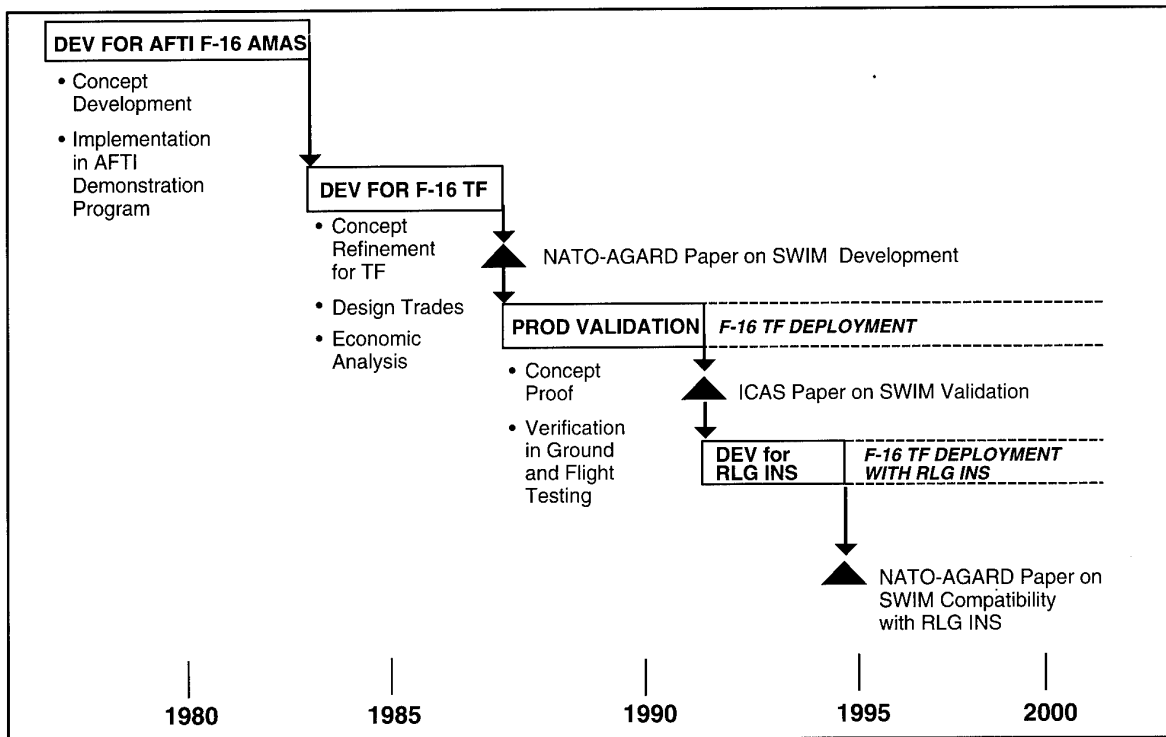


Figure 8 Lockheed Fort Worth Company SWIM Chronology

### RLG INS COMPATIBILITY WITH F-16 TF SWIM

F-16 TF SWIM development and production validation was accomplished for a TF system suite with an LN-93 gimballed, mechanical gyro INS, as documented in the SWIM development paper<sup>1</sup> and SWIM validation paper<sup>2</sup>, which preceded this paper (shown chronologically in Figure 8). With the LN-93 gimballed, mechanical-gyro INS produced by Litton Systems Incorporated, the F-16 TF system with its SWIM features was found<sup>1,2</sup> to have an acceptable level of safety. Since then, a non-gimballed, strap-down RLG INS was procured by the USAF for F-16 installation. The effect of this change in INS on F-16 TF safety had to be determined via another SWIM analysis. This analysis was necessary to ensure that integration of the RLG INS with F-16 TF/SWIM was acceptable in terms of safety level. If not acceptable, changes to the F-16 TF system would be required to achieve a comparable level of safety to that of the F-16 TF system with the LN-39 mechanical-gyro INS. This SWIM analysis was conducted to establish RLG INS compatibility with F-16 TF/SWIM.

### RLG INS Compatibility Objective

The purpose of the SWIM analysis was to ensure

an acceptable level of safety for F-16 TF with an RLG INS installed. To establish this safety level, the critical failure rate of the RLG INS subsystem, the TF mishap rate, and the predicted F-16 mishap rate were to be determined. The analysis would evaluate undetected critical signal RLG INS failures and establish failure rates affecting TF. The resulting RLG INS critical failure rates, TF mishap rates, and F-16 mishap rates would be compared to the rates for the predecessor mechanical-gyro LN-39 INS. If failure rates were worse, additional SWIM features were to be defined and recommended for implementation by the USAF to achieve a predicted F-16 mishap rate at least as low as the predicted F-16 mishap rate with the LN-39 INS.

### RLG INS Operation

Instead of a traditional, gimballed gyro-reference INS, a strap-down, laser-based INS is advantageous for highly-maneuverable, modern fighter aircraft. Packaging is smaller and less complicated if gimbaling is not required. Also, reliability is greatly increased by eliminating the gimballed, mechanical gyro.

In the RLG component of an RLG INS, interference between two counter-rotating laser beams in

a single-plane, closed cavity creates a standing wave pattern. This standing wave pattern is the reference for the RLG since it remains fixed in inertial space because of relativistic considerations attributed to Sagnac<sup>3</sup> based on the invariance of the speed of light. The effect of this speed invariance on optical path length versus the direction of cavity rotation is known as the Sagnac effect. A detector mounted to the cavity is used to determine the number of minima of the fixed standing-wave pattern through which the cavity rotates during an angular change. Since the closed cavity supports a fixed number of resonant laser-beam wavelengths, the number of interference minima around the cavity circumference is known. Consequently, the direct angle change is determined from the number of minima counted by the detector during an angular change of the cavity.<sup>4</sup>

An alternative description more easily visualized, particularly for interferometers, can also be given. Consider a rotating, closed cavity with counter-propagating beams. A full circuit around the loop will appear to be a longer optical path to the beam traveling in the same direction as the rotation, when compared with the beam propagating counter to the rotation. This leads to a phase difference between the two beams. A detector sensitive to this phase difference then provides a measure of rotation.

Three mutually-orthogonal RLG units provide complete attitude information, including angular rate and angular acceleration via differentiation. When combined with three mutually-orthogonal accelerometers and using integration of the linear

accelerations, the resultant RLG INS measures complete aircraft state changes. Initial alignment of the RLG INS prior to takeoff provides the reference aircraft state to which the angular and linear changes are added to obtain the current aircraft state.

### RLG INS Description

The RLG INS is a form, fit, and function equivalent to the gimbaled, mechanical-gyro LN-39 INS. It is a self-contained, solid-state, strap-down INS incorporating three mutually-orthogonal RLG units and three mutually-orthogonal accelerometers. It is microprocessor controlled and interfaces with other aircraft subsystems via 1553B MUX bus or analog/synchro interfaces. The RLG INS provides all-attitude, complete aircraft state, including linear and angular position, velocity, and acceleration. Figure 9 summarizes RLG INS physical characteristics and performance capabilities.

The USAF selected two different RLG INS suppliers as alternate sources for the F-16 RLG INS. Honeywell Military Avionics Division supplies the H-423 RLG INS, and Litton Systems, Incorporated supplies the LN-93 INS. The characteristics and performance of both units are listed in Figure 9. Internal mechanization differences exist, including a triangular, closed laser path for the H-423 versus a square closed laser path for the LN-93, which were treated individually in the SWIM analysis. Other small variations in physical characteristics, such as a fraction of a pound weight difference, also exist. In those cases, the worst case value is given in Figure 9.

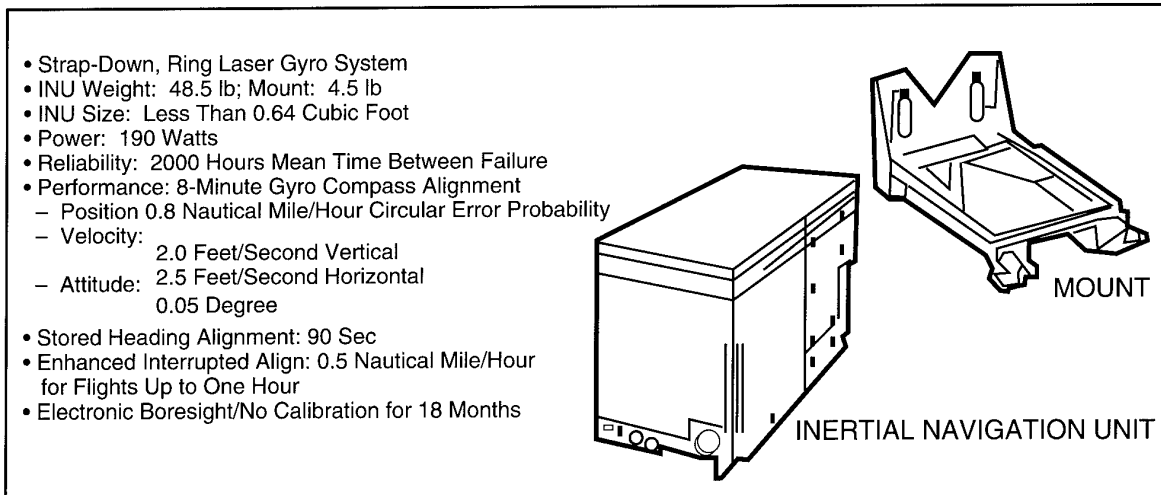


Figure 9 RLG INS System Description

## RLG INS DESIGN ENHANCEMENTS

As a serendipitous by-product of the in-depth circuit analysis required in a SWIM study, both RLG INS manufacturers discovered several design enhancements (primarily BIT software) that could be made to their designs at little cost. In every SWIM program conducted to date, similar design enhancements were achieved as a result of the intensive critical signal path scrutiny to which the subsystems are subjected.

These enhancements are not indications of specification deficiencies, since the analyzed subsystems had already met design specifications. Rather, the enhancements are ways to improve the subsystems beyond their specification requirements with minimal impact to program, schedule, and cost. A powerful argument for the SWIM process is the discovery and implementation of these design enhancements, which have occurred each time the SWIM process was applied, as documented in previous papers.<sup>1, 2</sup> The following enhancements can be incorporated at much less cost because they were discovered via SWIM analysis prior to the final production OFP update. This production OFP update is designated the Revision B update for both the Honeywell H-423 and the Litton LN-93 RLG INS subsystems.

### Honeywell H-423 Enhancements

Table 1 lists the H-423 RLG INS design enhancements, while the following discuss each enhancement and their effects.

**Table 1 H-423 RLG INS DESIGN ENHANCEMENTS**

- Decreased Response Time From BIT Detection to Failure Reporting on MUX Bus
- Improved Synchro Wraparound Test to Prevent Analysis of Wrong Data
- Logic to Prevent Test Mode Entry During Flight
- Improved Stability of Temperature Resolution Circuit (Hardware Change)
- Updated and Corrected Schematics, Specifications, and Operation Data

1. BIT Response Times (Software Change) – Response times from BIT detection to fault reporting on the MUX bus were adequate, but an improvement was identified to add a fault isolation routine after all 2 cycles per second BIT have been executed. The result is faster fault reporting.
2. Synchro Wraparound Test (Software Change) – A modification was identified that eliminates a condition whereby the test could analyze the wrong data if a 100 cycles per second interrupt occurred just before the test.
3. Additional Test Mode Entry Prevention (Software Change) – Logic was developed to prevent entry into test mode after a greater than 80 knots airspeed flag was set. This logic ensures the INS cannot enter test mode when the aircraft is in flight.
4. Temperature Resolution Circuit (Hardware Change) – A temperature stabilization circuit change was developed to better govern response to temperature variations. This circuit change improved RLG stability during temperature changes.
5. Specifications, Schematics, and Data (Documentation Change) – As a result of the SWIM analysis, errors and omissions were found and corrected in specifications and schematics. Updates were also made to operation descriptions and failure modes and criticality analyses, including effects of changes identified because of the SWIM analysis. The result was more accurate documentation and optimization for reliability and failure analyses.

### Litton LN-93 Enhancements

Table 2 lists the LN-93 RLG INS design enhancements, while the following discuss each enhancement and their effects.

1. BIT No. 1 (Software Change) – A navigation processor random access memory (RAM) test was performed only during initial BIT, leaving the possibility of undetected failure after initial BIT. The test was rewritten to perform periodic background tests of the RAM.

**Table 2 LN-93 RLG INS  
DESIGN ENHANCEMENTS**

- Changed RAM Test From Initial BIT-Only to Periodic BIT
- Added Lower Limit to Reasonable Angular Rate Tests to Ensure Detection of Frozen Zero Rate Output
- Added Lower Limit to Reasonable Acceleration Tests to Ensure Detection of Frozen Zero Output
- Changed Smoothing of Barometric Altitude Steps to Reduce Vertical Velocity Transients

2. BIT Nos. 154-156 (Software Change) – Tests were to verify that a reasonable amount of angular change per unit time (angular rate) occurs in the three mutually-orthogonal RLG units. It was discovered that a failure could occur that would result in a zero angular rate always being output without detection because the tests had no lower limit on reasonable change, only an upper limit (425 degrees per second). Tests were changed to include a zero degree per second lower limit, which ensured detection of a failure that could bias values below that corresponding to zero rate.
3. BIT Nos. 210-212 (Software Change) – These tests and the problem were identical to the problem with tests 154-156, except they involved velocity change per unit time (acceleration) instead of angular rate. A lower limit of 0 g was added with the existing upper limit of 12.5 g.
4. Step Altitude Input (Software Change) – INS vertical velocity transient response to steps in barometric altitude inputs from the CADC (used in stabilizing the INS vertical

velocity loop) met SWIM tolerances, but an alternate technique was developed after the SWIM analysis. The alternate technique achieves better smoothing of barometric altitude input steps, which reduces vertical velocity transients while maintaining good stabilization.

## RLG INS ANALYSIS RESULTS

The RLG INS unit critical signal failure rates, TF mishap rates, and predicted F-16 mishap rates are compared in Table 3 to comparable rates based on the predecessor LN-39 mechanical-gyro INS. The LN-39 INS is used as the standard for determining acceptable safety level and to determine if additional SWIM features need to be incorporated into the F-16 TF system, since TF safety with the LN-39 installed has already been judged acceptable by the USAF. Rates are presented as percent changes relative to the LN-39 rates.

As presented in Table 3, both the H-423 and the LN-93 RLG INS units have significantly lower critical signal failure rates and slightly lower TF mishap rates than the LN-39 mechanical-gyro INS and result in equivalent predicted F-16 system mishap rates. The predicted F-16 mishap rate change is negligible in spite of the improvement in RLG INS critical failure rate because of dominance by other low-altitude, high-speed effects (engine losses and bird strikes). As a result of the equivalent predicted F-16 mishap rate, no additional SWIM features need to be added for RLG INS compatibility with F-16 TF and its existing complement of SWIM features.

## DUAL USE

Since the RLG INS can be used for other military applications and other civilian applications, the improved critical failure rate of the RLG INS units, resulting from the F-16 TF/RLG INS SWIM compatibility analysis, is beneficial for

**Table 3 FAILURE RATES  
AND MISHAP RATES**

INS Subsystem	Change in INS Critical Failure Rate	Change in TF Mishap Rate	Change in Predicted F-16 Mishap Rate
LN-39 (Baseline)	0	0	0
H-423	76% Decrease	1% Decrease	Negligible
LN-93	68% Decrease	1% Decrease	Negligible

those other uses. In addition, application of the SWIM process to other systems using an RLG INS should be considered to maximize operational safety. Other dual-use applications that can benefit from the resultant RLG INS failure rate improvement (or conceivably, from a total system SWIM analysis) are found in both military and civilian examples.

### Military Dual-Use Applications

As stated in the background section of this paper, AMAS was the first application of SWIM, but that application used a gimbaled, mechanical-gyro INS as did F-16/LANTIRN TF. Consequently, the SWIM analysis portion of this paper, which shows the RLG INS to be safer than the previous mechanical-gyro INS for TF, is also applicable to AMAS. This is because the critical signals for command and control in AMAS are essentially the same as for TF, with some additional parameters related to weapon delivery that don't affect mishap probability beyond the parameters associated with TF.

Similarly to AMAS, integrated fire flight control (IFFC), ground collision avoidance system (GCAS), G-induced loss of consciousness (GLOC) recovery system, and applications of digital terrain system (DTS) involve controlled flight or controlled-flight recovery functions, which have a potential for high mishap rates, especially in the low-altitude flight regime. These functions, which were also based on a mechanical-gyro INS implementation, will also be recipients of the RLG INS

with its SWIM analysis safety validation for TF. These functions, will obviously benefit from an RLG INS with improved confidence in TF critical malfunction coverage. Unlike AMAS, however, these functions were never subjected to a SWIM analysis so that a safety improvement in one piece of the function architecture (the INS) cannot be inserted with the assumption that the overall function mishap rate is acceptable. Therefore, any flight-critical function should be subjected to a SWIM analysis for two reasons: (1) to validate an acceptable mishap rate or recommend changes to achieve such, and (2) because of the invariably discovered enhancements to the function design that increase safety via minimal cost software BIT changes. Figure 10 summarizes some of the other military applications benefitting from the RLG INS SWIM analysis. These applications could also benefit from a separate SWIM analysis.

### Civilian Dual-Use Applications

Civilian RLG INS applications in the area of navigation, including instrument landing system (ILS), air traffic control (ATC), and autopilot control (APC), also will benefit from use of the SWIM-analysis-improved RLG INS. These functions rely on accurate aircraft location and aircraft state, as provided by the RLG INS.

A promising, new commercial area for application of the SWIM-improved RLG INS and for the SWIM process itself is terrain referenced navigation (TRN) using a DTS database. Previous commercial airliners did not have an appropriate

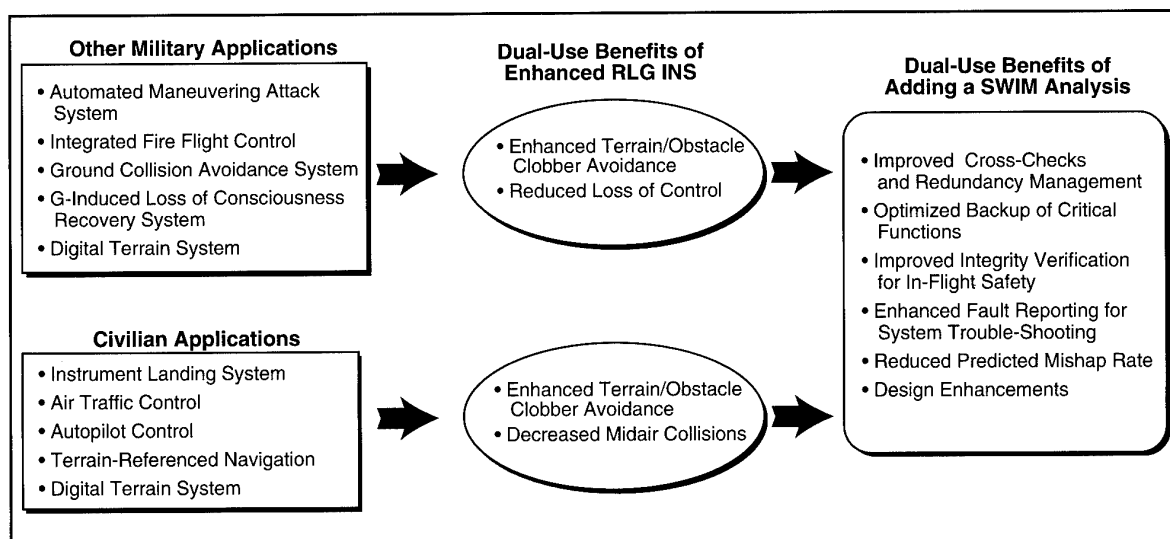


Figure 10 Dual-Use Applications Benefitting from RLG INS SWIM Analysis

SWIM monitor host site, such as a DFLCS. However, the DFLCS is being introduced into the commercial airliner world via aircraft, such as the Boeing 767, the Boeing 777, and other new airliners. With this DFLCS advent, a redundant, fault-tolerant network site is now available for critical failure detection for functions such as TRN. TRN requires the integration of the RLG INS with the DTS and other sensor inputs, such as a radar altimeter. Errors and misregistrations of the DTS database can be eliminated via verification and modification of the local database for specific commercial airport locations. The airliner crew can then be presented with a highly accurate display (in all weather) of terrain, obstacles, and runways in the airport vicinity.

Also, many current airliner architectures use multiple INS units without cross-check comparisons, relying entirely on each INS to test itself via internal BIT. In this architecture, if an INS declares itself failed, it is deactivated and another INS is used in a serial, backup role. However, with the DFLCS, parallel INS output comparisons can be made so that virtually all critical failures are detected. This increased assurance of covering critical failures enables automatic coupling of local airport area, customized, DTS-based TRN to enable safe, all-weather navigation and landings.

To achieve this enhanced TRN capability in commercial airliner applications would require a SWIM analysis of the TRN function, including all its components and would include specific architecture recommendations for RLG INS cross-check monitoring and additional SWIM features or monitors to be incorporated into the DFLCS OFP. These civilian applications, including TRN, are summarized in Figure 10.

## CONCLUSION

Both the H-423 and LN-93 RLG INS units are compatible with F-16 TF from a safety standpoint, based on lower INS critical failure rates, TF mishap rates, and equivalent predicted F-16 mishap rate to the predecessor gimbaled, mechanical-gyro LN-39 INS. In addition, design enhancements resulting from the SWIM analysis benefited the RLG INS units via an improvement in INS safety with minimal mechanization impact.

Other dual-use military and civilian applications of the RLG INS reap the benefits of improved

safety confidence from the SWIM analysis of the RLG INS and also inherit lower failure rate units as a result of the discovered design enhancements. Consideration of applying the SWIM process to other dual-use systems is recommended to maximize operational safety of those systems.

## REFERENCES

1. Blaylock, Swihart, Urschel, Integration of Advanced Safety Enhancements for F-16 Terrain Following, NATO-AGARD Conference Proceedings No. 439, November 1988.
2. Blaylock, Swihart, Urschel, Hicks, Validation of Advanced Safety Enhancements for F-16 Terrain Following, Proceedings of the 17th Congress of the International Council of the Aeronautical Sciences, September 1990.
3. Post, E.J., Sagnac Effect, Review of Modern Physics, Vol. 39, No. 2, April 1967.
4. Mark, J., et al, A Rate Integrating Fiber Optic Gyro, Journal of the Institute of Navigation, Vol. 38, No. 4, Winter 1991-92.



## SEA WAVE PARAMETERS, SMALL ALTITUDES AND DISTANCES MEASUREMENTS DESIGN FOR MOVEMENT CONTROL SYSTEMS OF SHIPS, WING-IN-SURFACE EFFECT CRAFTS AND SEAPLANES

A.V. Nebylov  
A.P. Vanayev  
V.V. Chernyavets

State Academy of Aerospace Instrumentation  
67 Bolshaya Morskaya  
St. Petersburg 190000, Russia

### SUMMARY

Advanced methods and means of controlled sea vehicle moving parameters and sea-way ones measurement are considered. Both directly measuring tasks and possibilities of control quality increasing of displacement and undispacement ships and sea flying vehicles under conditions of active wave disturbances are analysed. Design principles, some structural features and expected quality characteristics of device, being developed, for meter altitudes and distances measuring based on special phase radioaltimeter and inertial sensor integration are observed. When functioning in the sea-waves profile tracking mode, high measuring accuracy of sea-way and vehicle vertical moving parameters is provided. The mounting of several devices both on the left and on the right sides of vehicle allows to reconstruct the field of sea wave disturbances and to check roll and pitch parameters and draught or clearance as well. The conditions to be fulfilled for determining the main sea wave spread direction are investigated.

### INTRODUCTION

Sea-way is the most essential disturbance factor for all majority of ships and undispacement sea vehicles (hydrofoil, hovercraft, wing-in-ground effect crafts, seaplanes and sea helicopters during take-off and alighting) as controlled plants. Its influence effects undesirable oscillating movements appearance which make worse functional effectivity, safety and comfortability of such vehicles usage comparing to the case of calm sea. Perfection of methods and control means of sea vehicles under sea-way can be considered as one of the introduction of fuel saving technologies in transport aspects.

When calculating rolling, pitching and vertical tossing of ship and disturbed moving of other sea vehicles, disturbed sea surface with variable heights, slopes and orbital speeds is considered as unisotrope casual field, forming input casual process for some dynamic unit - controlled plant model. At the output of this unit corresponding reaction is observed, which can be calculated precisely enough using whole description of current values of wave field. However, knowledge of current value of even separate element of this field, for instance, of height value of wave surface

point near ship board, especially of several such elements allows to get probabilistic estimate of whole disturbance influence in view of determined space correlation of wave surface. This estimate can be accurate in utmost case of two dimensional regular sea-way, when all disturbance forces and heeling moments change their values synchronously with wave surface height oscillations in point of measurement but with another phase. Three dimensional being and irregularity of real windy sea-way complicate in some degree obtaining the estimate and decrease its accuracy. Due to this fact it is undoubtedly that control quality of transport vehicle moving on sea surface or near it can be increased when there are sensor units of sea wave current profile measuring on the board [1].

There are at least two variants of this information using for movement control quality increasing. They correspond to wave profile information processing channels, marked with 1 and 2 on generalized block-diagram of control system, shown on Fig. 1. In first variant, information about disturbances allows to realise principle of combined control by error and disturbing excitation. It is well known and theoretically proved but in navigation automation devices of current generation and sea transport vehicles autopilot practically is not used.

When introducing component, being determined by disturbance directly, in control law there appears some theoretical possibility to obtain invariance (undisturbability) of movement, that is impossible in principle when using control law by error. Even not reaching whole invariance because of insufficient effectivity of rudders or necessity of their resource economy, channel of control by disturbance would essentially widen control system optimization possibilities according to selected quality criterion. Practically significant quality criterions, for instance, maximal fuel economy, do not require usually whole invariance, but nevertheless make to appreciate in high degree the possibility of disturbance current information using in control law.

In second variant, on the base of wave profile current measurements, such their integral characteristics as overage values of altitude and period, course angle of wave spread main direction and others can be determined. Depending on these

characteristics it is expediently to readjust parameters of error-control main loop, i.e. to adapt control loop to sea-way characteristics.

Both mentioned variants of wave profile measurers using can be realized both due to modernization of serial autopilots and other movement control systems by means of connecting additional unit to standard contacts of this equipment, and due to developing perspective information-control complexes of next generation. Problem scales allow to estimate the need in wave profile board measurers only in Russia about 5-10 thousands of complete sets. Among potential users of equipment are shipowners, producers of displacement and undisplacement ships, WIG crafts, seaplanes and scientific-research and project organizations, producing transport vehicles trials in sea conditions.

## PREFACE OF PROJECT

There is great number of publications by problem of sea waves parameter measuring automation, majority of them is devoted to research of methods and measuring devices of sea-way integral characteristics. Distribution laws, one- and two-dimensional power spectrum, sea-way space spectrum, characteristics of sea surface reflection of electromagnetic radiation are determined under averaging over large squares and time intervals. Such measurements are most effective either when equipment is installed in aviation or space vehicles or when observing of sea surface is produced by ship radiolocator under small angles [2]. In fact all they assume not every wave profile tracking, but sea-way integral characteristics estimation according to indirect signs. Scarcely smaller group of papers is devoted to wave-sensors of contact type being installed on fixed base or produced as buoys. At last, there is some construction experience of unique ocean

research equipment for special scientific-research ships, where contact, buoy or other meters are adapted for operating under conditions of drifting ship.

All these investigations can not serve for creation of sea waves parameters measuring equipment suitable for systems of sea transport vehicle movement control. On the other hand there is another engineering field, advances in which are very useful for solving of this problem. This equipment measuring small altitude movement above sea surface is necessary for control systems of hovercraft, hydrofoil and especially WIG craft.

Last of the mentioned vehicles requires the most perfect system measuring movement parameters in vertical plane with high accuracy and inertionless, such system can be constructed only on the base of position and inertial meters integration. All of radar meters will measure not absolute, but comparative altitude, which is calculated as difference between current board altitude and wave profile altitude. To separate these two components of comparative altitude the additional information about vehicle vertical equipment is necessary, this information can be obtained from accelerometer with vertical axis of sensitivity [1,3].

So the problem of small altitude measurement of movement above rough sea surface is dual to one of sea waves profile measuring and both these problems can be solved only in one integrating measuring system. Similar measuring principle is realized on well-known today first Russian WIG crafts as "Orlenok" and "Lun" in board equipment developed in 60-70th. Its restricted functional facilities and obsolete elemental base caused necessity of creation measurers and second-generation control equipment for perspective WIG crafts, the last stimulated beginning of works being described in

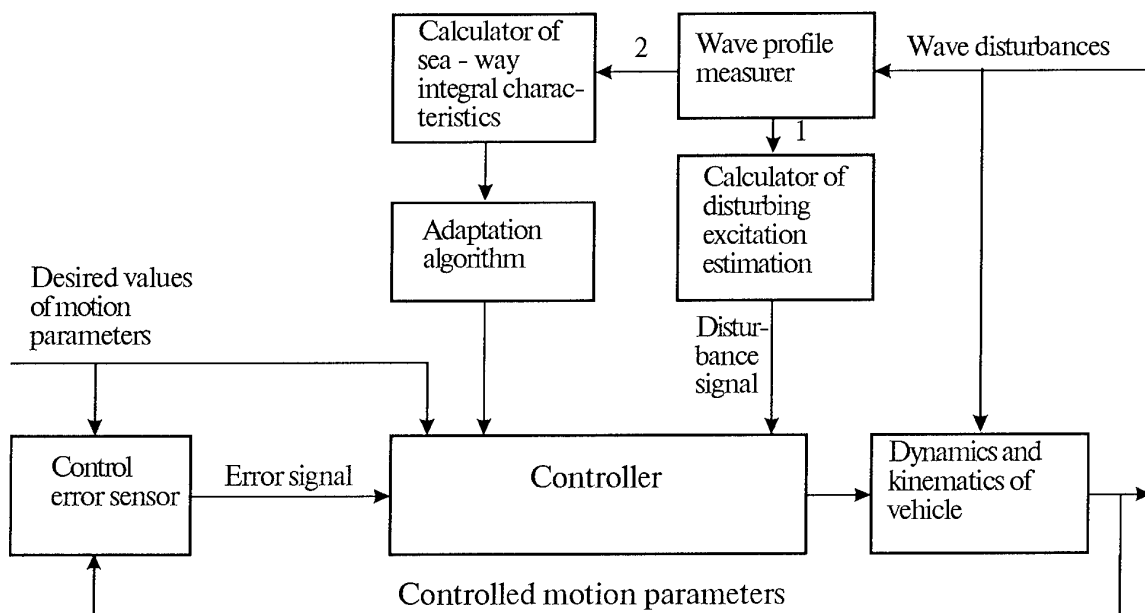


Fig.1. Block-diagram of motion control system using waves profile measurer.

this publication. Because of conversion these works acquired wider statement. Furthermore problem of sea waves measuring has been advanced in foreground but not the problem of movement altitude measurement, by this reason the number of potential customers was arisen. Designers received official support of several leading aviation and shipbuilding Russian firms, which proclaimed about interest in project.

### EQUIPMENT BEING DEVELOPED COMPOSITION

The described measurement complex structure is determined from wide functional possibilities guaranteeing necessity of its controlled naval different classes objects both floating and flying. The sphere of problems being accessible for solving is defined by the following basic functions: absolute altitude measurement related on sea surface undisturbed level, geometrical altitude measurement, i.e. instrument setting point elevation above disturbed sea surface, and following for wave profile as a difference of absolute and geometrical altitudes. The apparatus rocking mustn't prevent to specified parameters measurement high accuracy achievement substantially. The additional function, the existence of which is desirable is to determine the sea waves running direction. It can require the information not only about values but about waves disturbances speeds as well. The possibilities for accomplishing the functional transformations of altitudes and velocities estimations are to comply with angle and linear movement standard control algorithms and sea-way integral characteristic calculation statistic analyse algorithms either.

In construction the equipment is the two types unified modules collection. The first one is universal measurement module (UMM); the second one is integration block.

UMM is the digital output primary measuring converter. It operates as measurement basic function of object certain point altitude and wave altitude under that point and, if possible, wave speed. The number of UMM set on a one transport apparatus can be one, two and more, depending on measuring parameters composition, quality measurement requirements and size of apparatus. To decrease apparatus rocking influence on UMM working there are a compensation of corresponding errors in output signals of this block and some measures of its angle stabilization. As the easiest manner of coarse angle stabilization on a boat there can be considered a setting of UMM on a special arm with pendulum type suspension and angle oscillations damping. With the mooring automatization problem being solved, in boat using variants it is useful to provide rotation for the UMM sensitivity axis from vertical to horizontal position. Another variant of UMM horizontal applying is head-on-collision avoid car system.

The tie-in module is the specified digital computer which goal is to transform the information arriving from one or several UMM into form suitable to use in transport apparatus movement control system. By the way, this block can accomplish a weighted UMM signals summing, their dynamic correction (for instance, required phase shift), statistic averaging and other computing functions. The block has the standard interface, but if it's necessary to connect it to analog autopilots made years ago, there is possible to form analog

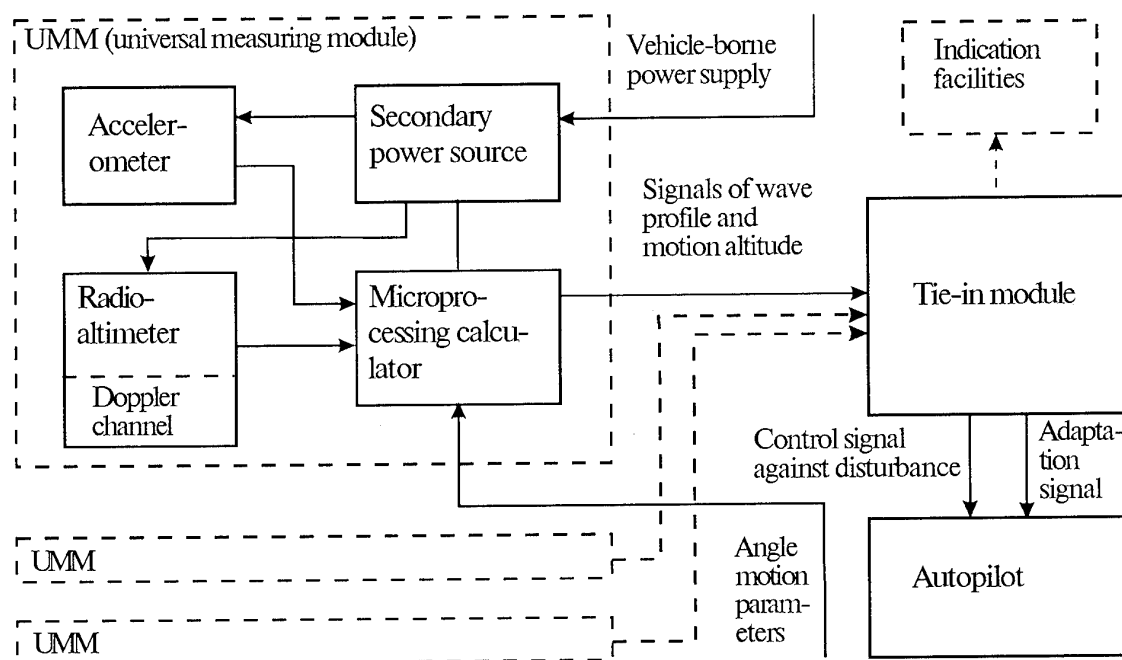


Fig.2. Block - diagram of information control complex elements interaction.

outputs. With the help of special electronic indication means if it's necessary the measured values change may be checked.

The measuring complex block-diagram is shown on Fig. 2, where the composition of UMM involving radioaltimeter, accelerometer, microprocessor block executing two directed sensors integration algorithms and secondary power source. In main variant of the device two component accelerometer is used. One of its sensitivity axis is vertical, the other one is oriented in lateral direction in order to check rocking parameters. The angle UMM movement information can be taken from other means being on the board.

## PHASE RADIOALTIMETER

For measuring sea surface altitude and profile it is supposed to apply without-contact measurer, as most suitable for broad class of ships and low-flying vehicles. In principle it is possible to use the devices of following types for it: - radioaltimeter, laser altimeter, ultrasonic and radioisotopic altimeters. Among these types of altimeters radioaltimeter is the most suitable, as measurer on different sea vehicles, not having their basic shortcomings, as following:

- laser altimeter in some degree by accuracy depends on rain, spray, mist and so on, because their particles have great back dispersion;
- ultrasonic altimeter also by accuracy depends on substance parameters, but its basic shortcoming as wide-purpose device is interference influence of engine noise and other apparatus parts; this interference for different types of devices has different spectral characteristics;
- radioisotope altimeter is unsafe for people device, and its accuracy in great degree depends on type of dispersion surface, besides it has low time stability of measurements.

In radioaltimeter parameter value depends on signal delay and is subsequently proportional to altitude being measured. Depending on modulation type radiated signal and parameter being measured radioaltimeters are divided into impulse ones, ones with frequency modulated signal and phase ones [4].

Impulse radioaltimeter is applied for distance measuring from several hundreds of meters and more, sometimes for distances measuring about several dozens of meters.

Radioaltimeters with frequency modulation of radiated signal are applied generally on altitudes from several dozens of meters to several hundreds of meters. In theirs measured parameter is frequency difference of radiated and received signals, caused by shift in time of frequency modulation function. For providing required accuracy when broadening measured altitudes range, serious difficulties in providing necessary value of radiated frequency variation by its modulation appear.

So for providing measurement mistake about several centimetre deviation (maximum changing) of radiating frequency is required to be equal several hundreds of MHz.

Phase radioaltimeter is the most suitable for small altitude measuring from portions of meter to several dozens of meters. Here the phase difference of radi-

ated signal frequency components is a measured parameter. For decreasing of measured frequency range, frequency difference of these components is chosen smaller. Because of it accuracy of phase radiometer in small altitudes is high in principle and depends on mistake of received signals phase measuring, which is about  $0.1^\circ - 0.2^\circ$  and mistake, caused by integral character of reflected signal formed from dispersion surface.

Two basic schemes of phase radioaltimeters are known: with phase difference measuring on Doppler shift frequency (here the beam is radiated as inclined); with measuring of phase difference on underbringing frequency (here the beam is radiated in vertical direction).

First of them is expediently to apply for combined measuring system of speed and altitude, when information of Doppler frequency is required, as in case of determining the waves direction.

Second scheme is expediently to apply when it is required to know only altitudes in all sea situation, also and steel, because vertical radiation has advantage comparing to the inclined one, that from sea surface in steel the reflected signal can be absent.

In phase radioaltimeters (Fig.3) extra high frequency signals of two neighbouring frequencies are radiated, after reflection signals are received:

$$u_1 = U \cos [(\omega_1 + \omega_D)t - k_1 h - \theta_0] = U \cos \theta_1,$$

$$u_2 = U \cos [(\omega_2 + \omega_D)t - k_2 h - \theta_0] = U \cos \theta_2,$$

where  $\omega_1, \omega_2$  - radiated frequencies,  $\omega_D$  - Doppler frequency,  $h$  - measured altitude,  $\theta_0$  - original phase,  $k_1 = 2\pi/\lambda_1$  и  $k_2 = 2\pi/\lambda_2$  - wave figures.

Phase difference  $\Delta\theta = \theta_1 - \theta_2 = (k_1 - k_2)h$  is measured either on Doppler  $\omega_D$  by inclined radiation or on intermediate frequency  $\omega_{IN}$  by vertical radiation.

Radiation frequencies for radioaltimeter are selected in range of three centimetres, that in contrast to millimetre range provides practical independence of measurements on spray, hydrometeors etc. Some increasing of receiver-transmitter dimensions comparing to millimetre range is not essential because of using extra high frequency track and antennas produced according to hybrid-strip-line technology.

Radioaltimeter mistake is several centimetre in broad range of sea surface states. Except of measurement method it is provided also by appropriate selection of wideness of beam of radiation about  $20^\circ$ .

The weight is about 4 kg.

## INTEGRATION ALGORITHM

Integration of radioaltimeter and accelerometer with vertical sensitivity axis is the only possible way of rather accurate estimation of radioaltimeter mounting point absolute height over the sea surface that is necessary for sea waves profile monitoring. General integration principles are well known and recommend to suppress in every sensor output signal such spectral components which are more corrupted by measurement noise than in other sensor output signal (or in other sensors, if there



synthesis may be easily fulfilled within correlation theory by optimal two-dimensional linear filtration technique. However it should be taken into account that meeting requirements of practice modern stage of linear filtration theory development is characterized by a great variety of excitations properties setting forms and analytical and numerical synthesis methods [5 – 7].

There is a tendency of excitation models roughing for increasing their authenticity, unparametric excitation classes are set when few prior information is available. For instance, it is possible to extract some field in excitations spectral densities functional space by setting upper and lower borders as known frequency functions (band model) or by limiting some excitation derivatives variances being spectral power density moments. For investigation of max errors values some excitations characteristics that are not statistical are useful, such as derivatives, finite differences and upper spectral frequency max values.

We would like to note that max error value characterizes quality of, for instance, flying close to the surface transport vehicle height measurement better than root-mean-square error value because inadmissible big departures of this coordinate from nominal value lead to the crash situation. Unfortunately, general using of Winer's and Kalman's synthesis techniques with correspondent excitation spectral-correlative description (which was not always true) resulted in ousting max error as accuracy criterium by root-mean-square one. However, when distribution law differs from the gaussian or is unknown it is necessary to check up the max error of at least part of excitations applied to the system and it cannot be strictly connected with the r.-m.-s. one. Regarding to the task in question it is sure that only sea waves ordinates and radioaltimeter error distribution lows are gaussian. Accelerometer error and object vertical movements do not submit to the gaussian low, these causal processes being not normalized either when passing through measuring system channels because corresponding channels have no narrow bandwidth. Resultant measurement errors  $e_h$  and  $e_k$  represent the sum of additive components each of which is connected with one of the excitations applied to the system, these excitation being either useful or interference. At least two of these components caused by accelerometer error and condition (2) inaccurate fulfilment cannot be gaussian. That's why  $3\sigma$  or  $5\sigma$  rules cannot be used for their max values checking – more detailed analysis with the use of special techniques is required. Resultant errors r.-m.-s. values also should be taken into consideration and be used together with those max values for measurements quality measure forming and system optimization. Investigation techniques developed for these purposes are described in detail in [5]. Investigation of synthesis task solution setting different variants showed that measuring system optimal structure is relatively independent of its functioning conditions nuances on different transport vehicles, however, filters  $W_{1,2,3}(s)$  parameters should be optimized and adjusted in every concrete case. That's why on base of simple physical ideas we shall explain expediency of the following transfer functions use in the system:

$$W_1(s) = \frac{b_{21} + b_{31}s}{A(s)}, \quad (3)$$

$$W_2(s) = \frac{b_{02} + b_{12}s + b_{22}s^2}{A(s)}, \quad (4)$$

where  $A(s) = 1 + a_1s + a_2s^2 + a_3s^3$ ,

$$\{a_i\}_1^3, \{b_{j1}\}_2^3, \{b_{j2}\}_0^2 \in (0, \infty).$$

Because the presence of quasicontant zero frequency component in accelerometer error  $v_4(t)$  is the essential factor, for its suppression filter  $W_1(s)$  must have pole near the point  $s = 0$  that is possible when  $W_1(s)|_{s=0} = b_{31}s$  or least when

$$W_1(s)|_{s=0} = b_{21} + b_{31}s, \quad (5)$$

where  $b_{21}/b_{31} \ll 1s^{-1}$ .

On the other turn, in the field of vehicle vertical acceleration spectrum substantial values, i.e. on rather high frequencies, the condition

$H_1(s)|_{s \rightarrow \infty} \approx 1$  must be fulfilled, that with  $W_4(s) \approx s^2$  (transfer coefficients of both primary sensors are conditionally considered to be equal to 1) gives

$$W_1(s)|_{s \rightarrow \infty} \approx 1/s^2. \quad (6)$$

From (5) and (6) it is seen that transfer function  $W_1(s)$  denominator power must be higher than its numerator power at least on 2, i.e. filter min. order is 3. Expression (6) corresponds to the simplest transfer function meeting the described requirements if  $a_3 \approx b_{31}$ .

Measured height infralowfrequency components, suppressed in accelerometer channel must be restored by radioaltimeter indications, that requires fulfilment of condition  $W_2(s)|_{s=0} \approx 1$ , and need of radioaltimeter wideband error suppression gives the condition  $W_2(s)|_{s \rightarrow \infty} \approx 0$ . When  $b_{02} \approx 1$ , transfer function (4) meets these requirements rather well.

In principle, full equality of transfer functions (3) and (4) denominators is not obligatory if condition (2) is not strict, however, in any case their equality simplifies both continuous and digital realization of integration filters. Condition (2) approximate fulfilment requirement combines filters coefficients by additional relationships  $b_{12} \approx a_1$ ,  $b_{21} + b_{22} \approx a_2$ . We would like also to note that for accurate fulfilment of condition (2) some radioaltimeter lag, characterized by its time constant  $T_{R4}$ , should be taken into account in transfer function  $W_2(s)$ , that may be represented as

$$W_2(s) = \frac{(b_{02} + b_{12}s + b_{22}s^2)(1 + T_{R4}s)}{A(p)}, \quad (7)$$

where  $T_{R4} \approx T_{R4}$ . However, because  $T_{R4}$  value is small substitution of (4) to (7) will not practically influence altitude measurement dynamic error, but will increase the error caused by radioaltimeter wideband error. That's why it is expedient to use the expression (4).

Fig. 5 shows transfer functions (3) and (4) continuous realization variant. If transfer functions (3) and (4) coefficients values required are approximately estimated filter  $W_2(s)$  may be represented as dynamic system with negative feedback coefficient equal to 1. In the open loop state transfer function of this system is

$$W_0(s) = \frac{K_3(1 + \tau_1 s + \tau_2 s^2)}{s^2(s + p_1)}, \quad (8)$$

all parameters are expressed through the  $K_3$  coefficient by the relationships  $\tau_1 = 2/K_3^{1/3}$ ,  $\tau_2 = \tau_1/\sqrt{2}$ ,  $p_1 = K_3^{1/3}/\rho$ , where coefficient  $\rho$  values of which should be chosen from the range  $10 - 10^3$  depending on the number of digits of digital calculator and on some other factors. Integrating filters amplitude plots corresponding to (3) and (4) are shown on Fig. 6. If to use the formula

$$W_2(s) = W_0(s) / [1 + W_0(s)], \quad (9)$$

$$W_1(s) = [1 - W_2(s)] / W_4(s) = [1 + W_0(s)]^{-1} s^{-2}$$

transfer functions (3) and (4) parameters may be also expressed through the  $K_3$  coefficient:

$$\begin{aligned} a_1 &= 2 / K_3^{1/3}, \quad a_2 = 2.02 / K_3^{2/3}, \quad a_3 = 1 / K_3, \\ b_{21} &= K_3^{-2/3} / \rho, \quad b_{31} = 1 / K_3, \quad b_{02} = 1, \\ b_{12} &= 2 / K_3^{1/3}, \quad b_{22} = 2 / K_3^{2/3}. \end{aligned} \quad (10)$$

In its turn, when estimating  $K_3$  coefficient acceptable value it may be taken into consideration that it depends on filter  $W_2(s)$  equivalent bandwidth, that may be controlled and that may be expressed by the formula (using (7) and (10)):

$$\begin{aligned} \Delta f &= \frac{1}{2\pi} \int_{-\infty}^{\infty} |W_2(j\omega)|^2 d\omega = \\ &= \frac{K_3 \tau_1 \tau_2^4 + \tau_1^2 - \tau_2^2 + p_1 / K_3}{2[(\tau_2^2 + p_1 / K_3) \tau_1 - K_3^{-1}]} \equiv 1.65 K_3^{-1/3}. \end{aligned} \quad (11)$$

Coefficient 1.65 in (11) corresponds to the value  $\rho = 10^2$ , but practically doesn't change when  $\rho$  increases or decreases on order. Parameters values determined by (10) should be considered just as rough initial approximation to the synthesis task solution that must be made more accurate using special calculating procedures taking into account optimization criterion, all excitations concrete characteristics and integrating algorithms digital realization features. After filters  $W_1(s)$  and  $W_2(s)$  digital equivalents numerical parametric optimization and absolute height measurements potential accuracy determination, the synthesis task of the filter  $W_3(s)$  providing waves profile measurement highest quality may be solved. To find initial approximation to the solution the formula

$W_3(s) \approx W_2(s) + s^2 W_1(s) / W_{R4}(s)$  is useful, however, numerical investigation allows to get truer result.

### MEASUREMENT ACCURACY ANALYSIS

In order to get approximate idea of measurements accuracy achievable let's analyse integration system errors in most typical modes of transport vehicle movement.

Considering at first movement absolute height  $h$  measurement errors due to wave interference we would like to note that in case of two-dimensional regular sea-way of loop type for any vehicle speed there is a heading under which encounter frequency of meeting with the wave will be zero or small. It is impossible to suppress this wave interference in

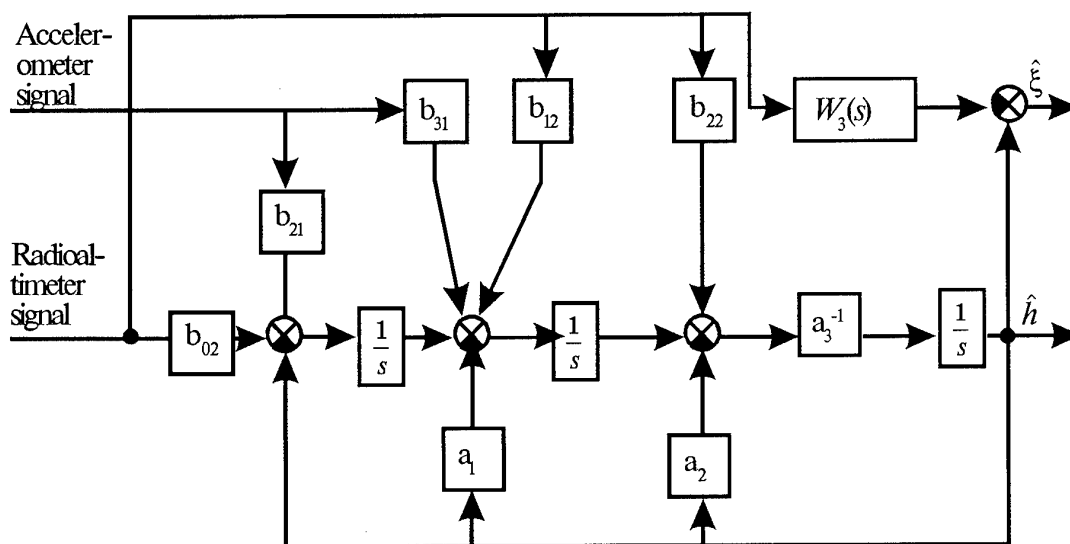


Fig. 5. The variant of integrating filter continuous prototype.

two components integration system that's why we will consider only situations that may be useful from the practical point of view when encounter frequency  $\Omega$  is rather high. Let's agree that in the coordinate system connected with the moving vehicle wave profile variation submits to the sine law  $\xi(t) = \xi_{\max} \sin(\Omega t + \varphi)$ . Then, corresponding measurement error amplitude is determined by  $e_{h\zeta_{\max}} = |W_2(j\omega)|_{\omega=\Omega} \xi_{\max}$ .

Using (4), (10) and (11) this formula may be substituted by approximate relationship

$e_{h\zeta_{\max}} \cong 1.21 \xi_{\max} \Delta f / \Omega$ , that is rather true under  $2\pi\Delta f \ll \Omega$ . Then, if the condition

$e_{h\zeta_{\max}} / \xi_{\max} \leq 0.025$ , is fulfilled, i.e. wave interference is suppressed up to the level 2.5%, we get the requirement to the equivalent bandwidth:

$$\Delta f \leq 0.02\Omega. \quad (12)$$

Frequency typical values for displacement ships may be 0.5–3 rad/s, for undisplacement ships, WIG-crafts and hydroplanes – 10 rad/s and more.

When analysing the influence of disturbances caused by three-dimensional irregular fully developed wind sea-way we use the formula, derived in

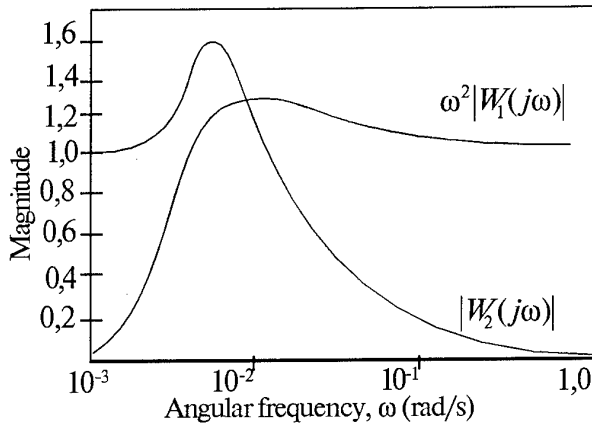


Fig.6. Amplitude plots of integrated measuring system channels.

[1], for wave ordinates spectral power level on zero frequency in moving coordinate system

$$S_{\xi}(0) = 0.383 h_{3\%}^3 V^{-1} \cos^2 \Psi, \quad (13)$$

where  $V$  is vehicle movement speed,  $\Psi$  - heading relatively to the wave spread main direction,  $h_{3\%}$  - provided sea waves height. The formula is true under  $V \geq 8.2 \sqrt{g h_{3\%}}$ , where  $g$  is free fall acceleration.

Using (13), the expression for correspondent measurement error r.-m.-s. value may be represented as

$$\sigma_{eh\zeta} = \sqrt{S_{\xi}(0) \Delta f} = 0.62 h_{3\%}^{3/2} \sqrt{\Delta f / V} \cos \Psi. \quad (14)$$

For instance, under  $h_{3\%} = 4\text{m}$  (incomplete sea-way of the force 6),  $\Psi = 45^\circ$ ,  $\Delta f = 0.01\text{Hz}$  and  $V = 150\text{ m/s}$  that is typical for big WIG-craft, formula (14) gives  $\sigma_{eh\zeta} = 0.031\text{m}$ .

It is clear that under  $\Delta f$  value decrease errors caused by wave interference decrease in any case, but accelerometer errors increase. Accelerometer scale quasiconstant zero shift caused by not ideal adjustment and inaccurate compensation of free fall acceleration has the most authentic numerical values among accelerometer error components.

We represent the value of this shift as  $\ddot{v}_{adr} = \varepsilon g$ , where  $g = 9.81\text{ m/s}^2$  and relative perfection level  $\varepsilon = 10^{-5} - 10^{-3}$ . Mentioned accelerometer error will lead to the error expressed by the formula (using (10) and (11)):

$$e_{hdr} = b_{21} \varepsilon g = 1.65^2 \varepsilon g / (\rho \Delta f^2).$$

Now, setting the acceptable value of this error  $e_h^0$ , we get one more requirement (additional to (12)) to the equivalent bandwidth

$$\Delta f \geq 1.65 \sqrt{\varepsilon g / (\rho e_h^0)}. \quad (15)$$

Fig.7 shows the plot of the opposite requirements (15) and (12). (15) right part values under  $e_h^0 = 0.05\text{ m}$  and different values  $\rho$  are shown as a function of accelerometer normalized error  $\varepsilon$  (lower horizontal scale) by dash lines, that represents lower limit of acceptable values  $\Delta f$ . Continuous line shows upper limit, corresponding to the inequality (12) right part depending on the values of typical frequency of meeting with the wave  $\Omega$  (upper horizontal scale). Upper and lower scales doesn't depend on each other and their position on the figure is determined only by the expediency to show most typical samples of  $\varepsilon$  and  $\Omega$  in the central part of the figure.

Fig.7 shows that in order to get acceptable measurements point on the ship board under encounter frequency of meeting with the wave  $\Omega$  of about 1 rad/s radioaltimeter channel equivalent bandwidth  $\Delta f$  should be about  $10^{-2}\text{ Hz}$ , and quasiconstant accelerometer error should not exceed  $10^{-4}\text{ g}$  level under  $\rho = 500 - 1000$ . It should be noted that these high values of coefficient  $\rho$  determining pole  $p$  value in transfer function (8) complicate integration algorithms digital realization because they require high accuracy of digital filters coefficients setting, i.e. it is necessary to use microprocessor computer with a great number of binary digits. For high speed transport vehicles values  $\Omega$  of about 10 rad/s are more typical, that allows to widen bandwidth  $\Delta f$  and either to use less perfect accelerometers with  $10^{-3}\text{ g}$  error or to decrease  $\rho$  values on 1 order.

Besides, error caused by quasiconstant accelerometer error it is possible to check other three its components.

Interference signal value slow variation at the accelerometer output with max speed  $\ddot{v}_{A\max}$  will give measurement error component in established mode:

$$e_{hdr1} = b_{31} \ddot{v}_{A\max} = \ddot{v}_{A\max} / K_3 = 1.65^3 \ddot{v}_{A\max} / \Delta f^3. \quad (16)$$

If to require to limit  $e_{hdr1}$  error by the 0.05m value, it is necessary to require in accordance with (16) under  $\Delta f = 10^{-2}\text{ Hz}$  to fulfil the condition  $\ddot{v}_{A\max} \leq e_{hdr1} \Delta f^3 / 1.65^3 = 0.05 \cdot 10^{-6} / 1.65^3 = 1.1 \cdot 10^{-8}\text{ m/s}^2$ ,



which is not too hard to be fulfilled.

Accelerometer scale coefficient instability of about  $10^{-4}$  even when movement height varies within 10m may lead only to the negligible measurement error component of about  $10^{-3}$  m.

Small uncontrolled inclinements of accelerometer sensitivity axis from the vertical line under vehicle tossing that cannot be algorithmically compensated result in measurement error due to accelerometer mounting point horizontal accelerations influence and free fall acceleration inaccurate compensation. Last component is more important and when inclinement angle varies by the sine low  $\gamma(t) = \gamma_{\max} \sin \Omega t$ , where  $\gamma_{\max}$  - uncontrolled inclinements amplitude, may be expressed by the formula

$$v_{Ay} = g(1 - \cos \gamma) = 2g \sin^2 \frac{\gamma}{2} \approx \frac{g}{2} (\gamma_{\max} \sin \Omega t)^2.$$

Error  $v_{Ay}(t)$  may be represented as sum of constant component and harmonic component with double tossing frequency which is not able to cause significant height measurement error.

Constant component is found by function  $v_{Ay}(t)$  values averaging for the half of tossing period:

$$\begin{aligned} \bar{v}_{Ay} &= \frac{\Omega}{\pi} \int_0^{\pi/\Omega} v_{Ay}(t) dt = \\ &= \frac{g}{2} \gamma_{\max}^2 \frac{\Omega}{\pi} \int_0^{\pi/\Omega} \sin^2 \Omega t dt = g \left( \frac{\gamma_{\max}}{2} \right)^2. \end{aligned} \quad (17)$$

As it was mentioned above in order to get rather small measurement error accelerometer error must meet the condition  $\bar{v}_{Ay} \leq 10^{-4} g$ . Then, using (17) we get the requirement  $\gamma_{\max} \leq 2 \cdot 10^{-2} \text{ rad} = 1.15^\circ$ . So, accelerometer sensitivity axis angular position control accuracy must be about  $1^\circ$ .

## DIGITAL REALIZATION

Filters  $W_{1,2,3}(s)$  shown on the integrated measuring system block-diagram are digitally realized that provides stability of their dynamic properties and possibility of parameters adaptation or program readjustment in different movement modes. Recursive digital filters of the third order are used with discrete transfer functions

$$D_1(z) = \sum_{i=0}^3 \beta_{i1} z^i / A_D(z), \quad D_2(z) = \sum_{i=0}^3 \beta_{i2} z^i / A_D(z),$$

the denominators of which are the same

$$A_D(z) = \sum_{j=0}^2 \alpha_j z^j + z^3. \text{ These filters coefficients}$$

are at first calculated on the base of correspondent continuous filters-prototypes  $W_1(s)$  and  $W_2(s)$  parameters and then are corrected during optimization taking into account features of microprocessor realization [1].

Discreteness period required of about  $10^{-1}$  s is determined first of all by the necessity of sea waves profile small features high accuracy reproduction

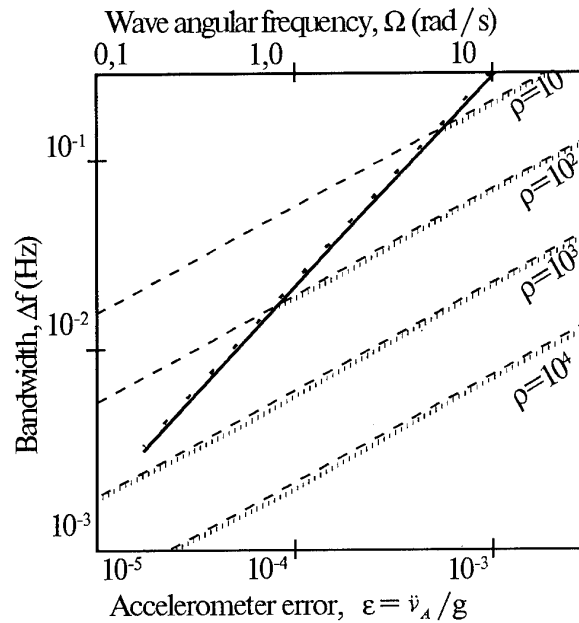


Fig. 7. Requirements to system bandwidth depending on wave frequency and accelerometer error.

especially under high speed of vehicle movement and allows to form measuring channels frequency characteristics desired up to frequencies of about 20 rad/s. Specificity of the system in question consists in the necessity of frequency characteristics form strict control not only for filters  $D_{1,2,3}(z)$  but also for hypothetical filter  $1 - D_1(z) - D_2(z)$ , that determines dynamic measurement error. Its properties are in fact determined by measuring channels desired frequency characteristics forming errors that must be negligible in the field of important frequencies of all the excitations applied to the system.

We would like to pay your attention to the necessity of frequency characteristics desired passing not only on frequencies close to the upper frequencies in the excitations spectrums but also on very low frequencies. Filter  $H_2(z)$  bandwidth of about  $10^{-2}$  Hz determines its weight function duration of about  $10^3$  s that is on 4 orders greater than discreteness period. Under this conditions desired dynamic properties forming high accuracy is possible only if digital filters coefficients required are adjusted very accurately, i.e. if multidigital microprocessor computer is used. Investigations and simulations showed that under big values of coefficient  $\beta$  computer must have 32 binary digits or more.

Accelerometer and radioaltimeter indications input into the computer must be performed through the ADC so that least-significant digit would correspond to not greater than  $10^{-4}$  m/s and  $10^{-2}$  m. Then quantization noise in ADC will not result in the noticeable measurements errors increase. Hence, under movement height variation range 100 m and possible accelerations within  $\pm 10$  m/s<sup>2</sup> range 14-digital ADC is required in accelerometer channel and 11-digital ADC in the altimeter channel.

## WAVE SPREAD DIRECTION DETERMINATION ALGORITHM

Waves moving direction knowledge is important factor to increase vehicle handling safety. It becomes especially substantial when WIG planes and seaplanes landing takes place. Besides, account of this parameter with the other sea-way characteristics allows us to save fuel, to select ship engine load optimally and to plan movement route.

Waves spread direction determination problem being complicated itself becomes more and more difficult when there is no prior information about this parameter and when it's necessary to determine it in all (from 0 to 360°) possible angles range. In the equipment in question several radioaltimeters mounted on the vehicle board and separated on some distance are supposed to be used for direction determination.

With vehicle moving, each altimeter takes down the wave surface profile. The closer altimeters are mounted to each other and the more sea-way looks like two-dimensional, the more similar profile describing functions are. Selecting the distance value between altimeters (not more than 10-20 m) one can achieve the profile form considerable similarity not only for two-dimensional sea-way but for three-dimensional one as well. In this case by corresponding processing of two functions, describing profiles, one can determine the time shift of one profile relatively to other, i.e. parameter proportional to vehicle and wave meeting angle value.

Generally, each signal in phase altimeter phase measurement channel looks like:

$$u = U \cos\{\omega_{BN} + \omega_B(t)t - \theta(h)\},$$

where  $\omega_{BN}$  — intermediate frequency which is equal to (10–15)  $10^3$  rad/s for phase radio altimeter;

$\omega_B(t)$  — received signal frequency shift due to sea surface speed vertical component;

$U, \theta(h)$  — amplitude and phase, depending on altitude  $h$ ;

$t$  — time.

The sea-way can be represented as a waves systems sum, in the easiest case as the sum of large scale  $\xi_g(\vec{r}, t)$  and small scale  $\xi_s(\vec{r}, t)$  two-dimensional sea-way components

$\xi(\vec{r}, t) = \xi_g(\vec{r}, t) + \xi_s(\vec{r}, t)$ , where  $\vec{r}$  — radius-vector.

Because of  $|\xi_s(\vec{r}, t)|^2 \ll |\xi_g(\vec{r}, t)|^2$  it is not considered when affecting vehicle and as the first approximation there'll be:

$$\xi(\vec{r}, t) = \frac{h_w}{2} \cos(\Omega_B t - \vec{k}_w \vec{r}),$$

where  $h_w, \Omega, \vec{k}_w$  — amplitude, frequency and wave vector of sea wave,

$k_w = 2\pi/\lambda_w$ , where  $\lambda_w$  — sea wave length.

For the easiest two altimeters case the meeting with wave angle measurement algorithm and, hence, the wave spread direction measurement algorithm can

be taken from the following relations (see also Fig.8):

$$\xi_1(\vec{r}_1, t) = \frac{h_w}{2} \cos(\Omega_B t - \vec{k}_w \vec{r}_1),$$

$$\omega_{B2}(t) = 2k v_{\max}^{orb} \sin(\Omega t - \vec{k}_w \vec{r}_2),$$

where  $k, v_{\max}^{orb}$  — wave number of SHF radiation and the maximal value (amplitude) of a sea waves orbital velocity in the same way

$$\psi_{12} = \overline{\xi_1(\vec{r}_1, t) \omega_{B2}(t)} = \frac{1}{2} k h_w v_{\max}^{orb} \sin\left(\frac{2\pi}{\lambda_w} L \sin\varphi\right),$$

$$\psi_{23} = \overline{\xi_2(\vec{r}_2, t) \omega_{B3}(t)} = \frac{1}{2} k h_w v_{\max}^{orb} \sin\left[\frac{2\pi}{\lambda_w} L \sin(\varphi + \varphi_0)\right],$$

$$\frac{\psi_{12}}{\psi_{23}} = \frac{\sin\left(\frac{2\pi}{\lambda_w} L \sin\varphi\right)}{\sin\left(\frac{2\pi}{\lambda_w} L \sin(\varphi + \varphi_0)\right)} \approx \frac{\sin\varphi}{\sin(\varphi + \varphi_0)}.$$

The last approximation is true under condition  $L \ll \lambda_w$ , and gives formula for calculation within the range from  $-90^\circ$  to  $+90^\circ$ . For range from  $-180^\circ$  to  $+180^\circ$  it's necessary to know whether wave directs to vehicle bow or stern.

Measuring of sea wave direction angle for all relationships of  $\lambda_w$  and  $L$  values is made by means of correlational processing of sea surface profiles, received from two radioaltimeters.

For two radioaltimeters (number 1 and 2 on Fig. 8) there is dependance:

$$\frac{\left(V \pm \frac{v_f}{\cos\varphi}\right)\tau}{L} = \operatorname{tg}\varphi,$$

where  $V$  — vehicle speed;

$v_f$  — wave phase speed;

$\tau$  — time shift of profiles in points 1 and 2.

In this formula  $v_f/\cos\varphi$  has positive sign, if wave directs to bow and negative if wave directs to stern.

This formula is transformed to the view:

$$\frac{V}{L} \cos\varphi \pm \frac{v_f \tau}{L} = \sin\varphi,$$

and from it, angle  $\varphi$  can be calculated; value  $v_f$  of phase speed in this formula is determined as function of waves height on the base of well-known empirical dependance.

Selection of concrete algorithm of value  $\varphi$  calculation is determined by different volumes of necessary operations and memory, which sharply increase for correlation processing under condition  $L \ll \lambda_w$ .

It is necessary to emphasize, that correlation processing algorithm requires at least two radioaltimeters, however, using of three radioaltimeters allows to get value of meeting angle for three pairs of measurers. By calculating the mean value of

these values (accounting their reduction to the horizontal plane of ship), accuracy and reliability of measurement are increased in addition. To calculate angle value within the range  $-180^\circ - +180^\circ$  it's necessary to determine, as it was already mentioned, whether sea wave has direction to bow, or stern of ship. For this aim two extra high frequency channels for determining of Doppler frequency and distance with the aid of two inclined rays, laying in different vertical planes, angle between planes being  $90^\circ$ , are introduced. Wave movement direction is determined for each ray, this direction being determined relatively to vertical plane and this plane being perpendicular to that vertical plane, where ray is lay. Orbital movement of water particles results in Doppler modulation of received signal frequency by law

$$\omega_{\text{mod}}(\vec{r}, t) = kU_{\text{max}}^{\text{orb}} a \sin \left\{ \Omega t - \vec{k}_w \vec{r} - \right. \\ \left. - \arctg[\cos(\Gamma_0 - \varphi_L) \operatorname{tg} \gamma_0] \right\},$$

where  $a$  - scale coefficient;

$\Gamma_0, \gamma_0$  - orientation angles of ray in space,

$\varphi_L$  - angle between wave movement direction and vertical plane, in which ray lays.

Angle  $\Gamma_0$  is read in horizontal plane from vertical one, in which ray lays. Angle  $\gamma_0$  is read from vertical axis.

Comparing phase  $\xi(\vec{r}, t)$ , we see that it differs from the last one by value

$$-\left\{ \frac{\pi}{2} + \arctg[\cos(\Gamma_0 - \varphi_L) \operatorname{tg} \gamma_0] \right\}$$

depending under given angles only on direction, determined by angle  $\varphi_L$ .

When determining wave movement direction, important feature of modulation function is that component of its phase

$\arctg[\cos(\Gamma_0 - \varphi_L) \operatorname{tg} \gamma_0]$  changes sign depending on wave direction angle relative to the radio-ray projection on horizontal plane. So for  $-90^\circ < (\Gamma_0 - \varphi_L) < 90^\circ$  it is positive, but for  $90^\circ < (\Gamma_0 - \varphi_L) < 180^\circ$  - negative.

After determination of wave direction for each this parameter is calculated for whole measurer by means of reduction of directions to frontal and back semiplanes of ship.

The device of Doppler frequency and distance determination by inclined radio ray has the circuit similar to that one of phase radioaltimeter but frequency shift unit may be absent in it.

## APPLICATION PECULIARITIES

Apparatus design is universal and allows to use it on transport vehicles of different types. However, application conditions may be different and they are briefly analysed here.

Initial aim at the WIG-craft movement parameters measurement task solution may be realized with confidence. The mode of movement at the height up to  $10^2$  m with the speed of about 10

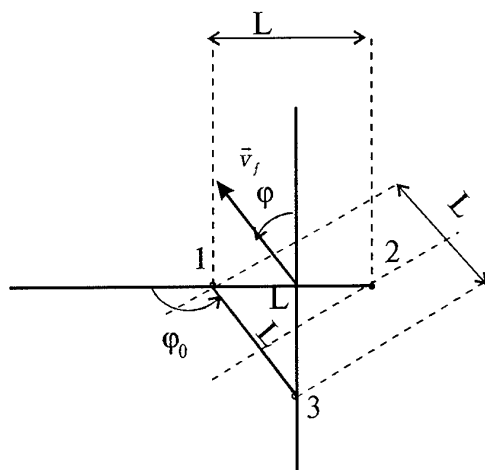


Fig. 8. Altimeters 1, 2, 3 positions diagram.

m/s which is typical for big WIG-craft is favourable for performance of both phase radioaltimeter and algorithms of its integration with accelerometer. High frequency of meeting with the wave and lack of vehicle substantial tossing allow to provide movement absolute height and waves profile measurement with r.-m.-s. errors about 5-10 cm even under the sea-way of the force 5-6 (except most unfavourable headings). Because movement refusal safety conditions require the presence of several radioaltimeters on board there is a possibility to use this excess for apparatus functional possibilities widening and measurements quality increasing. Detailed analysis of these possibilities with the wave disturbances space correlation taken into account is given in [1]. When choosing radioaltimeter mounting points it should be taken into consideration that vehicle pitching and rolling will interfere height measurements least of all when radioaltimeters are mounted near its gravity centre. However, when mounting radioaltimeters rather far from each other (for instance, on frame and on wings ends) it becomes possible to get information about inclination angles and to average statistically wave interference because of its decorrelation in different space points. Also, significant factors are spray and flood (because of this first Russian WIG-crafts had radioaltimeters at the nose), vibrations and short-period wings oscillations, the presence of rather perfect gyroscopic angular movement measurement facilities on the board. That is why radioaltimeters positions and their output signals application ways should be optimized when the whole on-board information control complex is investigated.

Peculiarities of apparatus use on seaplanes are determined by the requirements to the two functional tasks solution quality: first, sustaining the desired trajectory of movement in longitudinal plane during take-off and landing and, second, distant determination of sea-way parameters for final approach direction choice and, may be, landing point and moment optimization in accordance with the results of sea surface inclination forecasting in this point. In both

cases it is important that when illuminating sea surface from rather big height (more than 20-30 m under the force 5) waves in illumination spot are spacially smoothed that makes to consider radioaltimeter as LF space filter [1]. When measuring flight absolute height this space smoothing is useful, but when measuring waves profile and parameters it leads to the short-period spectrum components loss that should be taken into account when choosing apparatus application tactics.

The widest scale of apparatus application is possible on displacement ships where mounting of two or more UMMs on the right and left boards allows to form sea-way signal for use in autopilot mode, to determine sea-way parameters for ship heading and speed optimization task solution under sea-way, to determine ship rocking parameters (roll and trim), its draught during the movement in emergency mode and during shipment. When choosing radioaltimeters or UMMs mounting points on the ship it is necessary to take into consideration the mechanism of generation and propagation of the waves created by the ship movement itself. One of the variants of undisturbed waves profile measurement is to mount UMM on the ship bow. Due to relatively low speed of displacement ships encounter frequencies of meeting with big sea waves are low and may be about 1 rad/s that, as it was mentioned, complicates suppression of the wave interference to measurements and makes it possible only when radioaltimeter and high quality accelerometer signals are processed by 32-bit digital computer. Besides, this integrated measuring system may have rather big processing time of initial errors after switching on (about 10 min), that is the result of the radioaltimeter signal averaging on big time interval. However, when this transit process is finished waves profile and absolute height measurements are carried on without any significant lag.

Apparatus functioning conditions on undisplacement ships are more favorable because of high movement speed and, hence, higher frequency spectrum of wave excitations.

### CONCLUDING REMARKS

The usage of sea surface as a natural transport space is limited by the possible sea-way first of all. One of the few effective ways of this negative influence decreasing is sea-way conditions movement control system improvement and there is many unused reserves here. Two extreme cases cannot be certainly the satisfaction control problem solving: the complete leaving of transport vehicle to waves will and the attempt to keep out fully the waves influence on vehicle movement. The optimal solution should be trade-off and, realizing it, it is important both to synthesize vehicle movement trajectory on concrete part of wave surface and to force vehicle to move on it. Depending on designation and type of vehicle the optimal solving criteria differs but despite of all it is not possible without applicable control process information providing means. Namely, this circumstance stimulated the works to which the present publication is dedicated.

On account of a number of circumstances Russian firms are not considered to be authoritative suppliers

of autopilots for commercial ships. However, they have a great experience in creating of control systems for WIG-crafts and other undisplacement vehicles for non-commercial applying. They have also a good theoretical back-bag in this field. That is why there are preconditions for successful creation of suggested equipment. At the same time it is clear that this equipment can function most successfully as a part of united information control on-board complex which has still even been forming mainly by Russian shipowners from equipment imported. This explains our having interest in the interconnection with the world producers of sea-vehicle movement control equipment for equipment compatibility providing, its finishing for concrete objects, serial production mastering, particular components delivering, certification.

The possibility to use any proportional relative height sensor, if it can meet our function accuracy and reliability requirements, instead phase radioaltimeter included to UMM is substantial. In the same way it is possible to use phase radioaltimeter being developed as a separate sensor.

At last, another statement that equipment suggested suits ideally for functioning on the large WIG-craft board. Moreover, functioning conditions in this case will be more "soft" in comparison with displacement vessel. The creation of such type craft which corresponds by a number of parameters to the ideas of high speed, safe and environmental transport vehicle of 21st century could be a good proving ground for international cooperation.

### REFERENCES

1. Nebylov, A.V., "Measurement of parameters of flight close to the sea surface", St. Petersburg, SPSSAI, 1994.
2. Zagorodnikov, A.A., "Radiolocation monitoring of sea surface from flying crafts", Leningrad, Hydrometeoizdat, 1978.
3. Diomidov, V.B. and Nebylov, A.V. "Coordinate optimum estimation by data of positional radiotechnical sensor and accelerometer for the limited observation time. Transactions, pub.88, LIAP. 1974, pp. 16-21.
4. Zhukovsky A.P., ed., "Radioaltitude measurements theoretical foundations", Moscow, Sovetskoye Radio, 1979.
5. Besecersky, V.A., and Nebylov, A.V., "Robust automatic control systems", Moscow, Nauka, 1983.
6. Nebylov, A.V., "Robust way to the synthesis of complexed motion parameters measurer", Izvestia vuzov USSR - Priborostroenie, vol.40, N3, 1990, pp.85-90.
7. Nebylov, A.V., "Robust algorithms of discrete-data position sensor and continuous acceleration sensor complexing", Avtomatika and Telemekhanika, N5, 1994, pp.58-65.

The Application of Ada and Formal Methods to a  
Safety Critical Engine Control System

W.C.Dolman A.M.Ashdown  
Lucas Electronics  
York Road  
Hall Green  
Birmingham  
United Kingdom B28 8LN

by  
K J McCallion  
Procurement Executive, Ministry of Defence  
St Giles Court  
1-13 St Giles High Street  
London  
United Kingdom WC2 H8LD

Summary

The procurement executive of the UK Ministry of Defence, MoD (PE) identified Ada as the single preferred high level language for the implementation of defence real time operational systems from 1 July 1987. This meant that projects selecting an implementation language after that time must select Ada, unless there are sound and documented reasons for using an alternative.

MoD (PE) therefore decided to invite proposals for the High Order Language Demonstrator (HOLD) to examine the applicability of Ada to an aero gas turbine full authority digital engine control (FADEC), and awarded the contract to Lucas Electronics, Birmingham. This paper describes the work carried out by Lucas Electronics on this contract.

1.0 INTRODUCTION

The major potential benefit of the application of Ada to military systems, which led to its selection as the MoD (PE) preferred language, was the reduction of Life Cycle Costs. In addition, Ada is a truly international standard and, as a result, very wide support, in terms of Programme Support Environments (PSEs) and industry expertise, can be expected. Ada also provides facilities for structured design which holds the prospect for a modular approach with verifiable and re-usable software components.

MoD (PE) was concerned that Ada, and in particular its support environment, was not yet ready for incorporation into full development of high integrity software based systems such as flight safety critical FADEC's.

A FADEC is a real time control system. The control requires a fast execution time, typically in the order of 20ms, and all the functions must be computed within this time frame. The main functional activities are:-

- i) Input handling, including sampling, validation, averaging/filtering and scaling.
- ii) Control law computation.
- iii) Output handling, possibly including status and fault code data.

- iv) Fault monitoring and detection, state input checks and Built In Test (BIT).
- v) Fault handling, take action to implement fault procedures, for example change control lane or set system to a safe state.

There were two main areas of concern:-

Firstly the lack of visibility of the object code and its characteristics.

Although Ada lays down stringent requirements for the design of compilers, and the compilers have to be formally validated, there remains doubt about their integrity, and certainty of the object code produced actually representing that required by the source, and therefore their suitability for this application.

Secondly the size of code.

The use of the full Ada language with many compilers was understood to be inefficient in the production of object code, compared to the specialised lower-level languages being used for aero engine control. This would result in many times more computer memory space and processing power being used for a given function and would be a serious limitation to the use of Ada for aero engine control. However, it was considered that restrictions on the features used and selection of the compiler's optimisation features could greatly alleviate the problem.

A further area of interest to MoD (PE) was how the use of Formal Methods in the design of safety critical software could benefit the software development process. At the start of the HOLD programme Interim Defence Standard 00-55 [ref 1] was being prepared mandating the use of Formal Methods in Safety Critical software. However, very little experience of the use of such methods was available. A secondary aim of HOLD was to produce a formal specification of some components of the system and to formally verify the code implementation of these components.

## 2. PURPOSE AND SCOPE

The purpose of the HOLD programme was to examine the applicability of Ada to a military aero gas turbine FADEC. However, it was clear that much more could be undertaken whilst pursuing the top level objective. To ensure that the programme was as "real" as possible the contractor was required to base the programme on an existing in-service UK military FADEC.

The programme therefore covered:-

- i) Identification of the factors involved in the application of Ada to a flight safety critical control system.
- ii) The utilisation and critical assessment of design and development methods that will provide the best possible application of the language to this type of system, to meet both performance and integrity requirements.
- iii) Re-programming of the existing RB-199 flight certified Engine Electronic Control (EEC) in Ada.
- iv) The assessment of the efficiency of the executable code, and the resulting system performance and integrity, using the existing flight certified EEC as a benchmark.
- v) Assessment of the use of Formal Methods in the specification of a number of system components and the verification of their code implementations.

## 3. REQUIREMENTS OF A SAFETY CRITICAL ENGINE CONTROL SYSTEM

This section of the paper attempts to describe the features and life cycle of an aircraft engine control system which may set it apart from other avionic embedded software systems. The main purpose is to highlight the main differences so that some of the decisions described later in the paper can be better understood.

FADEC system software is generally set at the criticality level of "Level A" software as defined by RTCA/DO-178B [ref 4]. The "Requirements and Technical Concepts for Aviation. DO-178B Software Considerations in Airborne Systems and Equipment Certification" defines Level A software as:-

"Software whose anomalous behaviour, as shown by the system safety assessment process, would cause or contribute to a failure of system function resulting in a catastrophic failure condition for the aircraft."

The RB-199 engine control system used in HOLD was developed to an earlier standard, RTCA/DO-178 [ref 3]. Consequently, this standard was adopted for the HOLD programme so that direct comparisons between the flight certified engine control and HOLD could legitimately be made. The original RB-199 software was written in Lucas' own programming system, LUCOL<sup>1</sup>, which is an assembler based language.

It is worth pointing out at this stage that software, used for engine control, requires a computer system plus the associated input and output conditioning for it to operate and communicate with the outside world. The design of this system is of paramount importance, as the split of functions between hardware and software, with the safety features embedded in both, provides the safety critical system. The software is only part of the total system, and consequently cannot be considered in isolation.

### 3.1 Description of a FADEC

#### 3.1.1 FADEC Functionality

A FADEC, as shown in figure 1, comprises all the sensors, actuators and computing elements that realise engine management. The EEC is a major component of the FADEC. It is beneficial to later sections of this paper to segregate the "essential" FADEC functions from those functions arising as a result of "how" the system is implemented.

#### 3.1.2 Essential Functions

The primary purpose of the FADEC is to control a gas turbine installed on an aircraft throughout the flight envelope. Thrust demands from the cockpit and flight management computer are input to the EEC. The EEC utilises a set of control laws and schedules primarily based upon engine and airframe measurements of pressures, temperatures and speeds to control the engine by means of, fuel metering, variable guide vane actuation, engine igniter selection, engine bleed valve and thrust reverser operation.

#### 3.1.3 Additional Functions

The FADEC design is required to meet stringent integrity and reliability requirements. The architecture of the FADEC and of the EEC is designed to maximise fault accommodation. The additional functionality required of the EEC is to :-

- i) Condition, calibrate, validate and select input signals (critical inputs are normally duplicated).
- ii) Validate correct operation of and select output drives.
- iii) Detect dormant faults and reconfigure system.

<sup>1</sup>LUCOL is a Trademark of Lucas Industries Plc

- iv) Store all fault data for subsequent retrieval so that the status of the FADEC can be established.
- v) Provide test features to aid unit development.

### 3.2 Development Life Cycle

One of the major differences between an engine control system and other avionic systems is the software life cycle. Typical development life cycles for military and civil engines are 10 and 5 years respectively. During this time, the engine and its control system will be subjected to many changes with further modifications being embodied after entry into service.

The software life cycle normally begins with software requirements which, as a result of the state of the stage of development of the engine and its control system, are incomplete. A large number of modifications will be implemented in software since this is often easier and quicker, though not necessarily cheaper, than modifications to hardware. Some of these changes will be required to be carried out in short timescales, possibly less than 24 hours during particular stages of the development life cycle such as engine test cell operation. Thus the software teams do not have the luxury of frozen, complete and unambiguous requirements until quite late in the project life cycle.

It is therefore important that the software environment employed is flexible but must provide a top quality product without reliance upon formal verification as this task is impractical during the engine development process.

### 3.3 Software Verification

The verification of software is a very important, if not the most important, stage of a software life cycle. The outcome of the verification stage is to show that the software fully meets its requirements. There are many facets of verification including functional testing, structural testing, code review, static testing etc. To be able to meet the safety levels required for safety critical software the testing methodology employed must be against the target code resident in this target environment. If testing is carried out against source code, emulators, simulations etc then this will only be acceptable if the following conditions apply:-

- i) The source code to target object code process has itself been verified or is completely analysed.
- ii) The tools used in the process are themselves verified to the same level as the software criticality level.

## 4.0 HOLD METHODOLOGY

The approach adopted for the development of HOLD was to reprogram one lane of an existing FADEC unit. The unit chosen was a dual lane EEC i.e. it had two identical independent lanes for dry engine control and a third common lane of control for reheat. The advantage of choosing this unit was that we could replace one lane with the code developed for HOLD whilst retaining the original software of the other lane. This meant that during testing of the unit we could freely change lanes between the two different version of the software to compare performance.

The starting point for the software development was the software requirements that had been used to develop the original software.

### 4.1 Requirements Capture

We decided that the most advantageous way to proceed was to use some form of computer aided software engineering (CASE) tool to capture the existing software requirements. This approach was used to ensure that all the software requirements were captured in such a way that the subsequent design and implementation of the Ada solution mirrored the existing software. This provided reliable comparisons between the two systems. There are many methodologies available that come under the umbrella of requirements capture or analysis and design methods, such as CORE, MASCOT, SSADM, OOD, Jackson etc, but we decided to use Yourdon<sup>2</sup>. This choice was based mainly on two factors, firstly our knowledge and experience with Yourdon over several years and secondly the availability of in-house tool support for this methodology. We had available in-house the CASE tool Teamwork<sup>3</sup> which implements a Yourdon based system analysis methodology and also has support for structured design.

The first task in the requirements capture process was the analysis of the system. This was achieved in the Yourdon methodology by creating the top level context diagram which defined the inputs and outputs of the system and thus placed bounds on the extent of the system (see figure 2).

### 4.2 System Breakdown

The next phase of the requirements capture process was to break down the context diagram, through several steps, into smaller, and logically independent, functional tasks. The first stage of this process was straightforward. As the EEC performs two different functions, dry engine control and reheat control, the first level of partition was to split the context diagram along this functional boundary. Then as the dry engine control consists of a dual lane system the next level of partition was to split the dry engine control function into the functions of the two lanes, termed lane A and lane B.

<sup>2</sup>Yourdon is a trademark of Yourdon Inc

<sup>3</sup>Teamwork is a trademark of Cadre Technologies Inc

As the lanes are functionally identical we then proceeded by continuing the partition for just one of the lanes.

For HOLD this process of gradually splitting the overall task into smaller and smaller items was terminated when further partitioning yielded no benefits. The decision as to where to stop the process was to a large extent arbitrary. The main goal was to reach a point that did not over or under partition a function. If the level was taken too low then individual functions could be fragmented and not easily assimilated. If the level was too high then functions would be too large and complex.

When the partitioning had been completed the end process had to be defined. This was achieved using the process specification (P-Spec) feature of Teamwork.

#### 4.3 Structural Design

The task of structural design can be thought of as one of organisation. The objective is to take a set of specific requirements and organise them into coherent groups that will fit into the chosen hardware environment. If this is performed adequately then the task of the software design for the individual elements will, in concept, become trivial.

It is thus at this stage that the real world environment has to be considered. In essence the Yourdon analysis of the software requirements has no knowledge of real time aspects of the engine control functions, or of any physical limitations such as size of memory available.

So the structural design was tackled with two different approaches; a "bottom up" approach to create the structure charts for the individual processes and a "top down" approach for the executive structure controlling the order and sequence of execution of the processes. An overview of the development process is shown in figure 3.

##### 4.3.1 Process Structure Charts

The functionality of individual processes within the requirements analysis was transferred to a structure chart format to represent the software design of each component. These structure charts show the design tree of the software and how it is arranged into various blocks consisting of functional modules and data only modules. Each functional module is defined by a module specification (M-Spec).

##### 4.3.2 Executive Structure Charts

The executive structure charts fall into two types. Firstly there are the simple ones that reflect the dataflow diagram breakdown. These charts are used to define the calling sequence of the various modules which is not always obvious, or defined, in the dataflow diagram representation. This is an important feature which cannot be overlooked even though on the surface it seems to be a trivial task.

The second kind of structure chart is the overall executive which is typical of an engine control requirement. This is where real world detail has to be added in the form of power-up/initialisation requirements and iteration rates for the various processes.

It is this implementation of the software requirements into real iteration levels which causes problems especially where a function has to be split between two different levels. This means that in designing the structure charts there is not a one to one relationship between a P-Spec and a structure chart.

#### 4.4 Formal Methods Integration

In considering the application of Formal Methods to the HOLD programme, we decided that the best level at which to introduce such techniques would be at the P-spec level.

We already had experience of the use of Formal Methods, in terms of the use of static analysis applied to small sections of assembler code. The next logical step was to move this process up a level to a small section of high level language code, and as such the P-Spec seemed the most appropriate.

There are many different functions within an engine control system and we decided to choose a representative sample of these functions for investigation. Four P-Specs were chosen. Two of these were engine control functions, one of which fell into the classical control area and involved lead-lag compensation, gain, lowest and highest wins elements etc., and the other fell into the logic area and involved sequencing functions. The third P-Spec was chosen from the area of signal validation involving range, rate of change and cross checks on a signal. The fourth function was selected from the area of the control associated with fault logging and diagnostics.

Our approach to the Formal Methods representation of these functions was firstly to select the language in which to represent them. There are several Formal Methods available and in choosing one we set out several criteria on which we based our selection. One factor in our choice was that the method should be widely accepted and supported. We wanted a method that was in popular use by the rest of the industry and one that was likely to stay in use for the foreseeable future. The method must also be supported in terms of training and course availability and ideally would also have tool support available for automation of the Formal Method specifications and proof checking. For these reasons we chose the Vienna Development Method (VDM) which also had the added benefit of being the easiest to integrate with our existing systems.

The next step was to look at the implementation of the specification from a general point of view. A digital engine control is a system which regularly samples its inputs and updates its outputs. On this basis it was decided to formalise each P-Spec as a relation between the history of sampled inputs and the history of updated outputs.



As an example consider the P-Spec which contains, in part, the simplified requirement to operate an engine compressor bleed valve :-

"the valve should be opened on receipt of the pilot signal and held open for a period of  $n$  seconds after the pilot signal is removed."

Using the state :-

**state** State of

*pilot-signal-history* : B\*

**init**(mk-State(*pilot-signal-history*))  $\triangle$  *pilot-signal-history* =  $\square$

**end**

Which can then be formalised with the following VDM operation :-

VALVE-CONTROL-P *pilot-signal* : R) *valve-open* : B

**ext wr** *pilot-signal-history* : B\*

**post** *valve-open* = (*pilot-signal*  $\vee$

$\exists i \in \{1, \dots, n \times \text{CycleFrequency}\} \bullet \text{pilot-signal-history}(i)$  :

*pilot-signal-history* = *pilot-signal*  $\overleftarrow{\text{pilot-signal-history}}$

This specification may be read as :-

"The valve is open either if there is a pilot signal on this cycle or if there was a pilot signal in the last  $n \times \text{CycleFrequency}$  cycles. The state variable *pilot-signal-history* holds the status of the pilot signal over all previous cycles so that the second part of the condition can be evaluated."

When writing such specifications a number of problems of incompleteness and interpretation can arise. For example, how far back in a sample history should one look to determine whether values are increasing or decreasing? The production of formal specifications from an informal requirements definition can be a valuable way of revealing ambiguities and omissions.

The proof, in general, that a formal design meets its formal requirement specification is very difficult. In the HOLD project this problem has not been addressed because one can not prove correspondence between a component of the requirement (P-Spec) and separate parts of the design, i.e. the M-Specs which taken together within the overall design implement the requirement. For this reason the specification of the VDM operation associated with each M-Spec was a formalisation of the function of the design described by the M-Spec.

For the example given we would formalise the M-Spec as follows :-

VALVE-CONTROL-M (*pilot-signal* : R) *valve-open* : B

**ext wr** *signal-count* : Z\*

**post** (*valve-open* = (*signal-count* <  $n \times \text{CycleFrequency}$ ))  $\wedge$

(*pilot-signal*  $\Rightarrow$  *signal-count* = 0)  $\wedge$

( $\neg$ *pilot-signal*  $\wedge$   $\overleftarrow{\text{signal-count}} < n \times \text{CycleFrequency} \Rightarrow$

*signal-count* =  $\overleftarrow{\text{signal-count}} + 1$ )  $\wedge$

( $\neg$ *pilot-signal*  $\wedge$   $\overleftarrow{\text{signal-count}} \geq n \times \text{CycleFrequency} \Rightarrow$

*signal-count*  $\geq n \times \text{CycleFrequency}$ )

The state variable *pilot-signal-history* has been replaced by the state variable *signal-count*, which has the value of the number of cycles since the last pilot signal occurred.

#### 4.5 Programming Environment

In considering the application of Ada to a real time engine control system there were two main areas that we had to investigate. Firstly there were the safety aspects of the language and secondly there were the timing implementations.

##### 4.5.1 Safety Critical Language Features

In any High Level Language (HLL) there are generally features that are not desirable in safety critical systems. The failure of the software to complete a function is a serious error not merely an inconvenience. For example it is of critical importance that any function in the software has an explicit entry and exit condition. For this reason loop constructs of the type DO-UNTIL, DO-FOR and DO-WHILE are avoided especially where the loop parameter is determined at the run-time of the system. For a similar reason the use of GO-TO type constructs should be avoided as they permit ad-hoc entry to and exit from functions.

Another major feature of safety critical engine control systems is that in general the hardware environment is composed of a custom made unit. This means that any software language used to program these units must have the ability to interface with the unique hardware of the unit. This is available with Ada, and with other languages, by means of an interface with assembly language components. The hardware constraints also limit in a system the amount of memory available and for this reason it is preferable to know in advance how much storage is required. Thus features which dynamically allocate memory at run-time must be avoided. Ideally all the memory should be statically defined at compile or link time, or in the case of a stack for example the bounds of the memory requirements should be calculable.

#### 4.5.2 Time Critical Language Features

A typical engine control system runs at an iteration rate in the region of 20 milliseconds, the time being chosen to achieve satisfactory engine control response. Thus time is critical in an engine control environment as there is no option available to increase the run-time of the software. For this reason the efficiency of the language is of prime importance. From experience we knew that the run-time system was going to be an important area to investigate, not only in respect of Ada itself but also in respect of the particular compiler selected.

We required a run-time system that could provide a simple and quick interrupt transfer mechanism without the use of tasking because of the time response associated with this feature of Ada.

Another feature of Ada that we wished to avoid was the use of exception handlers. The main source of exceptions in an engine control system is due to integer overflow. As integer operations are widely used this would need in theory an exception handler for each operation as the result required would be different in each case. This approach would place a unacceptable overhead on the execution time of the code. The preferred method was to design against overflow conditions, so the exception handlers became redundant.

### 5. RESULTS OF PROGRAMME

#### 5.1 Ada in a Safety Critical Environment

The three main features which affected the application of Ada to a safety critical environment that emerged as a result of the HOLD programme were the provision of a safe sub-set of Ada, the Ada run time system and the validation of the compiler.

##### 5.1.1 Safe Ada Sub-set

As a result of the requirements set out in section 4.5 we selected the XD-Ada compiler from SD-Scicon since it had a minimal run time system, which could also be tailored to our own individual requirements. The selection was also influenced by the needs to operate on our own computer system in terms of target/host configuration.

In considering the possible need to apply restrictions to the Ada language we looked for a way of providing a safe sub-set of the language. Ideally we required some way to automatically test code for illegal construct usage. There was, and still is, a very limited set of products in this field but one which fitted not only our requirements for a safe sub-set, but also our needs in the integration of Formal Methods, was SPARK (SPADE<sup>4</sup> Ada Run time Kernel).

SPARK has a tool, the SPARK Examiner, which checks Ada source code for a variety of restricted features and issues warnings if any code violates these conditions.

The tool also performs tasks associated with the static analysis of the code. This provides flow checking of the code as well as verification condition generation and proof checking. These last two elements fitted well with the integration of Formal Methods in the generation of the code. We could thus use formal specifications to generate pre- and post- conditions in the Ada code which we could then prove using the SPARK Examiner.

#### 5.1.2 Ada Run-time System

Our work on the assessment of run time systems suitable for this application, as part of the selection of an Ada compiler has shown that the area of "bare micro" targets is being addressed by compiler vendors. As recently as seven years ago it would have been impossible to purchase anything other than a large run time system aimed at a large computer system target. Now more attention is being focused on almost "bare micro" target systems. The fact that we have been able to take an off the shelf system, albeit with some tailoring, is testimony to this development. Using this supplied system we developed a bare run time system consisting of interrupt servicing and test port communication, into which the rest of the code was integrated.

#### 5.1.3 Ada Validation

Another critical problem with the use of Ada is the current requirement to use a validated compiler and the necessary reliance that is placed on its correct operation. In general the approach used for safety critical software involves verifying the code produced down to object code level. With most HLLs the traceability from source code to target object code is difficult, especially where features such as optimisation are used.

If it is a certification requirement that engine control manufactures still have to verify down to object code level then this could prove a very time consuming task. It also has to be born in mind that control manufactures may not have the necessary expertise to analyse the intricacies of an Ada compiler output. On the other hand if they are allowed to rely on the validation of the compiler and there is found to be an error in that compiler then who is responsible? It is believed that at present compiler suppliers absolve themselves of such responsibilities.

### 5.2 Analysis of Software Development Processes

#### 5.2.1 Software Specification and Design

The analysis of the software requirements document using the Yourdon methodology has resulted in a very easy to read document. It must be remembered, however, that the methodology only serves as a tool to represent the software requirements. It only helps to specify the requirements, in so far as laying them out in a clear manner so that ideas can be communicated easily.

---

<sup>4</sup>SPADE is a trademark of Programme Validation Limited

As is the case with the software requirements, the use of structure charts generated from the dataflow diagram breakdown provided a clear description of the software design. The main problems, as with all systems, is that of transition from what is required to how it is to be implemented. The addition of implementation dependent features at the software design stage tends to obscure the flow of information from the analysis to the design phase. This problem can be overcome, however, if the analysis is performed with the implementation in mind.

### 5.2.2 Application of Formal Methods

The choice of VDM was well suited to the formalisation of the specification and designs, and the Adelard SpecBox tool used provided effective VDM support.

The Ada restrictions imposed by SPARK did not seriously constrain programming, and transcription of pre- and post-conditions from VDM specifications to SPARK code was conceptually straightforward. Experiences in using the SPARK examiner were generally favourable.

As for the integration of structured design, Formal Methods and Ada programming, one crucial question is how far the use of the design method should be taken, before employing the programming language itself for design refinement. When a program is to be implemented in an assembly language, the distinction between design and coding is clear, because an assembly language has very limited expressive power and it offers very little support for abstraction. If the target language is Ada however, one can exploit its expressive power, to describe designs more precisely than any structured design method. The experiences with HOLD suggest that in future software developments of this kind it would be beneficial to make a much earlier transition from Yourdon design, to design and development directly in SPARK, with extensive use of well-chosen packages and subprograms.

The Formal Methods approach employed on HOLD is considered to have been successful, fully meeting its, somewhat limited, objectives. The next, more exacting, test of the applicability of the formal approach, and of the feasibility of applying the Interim Defence Standard 00-55, would consist of a review, and formalisation in VDM, of the complete statement of requirements. We believe this would be possible, and very instructive.

### 5.2.3 Development Process Efficiency

The productivity metrics used in the analysis of the programme costs for HOLD have been based on in-house values currently in use for software development. These figures were applied to the original LUCOL Software for the EEC and then broken down into the four broad areas of requirements capture, design, code and verification. These figures were then compared to the actual hours spent on each of these tasks for HOLD.

If the figures are compared as a whole, the time spent on the HOLD programme has been double the time we would have expected for the same software using the LUCOL System. Part of the increase may be attributed to the investigative nature of the HOLD programme and the associated extra tasks that such a programme entails.

The management overhead, for example, is far more than we would expect on an equivalent project due to the extra number of meetings held and reports produced. There were also some extra tasks like that of validation, the Formal Methods investigation and the Ada compiler selection. Once all these factors have been taken out the comparison showed that the increase was around 80% with most of the increase attributable to the code and verification tasks.

The tasks of software requirements capture and software design using Teamwork have been respectively 30% and 40% more expensive than traditional methods. Part of this increase can be put down to the learning process associated with the new methods and the experience level of the personnel involved. Taking these factors into account it is estimated that there will, at the end of the day, be a 10% to 20% overhead in using this methodology. This should, however, pay for itself in the long term as the quality of documentation produced is higher which should reduce the overall programme costs.

As for the code and verification tasks, these have proved more time consuming, being on average 40% greater than the existing system. Again part of this can be attributed to gaining experience with the use of Ada and SPARK. The use of SPARK and the extra effort that it requires in annotating the code with derives lists is a task that has no direct comparison in the existing system. Even so these factors can only account for around 50% of the increase at most. There is still a large element that can only be attributed to Ada itself. It must be remembered that Ada, and to a lesser extent SPARK, is a rich complex language. This has made it very difficult to debug and test. One of the main attributes of Ada is its principal of information hiding which makes testing, especially requirements testing, complex. If internal data is not accessible then it is very hard to determine if a programme is operating correctly and almost impossible to debug. This can only be overcome by defining data globally for test purposes or by the use of analysers.

There will be an overhead on any programme that uses Formal Methods and Ada if they are applied in the wrong environment. Where software requirements can be fully defined then the use of the methodologies used on HOLD, will lead to an overall reduction in programme time scales and an improvement in quality. It is strongly recommended, however, that for initial development work these methods are not adopted rigorously. The framework of the methods should be used to ease the transition to the full methodology, but flexibility should be allowed in light of the imprecise nature of requirements that generally exist at the start of a project.

### 5.3 Applicability of Ada in a Real Time Environment

The results of the HOLD programme indicate that Ada can be used in a real time safety critical environment but great care has to be taken in its use. There are also some constraints that have to be applied which restrict the use of the full richness of the Ada language.

The main constraints in the use of any language for a real time application is the efficiency of the code produced. As detailed in section 5.4 it can be seen that with care the efficiency of Ada code can be made to approach that of assembler languages but there will always be an overhead. This is only to be expected when you try to apply a general language like Ada rather than a language specifically tailored for real time applications. This trade off is one that has to be considered as part of the overall programme development costs.

We have shown that, in the development of Ada code for HOLD, there have been very few problems in its adaption for use in specialised target hardware. The assembler routines for specialist I/O functions in the EEC have been developed as a package of functions which were easily incorporated using "pragma INTERFACE" and the run time executive was developed by fairly simple tailoring of the supplied system.

Our approach to exception handling, of not introducing them because of their time overhead, has shown to be successful. The method we have adopted of ensuring that exceptions cannot be raised does have an overhead but this is much smaller than that which would have to be carried if exceptions were handled. This approach does compromise the principles of Ada somewhat but may be one of the sacrifices that has to be made if Ada is to be widely adopted for real time systems. This approach to exception handling also fits in with the approach adopted by SPARK which also prohibits them.

The use of SPARK posed no real problems other than the time taken to add derives lists to the code which in some cases was considerable because of their length. The adoption of SPARK did impose a slight change in programming style but this was fairly easy to get used to with a little practice. In general these changes in style were of positive benefit as they force the programmer to think about the code layout in a more structured manner.

Much better use of SPARK could have been made, however, if it had been used earlier in the process e.g. if the P-specs had been written in VDM and their corresponding M-Specs in SPARK. The derives list could then have been related to the dataflow in and out of the dataflow "bubble". The reason why our derives lists were so long is due to the fact that all the data in these lists went down to the elemental data level. If data had been combined together, as for composite elements in dataflow diagrams, then the list would have been shorter but less explicit. This is due to the fact that you would be able to check that the correct composite dataflow was being used but not if the particular element within that flow was correct.

This is another trade off that will have to be made in the design process and one that will affect the approach to the Yourdon breakdown especially if SPARK is used earlier in the design process.

The only other problem encountered with SPARK was the inability to use the SPARK Examiner on the top level procedures. The Ada code was written to interface the three main routines, fast level, slow level and base level, to the run time executive as exception handlers, which had to be "hidden" from SPARK. Data is communicated between these levels using global data in the WORLD package. This setup is typical of a real time engine control whereas more traditional programmes consist of a single main program element. It is because of this arrangement that SPARK cannot be used i.e. where data is defined in an external package. This could be overcome using access types to communicate data but this is thought to be risky due to the storage allocation associated with access types and their imposition on the run time code. This problem needs more investigation before an acceptable approach could be recommended.

### 5.4 Analysis of Produced Code

#### 5.4.1 Memory Analysis

With regard to the utilisation of memory the Ada system was only 10% larger than the existing software in terms of PROM usage. This factor is so small in terms of the memory generally available with systems that it is almost insignificant.

The equivalent figures for RAM usage are difficult to compare directly. The Ada code for HOLD uses approximately 3 K bytes in directly allocated RAM, the rest of available RAM is allocated automatically to the stack of which only a few hundred words are actually used. For the existing software only 1 K bytes are allocated directly but another 2 K bytes are assigned to fixed memory locations for compatibility with earlier EEC's. The stack on the existing system only occupies around 50 words. Thus to all intents the figures appear to be around the same value with the Ada figure only being slightly larger due to the stack usage. As with the PROM memory this difference is insignificant considering the amount of memory generally available.

#### 5.4.2 Timing Analysis

On the surface the timing analysis produced some unusual contradictions. The analysis of equivalent modules, comparing functions in Ada that were representative of simple single functions in the existing system, showed that some functions were very slow, some over 5 times slower, these being the functions that were executed by calls. The functions that were in line, however, were faster than their existing counterparts. This would lead to the conclusion that Ada was likely to be very much slower.

However when figures for the overall time taken to complete the slow level tasks were examined they were found to be around 17 milliseconds for Ada and 16 milliseconds for the existing system, indicating that there is little difference between the two systems.

This contradiction was resolved by more detailed examination of the elements that make up these two values. The answer lies in the fact that due to the design of the hardware having to conform to fit in with an earlier standard of EEC the hardware functions are very time consuming. The A. to D. conversion alone takes around 10 milliseconds in the Ada software and around 12 milliseconds in the existing software.

Thus if allowances of 11 and 13 milliseconds respectively are allowed for these hardware elements, then the comparative figures come down to 6 and 3 milliseconds. This means that in general Ada is likely to be in the order of a factor of two slower than an equivalent function written with the existing language. This two to one ratio is also reflected in the comparison of a large sections of code e.g. procedures.

When optimisation is applied to the software, the slow cycle time for Ada reduces to approximately 15 milliseconds. Applying the same assumptions as before, this means that the overhead of Ada is reduced from 100% to 30%. This figure is again reflected well in the comparison of large sections of code.

#### 5.4.3 Hardware Effects

The main effect that Ada will have on the design of engine control systems is in the area of processor selection. It has been shown that there is little overhead in the selected approach as far as memory is concerned, the only overhead being in throughput which will require a more powerful processor to be selected.

The processor selection question will also depend on which processors have validated, or even un-validated, compilers available. In general most of the main stream processors are covered by a wide variety of available compilers but there is also a trend to the use of small micro-controllers that have on board PROM, RAM, A. to D.s, D. to A.s etc. Where these processors have been derived from a existing processor with Ada support available then it is likely that compiler support will be supplied, but some micro-controllers do not fall into this category. The other consideration is to ensure that the compiler has the correct host availability. Again with most of the main stream processors a wide variety of host configurations are available.

## 6. CONCLUSIONS

The overall conclusion is that Ada can be used for such real applications but there are several provisos to this statement:-

- a) A safe subset, such as SPARK must be used.

- b) Allowance must be made in the choice of processor to allow for the overhead of an Ada system. This choice may be mitigated by compromises to the Ada such as increased use of imported assembler or by the use of optimisation.
- c) The verification of Ada systems is limited to the Ada source code level. This will place much greater emphasis on the validation of compilers, the procedures and the tools used in development of Ada software.

The conclusions regarding the use of Formal Methods are that they provide a rigorous methodology for specifying requirements but are only really useful if applied in the right context. For example at present the usefulness of transforming a control law diagram into a Formal Method specification is suspect. Most engineers in the engine control business can understand and translate into code such a diagram more reliably than they could a Formal Method specification.

There is thus a bridge to be crossed between the world of engineering and the mainly mathematical and computer science orientated communities. This will only be crossed slowly with training and gradual adoption of Formal Methods into programmes.

### 6.1 Future Work

There is a considerable amount of work being undertaken within the UK software engineering community into ways of producing good quality software. MoD (PE) has been active in this arena and has issued Interim Defence Standards (IDS) 00-55 [ref 1] and 00-56 [ref 2] to ensure that real time operational software for defence equipment is produced to adequate standards. Furthermore, MoD (PE) has funded a number of studies into current and future software engineering practices, one example being the HOLD programme.

A particularly interesting result of HOLD was confirmation of the advantages to be gained from using Formal Methods in the software development process. As stated earlier, however, one of the main disadvantages of such methods is their complexity which makes them difficult to understand by all but a few specialist software engineers.

To combat this, MoD (PE) and Lucas Electronics are currently engaged in a follow on study to the HOLD programme in an attempt to define a methodology which will make these techniques more understandable and acceptable to the majority of control engineers. Such a methodology must have the mathematical rigour necessary to comply with IDS 00-55 [ref 1] while being sufficiently simple for use by control engineers without extensive Formal Methods experience. Such a methodology must be able to capture software requirements effectively, provide a means of animating these requirements at an early stage and produce formal proofs against which the final code can be checked.

A further requirement is for such a methodology to be able to deal with the strict-timing requirements of a typical engine control system in a formal way. This work is being undertaken by Lucas Electronics and jointly funded by MoD (PE) and Lucas.

The imminent introduction of Ada 9X is also causing a great deal of interest within the Ada community. MoD (PE) is currently defining an Ada 9X transition plan and some thought has been given to the effects that a transition to Ada 9X will have on the safety critical software within a FADEC. Although it is generally accepted that a "safe" subset of the Ada language must be used in applications of this type, there may well be new features provided by Ada 9X which would be of benefit and could result in an extension of this subset. Furthermore, there may well be differences in the object code produced by Ada 83 and Ada 9X compilers in terms of memory usage and speed of operation which could have a significant effect on the operation of the FADEC. MoD (PE) and Lucas are therefore discussing the possibility of conducting a further study to investigate these effects in more detail.

## 7. ACKNOWLEDGEMENTS

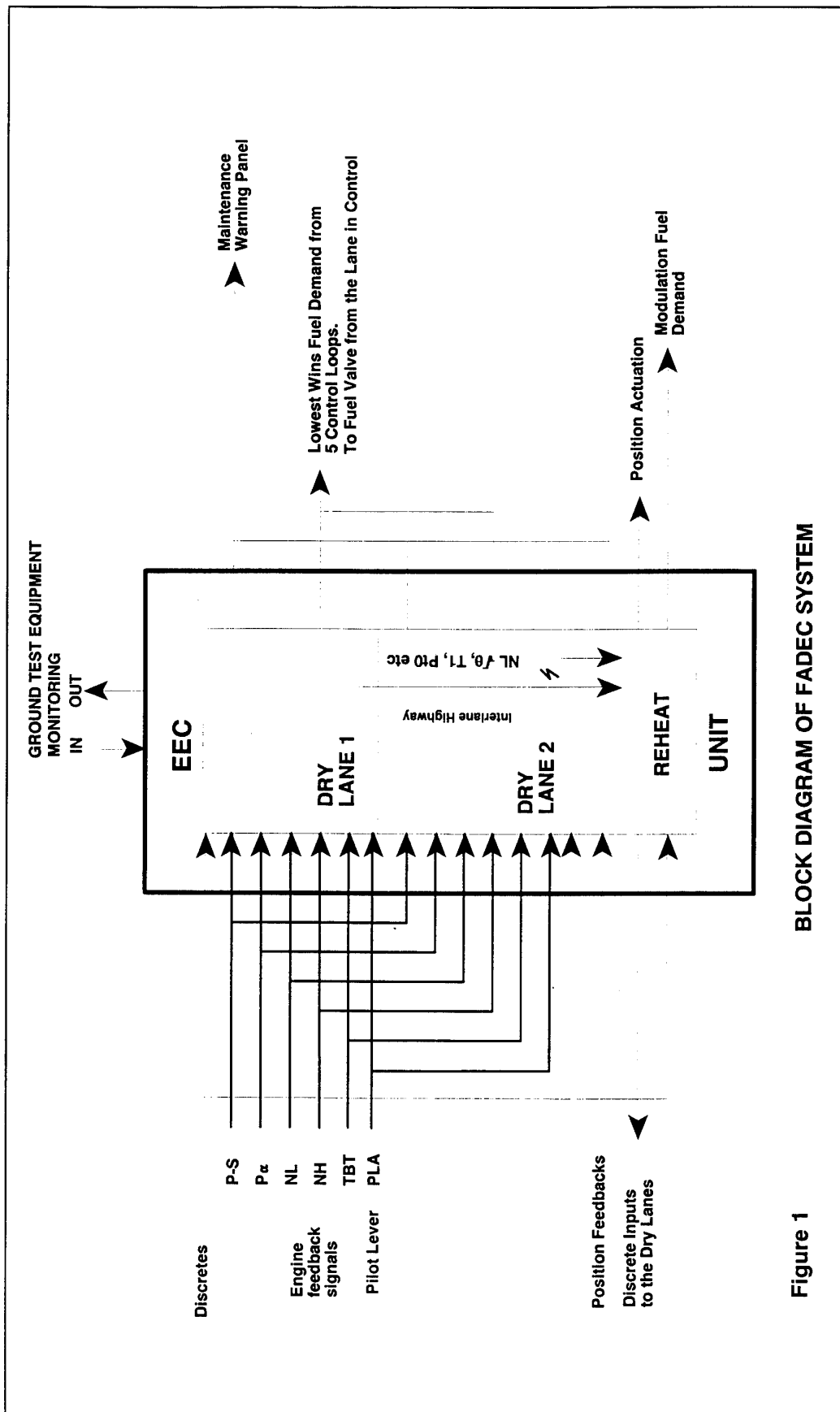
The authors would like to thank MoD (PE) and Lucas Electronics for their support in presenting and publishing this paper.

The authors would also like to place on record their appreciation for the support of their colleagues in preparing this paper and for their contribution to the HOLD project. This also applies to other companies involved in the HOLD project, in particular Program Validation Limited.

The opinions expressed in this paper are entirely those of the authors and do not necessarily represent those of their respective organisations.

## REFERENCES

- [1] DEF STAN 00-55      The Procurement of Safety Critical Software in Defence Equipment, Interim, April 1992.
- [2] DEF STAN 00-56      Safety Management Requirements of Defence Systems containing Programmable Electronics. Draft, February 1993.
- [3] RTCA/DO-178      Radio Technical Commission for Aeronautics - Software Considerations in Airborne Systems and Equipment Certification
- [4] RTCA/DO-178B      Requirements and Technical Concepts for Aviation - Software Considerations in Airborne Systems and Equipment Certification.



BLOCK DIAGRAM OF FADEC SYSTEM

Figure 1

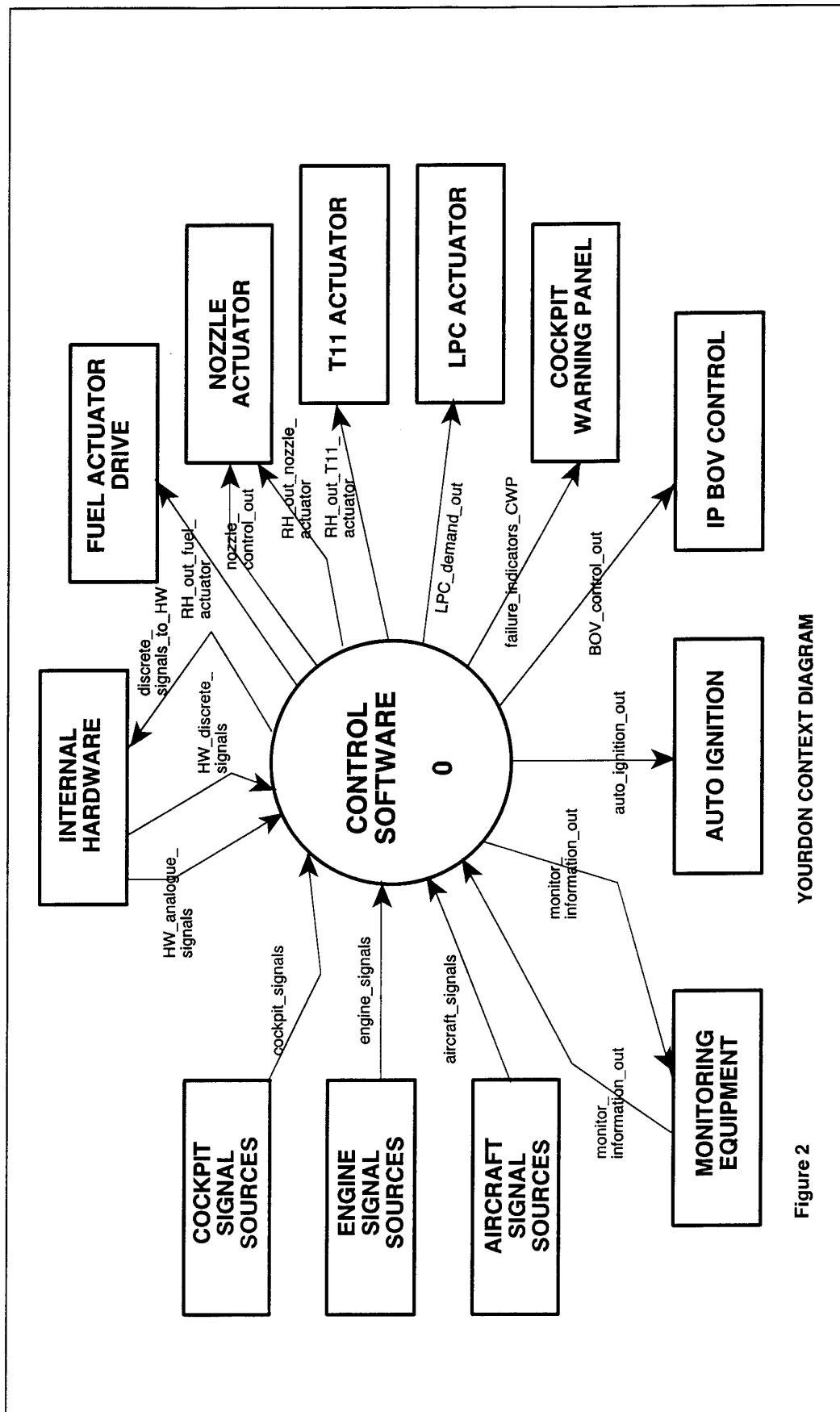


Figure 2

YOURDON CONTEXT DIAGRAM



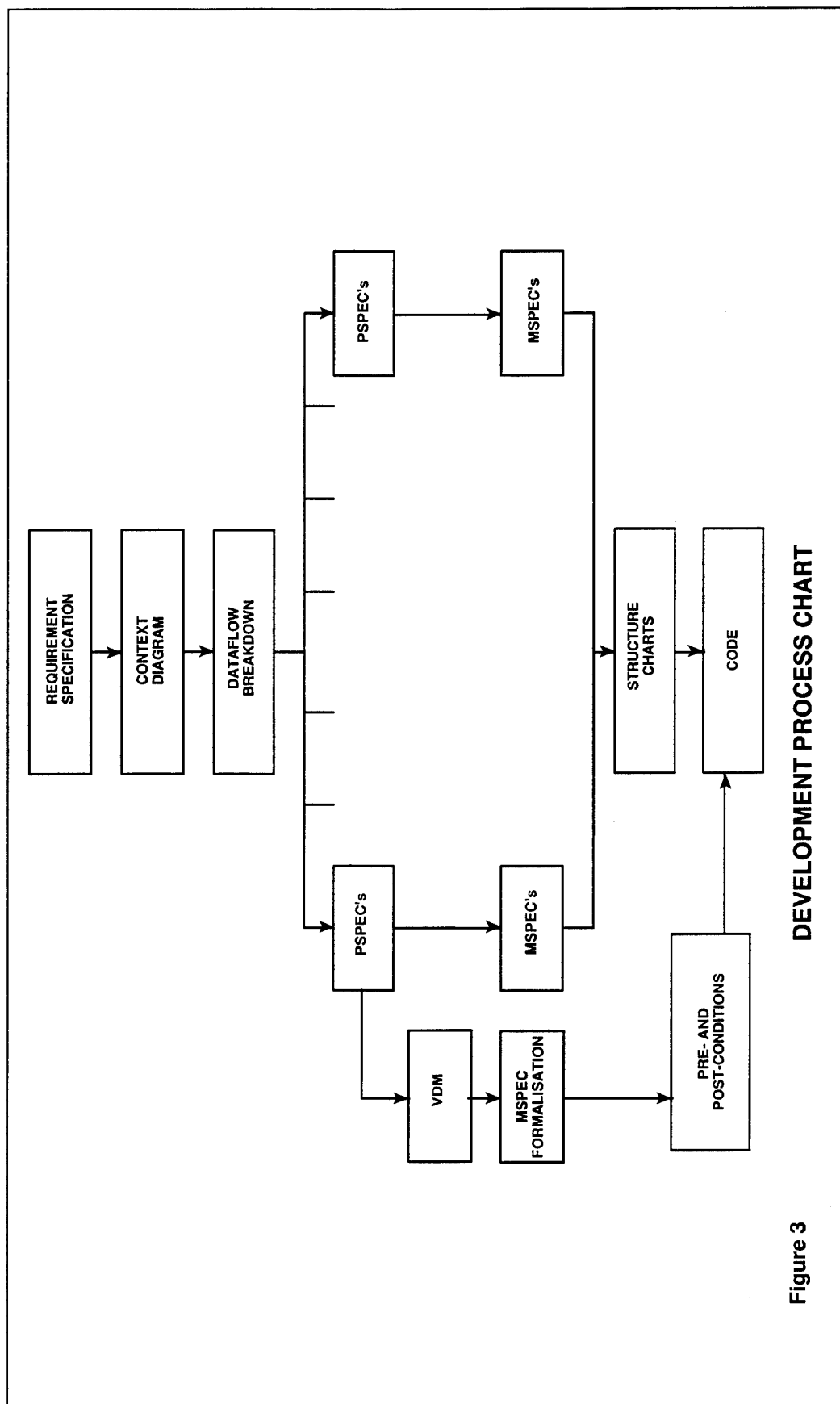


Figure 3

## SOLID-STATE DATA RECORDER, NEXT DEVELOPMENT AND USE

J. Vidiečan

J. Kozák

K. Horák

J. Svoboda

VZLÚ - SPEEL Ltd.

Beranovych 130

199 05 Praha 9, Czech Republic

### SUMMARY

The use of Data Recorders on board of aircrafts for crash and later for maintenance and logistic purposes is well known already for decades as "black box" installation.

Due to higher requirement on safety and economy of ground transport vehicles operation, such devices are already used in selected types of these vehicles.

The use of new technology - Solid-State Memories - enables to increase technical parameters of such recorders (number of registered parameters, MTBF), reduce the mass, space and requirements on technical assistance during operation.

Besides aircraft application started the first use of Solid-State technology in the development of Railway Electronic Tachograph.

In the paper technical data and description of such recorders for aircraft and ground based vehicles are given. Also results of nowadays application of these devices and different methods and software for evaluation are also presented.

### 1 INTRODUCTION

VZLU-SPEEL Ltd. (SPEcial ELectronics) was established in 1993 as the successor of Automation and Aircraft Diagnostics Division of Aeronautical Research and Test Institute, Praha, Czech Republic.

VZLU-SPEEL Ltd. with its 23 employees, from which more than one half has a complete technical university education, goes on in the equipment development for aircraft diagnostics, which started already in 1960 with the development of Mobile Automatic Test Equipment (ATE) for the L 39 jet trainer. This diagnostic equipment marked KL 39 (Fig.1) was in series production in

LETOV Enterprise of the AERO Concern Company nearly till 1988.[1] In 80ties the Test and Diagnostic System - KDS was developed for the L 39MS jet trainer and modifications of this system for L 59E and commuter aircraft L 410 and L610 were also developed (Fig.2),[2,3]. On-board part of these systems - PARES 39, PARES 610 - were produced in series by Aritma-Prague Company. For L59E aircraft (producer Aero Vodochody) VZLU-SPEEL Ltd. is producing in series ground based part of this diagnostic system marked GEE 59E, the on-board part marked PARES 59E is produced in series by Unimer-Prague Company.

### 2 SOLID-STATE FDR

VZLU-SPEEL Ltd. finished in 1993 the development and started the series production and deliveries of crash protected Solid-State Flight Data Recorder marked FDR for Czech manufactured aircraft types L 39, L 59 and future types L 139 and L159.(Fig.3,4),[4,5].

The FDR 39T model can be used as more reliable and modern replacement of mechanical recorder of SARPP-12 type, where existing aircraft wiring is used, only another mechanical fixing of FDR 39T block is necessary.

#### Basic technical data of FDR:

Dimensions and weight: 252 x 233 x 116 mm  
8,2 kg

Power supply and consumption: 28 VDC, 9 W

Storage capacity: according the wish of the customer, in the range from 4 to 32 flight hours.

Registration accuracy:  $\pm 1\%$  and better

Operation temperature: -55 to 60°C

Memory operation life: 25 years or 10000 registration cycles

Sampling rate and sequence of parameters is programmable. The registered data organization ensures the minimal information drop-out in the case of memory failure.

The FDR complet meets selected MIL Std 810C mechanical and temperature requirements and TSO C51a memory crash protection requirements.

For recorded data evaluation and FDR operational testing the Ground Evaluation Equipment of the type GEE using PC/AT is used as in portable (Notebook with RS232 databus), so in desk-top arrangement.

For quick downloading of data from FDR, Portable Memory Unit working with RS422 databus is delivered.

The complet is equipped with SOFTWARE which can be divided into three parts:

General SW:

Norton Commander 3.00 and higher

User s general SW:

LOAD (for data transfer from FDR into Hard Disk of used PC)

VIEW (for off-line graphic or digital presentation of data stored on HD)

REAL (for on-line display of measured parameters at the aircraft)

CALB (for FDR sensors calibration)

TEST (for FDR operational testing)

User s type SW:

GALD (graphic analysis)

EXTS (aircraft technical state express analysis)

EXPI (crew operation express

LIFE (engine usage and life monitoring)

FRAME (aircraft structure life monitoring)

ANIM (flight animation)

Other nonspecified software can be created according the wish of the customer.

Besides tasks in Avionics, VZLU-SPEEL Ltd. developed and delivers Electronic Tachograph with Solid-State Memory for the use in driving railway and Metro vehicles.

### 3 ELECTRONIC TACHOGRAPH

This device equipped with Solid-State Memory is intended for measuring, indication and record of the course of railway driving vehicle motion.

The measurement and processing of sampled data is provided by microprocessor system. Also the function and communication with display panel and the control of the memory module are performed by microprocessors. (Fig.5).

On the communication and display panel (Fig.6) are presented:

- on the circular dial composed of LED diodes the velocity of the vehicle in the range 0 to 100 km/h, resolution 2km/h
- on the seven segment LED indicator one of following parameters is displayed:
  - real velocity of the vehicle in the range 0 to 100 km/h, resolution 1 km/h
  - vehicle run away in the range 0 to 9,999999 kms, resolution 1 km
  - real time 0 to 23 hours, 59 minutes, 59 seconds, accuracy 43s/day.

### Basic technical data of RRM-3

- Solid-State FLASH EEPROM memory 0,5 MB (30 hours of operation)
- inputs and outputs: high resistivity against external electromagnetic interference (optically separated).
- power supply 72 V DC, 55 W
- autonomous real time circuit - supplied by "LI" battery for min.5 years
- operation temperature: - 20 to 40°C
- mass: electronic tachograph (ET) 2,5 kg  
power supply (PS) 1,5 kg
- conforms to IEC/TC9 standard
- dimensions: ET: 160 x 280 x 100 mm  
PS: 100 x 220 x 75 mm

Input parameters:

- optical RPM sensor (15 V)
- 7 on-off parameters (50 to 95 V DC)

Registered data:

a) service data:

- ET serial No.
- Vehicle No.
- Other cars of the train No.
- Operator s personal No.
- Train No.
- Driver s personal No.

b) time - hours, minutes, seconds

c) vehicle velocity 0 to 100 km/h

d) direction of motion (forward, backward)

e) 7 on-off signals:

- electrodynamic brake
- pneumatic brake
- ARS switching on
- use of watchfulness knob
- allowed codes of ARS 20,40,60,80 km/h
- forbidden code of ARS 0 km/h
- reserve

Registered data downloading may be

performed directly to PC or via Portable Memory Unit, which enables to serve without interruption for 16 electronic tachographs. The evaluation is performed on PC/AT in configuration:

- PC/AT IBM compatible, min.16 MHz
- Hard Disk 40 MB and more
- 1 MB RAM and more
- color monitor
- keyboard
- graph. PCB EGA 256 kB
- mouse
- 2 serial ports
- FD 5,25" 1,15MB and 3,5" 1,44 MB
- Epson printer
- Operational system MS DOS 5.0
- Software cache Smart Drv.sys.256 kB
- Smart Drv.exe and more

User s software:

ETView 01 program - enables evaluation of records stored in the ET Solid-State Memory as follows:

- to read data stored in the ET Memory
- to read data downloaded in the HD of the computer
- to display individual records in graphical form on the screen
- to display additional information to the displayed graphics (e.g. Driver s personal No., Vehicle s No., Date of the route, etc.)
- to measure run distance between two arbitrary points of the record
- to print required part of the record both in the graphical so in digital form (table)

Outputs of the ETView 01 program:(Fig.7,8)

- on the screen:- velocity in analog form
- 7 on-off parameters time
- axle scale in 8 grades,
- exact velocity and on-off signals reading in selected time point
- on the printer:- hard copy of selected time interval on the screen,
- digital presentation of data (table)

To each data print-out the information block about the record is added.

ETPmu 01 program is intended for downloading of data stored in PMU into the HD of the computer with the speed 15200 bd/s. The program generates automatically titles of stored files in the format ( CCC-vehicle No., DD-day, MM-month, P-sequence of records).

#### 4 REFERENCES

1. Kozák J.: "Diagnostische Einrichtung zur Feststellung des Technischen Zustandes von Maschinen und Anlagen", Die Technik, 31Jg.Januar 1976, Berlin, pp.23-27. (in German)
2. Kozák J.: "Exhibit of the Brno Fair - The 2nd Generation ATE", Letectví a kosmonautika No.18, 1984, Praha, pp.15,16. (in Czech)
3. Janoušek I., Kozák J., Taraba O. : "Technická diagnostika", Praha, Czechoslovakia, SNTL 1988 (in Czech)
4. Kozák J. et al.: "Czechoslovak Development and Experience in FLight Data Recorder Readout and Analysis" DLR Mitt. 92-01, Braunschweig, Germany, 2/1992, pp. 185-200. (in English)
5. J. Vidiečan, J. Kozák: "Solid-State Data Recorder, Next Development" DLR Mitt. 94-01, Braunschweig, Germany, 2/1994, pp. 663-674. (in English).

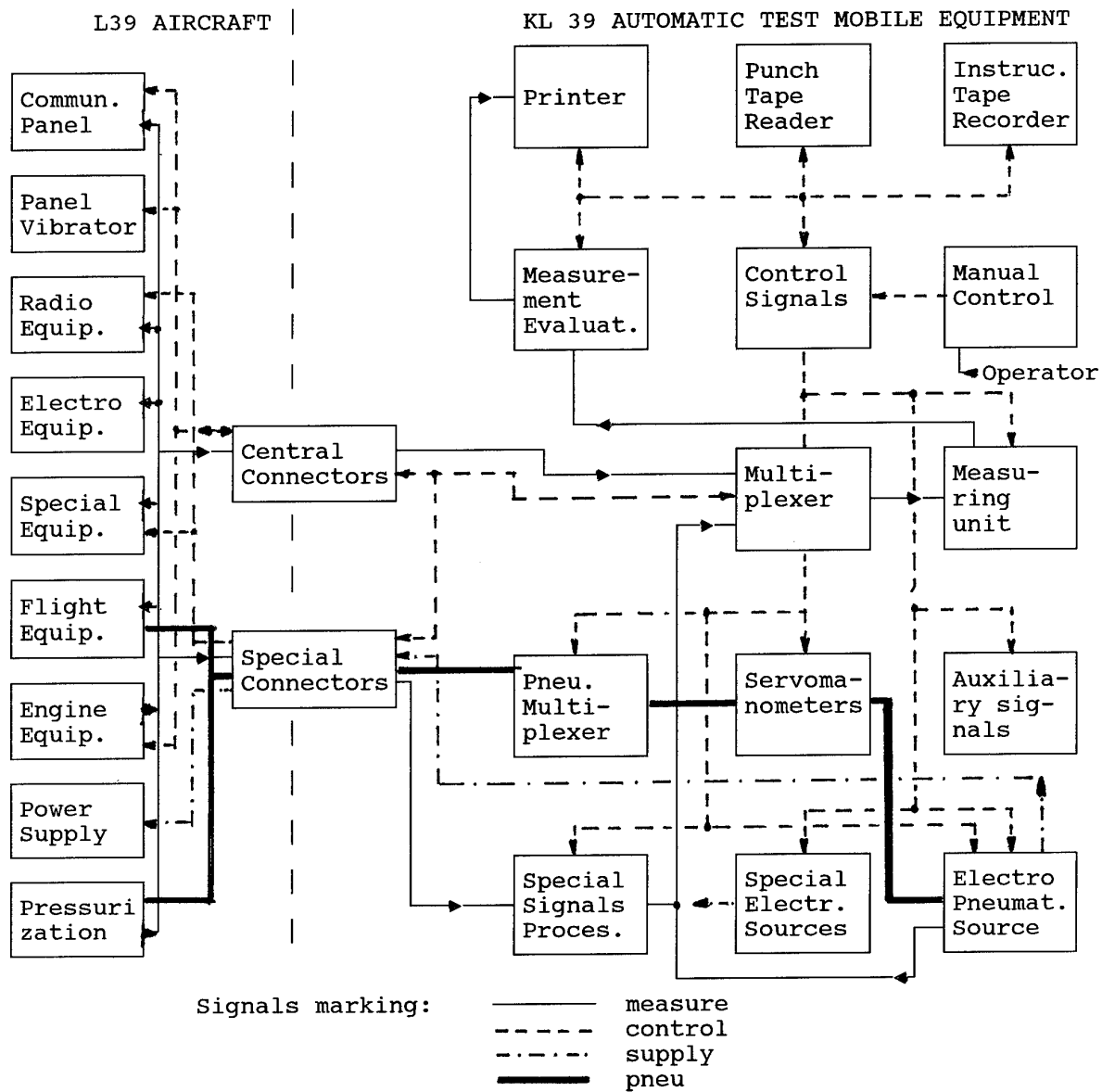


Fig.1. Block Diagram of Mobile Automatic Test Equipment and its Connection to Aircraft.

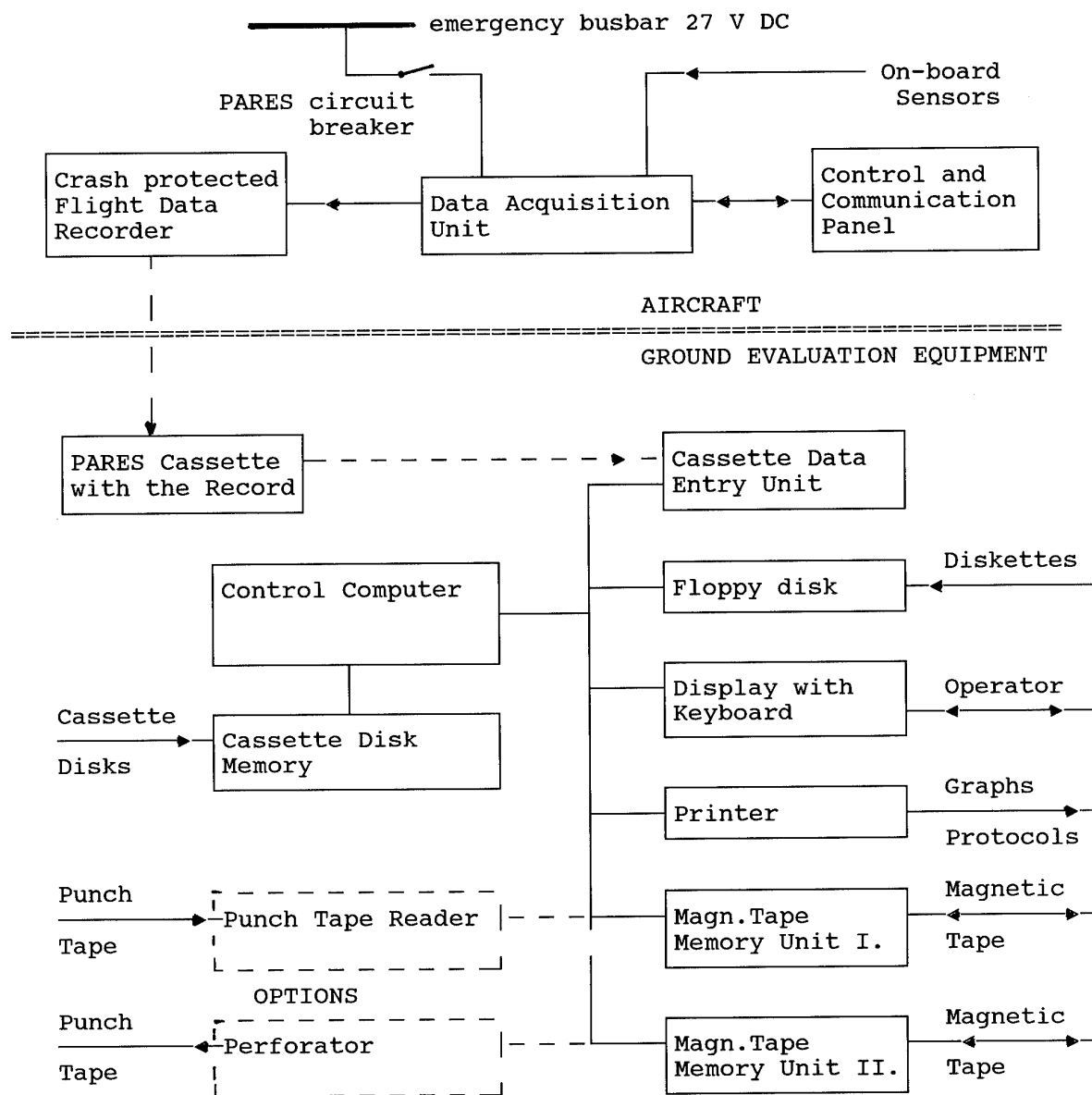


Fig.2. Block Diagram of the Test and Diagnostic System

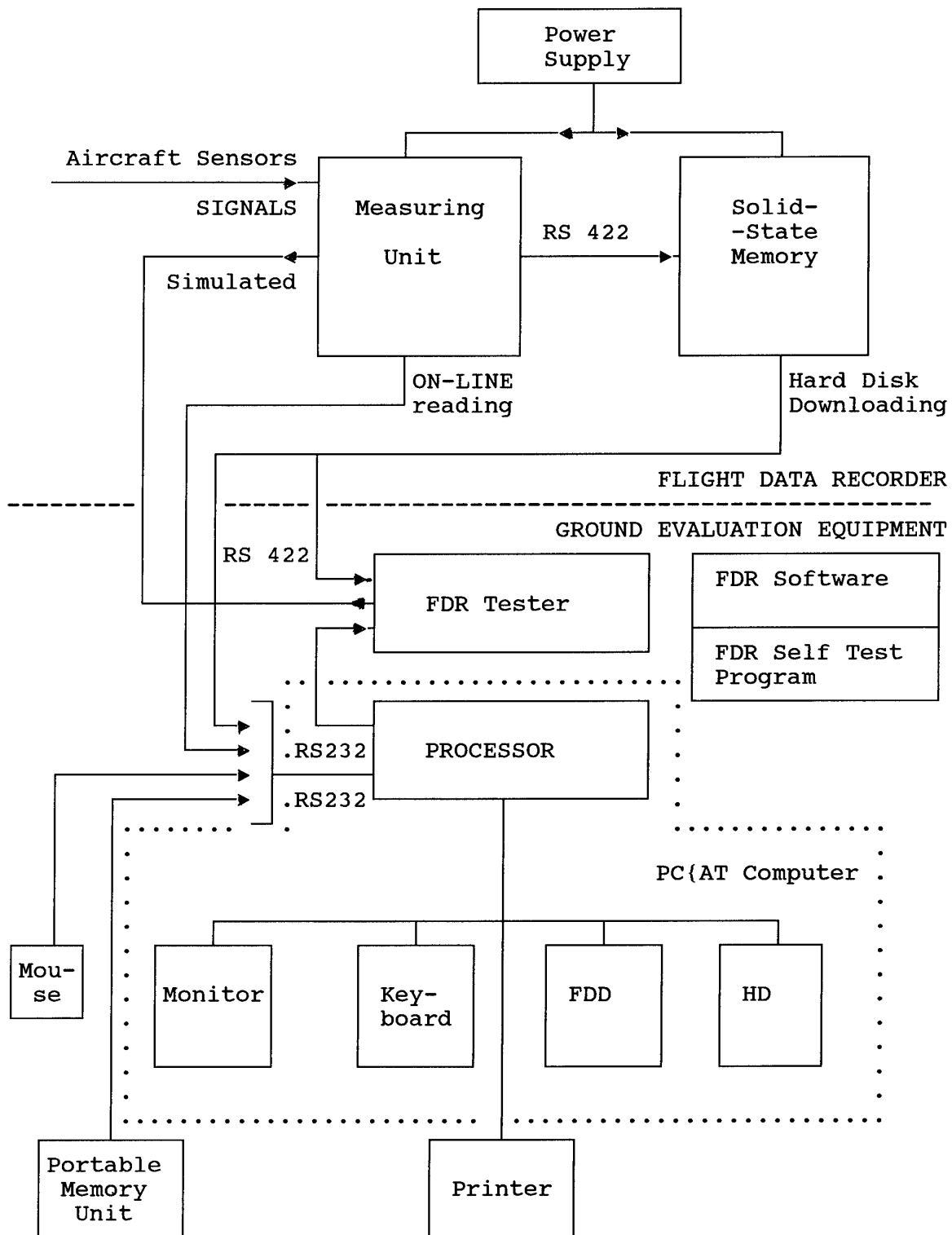


Fig.3. Solid-State FDR and Ground Evaluation Equipment Block Diagram.

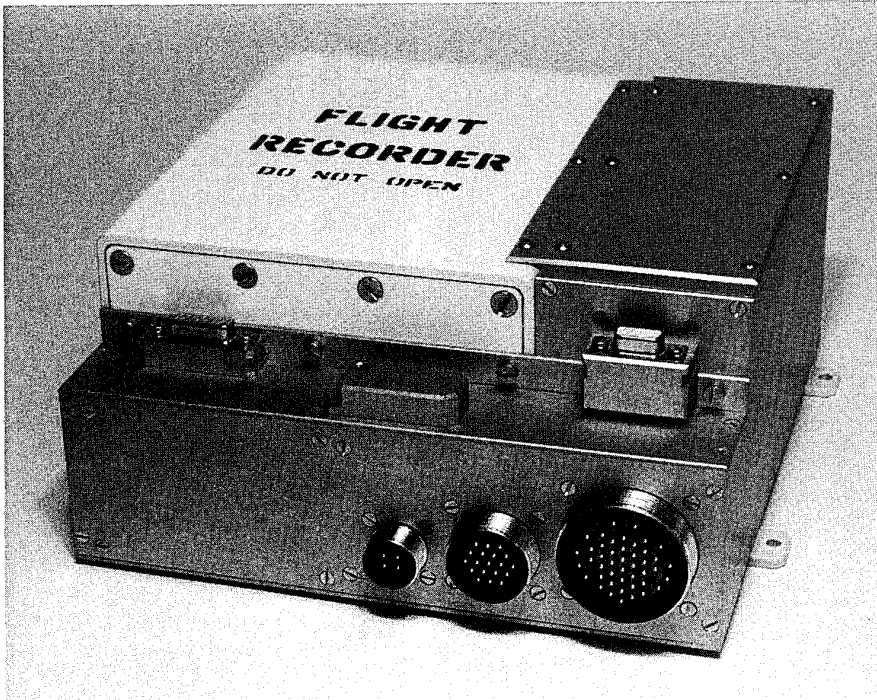


Fig.4. Crash protected Solid-State Flight Data Recorder



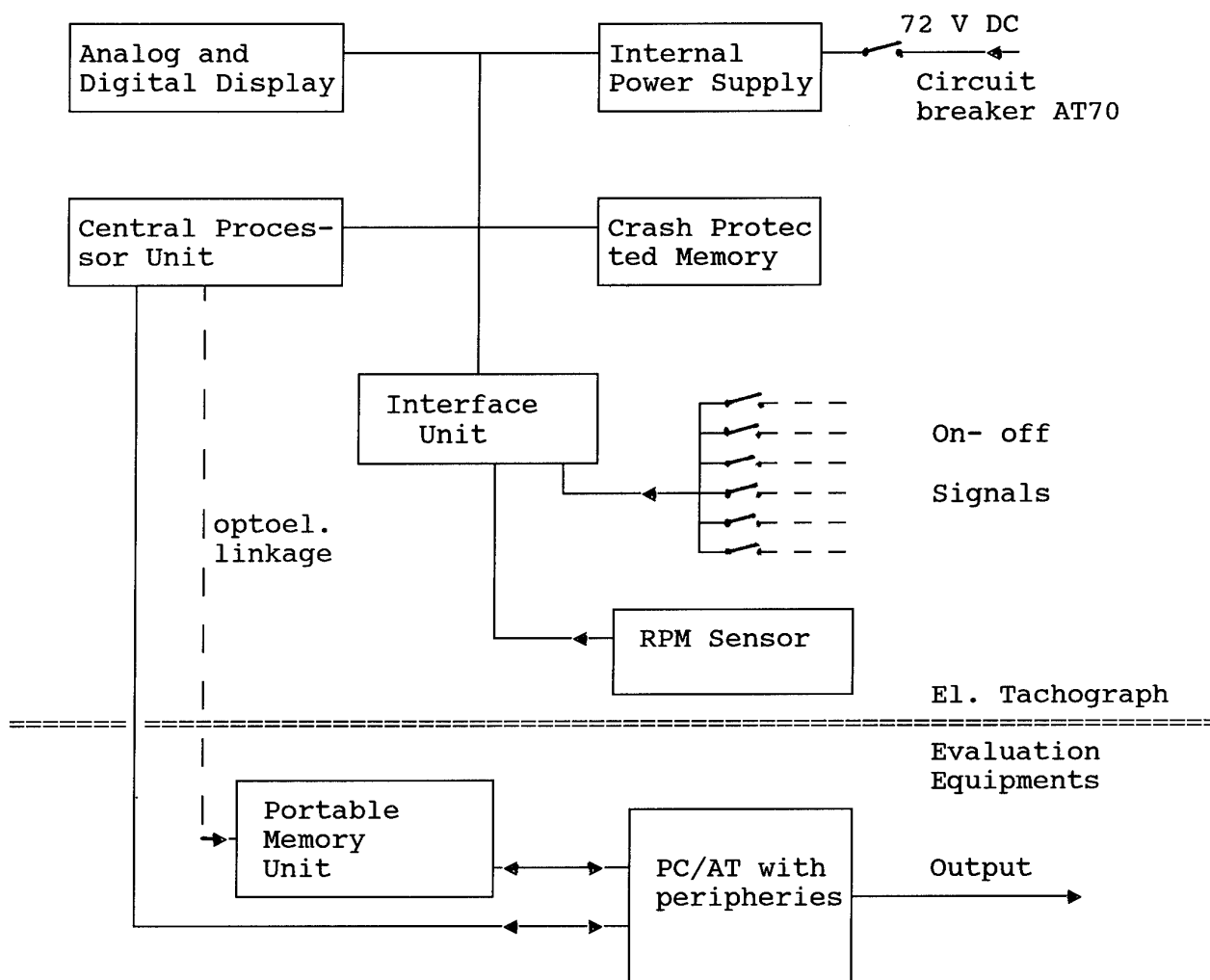


Fig.5. Block Diagram of Electronic Tachograph

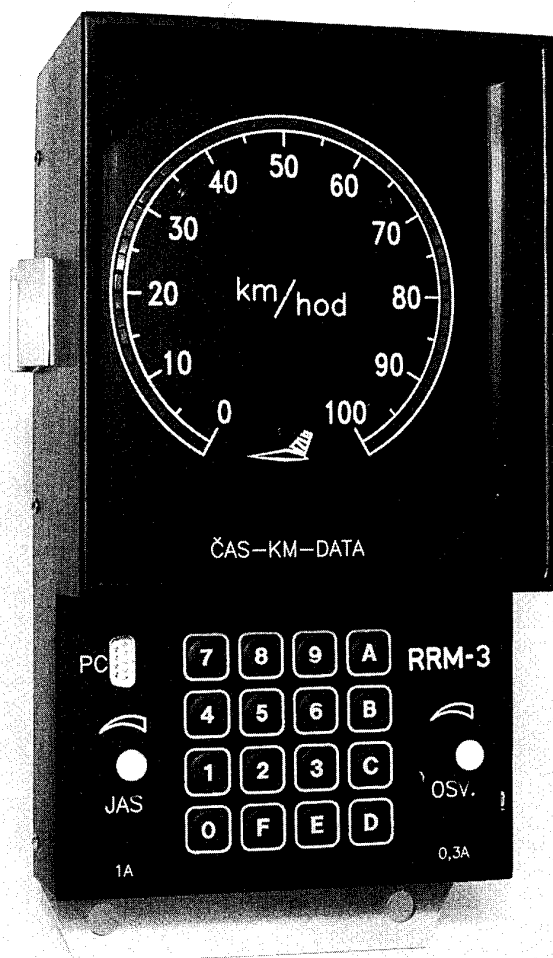


Fig.6. Solid State Electronic Tachograph for METRO Vehicles.

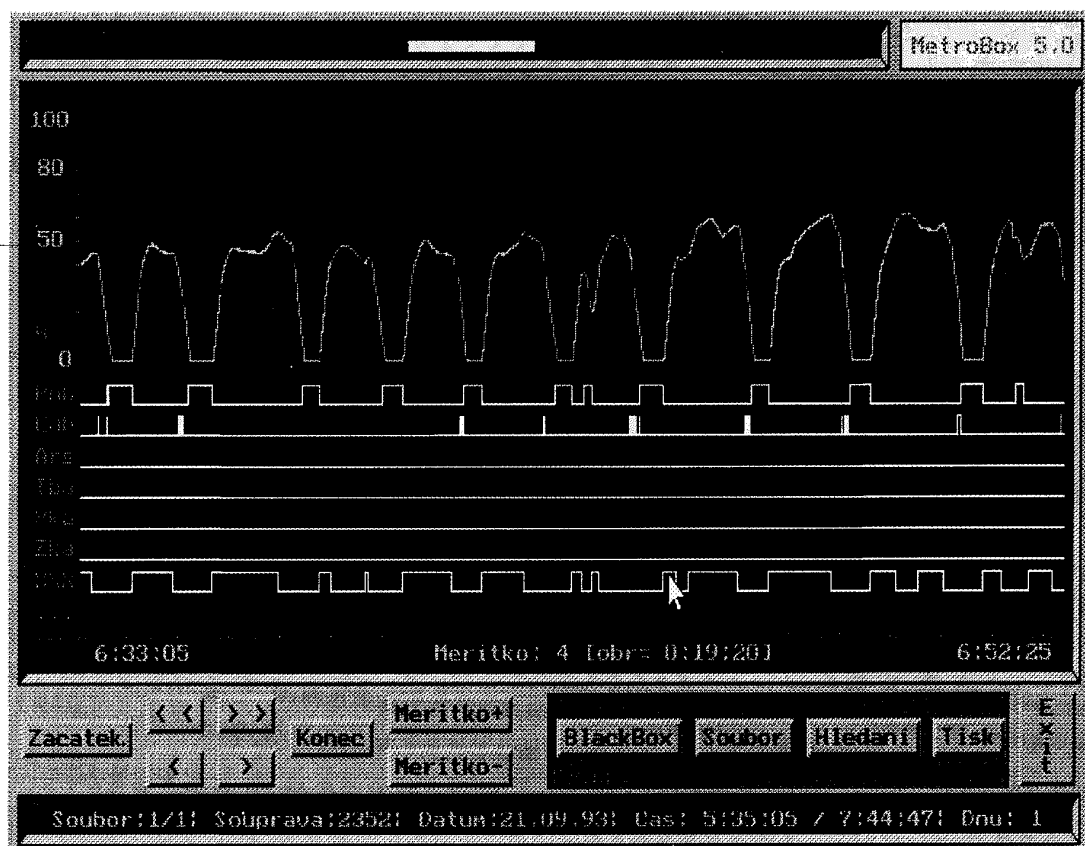


Fig.7. Example of analog data presentation recorded into Electronic Tachograph -scale 4

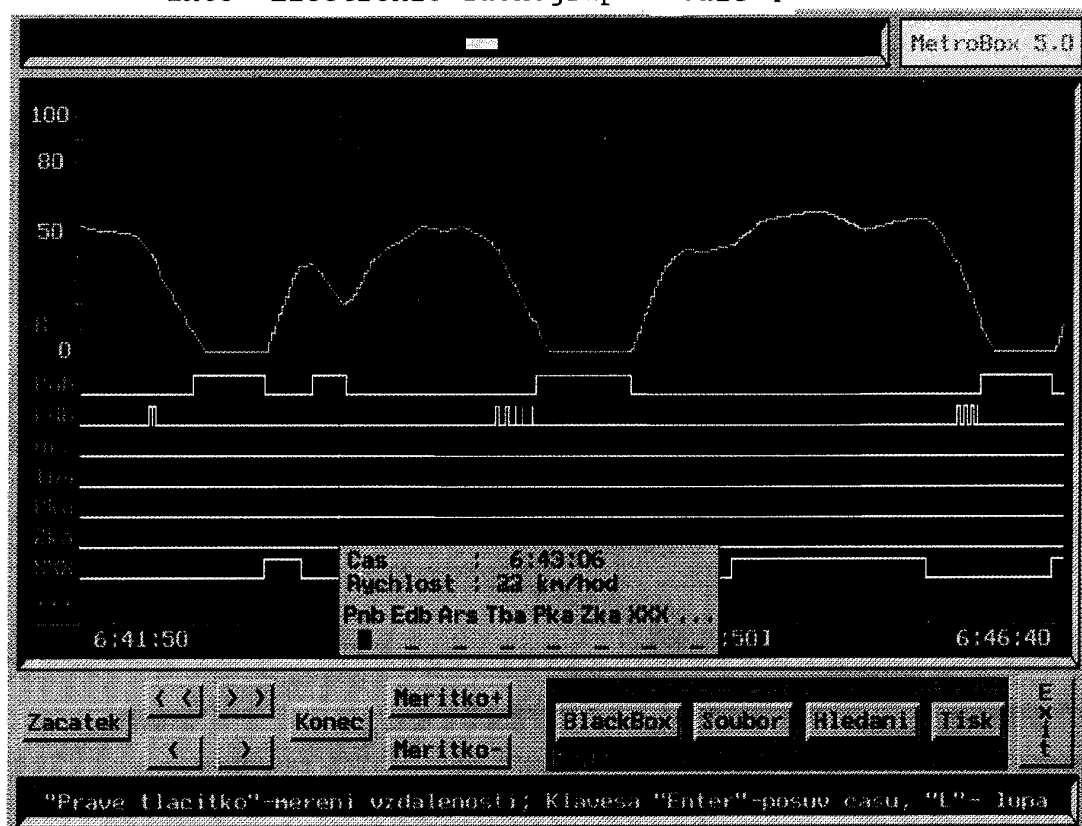


Fig.8. Example of analog data presentation recorded into Electronic Tachograph -scale 2

## GPS-BASED NAVIGATION FOR SPACE APPLICATIONS

C.CHAMPETIER, T.DUHAMEL, M.FREZET

MATRA MARCONI SPACE  
31, Rue des Cosmonautes  
31077 TOULOUSE CEDEX  
FRANCE

## SUMMARY

We present in this paper a survey of the applications of the GPS system for spacecraft navigation. The use of the GPS techniques for space missions is a striking example of dual-use of military technology; it can bring vast improvements in performances and, in some cases, for a reduced cost.

We only deal in this paper with the functional aspects and performances of GPS uses without addressing the issues of hardware implementation where current developments are leading to an increased miniaturisation of the GPS receiver hardware.

We start this paper with a general overview of the GPS system and its various uses for space missions. We then focus on four areas where MATRA MARCONI Space has conducted detailed analyses of performances: autonomous navigation for geostationary spacecraft, relative navigation for space rendez-vous, differential navigation for landing vehicles, absolute navigation for launchers and reentry vehicles.

**Keywords:** GPS, autonomous navigation, rendez-vous, geostationary spacecraft, launcher, reentry.

## 1. INTRODUCTION

Spacecraft navigation has been essentially performed up to now through tracking from ground stations. Three types of measurement are used for tracking spacecraft:

- measurement of the time of propagation of RF signals between accurately positioned reference ground stations and the orbiting spacecraft.
- measurement of the Doppler shift of an RF signal from the orbiting spacecraft.
- measurement of the line-of-sight direction of the orbiting spacecraft relative to the ground station.

Time or Doppler measurements are inherently more accurate than angle measurements and consequently preferred in most applications. The tracking and measurement processing is performed on the ground which implies maintenance and operation of expensive ground facilities for the whole duration of the spacecraft mission.

To reduce dependence on ground facilities, various autonomous navigation systems have been considered in the past based for example on optical sensors using the Sun, Moon or stars to position the spacecraft. The advent of the NAVSTAR Global Positioning System (GPS) has offered a new and very effective way of performing autonomous navigation for spacecraft in the vicinity of the Earth.

The basic principle of GPS system is to replace external natural reference such as stars by a large number of satellites whose position at any time is very accurately known and transmitted to the users so that by triangulation

the position of the user can be computed (relative to any reference frame whose orientation is known relative to the GPS reference system). The basic measurement is a measurement of time of propagation between the GPS satellites and the user which can be performed with a very high accuracy. Another advantage of the GPS navigation is the augmented coverage of the user spacecraft orbit due to the large constellation of satellites as compared to the coverage available with scattered tracking stations.

We present in this paper an overview of the GPS system and its possible uses for navigation in space applications. We then present the GPS navigation performances for four specific applications:

- autonomous navigation of geostationary spacecraft which represent the largest segment of the commercial space market
- relative navigation during rendez-vous phases between two spacecraft
- differential navigation for landing space vehicles such as a reentry spaceplane
- absolute navigation for launchers or reentry vehicles where GPS navigation is coupled with inertial navigation

## 2. GPS SYSTEM OVERVIEW

The NAVSTAR GPS system is based on a constellation of 24 satellites placed in circular orbits at an altitude of 20185 km (corresponding to a 12-hour orbital period). The GPS Satellites (GPSS) are distributed in 6 orbital planes with a 55 degree inclination. The position of each GPSS is supposed to be very accurately known and broadcast, in the form of periodically updated ephemerides, to all the potential users.

A GPS measurement is basically a pseudo-range information given by a measurement of the time of propagation of the signal between a GPS Satellite (GPSS) and a user. A pseudo-velocity (or integrated Doppler count) measurement can be also performed by using the Doppler effect on the GPS signal carrier. The pseudo-range measurement can be written as :

$$\|R_H - R_{GPSS}\| + c \cdot (T_H - T_{GPS}) = \|R_H - R_{GPSS}\| + c \delta t$$

where  $R_H$  is the user spacecraft absolute position,  $R_{GPSS}$  the GPSS absolute position,  $T_H$  the user spacecraft time,  $T_{GPS}$  the GPS time (the GPSS are all synchronised). A simple triangulation from 3 pseudo-range measurements would yield the desired absolute position measurement if  $T_H$  was equal to  $T_{GPS}$ . As the user and GPSS clocks are not synchronised, a fourth pseudo-range measurement is required to recover a reliable position estimation. The triangulation accuracy crucially depends on the geometric distribution of the GPSS in visibility. If  $u_i$  designs the unit vector defining the LOS spacecraft-GPSS $_i$  including as a fourth component the value of the user clock offset relative

to the GPS time, and  $H$  the  $4 \times 4$  matrix  $\begin{bmatrix} u_1^1 & u_2^1 & u_3^1 & u_4^1 \end{bmatrix}$  of the selected LOS, then the positive number  $\tau (H^T H)^{-1}$

(called the Geometric Dilution of Precision (GDOP)) characterises the achievable positioning performances: the smaller it is, the better the localisation accuracy. With more than four GPSS in visibility, a selection which minimises the GDOP is recommended. Otherwise with less than four GPSS in view, in the frame of a pure GPS fix navigation, the position is no longer observable due to the clock drift. The frequency of such inobservability conditions is highly dependent on the receiver antenna RF aperture.

The main source of GPS measurement errors comes from the selective availability (SA) concept: for civil applications, a low frequency coded degradation is superimposed to the original signal. This signal degradation is not well known but its contribution to the final performance is undoubtedly very important. The error model that can be used for the pseudo-distance/pseudo-velocity measurements is the following :

Sources	Error (1 $\sigma$ )
long term SA + GPSS ephemeris + satellite clock	30 m (bias)
short term SA	11 m (bias)
ionosphere	15 m (bias)
GPS receiver noise	10 m
pseudo-velocity	0.2 m/s

Table 1 - Main GPS error sources

The above values correspond to the Standard Positioning Service using the so-called C/A code with a carrier frequency  $L1 = 1575.42$  MHz. For obvious reasons, the Precise Positioning Service which can provide much higher accuracy than the Standard Positioning Service but can be encrypted by US authorities is not usually considered for space applications.

Another important error source not included in the above table is due to multipath effects created by the environment of the GPS receiver antenna. These multipath effects usually vary with the direction of the GPSS relative to the antenna and can be important for the higher accuracy applications.

### 3. SURVEY OF SPACE APPLICATIONS OF GPS

#### 3.1 Absolute navigation

For most space applications, absolute navigation is performed according to the scheme shown on figure 1. The main feature of this scheme is the sequential treatment by a navigation filter of the GPS elementary measurements and hybridation with an orbit model; no attempt is made to compute the so-called GPS fix from four measurements from four different GPS satellites. Each pseudo-distance and pseudo-velocity data is treated separately by the filter: the partial measurement matrix makes it possible for the filter to compute the correct weight to be applied on each coordinate depending on the relative direction of the GPS satellite. This technique greatly improves the navigation accuracy and also improves the performance in degraded GPS satellites configurations: in such cases, the filter will bring new information where it is available and keep confidence in the prediction model for the other coordinates.

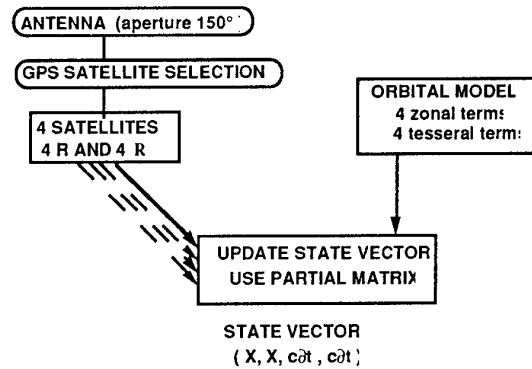


Figure 1 - GPS absolute navigation filter

The predicted performances with/without the pseudo-velocity measurement on a free trajectory and on a manoeuvring trajectory for a low Earth orbit spacecraft are the following :

	position (3 $\sigma$ )	velocity (3 $\sigma$ )
with manoeuvres		
range	120 m	14 cm/s
range & range rate	30 m	4.5 cm/s
w/o manoeuvres		
range & range rate	75 m	28 cm/s

Table 2 - GPS absolute navigation performances

The overall performances are excellent as compared to the usual navigation requirements: therefore an intermittent mode can be defined in coasting flight where the navigation filter performs only prediction calculation during a large period of time and use GPS measurements to update the estimates and recover the converged regime. The preliminary performances calculations have shown that the GPS receiver could be remain in dormant mode 50% of the time outside manoeuvring trajectories for a LEO mission. The range-rate measurement is treated separately in order to assess its influence on the final performance and its inclusion or not in the measurement process for operational constraints; even if not necessary for the pure navigation performances in coasting flight, it decreases the convergence time and therefore facilitates the intermittent mode. Furthermore range-rate measurements improve the navigation performance considerably during the manoeuvring phases.

#### 3.2 Relative navigation

When two spacecraft are fairly close together, such as during rendez-vous phases, it is possible to perform relative GPS navigation which provides improved accuracy on the relative position of the spacecraft. The technique of relative navigation is based on one spacecraft transmitting its dated GPS receiver data to the other and processing the difference between the GPS data of the two spacecraft through a filter which takes into account a model of the relative dynamics of the two spacecraft. The advantages of this technique are that:

- low frequency errors (such as ionospheric propagation errors and selective availability) are cancelled.
- the relative motion information is a direct output of the navigation filter.

The typical relative position accuracy achievable between two cooperative spacecraft in a rendez-vous phase is

approximately 1m in position and 1 cm/s in velocity (1 $\sigma$  values). Further details on the relative navigation techniques for rendez-vous are given in section 5.

### 3.3 Differential navigation

In differential navigation applications, a ground station with an accurately known position is used to estimate the biases attached to each visible GPSS (assumed to be the same as those visible from the moving space vehicle). These biases (or differential corrections) are then transmitted to the spacecraft through a radio link or in the same form as the GPS signal (the ground station is then called a pseudolite) and used to correct the navigation estimates on-board the vehicle.

As for relative navigation, the differential navigation technique eliminates the low frequency errors while keeping the navigation filter structure used for absolute navigation. This approach is particularly useful for the reentry approach and landing phases of spaceplane such as Hermès. The differential navigation performances achievable are detailed in section 6.

### 3.4 Precise orbit determination

In precise orbit determination applications such as for the TOPEX/POSEIDON mission, differential navigation is performed relative to a large number of ground using not only range and range-rate measurements but also GPS signal carrier phase measurements. The navigation performance achievable in that case is of the order of a few centimeters (see [4]) which requires:

- the use of as many GPS spacecraft are visible at any time, i.e. a receiver with up to 12 channels.
- extensive ground processing of the data and hybridation with complex orbit models.

These centimeter level accuracies are not achievable in real-time and are reserved for scientific applications such as oceanography or geodesy.

### 3.5 GPS/INS navigation

The basic navigation technique for launcher and reentry vehicles is inertial navigation i.e., integration of sensed forces and gravity in a known reference frame. GPS measurements can be used to aid the Inertial Navigation System (INS) in the following way:

- GPS updates can be used to bound the error growth of the INS
- they can also be used to estimate and correct biases of the INS
- a GPS fix can be used to initialise the INS

The INS can also be used to improve GPS navigation:

- by bridging gaps in the GPS satellites coverage of the trajectory
- by facilitating GPS satellites reacquisition after a period of masking
- by allowing a dynamic tracking of the GPS satellites

Because of all these advantages, coupling of GPS and INS has been envisaged recently for launchers and reentry vehicles; examples of performance evaluation are detailed in section 7.

## 4. AUTONOMOUS NAVIGATION FOR GEOSTATIONARY SPACECRAFT

The use of a GPS receiver for autonomous navigation of geostationary spacecraft was investigated at MATRA MARCONI Space in the frame of future French Telecommunications Satellite Programme, STENTOR. Performance analyses were conducted assuming a GPS receiver in C/A mode with Selective Availability on. The two main parameters affecting the performance are the maximum aperture of the GPS satellites antenna main beam (which is a driving parameter for the link budget) and the receiver's clock stability.

### 4.1 Sources of errors

#### *Ionospheric effects*

The GPS measurements are affected by the ionospheric effect. To model this error we assume that for measurements with a line-of-sight from the GEO to the GPS satellite away from the Earth by more than 1000 km, the ionospheric errors can be neglected. By contrast, measurements with a line-of-sight from the GEO to the GPS satellite closer than 1000 km from the Earth are not taken into account. The equivalent limitation for the angle Earth centre- GPS satellite - GEO satellite is  $\theta > 16.1$  degree whereas the Earth horizon limitation is only  $\theta > 13.9$  degree.

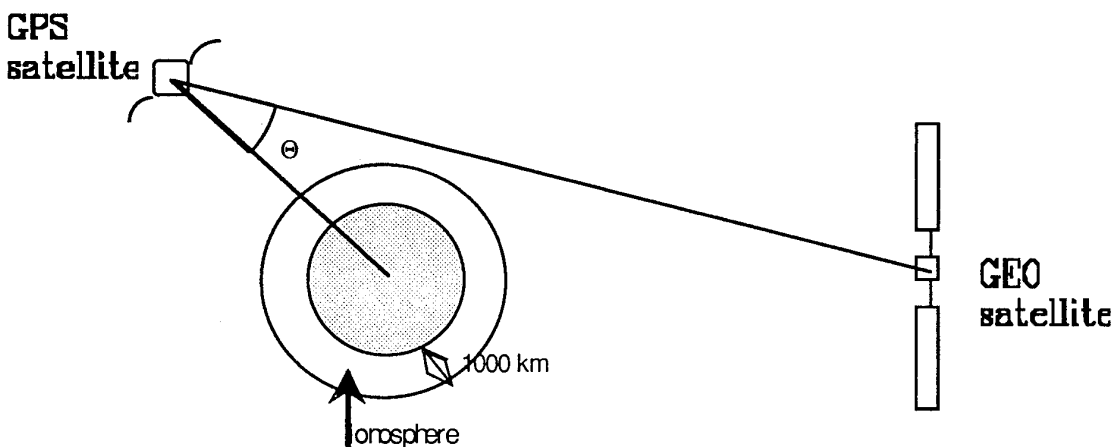


Figure 2 - GEO spacecraft geometry relative to GPS

#### GPS ephemeris errors

The uncertainties on the knowledge of the orbits of GPS satellites are modelled as biases which are supposed to be the result of a Gaussian process with a position uncertainty of 12m ( $3\sigma$ ) and a velocity uncertainty of 0.12 cm/s ( $3\sigma$ ).

#### Receiver clock errors

The main error source consists in the fluctuation of the clock drift. This fluctuation is modelled by a Markov process (slowly evolving bias) characterised by a time constant of 7200 s; the standard deviation of this error characterises the stability of the clock. The typical values considered in this study are  $10^{-7}$ ,  $10^{-8}$  and  $10^{-9}$  s/s ( $3\sigma$ ).

#### Range measurement errors

The GPS is used in C/A mode with SA. In these conditions, only the range measurements are used and their errors are modelled as follows: measurement noise of 30 m ( $3\sigma$ ) and a SA error made of one short term Markov process ( $\tau=180$  s  $1\sigma=25$ m) and one long term Markov process ( $\tau=7200$  s  $1\sigma=30$ m).

#### Dynamic model errors

The dynamic errors which are taken into account correspond to a perturbing acceleration with the following components are ( $1\sigma$  values): along track,  $\sigma_X=5 \cdot 10^{-9}$  m.s $^{-2}$ , cross track,  $\sigma_Y=10^{-8}$  m.s $^{-2}$ , radial,  $\sigma_Z=5 \cdot 10^{-9}$  m.s $^{-2}$ . The order of magnitude of these errors is very pessimistic in comparison with the accuracy of the orbit propagators that are envisaged for the autonomous navigation application. In fact, this continuous acceleration should roughly lead to the same level of uncertainty on the knowledge of the orbit as the realisation errors of the station keeping manoeuvres would. Of course, the modelling of the manoeuvre realisation errors by a continuous acceleration instead of discrete random impulses is not very realistic. However, when considering a posteriori the accuracy on the knowledge of the velocity of the spacecraft obtained with SA and standard receiver clock, one can notice that this accuracy (of the order of the cm/s) is far larger than the expected discrete realisation errors (less than 1 mm/s).

### 4.2 Covariance analysis method

The classical formulation of the equations of the linearised Kalman filter allow one to compute the propagation of the covariance matrix associated to the estimation error of the state vector as a function of the error models only (independently from the values of the measurements themselves). In order to make such a covariance analysis more representative of the actual performance of the estimation, the method consists in two steps:

- in the first step, the state vector is made of 8 parameters (6 for the estimated position and velocity of the spacecraft, 2 for the bias and the drift of the GPS receiver clock). This 8-component filter is representative of the on-board filter. It is set with dynamic noise and measurement noise matrices chosen a priori large enough to ensure the robustness of the filter with respect to non modelled errors such as ephemeris biases or SA biases.

- the second step is representative of the real behaviour of the on-board filter (with gains computed in the first run). In addition to the 8 solved-for parameters, the state vector includes additional "considered" parameters corresponding to errors such as ephemeris biases or SA. The evolution of these parameters is modelled as a constant bias or a markov process. They contribute in the propagation and in the correction phases of the covariance matrix.

A meaningful orbit determination accuracy can only be extracted from the covariance matrix at the end of the second step; the covariance matrix at the end of the first step only corresponds to the ideal performance of the filter,

not its performance in real-life conditions. Nevertheless, the covariance matrix of the first step, which is usually optimistic (measurement biases are taken into account only by increasing the measurement noise covariance matrix), can be used for comparison purpose in the frame of parametric studies.

### 4.3 Parametric analyses

When considering for example a  $10^{-8}$  clock stability and a 15 minutes interval between measurements, the clock drift may induce a  $9 \cdot 10^{-6}$  s error on the receiver date between two consecutive corrections, which is equivalent to a 2700 m ranging error. In those conditions, it does not seem possible to achieve an orbit determination with a sufficient accuracy. One can easily understand that the time interval between the measurements should first be reduced but one should also notice that when we have visibility of two (or three) GPS satellites at the same time, the observability of the receiver's clock error is increased. The possibility of getting measurements from different GPS satellites and the frequency of such opportunities is directly linked to the maximum value allowed for  $\theta$ . In order to better understand the relative importance of these different factors, a first cut analysis based on the first step of the covariance analysis described above was performed with different values of  $\theta_{\max}$ , different time interval values between two corrections and different clock stabilities. For each parametric analysis, three different approaches concerning the visibility of several GPS satellites at the same time were used: in the first case all the available measurements are taken into account by the filter, in the second case only the measurements corresponding to a date when several GPS satellites are available are considered, in the third case, only one measurement is considered at each time interval (if two satellites are visible at the same time, one of the measurements is skipped). The main conclusions of the parametric analyses are:

- 1 min can be considered as a baseline for the time interval between two corrections (it allows the accuracy of the orbit determination to be divided approximatively by two in comparison with a 5 min interval).

- using a standard crystal clock, the convergence of the orbit determination is mostly ensured by the simultaneous visibility of several satellites, or, in the case of a reduced time interval between the corrections (1min), when two consecutive measurements correspond to two different GPS satellites. This fact is illustrated by Figure 3: this case corresponds to a  $10^{-8}$  clock stability  $\theta_{\max}=19$  degree and a time interval between measurements of 1 min. The absolute position and velocity accuracies are shown between 24 and 56 hours after the beginning of orbit determination (the initial uncertainty on the knowledge of the orbit is taken to be very large). The visibility of the GPS satellites is also shown, so that it permits the discrimination of the multiple visibility cases and of the cases corresponding to a rapid succession of different GPS satellites.

The second step runs performed with a time interval between measurements of 1 min (all the available measurements taken into account) for various values of  $\theta_{\max}$  and of the receiver clock stability showed that a trade-off between these two parameters had to be found; for example  $\theta_{\max}=17$ deg and stability  $10^{-7}$  s/s or even  $10^{-8}$  s/s do not allow a satisfactory convergence of the orbit determination. A suggested compromise is  $\theta_{\max}=19$  degree and a  $10^{-8}$  s/s stability; in these conditions a longitude window of less than  $\pm 0.05$  degree is achievable in the frame of an autonomous station keeping. The accuracy on

the knowledge of the orbit is better than the accuracy usually achieved with a ground based orbit determination

involving a single station with ranging and tracking measurements.

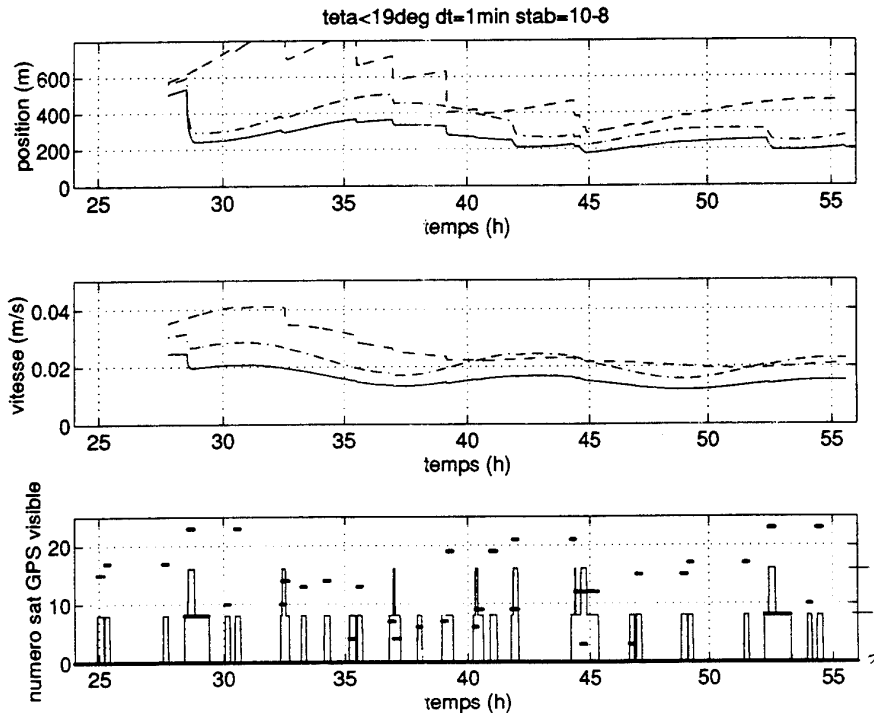


Figure 3 - Orbit determination convergence for a clock stability of  $10^{-8}$

The values in table 3 and 4 were obtained during the 6 last hours of a 72-hour long orbit determination period. The orbit determination accuracies are given in the local orbital frame X,Y,Z ( in-track, cross-track, radial position and velocity). Table 3 contains the results obtained for various values of  $\theta_{max}$  and a  $10^{-9}$  receiver's clock stability, table 4 contains the results obtained for  $\theta_{max}=19$  degree and various values of the receiver's clock stability.

$\theta_{max}$ degree	X m	Y m	Z m	VX mm/s	VY mm/s	VZ mm/s
21	310	130	95	13,5	9,0	7,0
19	380	160	140	19,0	11,5	9,5
17	640	210	170	26,0	18,0	13,0

Table 3 - Orbit determination accuracy for a  $10^{-9}$  receiver clock stability

clock stability (s/s)	X m	Y m	Z m	VX mm/s	VY mm/s	VZ mm/s
$10^{-9}$	380	160	140	19,0	11,5	9,5
$10^{-8}$	430	200	230	26,0	15,0	12,5
$10^{-7}$	480	240	240	33,0	18,5	16,0

Table 4 - Orbit determination accuracy for a 19 degree maximum aperture of the GPS main beam

The GPS can be envisaged as an autonomous orbit determination means for a geostationary spacecraft even

with a low cost standard receiver clock, even in presence of Selective Availability. A trade off has however to be found between the clock stability and the link budget. A typical choice would be a  $10^{-8}$  clock stability and a minimum of 19 degree for  $\theta_{max}$ . Another advantage of this localisation technique is its possible application in the frame of the colocation of several inside the same orbital window. It should then enable a very precise relative orbit determination (due to the cancellation of most biases which are common to the colocated satellites.).

## 5. RELATIVE NAVIGATION FOR RENDEZ-VOUS

GPS navigation is the ideal candidate for autonomous on-board orbit estimation in low Earth orbit rendez-vous missions. The accuracy of absolute orbit determination is completely adequate and it offers the following mission-oriented advantages :

- relative GPS navigation technique provide relative navigation during rendez-vous
- GPS can be used during reentry (if any)
- differential GPS can be used during landing (if any)

A great deal of effort has been devoted in Europe to rendezvous missions in the frame of the Hermès-Columbus projects. MATRA MARCONI Space as responsible of the Hermès Navigation and Orbital Guidance has developed, before the project was cancelled, a preliminary design of the on-board absolute and relative navigation filters [2]. In this design, range and Doppler (range-rate) measurements were processed.



Relative GPS (RGPS) navigation will be implemented by MATRA MARCONI Space in the frame of the ATV Rendezvous Predevelopment (ARP-Kernel) programme. This navigation filter will also incorporate Doppler measurements but under the form of Integrated Doppler Count.

In the rendezvous phase of the mission, the target (we assume in the following that the target is the Space Station) is assumed to be equipped with GPS receivers and to transmit its own GPS pseudo-range to the chaser. An important improvement of the simple scheme of differentiating the chaser GPS absolute navigation and the target absolute navigation can be achieved by directly comparing the pseudo-range and pseudo-velocity measurements of both vehicles. This technique leads to an accurate relative position/velocity information because the slowly varying SA bias as well as the propagation disturbances and the GPSS ephemeris biases are nearly eliminated.

The overall principle of the relative GPS update can be illustrated as follows. If one neglects the clock variables, we can write:

$d_1 = \|R_{GPSS} - R_{SS}\|$  measurement of the target ( $R_{SS}$  is the absolute position of the target)

$d_2 = \|R_{GPSS} - R_H\|$  measurement of the chaser ( $R_H$  is the absolute position of the chaser)

$R = R_{SS} - R_H$ , the relative position

then we have :

$$d_1 = \|R_{GPSS} - R - R_H\|$$

and

$$\frac{\partial d_1}{\partial R_H} = \frac{\partial d_1}{\partial R}$$

$$\frac{\partial d_2}{\partial R_H} = \frac{\partial d_1}{\partial R_H}$$

This symmetry of the equations due to the very short distance between the 2 spacecraft compared to the distance to the GPS satellite, allows to assume that the innovation contained in  $d_1-d_2$  will be directly related to  $R$ , the relative position between the chaser and the target. The residual term  $\partial(d_1-d_2)/\partial R_H$  represents the coupling between absolute and relative navigation. Due to the geometry of the relative spacecraft motion, it can be neglected and the difference between the elementary GPS measurements can be used as a measurement of the relative position/velocity.

The overall filter scheme is illustrated on figure 4. The relative navigation filter estimates at least the relative position, relative velocity and clock variables. The absolute navigation filter continues to be activated during the relative navigation: it is used for measurements prediction as well as for the partial measurement matrix calculation. This filter architecture minimises the constraints imposed by the chaser to the target : the only requirement is that the target provides to the chaser its dated elementary GPS data (range & range rate) obtained of course with the same GPS satellites. The absolute chaser filter can be used to compensate a difference of date between the measurements. In any case residual errors due to the non-simultaneity of the chaser and the target measurements are negligible if a synchronisation better than 1 second can be achieved. On the contrary, the GPS receivers noise is amplified by a factor  $\sqrt{2}$ .

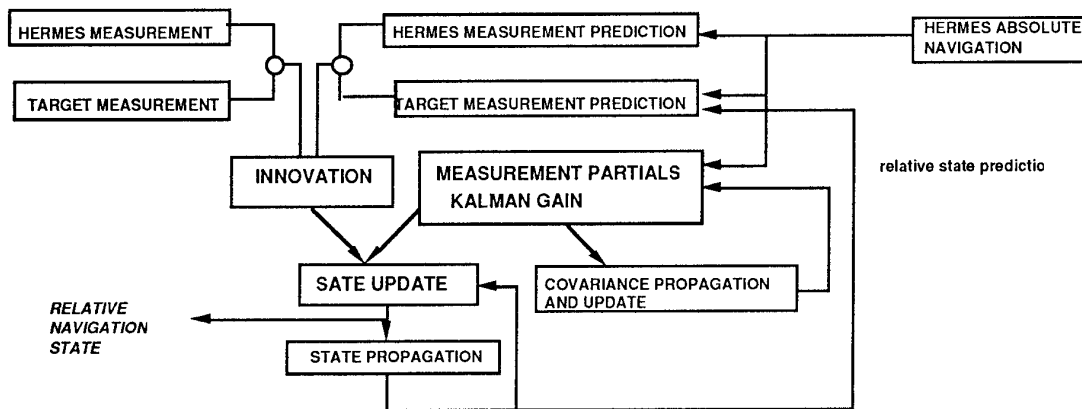


Figure 4 - Relative GPS navigation principle (HERMÈS application)

The performances obtained in homing and closing rendezvous approaches are given below. The homing phase allows the chaser to reach the target orbit (starting a few kilometers under the target orbit). The closing phase is a phase where the chaser moves towards the target using for instance V-bar hops (from typically 1 kilometer to about 200m). The unmodelled perturbations which are considered for designing the Kalman estimator are

- the error on the thrust estimate (including attitude estimation error, thruster misalignment, thrust error, etc.)
- the dynamic model errors (neglected terms in the relative motion equations, target orbit eccentricity, etc.)
- the error on the differential air drag estimation

- the differential effect of the J2 gravity term

The target is assumed to perform no translational manoeuvre. The position and velocity errors (at  $3\sigma$ ) are illustrated on figures 8 and 9 for respectively the homing and closing phases. The position error is expressed in percentage of the distance between chaser and target and the axis limit corresponds to the requirement. The shaded part illustrates the difference between the cases with and without the range-rate measurements. The major reason for improvement of the accuracy at lower distances is the better filtering of the GPS measurements by the more and more accurate relative motion model.

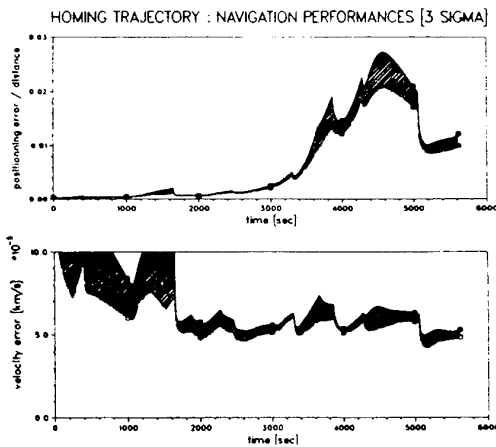


Figure 5 - Relative GPS navigation performance in Homing

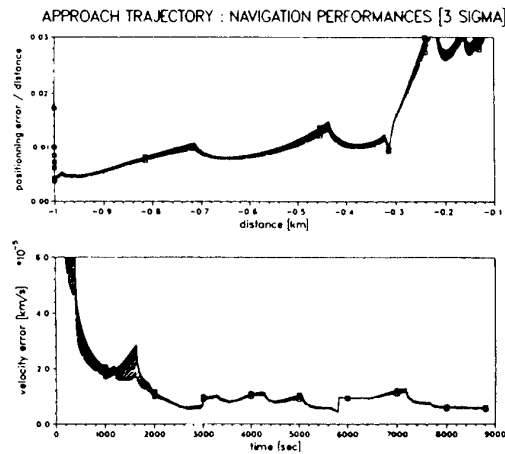


Figure 6 - Relative GPS navigation performance in closing

## 6. DIFFERENTIAL NAVIGATION FOR LANDING VEHICLES

GPS-based differential navigation for landing has been extensively analysed at MATRA MARCONI Space in the frame of the Approach and Landing Navigation studies for the Hermès vehicle. To satisfy the stringent accuracy requirements of the landing phase of Hermès (see table 5 below), a dedicated navigation concept based on GPS in differential mode was designed.

Flight conditions	Final Phase	Final Flare	Touch Down
Range-to-go (km)	10	1	0
Error on X (m)	500	50	50
Error on Y (m)	500	20	10
Error on Z (m)	200	5	1.5
Error on VX (m/s)	5	3	3
Error on VY (m/s)	5	2	2
Error on VZ (m/s)	3	0.5	0.3

Table 5 - Performance requirements for DGPS Navigation (4.45S)

In its nominal mode, the navigation system relies on the hybridation of the measurements issued from the following redundant equipment: 4 Inertial Measurement Units (IMU), 2 GPS receivers, 3 Radio-Altimeters. The radio-altimeters are only used to improve the navigation performances along the vertical axis. As during the whole descent phase, the vehicle position and velocity are predicted at high frequency (typically 12.5 Hz) from the integration of the IMU acceleration measurements and an on-board gravity model; this prediction is updated at 1Hz by the on-board GPS measurements (pseudo-range and pseudo-velocity). At typically 50km from the runway (25 km altitude, Mach 2), the navigation system enters the differential GPS mode. Then, it receives information from the ground which permits to correct the main errors corrupting the on-board GPS measurements. The principle of this correction is the following. The ground station is assumed to receive the signals from the same satellites as the landing vehicle. The

errors introduced by the selected availability on each signal are identified using to the very accurate knowledge on the ground station location. These errors are then sent back to the on-board navigation system which eliminates them from the on-board GPS measurements. Analysis has shown that the key drivers of the resulting navigation performances are the following:

- the characteristics of the on-board GPS receivers (pseudo-range and pseudo-velocity measurement noises, GPS antenna field of view for a given configuration),
- the SA bias on pseudo-velocity before and after correction by the ground,
- the characteristics of the differential GPS correction (transmission delay, correction update period),
- the on-board clock residual bias in this mode.

Extensive covariance analysis runs and sensitivity analyses based on very realistic DGPS correction error models identified from ground experiments have allowed to specify on-board and ground GPS segments for the differential GPS mode. The following hypotheses have been taken into account in the analyses:

- station receiver position error: 1m ( $1\sigma$ )
- station receiver Doppler error: 0.004m/s ( $1\sigma$ )
- DGPS error due to iono- and tropo-spheric propagation:  $3.10^{-3} \Delta h$
- other DGPS errors terms: 2nd order Markov process with 0.004 Hz frequency and 0.001 damping (amplitude kept as a parameter)
- GPS receiver noise: 10m ( $1\sigma$ ), 4 mm/s ( $1\sigma$ )
- GPS antenna field of view: 75° half cone angle
- radio altimeter bias: 2/3% of height +20cm
- radio altimeter noise: 1/3% of height

The contribution of all the DGPS error sources on the performance has been assessed along reference trajectories up to the touch down. Table 6 gives a synthesis of the error budget at runway threshold. The main specifications derived from this analysis are summed up in Table 7. As a result, the applicability of Differential GPS navigation for the landing of a space vehicle such as Hermès has been demonstrated.

CONTRIBUTOR	PARAMETER SPECIFICATION ( $1\sigma$ )	CONTRIBUTION ( $1\sigma$ )						COMMENTS
		X m	Y m	Z cm	Vx cm/s	Vy cm/s	Vz cm/s	
Initial errors	Pos(m (53,19,20) Vcl(cm/s) (9.1,8.6,9.7)	0.1	-	0.2	0.1	0.2	0.2	Main contributor
Model errors		0.1	0.1	0.3	0.9	1.1	0.7	
IMU errors (gmi,asf)		-	-	-	-	-	0.1	
Attitude error	0.24° ( $3\sigma$ )	0.1	0.3	0.1	3.6	5.7	0.2	
SV clock bias on pseudo-range	0.005m/s <sup>2</sup> $\Delta t^2/2$	0.2	0.2	-	0.1	0.1	-	
S/A bias on pseudo-velocity	0.005m/s <sup>2</sup> $\Delta t$	2.0	1.8	-	2	2	-	
Measurement noise		1.0	0.8	0.1	0.3	0.5	0.8	
Measurement bias	DGPS: 7.10 <sup>-5</sup> d + 3.10 <sup>-3</sup> $\Delta h$	0.4	0.7	20.8	1.3	2.3	2.7	Main contributor
TOTAL	Case 2	2.1	2.0	21	9	12	3.8	
Requirement		11.1	2.2	33	67	44	6.7	

Table 6- Error Budget at Runway Threshold

Specified Parameters	Specified Value ( $1\sigma$ )
Pseudo-range measurement noise	10m
Pseudo-velocity measurement noise	4mm/s
S/A bias on pseudo-velocity (w/o DGPS correction)	0.05m/s
GPS antenna field of view	75°
DGPS correction delay (max value)	0.5s
DGPS correction update period	20s
On-board clock residual bias in DGPS mode	0.005m/s <sup>2</sup>
Residual S/A bias on pseudo-velocity	0.005m/s <sup>2</sup>

Table 7 - Specifications of DGPS Space and Ground Segment

## 7. ABSOLUTE NAVIGATION FOR LAUNCHERS AND REENTRY VEHICLES

### 7.1 GPS navigation for reentry vehicles

GPS use is now on the way to replace purely inertial reentry navigation for experimental flights (HOPE/OREX, ARD) and future European manned missions (CTV). The main advantages of the GPS use in a reentry mission are to decrease the requirements on the Inertial Measurement Unit (IMU) and on the accuracy of the last attitude external update before reentry, which are constrained by the desired landing accuracy and the reentry trajectory profile (duration and decelerations). The complete hybridation of GPS and inertial measurements in a Kalman filter during reentry allows not only to maintain a very good knowledge on the vehicle position and velocity, but also to improve the attitude estimation performance as long as sensed accelerations are one order of magnitude higher than accelerometers biases. The drawbacks related to the GPS use in reentry mainly concern the black-out phase where GPS measurements are expected to be absent (a Drag Derived Altitude updating measurement can be envisaged),

visibility and tracking problems resulting from the vehicle attitude high dynamics (implying to use at least two antennas), and reacquisition delays induced at the end of the black-out phase, which must be minimised (typ. a few tens of seconds) by an adequate on-board storage of visible GPS satellites and reentry vehicle relative positions to allow a good restart.

MATRA MARCONI Space has recently carried out preliminary navigation analyses in the frame of the ESA CTV (Crew Transport Vehicle) phase 0 and ACRV (Assured Crew Return Vehicle) phase A studies (see [5] & [6]), aimed at specifying the IMU class and the attitude sensor performances. It has been shown that using GPS, an Ariane 5 class IMU with an Earth sensor attitude update before reentry could meet navigation performance requirements at the end of black-out compatible with a landing accuracy of 9km at  $3\sigma$  (with a ballistic parachute) or 1.5km at  $3\sigma$  (with a parafoil). Such a solution was also shown to be compatible with the required attitude knowledge down to landing (typ. 0.45°,  $3\sigma$ ), while the GPS position/velocity estimation accuracy (typ. 184m, 22cm/s,  $3\sigma$ ) comfortably

covers post black-out navigation needs, including landing systems under parafoil.

## 7.2 GPS navigation for launchers

The launch phase presents characteristics similar to the reentry phase, i.e. initial attitude alignment followed by an accelerated phase possibly separated by ballistic phases before orbit injection. Usually launcher navigation relies on an accurate IMU for gyrocompass alignment and position/velocity/attitude estimation up to orbit injection. Typical orbit dispersions for an Ariane 5 Sun Synchronous Orbit, mainly due to navigation divergence, are 4km at  $1\sigma$  on the semi-major axis and  $0.04^\circ$  at  $1\sigma$  on the inclination, with an IMU class of  $0.01^\circ/\text{h}$ ,  $100\mu\text{g}$  at  $1\sigma$ . Although GPS use cannot totally replace an IMU for alignment and continuity of measurements, it may increase the final performance and relax specifications on the IMU.

A performance analysis has been carried out at MATRA MARCONI Space in the frame of the CNES-funded programme on the European Small Launcher (ESL), aimed at launching 1-ton payloads in low Earth orbits (typ. 700km), with injection performances similar to Ariane 5, but at a very reduced cost. The use of GPS on-board Ariane 5 has already been envisaged for ground localisation purposes, showing no critical problem concerning GPS satellites visibility (two antennas seem enough) and on-board implementation. For ESL, the use of GPS navigation inside the on-board GNC loop is supposed to relax IMU specifications, therefore the induced costs, while maintaining or improving the final injection performance (see [7]).

The results of the preliminary performance assessment carried out at MATRA MARCONI Space accounting for specific constraints of the ESL trajectory (ballistic phases, circularisation boost) have shown that final orbit injection performances can be increased using a relaxed IMU hybridised with a GPS (Table 8). The limitation in the refinement of the IMU specifications has been found to be the alignment accuracy which implies a large additional correction  $\Delta V$  if not compensated by the 1<sup>st</sup> and 2<sup>nd</sup> solid propulsion stages (there is no  $\Delta V$  penalty for the IMU performance displayed in the table). The attitude estimation accuracy can take full advantage of the IMU/GPS hybridisation during highly accelerated phases, as shown in Figure 7.

navigation system	IMU alone, Ariane 5 class : $0.03^\circ/\text{h}$ , $300\mu\text{g}$ $3\sigma$	Hybridised IMU / GPS, IMU class : $0.1^\circ/\text{h}$ , $300\mu\text{g}$ $3\sigma$
performances at orbit injection ( $1\sigma$ )	$\Delta a = 5.75\text{km}$ $\Delta i = 0.043^\circ$ attitude : $0.085^\circ$	$\Delta a = 2.25\text{km}$ $\Delta i = 0.014^\circ$ attitude : $0.1^\circ$

Table 8- Preliminary performance results for GPS-aided launcher navigation

Current investigations are aimed to refine these preliminary results and examine potential solutions to improve the initial IMU alignment accuracy.

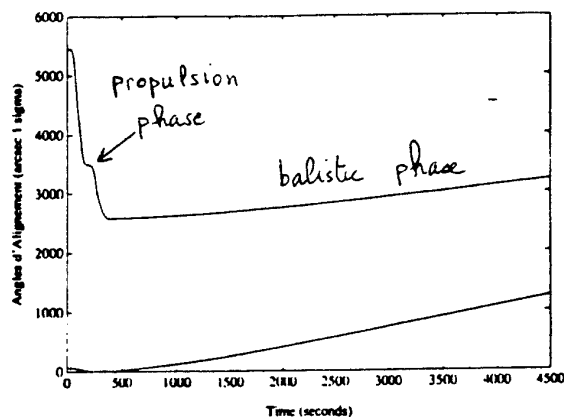


Figure 7 - Attitude estimation improvement by IMU/GPS hybridisation in accelerated phases

## 8. CONCLUSION

Through the examples presented in this paper, we have demonstrated the usefulness of GPS navigation for many space missions. It generally brings improvements both in performance and autonomy and reduction in cost relative to the previous means of navigation.

Although no GPS navigation system is currently operational on-board a spacecraft, many experiments or commercial implementations are planned in the near future which will confirm the expected gains and probably make GPS navigation the preferred means of navigation for future spacecraft.

## 9. ACKNOWLEDGEMENTS

This paper includes important contributions from D.Breton and P.Régner from MATRA MARCONI Space.

## 10. REFERENCES

- [1] NAVSTAR Global Positioning System (GPS) - System Characteristics, Standardization Agreement, MAS, NATO, STANAG 4294.
- [2] M.Frezet, P.Riant, Hermès Navigation and Orbital Guidance, *Proceedings of the 1st ESA Internat. Conf. on 'Spacecraft Guidance, Navigation and Control Systems*, Noordwijk, June 1991.
- [3] C.E.Cohen, *Attitude Determination using GPS*, PhD thesis, Dept of Aeronautics and Astronautics, Stanford University, December 1992.
- [4] E.T. Hesper, B.A.C. Ambrosius, K.F. Wakker, Landsat5 and Topex/Poseidon Orbit Determination from GPS Observations, *Proceedings of the 2nd ESA Internat. Conf. on 'Spacecraft Guidance, Navigation and Control Systems*, Noordwijk, April 1994.
- [5] Crew Transport Vehicle Phase 0 Study, *GNC System Detailed Design*, Technical Note S414/NT/55.94, MATRA MARCONI Space, June 1994.
- [6] Assured Crew Return Vehicle Phase A Study, *GNC Studies*, Technical Note ACRV/NT/CH/75.93, MATRA MARCONI Space, December 1993.
- [7] *Etude GNC des Spécifications du Système de Navigation et d'Estimation d'Attitude du lanceur ESL*, Technical Note AL/NT/14/0068-MATR, MATRA MARCONI Space, March 1994.

# Integrated Special Mission Flight Management for a Flight Inspection Aircraft

A. Redeker  
M. Haverland

Aerodata Flugmeßtechnik GmbH  
Rebenring 33  
D-38106 Braunschweig

## 1. SUMMARY

Flight Inspection of military and civil radionavigation aids requires calibration aircraft with a complex mission equipment. The measurement patterns and their flight procedures differ from usual flight procedures, which cannot be performed with normal flight management/autopilot systems. On the other hand there is a requirement for an automatic guidance, in order to increase the reproducibility of calibration results and to assist the crew operating in areas with high traffic density.

Special mission flight management systems, which are available on the market, are not an elegant solution for flight inspection applications. The flight inspection system (FIS) contains already all elements of a flight management system (FMS), and the FIS has a more comprehensive information on navigational data.

The system approach of an integrated FIS/FMS system is presented, where special mission profiles are generated and interfaced to the autopilot. Flight test results and operational experience are reported.

## 2. INTRODUCTION, STATE OF THE ART

The purpose of flight inspection is to calibrate and verify radio navigation systems for precision approach, landing, and enroute navigation. Even with GNSS (Global Navigation Satellite System) based air traffic navigation coming up at the horizon, conventional radio navigation systems will be installed for a lot of years and will require commissioning and periodic flight inspections.

Flight inspection aircraft are equipped with a complex measuring equipment. The subject of this paper is part of an integrated flight inspection system which is already in regular operation. To understand its purpose it is useful to know the main components and function of such a flight inspection equipment (fig. 1), which are summarized here briefly:

- a variety of calibrated radionav receivers detect the signals of the radionav facilities under test
- independent precision navigation systems enable the comparison of radionav receiver signals with a reference position
- an operator console with a computer system for data acquisition, evaluation, and storage enables the flight test engineer to observe and evaluate the calibration process

Calibration procedures require the performance of flight profiles like orbit flights or ILS quarter sector approaches, which differ from normal airline procedures. The task of flight calibration requires a very close cooperation between pilot, flight inspector, and air traffic control.

State of the art flight inspection systems have poor provisions for autopilot and cockpit interfacing. The already mentioned unusual flight procedures are flown manually because normal flight management systems are not capable to do this. Information exchange between flight inspector and pilot is performed by voice/intercom. The flight inspector communicates with the ground staff at the facility under test and with the pilot, who has additional communication with air traffic control.

The worldwide pressure for a reduction of air traffic control costs forces the flight inspection organisations to efficient operation with less disturbance of regular air traffic. As the flight inspection aircraft is a very expensive investment, a high amount of successful daily calibration flight hours per aircraft are necessary for economic reasons.

Regarding that from its nature the flight inspection business puts a high workload both on pilot and flight inspector, it is necessary to reduce their load with technical measures to receive results with proper quality during the whole mission.

The presented approach of an integrated special mission flight management (SM-FMS) and cockpit information system has the primary goal to assist the mission crew offering efficient and ergonomic working procedures.

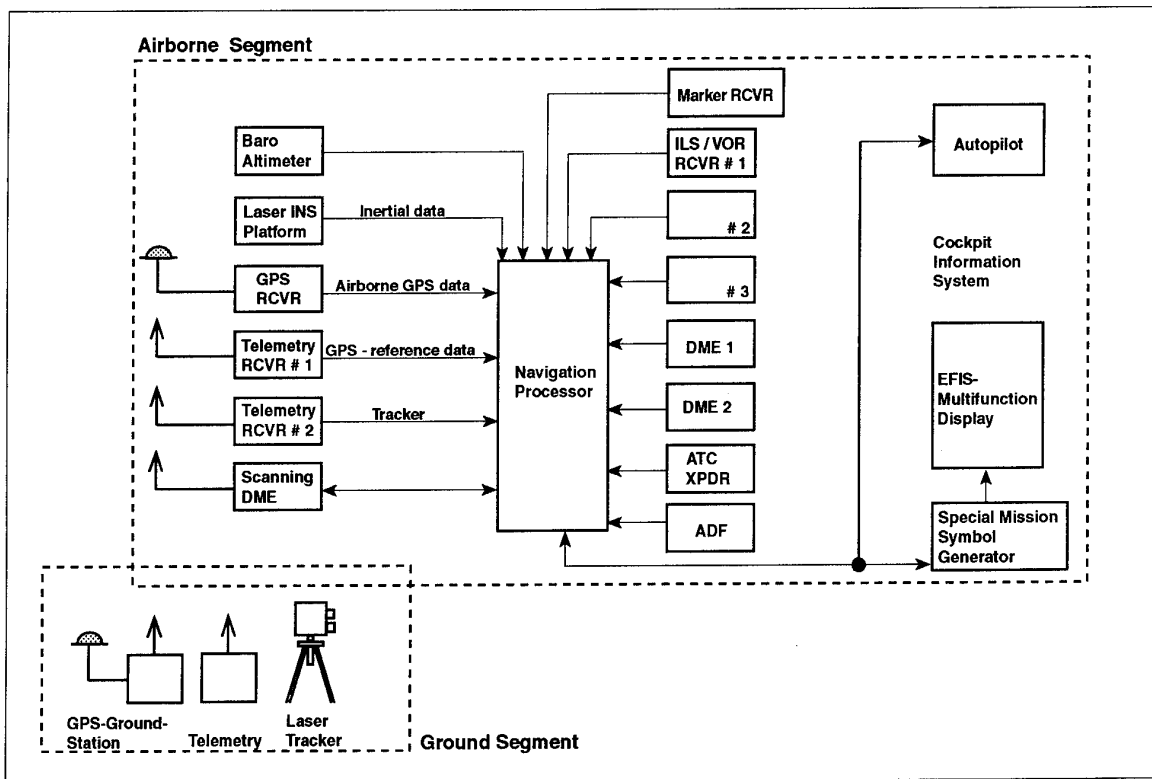


Fig. 1: Functional Block Diagram of a Flight Inspection System

### 3. TECHNICAL CONCEPT

Due to its position reference the FIS has much more precise position information available than the primary aircraft equipment. The flight inspection system software knows, which special flight paths are to be flown, because it evaluates flight data from these flight profiles. As the FIS data processor also includes realtime software processes, it can also overtake steering signal generation for aircraft guidance.

Using these resources for flight guidance purposes seems to suggest itself. The idea is to generate special flight path patterns with the FIS data processor and to interface the aircraft flight guidance system. This is an elegant solution because it avoids the installation of a special mission flight management system, which has anyway to be supplied with information from the FIS.

For the realization of this idea, one general problem has to be solved: The airworthiness certification status of the FIS mission equipment is different from that of the primary aircraft equipment. The airworthiness certification process for the mission equipment ensures the mechanical and electrical compatibility of the installation with the type certification of the aircraft platform and its primary equipment. It does not cover the proper function of the system concerning its flight inspection task.

For economical reasons, a solution can only be found if it can be avoided to upgrade the FIS to the status of primary aircraft equipment. This is possible and shown in the next chapter.

Additional to the flight guidance task there is a need to supply the pilot with information from the FIS to inform him about the intentions of the flight inspector or to assist him for manual flight of special mission profiles. The idea is to present this information on an EFIS multifunction display (EFIS = Electronic Flight Instrument System).

### 4. REALIZATION

As stated before it was essential to find a solution to use "non essential" mission equipment hardware for the flight guidance task.

The following method could be successfully realized and shall be described in a simplified way (see Fig.2):

- the aircraft autopilot is used in a low level mode like "bank and pitch command"
- the FIS calculates the outer autopilot loops and outputs bank and pitch steering commands to the primary autopilot

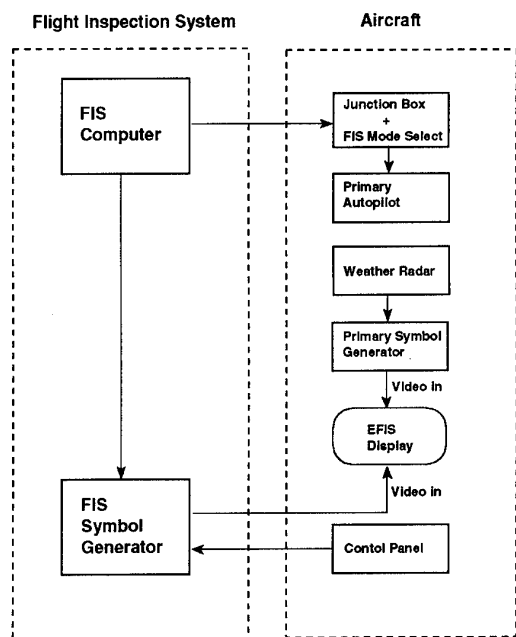


Fig. 2: Flight Inspection System and Aircraft Installation

a junction interface between autopilot and FIS ensures that the "special mission autopilot mode" with FIS-Guidance can only be activated under special conditions. This junction box has to be certified like primary equipment. Together with a watchdog it observes that the FIS computer is still active to process autopilot algorithms. It also activates a yellow indicator in the cockpit to show the pilots that the autopilot is in FIS-mode. Should the operator leave the realtime flight inspection software or shutdown the computer, the autopilot is disconnected.

This method has the advantage that it requires limited certification efforts, because the primary autopilot is operated in an unmodified way. Only a few signal input lines, which are normally input by control elements from the autopilot control panel in the cockpit, are supplied by the FIS instead of the pilots. Internal safety loops of the autopilot like attitude angle or rate limitations are unaffected and still in use. The certification of the basic autopilot covers the possibility that his signal inputs are fed with useless data because one of the connected devices could fail. This means that also the FIS may output a senseless bank or pitch command at any time. As long as the pilot has still unmodified primary instruments, there is no discussion about the reliability of the FIS computer and its outer autopilot loops necessary for airworthiness certification.

The cockpit information system has been realized with an EFIS multifunction display. This display is normally used for weather radar information, driven by a symbol generator from the primary equipment. It can be switched to a special symbol generator which is integrated in the FIS installation. The pilot can select the following information on a mode switching unit:

- special mission Attitude Direction Indicator (SM-ADI)
- special mission Horizontal Situation Indicator (SM-HSI)
- moving map display
- moving map including airway display (enroute mode)
- approach chart display
- text information from the FIS

The moving map is generated from an official Jeppesen data base which is merged with the station data library from the flight inspection system. This is useful because the flight inspection business requires a number of locations which are not published in official data bases.

As the flight inspector at the FIS console needs some information about the aircraft itself, he has access to similar information than the pilot. On one of his computer screens he has the permanent display of SM-ADI/HSI. On request he can call the moving map display as well. This information keeps him in the loop and enables a very efficient cooperation with the flight deck.

## 5. OPERATIONAL ASPECTS

At the beginning of a mission with the startup of the flight inspection console, the special mission symbol generator is initially loaded with map information. After initialization it is permanently supplied with 10 Hz position data from the integrated positioning system of the FIS. It is a best position, which is Kalman filtered from different sensor sources like satellite navigation (GPS), differential satellite navigation (DGPS), inertial laserplatform (INS), and laser-tracker data.

If the flight inspector prepares a mission profile by command inputs at the FIS console, a message about his intention is sent to the display generator and informs the pilot on the text page. A shortest flyable flight path from the present aircraft position and heading to the starting point of the mission profile is generated as well as the mission profile itself. This recommended flight path is displayed on the moving map. If the pilot accepts it, he engages the autopilot in the FIS-mode and the aircraft follows the flight profile.

The radius of curved flight patterns is generated with regard to actual airspeed and a limited bank angle.

## 6. OPERATIONAL EXPERIENCE

The experience from half a year's flight inspection operation has shown that flight inspectors and pilots were quickly trained and highly motivated to use the possibilities of the special mission flight guidance system and the cockpit information system. Nearly all mission profiles including ILS calibrations are flown now with autopilot. Especially ILS quartersector approaches, which are difficult to fly manually are made with Differential GPS coupled autopilot. Hundreds of approaches like this have been performed in the meantime.

## REPORT DOCUMENTATION PAGE

<b>1. Recipient's Reference</b>	<b>2. Originator's Reference</b> AGARD-CP-556	<b>3. Further Reference</b> ISBN 92-836-1016-4	<b>4. Security Classification of Document</b> UNCLASSIFIED/ UNLIMITED												
<b>5. Originator</b> Advisory Group for Aerospace Research and Development North Atlantic Treaty Organization 7 rue Ancelle, 92200 Neuilly-sur-Seine, France															
<b>6. Title</b> Dual Usage of Military and Commercial Technology in Guidance and Control															
<b>7. Presented at</b> The Guidance and Control Panel 59th Symposium held in Pratica di Mare (Rome), Italy, from 20th to 21st October 1994															
<b>8. Author(s)/Editor(s)</b> Multiple			<b>9. Date</b> March 1995												
<b>10. Author's/Editor's Address</b> Multiple			<b>11. Pages</b> 192												
<b>12. Distribution Statement</b> There are no restrictions on the distribution of this document. Information about the availability of this and other AGARD unclassified publications is given on the back cover.															
<b>13. Keywords/Descriptors</b> <table border="0"><tr><td>Guidance</td><td>Navigation sensors</td></tr><tr><td>Guidance computers</td><td>Navigational computers</td></tr><tr><td>Control equipment</td><td>Data fusion</td></tr><tr><td>Dual use technologies</td><td>Laser gyroscopes</td></tr><tr><td>Multisensors</td><td>Global positioning system</td></tr><tr><td>Integrated systems</td><td></td></tr></table>				Guidance	Navigation sensors	Guidance computers	Navigational computers	Control equipment	Data fusion	Dual use technologies	Laser gyroscopes	Multisensors	Global positioning system	Integrated systems	
Guidance	Navigation sensors														
Guidance computers	Navigational computers														
Control equipment	Data fusion														
Dual use technologies	Laser gyroscopes														
Multisensors	Global positioning system														
Integrated systems															
<b>14. Abstract</b> <p>This volume contains the Technical Evaluation Report and the 19 unclassified papers, presented at the Guidance and Control Panel Symposium held in Pratica di Mare (Rome), Italy, from 20th to 21st October 1994.</p> <p>The papers presented covered the following headings:</p> <ul style="list-style-type: none"><li>• Dual-use Opportunities and Missions</li><li>• Navigation Sensors for Dual-use Applications</li><li>• Multi-sensor Navigation Applied to Dual-uses</li><li>• Dual-use Technology for Air-Ground Operations</li><li>• Dual-use Applications of G&amp;C Technology</li></ul>															



Aucun stock de publications n'a existé à AGARD. A partir de 1993, AGARD détiendra un stock limité des publications associées aux cycles de conférences et cours spéciaux ainsi que les AGARDographies et les rapports des groupes de travail, organisés et publiés à partir de 1993 inclus. Les demandes de renseignements doivent être adressées à AGARD par lettre ou par fax à l'adresse indiquée ci-dessus. *Veuillez ne pas téléphoner.* La diffusion initiale de toutes les publications de l'AGARD est effectuée auprès des pays membres de l'OTAN par l'intermédiaire des centres de distribution nationaux indiqués ci-dessous. Des exemplaires supplémentaires peuvent parfois être obtenus auprès de ces centres (à l'exception des Etats-Unis). Si vous souhaitez recevoir toutes les publications de l'AGARD, ou simplement celles qui concernent certains Panels, vous pouvez demander à être inclut sur la liste d'envoi de l'un de ces centres. Les publications de l'AGARD sont en vente auprès des agences indiquées ci-dessous, sous forme de photocopie ou de microfiche.

CENTRES DE DIFFUSION NATIONAUX

## ALLEMAGNE

Fachinformationszentrum,  
Karlsruhe  
D-76344 Eggenstein-Leopoldshafen 2

## BELGIQUE

Coordonnateur AGARD-VSL  
Etat-major de la Force aérienne  
Quartier Reine Elisabeth  
Rue d'Evere, 1140 Bruxelles

## CANADA

Directeur, Services d'information scientifique  
Ministère de la Défense nationale  
Ottawa, Ontario K1A 0K2

## DANEMARK

Danish Defence Research Establishment  
Ryvangs Allé 1  
P.O. Box 2715  
DK-2100 Copenhagen Ø

## ESPAGNE

INTA (AGARD Publications)  
Pintor Rosales 34  
28008 Madrid

## ETATS-UNIS

NASA Headquarters  
Code JOB-1  
Washington, D.C. 20546

## FRANCE

O.N.E.R.A. (Direction)  
29, Avenue de la Division Leclerc  
92322 Châtillon Cedex

## GRECE

Hellenic Air Force  
Air War College  
Scientific and Technical Library  
Dekelia Air Force Base  
Dekelia, Athens TGA 1010

## ISLANDE

Director of Aviation  
c/o Flugrad  
Reykjavik

## ITALIE

Aeronautica Militare  
Ufficio del Delegato Nazionale all'AGARD  
Aeroporto Pratica di Mare  
00040 Pomezia (Roma)

## LUXEMBOURG

Voir Belgique

## NORVEGE

Norwegian Defence Research Establishment  
Attn: Biblioteket  
P.O. Box 25  
N-2007 Kjeller

## PAYS-BAS

Netherlands Delegation to AGARD  
National Aerospace Laboratory NLR  
P.O. Box 90502  
1006 BM Amsterdam

## PORTUGAL

Força Aérea Portuguesa  
Centro de Documentação e Informação  
Alfragide  
2700 Amadora

## ROYAUME-UNI

Defence Research Information Centre  
Kentigern House  
65 Brown Street  
Glasgow G2 8EX

## TURQUIE

Millî Savunma Başkanlığı (MSB)  
ARGE Dairesi Başkanlığı (MSB)  
06650 Bakanlıklar-Ankara

**Le centre de distribution national des Etats-Unis ne détient PAS de stocks des publications de l'AGARD.**

D'éventuelles demandes de photocopies doivent être formulées directement auprès du NASA Center for AeroSpace Information (CASI) à l'adresse ci-dessous. Toute notification de changement d'adresse doit être fait également auprès de CASI.

AGENCES DE VENTE

NASA Center for  
AeroSpace Information (CASI)  
800 Elkridge Landing Road  
Linthicum Heights, MD 21090-2934  
Etats-Unis

ESA/Information Retrieval Service  
European Space Agency  
10, rue Mario Nikis  
75015 Paris  
France

The British Library  
Document Supply Division  
Boston Spa, Wetherby  
West Yorkshire LS23 7BQ  
Royaume-Uni

Les demandes de microfiches ou de photocopies de documents AGARD (y compris les demandes faites auprès du CASI) doivent comporter la dénomination AGARD, ainsi que le numéro de série d'AGARD (par exemple AGARD-AG-315). Des informations analogues, telles que le titre et la date de publication sont souhaitables. Veuillez noter qu'il y a lieu de spécifier AGARD-R-nnn et AGARD-AR-nnn lors de la commande des rapports AGARD et des rapports consultatifs AGARD respectivement. Des références bibliographiques complètes ainsi que des résumés des publications AGARD figurent dans les journaux suivants:

Scientific and Technical Aerospace Reports (STAR)  
publié par la NASA Scientific and Technical  
Information Division  
NASA Headquarters (JTT)  
Washington D.C. 20546  
Etats-Unis

Government Reports Announcements and Index (GRA&I)  
publié par le National Technical Information Service  
Springfield  
Virginia 22161  
Etats-Unis  
(accessible également en mode interactif dans la base de  
données bibliographiques en ligne du NTIS, et sur CD-ROM)



7 RUE ANCELLE • 92200 NEUILLY-SUR-SEINE  
FRANCE

Telefax (1)47.38.57.99 • Telex 610 176

**DISTRIBUTION OF UNCLASSIFIED  
AGARD PUBLICATIONS**

AGARD holds limited quantities of the publications that accompanied Lecture Series and Special Courses held in 1993 or later, and of AGARDographs and Working Group reports published from 1993 onward. For details, write or send a telefax to the address given above. *Please do not telephone.*

AGARD does not hold stocks of publications that accompanied earlier Lecture Series or Courses or of any other publications. Initial distribution of all AGARD publications is made to NATO nations through the National Distribution Centres listed below. Further copies are sometimes available from these centres (except in the United States). If you have a need to receive all AGARD publications, or just those relating to one or more specific AGARD Panels, they may be willing to include you (or your organisation) on their distribution list. AGARD publications may be purchased from the Sales Agencies listed below, in photocopy or microfiche form.

NATIONAL DISTRIBUTION CENTRES

**BELGIUM**

Coordonnateur AGARD — VSL  
Etat-major de la Force aérienne  
Quartier Reine Elisabeth  
Rue d'Evere, 1140 Bruxelles

**CANADA**

Director Scientific Information Services  
Dept of National Defence  
Ottawa, Ontario K1A 0K2

**DENMARK**

Danish Defence Research Establishment  
Ryvangs Allé 1  
P.O. Box 2715  
DK-2100 Copenhagen Ø

**FRANCE**

O.N.E.R.A. (Direction)  
29 Avenue de la Division Leclerc  
92322 Châtillon Cedex

**GERMANY**

Fachinformationszentrum  
Karlsruhe  
D-76344 Eggenstein-Leopoldshafen 2

**GREECE**

Hellenic Air Force  
Air War College  
Scientific and Technical Library  
Dekelia Air Force Base  
Dekelia, Athens TGA 1010

**ICELAND**

Director of Aviation  
c/o Flugrad  
Reykjavik

**ITALY**

Aeronautica Militare  
Ufficio del Delegato Nazionale all'AGARD  
Aeroporto Pratica di Mare  
00040 Pomezia (Roma)

**LUXEMBOURG**

*See Belgium*

**NETHERLANDS**

Netherlands Delegation to AGARD  
National Aerospace Laboratory, NLR  
P.O. Box 90502  
1006 BM Amsterdam

**NORWAY**

Norwegian Defence Research Establishment  
Attn: Biblioteket  
P.O. Box 25  
N-2007 Kjeller

**PORTUGAL**

Força Aérea Portuguesa  
Centro de Documentação e Informação  
Alfragide  
2700 Amadora

**SPAIN**

INTA (AGARD Publications)  
Pintor Rosales 34  
28008 Madrid

**TURKEY**

Millî Savunma Başkanlığı (MSB)  
ARGE Dairesi Başkanlığı (MSB)  
06650 Bakanlıklar-Ankara

**UNITED KINGDOM**

Defence Research Information Centre  
Kentigern House  
65 Brown Street  
Glasgow G2 8EX

**UNITED STATES**

NASA Headquarters  
Code JOB-1  
Washington, D.C. 20546

**The United States National Distribution Centre does NOT hold stocks of AGARD publications.**

Applications for copies should be made direct to the NASA Center for AeroSpace Information (CASI) at the address below.

Change of address requests should also go to CASI.

SALES AGENCIES

NASA Center for  
AeroSpace Information (CASI)  
800 Elkridge Landing Road  
Linthicum Heights, MD 21090-2934  
United States

ESA/Information Retrieval Service  
European Space Agency  
10, rue Mario Nikis  
75015 Paris  
France

The British Library  
Document Supply Centre  
Boston Spa, Wetherby  
West Yorkshire LS23 7BQ  
United Kingdom

Requests for microfiches or photocopies of AGARD documents (including requests to CASI) should include the word 'AGARD' and the AGARD serial number (for example AGARD-AG-315). Collateral information such as title and publication date is desirable. Note that AGARD Reports and Advisory Reports should be specified as AGARD-R-*nnn* and AGARD-AR-*nnn*, respectively. Full bibliographical references and abstracts of AGARD publications are given in the following journals:

Scientific and Technical Aerospace Reports (STAR)  
published by NASA Scientific and Technical  
Information Division  
NASA Headquarters (JTT)  
Washington D.C. 20546  
United States

Government Reports Announcements and Index (GRA&I)  
published by the National Technical Information Service  
Springfield  
Virginia 22161  
United States  
(also available online in the NTIS Bibliographic  
Database or on CD-ROM)



Printed by Canada Communication Group  
45 Sacré-Cœur Blvd., Hull (Québec), Canada K1A 0S7